SEISMIC VULNERABILITY ASSESSMENT OF RETROFITTED BRIDGES USING PROBABILISTIC METHODS

A Thesis
Presented to
The Academic Faculty

by

Jamie Ellen Padgett

In Partial Fulfillment
of the Requirements for the Degree
Doctor of Philosophy

School of Civil and Environmental Engineering
Georgia Institute of Technology
May, 2007

SEISMIC VULNERABILITY ASSESSMENT OF RETROFITTED BRIDGES USING PROBABILISTIC METHODS

Approved by:

Dr. Reginald DesRoches, Advisor
School of Civil and Environmental Engineering
Georgia Institute of Technology

Dr. Glenn Rix
School of Civil and Environmental Engineering
Georgia Institute of Technology

Dr. Bruce Ellingwood
School of Civil and Environmental Engineering
Georgia Institute of Technology

Dr. Ann Bostrom
School of Public Policy
Georgia Institute of Technology

Dr. Barry Goodno
School of Civil and Environmental Engineering
Georgia Institute of Technology

Date Approved: April 4, 2007

ACKNOWLEDGEMENTS

Through the course of our journey we are touched by a number of individuals, and my experience in graduate school has been just such an experience. I would like to thank those who have had an impact on this journey and have made these years at Georgia Tech so special.

I cannot express greatly enough my appreciation to my advisor, Dr. Reginald DesRoches. He has offered the knowledge, support, opportunity, mentoring, and friendship which have made my graduate experience so fruitful. I attribute much of my positive experience in graduate school and foundation for the future to him.

I would certainly like to extend my gratitude to my thesis committee members: Drs. Bruce Ellingwood, Barry Goodno, Glenn Rix, and Ann Bostrom. Their insight, critical assessment, and guidance throughout the course of my graduate studies is greatly appreciated–not to mention the essential courses that they offered in order for me to have a strong base to pursue the topics in my dissertation work. I would also like to acknowledge Drs. Laurence Jacobs and Kimberly Kurtis for their advice and encouragement of my academic career.

Georgia Tech has provided an excellent educational experience, and I would like to acknowledge the support I have received for pursuing a graduate degree at this Institution through the National Science Foundation and Earthquake Engineering Research Institute.

Additionally, the Mid-America Earthquake Center has sponsored this research project and provided numerous unique opportunities throughout my graduate program.

I have been fortunate to be surrounded by an excellent group of graduate students in the SEMM group who have offered technical knowledge, lively discussions, and friendship. Thanks to my wonderful officemates from 325 Mason: Jason, Brad, Laura, Monique, Masahiro, and Ben. I would like to extend a special note of appreciation to Bryant for his advice and willingness to endlessly discuss bridge fragility among other exciting topics. Thank you to others I have had the pleasure of being associated with in the Department, such as Leonardo, Matthew, Bassem, Murat, Emily, Junwon, Takao, and Parisa. I sincerely appreciate my wonderful friends outside Tech who continue to be so thoughtful and encouraging, and always provide an outlet for entertainment.

I am truly grateful for the unconditional support of my family, without which I would likely not be here today. My parents have offered endless support, confidence in me, wise advice, and love. I extend my sincere appreciation and love to them. Finally, I would like to thank my husband, Jonathan. His support, selflessness, groundedness, encouragement, and enduring love have meant the world to me throughout this process and always.

TABLE OF CONTENTS

LIST OF TABLES

LIST OF FIGURES

SUMMARY

While the 1971 San Fernando earthquake heightened the awareness of the seismic vulnerabilities of highway bridges and motivated seismic retrofit programs in California, seismic design considerations were not made in regions of moderate seismicity such as the Central and Southeastern United States (CSUS) until after 1990. This has resulted in an inventory populated with highly vulnerable bridges for which states in the CSUS are now beginning to evaluate deficiencies and undertake seismic retrofit activities. There has been limited research to date to evaluate viable retrofit strategies for the bridges common in the region or support decision making on seismic upgrade. However, an emerging tool in seismic risk assessment, bridge fragility curves, provides valuable support for risk mitigation activities.

There is an urgent need for the development of fragility curves for retrofitted bridges, particularly for the CSUS. These fragility curves are conditional probability statements of potential levels of damage over a range of earthquake intensities. The development of reliable retrofitted bridge fragility curves would allow for assessment of the effects of various retrofit measures on the performance of different CSUS bridge types. Therefore, a primary objective of this work is to develop a methodology for fragility assessment of bridge retrofit, in order to support seismic risk mitigation efforts in the region.

A range of potential retrofit measures for typical classes of bridges in the CSUS are evaluated ranging from response modification to capacity enhancement or partial replacement. This is accomplished by developing detailed analytical models of the retrofitted bridges and subjecting them to suites of synthetic ground motions appropriate for the region of interest. The impact of retrofit on the demand placed on various critical components in the bridge is captured through the development of joint probabilistic seismic demand models (PSDMs). The potential for meeting different measures of performance is assessed incorporating both the uncertainty in the seismic demand and capacity in order to develop the fragility curves. Appropriate levels of uncertainty are evaluated and propagated through the analysis. The fragility curves reveal the impact of retrofit not only on component vulnerability, but on bridge system performance. The results indicate that different retrofits become more effective depending upon the bridge type and damage level of interest. Frameworks for the use of the fragility curves in retrofit selection are highlighted including performance-based retrofit and cost-benefit analyses. These types of assessments illustrate the vital role the retrofitted bridge fragility curves developed as a part of this work play in supporting risk mitigation efforts for transportation networks.

CHAPTER I

INTRODUCTION

1.1 Problem Description

Earthquake damage in recent decades has revealed that bridges are one of the most vulnerable components of the transportation system. Damage to bridges can cause significant disruption to the transportation network, posing a threat to emergency response and recovery as well as resulting in severe economic losses for a region. The transportation system of the Central and Southeastern United States (CSUS) is particularly at risk because of the history of large but infrequent events and the fact that many of its bridges were designed with little or no seismic consideration. Previous studies have estimated that a major earthquake in the CSUS could result in economic losses in excess of $200 billion (Abrams, 2003).

In an effort to mitigate potential damage, bridges with inadequate seismic detailing may be seismically retrofit. Following the 1971 San Fernando Earthquake, the California Department of Transportation (Caltrans) implemented a state-wide bridge retrofit program to systematically address the deficiencies of existing structures (Mellon and Post, 1999). The state's current Seismic Safety Retrofit Program, established in 1989, involves over 2,200 bridges at an estimated construction cost of $8 billion (Caltrans, 2003). Other West-Coast states such as Oregon and Washington have established similar programs.

In recent years, awareness of the potential seismic hazard in the CSUS has increased, and has precipitated seismic retrofit activities and evaluations in some CSUS states. However, this has led to a question of the viability of different retrofits for bridges common to this part of the country, and prompted concern over the cost of the large number of bridges that may require retrofit. CSUS resources for seismic retrofit are limited, and investment in seismic upgrade must be made efficiently. Little technical support has been offered to date for evaluating the impact of various retrofit measures on the seismic performance of bridges in the region. There is a strong need for a comparative assessment of the viability of various retrofit strategies for typical CSUS bridges.

One approach to facilitate decision making for seismic bridge retrofit in the CSUS is the use of bridge fragility curves. Bridge fragility curves are conditional probability statements providing an enhanced understanding of expected seismic bridge performance. They indicate the probability of the bridge being damaged beyond a given state for various levels of ground motion intensity. The availability of reliable retrofitted bridge fragility curves would allow for assessment of the effects of various retrofit measures on the performance of different CSUS bridge types. Such tools could offer support for identifying retrofit measures for bridges common to the region, and provide essential tools for decision-support frameworks such as performance-based retrofit and cost-benefit analyses. An emerging approach for evaluating the seismic risk to regions or infrastructure systems, such as transportation networks, is the seismic risk assessment (SRA) methodology. Fragility curves are essential inputs to this framework and coupling retrofitted bridge fragility curves with the framework would support effective investment in seismic risk mitigation rooted in evaluating retrofit impact on regional and system performance.

1.2 Objectives and Scope

This research aims to provide enhanced understanding of the impact of various retrofit strategies on the seismic performance of typical CSUS bridges through the use of probabilistic methods. A primary objective is to develop an approach for vulnerability assessment of retrofitted bridges, in order to provide the first set of fragility curves for general classes of retrofitted bridges. The intention is to provide support for seismic risk mitigation efforts for transportation networks by offering insight on the relative benefits of different retrofit measures and providing essential tools for decision support frameworks. In order to achieve these goals, care is taken in evaluating the effect of retrofit and providing appropriate details on the fragility methodology for development of reliable fragility curves for classes of retrofitted bridges.

The associated research tasks include the following:

- Evaluation of the viable retrofit measures performed in the Central and Southeastern United States. Identification of potential measures to be incorporated in the study and vulnerable bridge types to be examined.
- Development of detailed 3-d analytical models of the retrofitted bridges.
- Deterministic analysis of the classes of typical bridges in their as-built and retrofitted conditions. This allows for determination of likely critical components and the effect of retrofits on the various component responses.

- Identification and probabilistic modeling of potentially uncertain modeling parameters. Screening of the most significant modeling parameters for incorporation in the simulation for fragility assessment.

- Determination of damage states and limit state capacities for bridges. Assessment of bridge damage-functionality survey results for recommendation of damage states and refinement of limit states for bridge components such that they have a consistent implication of allowable traffic capacity.

- Development of component and systems level fragility curves for classes of retrofitted bridges. Comparison of the relative performance of bridge components and systems under various retrofit measures.

- Exploration of the sensitivity of the fragility estimates to various levels of uncertainty treatment, including sources stemming from ground motion, geometric, and analytical modeling parameters.

- Illustration of the use of retrofitted bridge fragility curves for risk mitigation activities.

1.3 Dissertation Outline

The content of the dissertation is organized into the following chapters:

- **Chapter 2** provides an overview of seismic retrofit of bridges in the Central and Southeastern US (CSUS), including the current state of practice and research studies

on retrofit of bridges common to the region, as well as a summary on previous research in the area of bridge fragility. Potential methodologies and studies focused on the development of fragility curves for retrofitted bridges are emphasized.

- **Chapter 3** presents the five retrofit measures considered as a part of this work. The Chapter highlights the overall retrofit objective, past experimental testing, typical details, and analytical modeling of the retrofits.

- **Chapter 4** provides a deterministic performance evaluation of classes of retrofitted bridges. It presents the four typical classes of CSUS bridges examined in this study along with the analytical modeling approach, response characterization of the retrofitted bridges, and a summary of the influence of retrofit on the seismic response of the different retrofitted bridges.

- **Chapter 5** assesses the sensitivity of the response of the retrofitted bridges to modeling parameter uncertainty, by evaluating the significance of various modeling parameters through a screening study.

- **Chapter 6** presents a study to evaluate the relationship between bridge damage and functionality which will be used to refine the limit state capacities for forthcoming probabilistic assessment of bridge performance.

- **Chapter 7** provides the methodology for fragility curve development for general classes of retrofitted bridges. The Chapter discusses the details for the approach including ground motions used, joint probabilistic seismic demand models, capacity estimates, component fragility curves, and the development of retrofitted bridge

system fragility curves. The sensitivity of the system fragilities to various levels of uncertainty treatment is examined. The resulting fragility curves developed for a range of CSUS bridge types and retrofit measures are presented.

- **Chapter 8** offers frameworks for applying the retrofitted bridge fragility curves to support seismic risk mitigation efforts. This includes supporting implementation through simplified fragility parameters and modification factors, supporting retrofit decision making through a framework for performance-based retrofit assessment or cost-benefit analyses, as well as the use of such fragilities in a regional seismic risk assessment.

- **Chapter 9** summarizes the research and draws conclusions, as well as discusses the anticipated impacts of the work and suggestions for future research.

CHAPTER II

OVERVIEW OF BRIDGE RETROFIT AND FRAGILITY STUDIES

Following the 1971 San Fernando Earthquake, the California Department of Transportation implemented a state-wide bridge retrofit program to systematically address the deficiencies of existing structures (Mellon and Post, 1999). Damage from past events has provided evidence of the vulnerability of common bridge types, performance of retrofits, and need for future retrofit (Cooper et al., 1994; Seible and Priestley, 1999). Multi-frame concrete bridges that have short seat widths have been identified for restrainer retrofit, and those with squat columns or pre-1971 designed columns with inadequate transverse reinforcement and lap splices have been targeted for column jacketing. However, there have been few investigations of the most appropriate potential retrofits for typical Central and Southeastern US (CSUS) bridges. The region has a significantly different bridge stock than the West Coast, with a large percentage of the inventory consisting of multi-span simply supported, multi-span continuous, and simply supported steel and concrete girder bridges (Nielson, 2005b). An evaluation of current retrofit practice in CSUS, studies on retrofit of CSUS-type bridges, and the state-of-the art in bridge fragility curve development help to illustrate the state of the practice and needs in the area of bridge retrofit evaluation for the CSUS.

2.1 Seismic Retrofit of CSUS Bridges

2.1.1 Seismic Retrofit Practice in the CSUS

The majority of bridges in the Central and Southeastern United States (CSUS) were designed with little or no seismic consideration. Typical bridge deficiencies have been identified as inadequately detailed columns with limited ductility capacity and low shear strength, brittle steel bearings, short seat widths, and inadequately reinforced pile caps among others (DesRoches et al., 2004). Common challenges for bridge assessment in low-to-moderate seismic zones such as the CSUS have been identified by DesRoches et al. (2000). These include (1) the infrequent nature of the major or moderate earthquakes leading to little understanding of large earthquake characteristics; (2) the lack of adequate seismic design in much of the bridge inventory; (3) the vague understanding of the earthquake source and mechanism; and (4) the potential for a more wide-spread damage area based on the attenuation in the CSUS. In recent years, the community has begun to recognize the potential vulnerability of these bridges and of new bridges in the region. Recent changes in the design recommendations have included the recommendation of a design earthquake that has a 2% probability of exceedance in 50 years (an earthquake with a mean recurrence interval of 2475 years) in the FEMA 302 *NEHRP Recommended Provisions for Development of Seismic Regulations for New Buildings and Other Structures* (FEMA, 1997). States in the CSUS region have begun to assess the vulnerability of their inventory and some have begun to undertake seismic retrofit activities. Many states in this region are challenged with investing limited resources available for seismic upgrade.

The Central US Earthquake Consortium (CUSEC) has collaborated with the US Department of Transportation to prepare a monograph that helps to increase the awareness of the earthquake risk to transportation systems in the Central US (CUSEC, 2000), focusing on the vulnerable regions of Arkansas, Illinois, Indiana, Kentucky, Mississippi, Missouri, and Tennessee. They discuss and encourage mitigation efforts, including development or adoption of sufficient design criteria, and bridge retrofit programs that implement technologies that are new and innovative in the CUS community. Examples of the current state of practice in seismic retrofit of bridges in the Central and Southeastern US is presented below. This includes protection of a number of different bridge components using a range of retrofit measures and approaches.

2.1.1.1 Column Retrofit

States in the CSUS region have used a number of different approaches to target the improved performance of non-seismically detailed columns. A vast majority of the columns in typical CSUS bridges are concrete columns, for which a variety of retrofit measures have been proposed. While full column replacement is sometimes an option, states often adopt less costly and invasive alternatives. The general retrofit strategy for these columns often includes some sort of encasement in order to improve the shear or flexural strength, flexural confinement and ductility capacity, or lap splice performance.

Steel jackets are a common approach to retrofitting deficient columns in the CSUS. Partial column casings often target the plastic hinge regions by providing enhanced confinement for increased ductility capacity, or target locations of the lap splices for improved bond transfer. Full height jackets also improve the shear strength of the column. Examples

of a partial height steel jacket in St. Louis, MO and full height column retrofit in Tennessee are shown in Figure 2-1. Over a dozen bridges in Tennessee have been retrofit with these jackets.

2-1(a): **2-1(b):**

Figure 2-1: Examples of (a) partial height steel jackets in MO and (b) full height steel jackets in TN.

Concrete overlays are often used to provide confinement for enhanced ductility capacity, and less often as measures to increase a column's flexural strength since this is not often required or desired. Both longitudinal and transverse reinforcement may be provided in these casings, and in some instances the concrete overlay is used in conjunction with a steel jacket retrofit. The construction of a concrete encasement in Memphis, TN is shown in Figure 2-2(a) and a completed partial height encasement in Illinois is shown in Figure 2-2(b).

Other column retrofit measures which have been performed in some states but are less common on average include cable column wraps (or external prestressing),and jacketing

2-2(a):

2-2(b):

Figure 2-2: Concrete column overlay (a) during construction in TN and (b) as a partial encasement in IL.

by fiber composite wraps, which may be continuous or applied in strips. Examples of these column retrofits performed by the Illinois DOT are shown in Figure 2-3. The main objective in most cases is to provide confinement for the concrete columns.

2.1.1.2 Isolation

Isolation strategies are adopted to limit the forces transferred to deficient substructure elements and as a means to replace existing bearings. While the replacement of existing vulnerable bearings, such as shown in Figure 2-4, with isolation bearings is slightly more intrusive than other measures, several states have employed this retrofit approach. States in the Central and Southeastern US have performed retrofit with a relatively limited number of bearing types. Laminated elastomeric bearings have been used in several states (Figure 2-5(a)). Others have used energy dissipating sliding bearings (Figure 2-5(b)), as well

2-3(a):

2-3(b):

2-3(c):

Figure 2-3: Other column retrofits with (a) cable wraps or (b and c) fiber composites performed in IL.

as lead rubber bearings or friction pendulum bearings, which are found on the Hernando DeSoto Bridge crossing the Mississippi River between Arkansas and Tennessee (2-5(c)).

2-4(a):

2-4(b):

Figure 2-4: Potentially vulnerable existing steel (a) fixed and (b) rocker bearings.

2-5(a):

2-5(b):

2-5(c):

Figure 2-5: Isolation bearings found in the CSUS: (a) laminated elastomeric, (b) sliding, and (c) friction pendulum bearings.

2.1.1.3 Longitudinal Restrainer

Longitudinal restrainers are often implemented at the expansion joints between adjacent decks or at the deck-abutment interface to limit deck displacement and reduce the potential for span unseating. In the CSUS, these restrainers often take the form of cable restrainers. For simply supported bridges, as are typical in the CSUS, cables may be anchored to the girder and then wrapped around the bent cap or anchored directly between the girder and bent cap as shown in Figure 2-6(a). An alternate configuration would be for the cables to be mounted directly between adjacent girders as shown in Figure 2-6(b), however this has been recognized as a less appropriate method for bridges with short seat widths (Keady et al., 2000). Field implementation of a common set of CSUS restrainer cable details is shown in Figure 2-7 for a bridge in TN, where the cables are connected from the girders to the abutment as well as between the girders and bent cap. Over 200 bridges have been retrofit with steel restrainer cables in the state of Tennessee alone, and a number of similar retrofit projects have been performed in other Central and Southeastern US states.

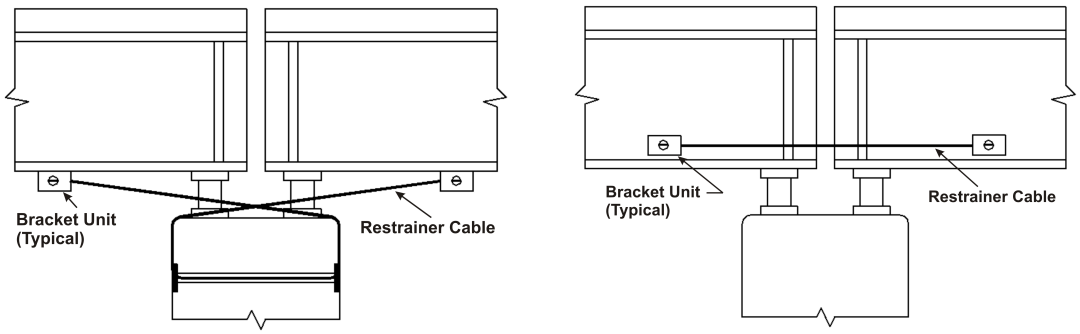

2-6(a): **2-6(b):**

Figure 2-6: Two potential restrainer configurations.

Figure 2-7: Common CSUS restrainer cable retrofit details as performed in TN.

Another type of restrainer is high strength bar restrainers, which are often stiffer yet more ductile than the cable restrainers. These have been used less frequently in the CSUS yet examples exist in different arrangements in IL and MO (Figure 2-8).

2-8(a):

2-8(b):

2-8(c):

Figure 2-8: High strength bar restrainers in (a) MO and (b and c) IL.

2.1.1.4 Other Longitudinal Restraint and Response Modification Devices

Other devices that modify the longitudinal response of bridges have been employed in bridge retrofit, often to either prevent excessive movement of the superstructure or to provide energy dissipation. A relatively simple alternative method to restrainer cables is the use of stoppers, or bumper blocks. An example is shown in Figure 2-9(a). As previously shown in Figure 2-7, the bumpers may be used in conjunction with restrainer bars. Shock transmission units (STUs) have also been used to modify the longitudinal response, as shown in the Poplar Street Bridge in MO (Figure 2-9(b)). These devices allow for slow motion, such as thermal movements, yet rigidly restrict rapid motion, such as that induced by earthquake loading. These retrofits all serve as displacement limitation devices and provide load transfer at the location of implementation.

2-9(a):

2-9(b):

Figure 2-9: Retrofits performed in MO using (a) bumpers and (b) shock transmission units.

2.1.1.5 Shear Keys and Transverse Restraint

Transverse restraint of the superstructure is often provided to keep the superstructure from sliding off its supports should the bearings fail in the transverse direction, and is recommended for common CSUS conditions such as when high steel rocker bearings are used, or limited transverse seat is available (FHWA, 2006). Shear keys often take the form of reinforced concrete blocks doweled into the bent beam, which have been used in TN and MO among other states (Figure 2-10(a)). In some cases they are added as keeper brackets to the bearing assembly, as shown in Figure 2-10(b), and less often as transverse steel bumper assemblies.

2.1.1.6 Seat Extenders and Catcher Blocks

Since many of the bridges in the CSUS have relatively short seat widths and unseating is a concern, another popular retrofit measure is the use of seat extenders. Rather than alter

2-10(a): **2-10(b):**

Figure 2-10: Transverse restraint provided by (a) concrete shear keys and (b) keeper brackets.

the response of the bridge in the longitudinal direction, they serve as a failsafe to deck collapse by providing an extended support length. Most commonly, the seat length for a simply supported bridge may be extended at the abutment or bent through the addition of a concrete corbel or steel bracket as illustrated in Figure 2-11. Tennessee has performed a number of retrofits with seat extenders in bridges crossing I-40, as shown in Figure 2-12(a). Figure 2-12(a) shows less conventional seat extender details used on US40 in Missouri. Catcher blocks perform a similar function of supporting the span given it has fallen off of its bearing or the bearing has failed, and have also been used in MO. However, catcher blocks are elevated to a height just under the girders and are often used either when the deck is supported by tall bearings, and/or there is not sufficient room to anchor seat extenders as in Figure 2-12(c).

2.1.1.7 Footing Retrofit

The foundations of most CSUS bridges were not designed considering seismic loading and may be susceptible to damage, yet the *Seismic Retrofit Manual* (FHWA, 2006) indicates

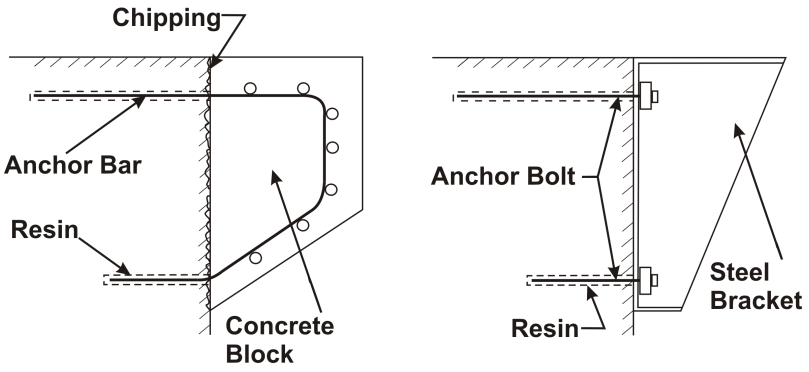

Figure 2-11: Corbel and bracket seat extender details.

2-12(a): **2-12(b):** **2-12(c):**

Figure 2-12: (a) Traditional seat extender retrofit in TN, (b) beam extender in MO, and (c) catcher block.

that collapse due to structural failure of footings and foundations is rare. Additionally, such retrofits are expensive and disruptive. As a result, relatively few foundation retrofits have been performed in the CSUS. Those performed have included footing strengthening by adding pile cap reinforcement and concrete overlay (Gupta and Hartnagel, 2003) in TN, or extending the foundations and adding piles (Anderson and Gruendler, 1995) in IL.

2.1.1.8 Bent Cap Retrofit

Bent caps which serve to transfer loading from the bearings to the columns may be deficiently reinforced for either shear or flexural loading. The general approach to bent cap retrofit is to enhance the shear or flexural strength to sufficient levels such that the columns form plastic hinges before damage occurs in the bent beam (Priestley et al., 1996). Both IL and MO have retrofitted bridge bent beams (or bent caps). The most common measure includes providing pre-stressing of the beam through external tendons, as shown in Figure 2-13(a) (MO), where the pre-stressing essentially enhances the strength of the bent cap by providing an axial compression force on the beam. Other retrofit approaches include providing external shear reinforcement, as has been performed in IL (Figure 2-13(b)), adding reinforced concrete bolsters to the existing cap beam face to increase the level of shear and flexural reinforcement, or completely encasing and reinforcing the beam (Figure 2-13(c) in TN).

2.1.2 Analytical and Experimental Studies on Retrofit of CSUS Type Bridges

While there have been many studies that evaluate the performance of various bridge components following retrofit, few have investigated the response of the CSUS-type bridge

2-13(a):

2-13(b):

2-13(c):

Figure 2-13: Bent cap retrofits with (a) pre-stressing in MO, (b) shear reinforcement in IL, and (c) reinforced concrete encasement.

systems and impact of retrofit on various components within the system. In general, studies often evaluate the efficacy of retrofits for other types of bridges, such as multi-frame concrete bridges, or the impact of retrofit on improving a particular bridge component response. These approaches include strengthening, such as the use of steel restrainer cables (Saiidi et al., 1996; Selna et al., 1989); capacity improvement, for example steel jacketing of columns (Chai et al., 1991; Zhang et al., 1999); force limitation or response modification, such as implementing an isolation strategy (Ghobarah and Ali, 1988; Kelly, 1998); and other bridge retrofit approaches (Priestley et al., 1996). However, there have been relatively few studies that have explored the impact of various retrofit measures on the seismic response of common classes of bridges in the Central and Southeastern US, such as multi-span steel or concrete girder bridges, which have been revealed to have potentially significant seismic vulnerabilities. Those that have often focus on a particular bridge's response under a given retrofit, rather than aiming to evaluate a class of bridges and compare the effectiveness of various potential measures.

DesRoches et al. (2003) performed full-scale tests of cable restrainers in a simply supported steel girder bridge and provided cable connection recommendations for these bridge types that were subsequently implemented in the CSUS. Saiidi et al. (2001) evaluated different restrainer design methods for multi-span simply supported (MSSS) bridges using two- and five-span steel girder bridges. They concluded that while the use of restrainers tended to decrease the critical relative displacements, the reduction was not necessarily proportional to the number of restrainers used, and that the bearing strength has a significant impact on the response. A multi-span simply supported steel girder bridge was analyzed by Caner et al. (2002) under link slab retrofit (a provision for continuity between decks

that may serve as an alternative way of reducing span separation or unseating). They found that the retrofit improved the seismic performance by reducing relative displacements or potential unseating and noted that abutment forces were increased.

Ductile end-diaphragm systems were investigated as retrofits which help to provide energy dissipation and limit the forces transferred to vulnerable substructure elements in work by Zahrai and Bruneau (1999). They found that the retrofits showed promise, particularly for bridges having long spans and few steel girders. Maleki (2004) considered the effects of side retainers (or keeper plates) on single span bridges with non-seismic elastomeric bearings, and concluded that the gap between the bearings and keeper should be considered in order to avoid underestimating the forces transferred to the substructure. Dicleli and Mansour (2003) investigated the use of friction pendulum bearings (FPB) vs. a footing retrofit strategy a multi-span continuous concrete girder bridge in IL and compared the demand on the abutments, piers, and bearings, and compared the costs of the two bridge retrofits. Other researchers (Jangid, 2004; Liao et al., 2004; Yan et al., 2004) have analytically evaluated the effect of isolation on column response and deck displacement for specific bridges common to the CSUS, and indicated the potential for pounding between adjacent decks.

Extensive testing of single columns with steel jackets have been performed by Priestley et al. (1994a,b) and Chai et al. (1991). Zhang et al. (1999) has analytically evaluated various combinations of column jacketing of a multi-column bent, however the response of other bridge components was not modeled.

These studies have provided insight into the potential viable retrofit strategies for typical CSUS bridges. However, the number of studies addressing retrofit of CSUS bridges classes has been rather limited and they do not provide adequate relative comparison of

retrofit of CSUS bridges. The relative impacts of a range of different retrofit measures on the seismic performance of typical CSUS bridges has not been addressed. Moreover, probabilistic analyses of CSUS retrofit techniques have not been addressed. This is critical for assessing the potential of various retrofit measures to reduce likely damage in the bridges, and capturing the uncertainties associated with such a performance evaluation.

2.2 Fragility Curve Development and Application to Retrofitted Bridges

Fragility curves are a key input into a seismic risk assessment of transportation networks that allow an evaluation of the potential seismic performance of bridges in the system. The relative vulnerability of bridges in their as-built and retrofitted states may be presented through a comparison of their vulnerability functions or so-called fragility curves.

Fragility curves state the probability of entering a damage state given an input ground motion intensity parameter. This conditional probability can be expressed as:

$$Fragility = P[LS|IM = y] \tag{2.1}$$

where LS is the limit state or level of damage to the engineered system or component, IM is the ground motion intensity measure and y is the realized condition of the ground motion intensity measure, often expressed in terms of peak ground acceleration or spectral acceleration at the fundamental period. This fragility function represents the ability of an engineered system or component to withstand a specified event (Tekie and Ellingwood, 2003). Figure 2-14 depicts the continuous form of a set of fragility curves and their interpretation at a particular ground motion intensity.

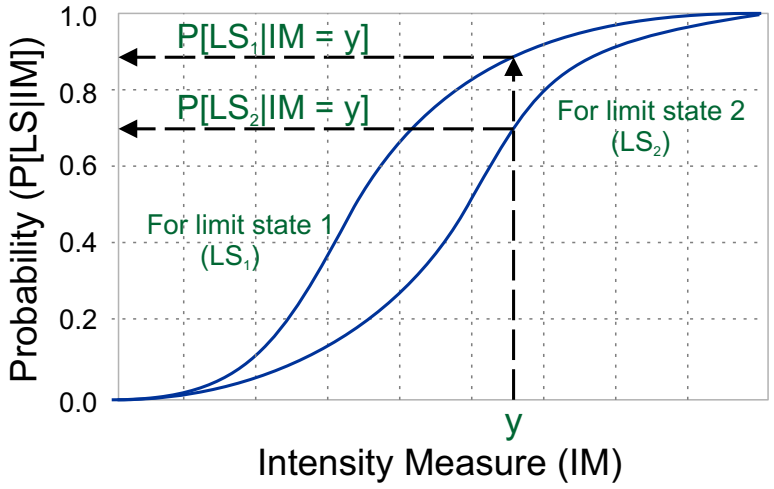

Figure 2-14: Fragility curve depiction

The relationship between bridge damage and ground motion intensity has been investigated for bridge systems since the 1980s and early 1990s, and an array of approaches and methodologies have been employed. Some retrofit measures may tend to alter this damage-ground motion intensity relationship. The potential impact of retrofit on the failure probability of a bridge is illustrated in Figure 2-15. Only in recent years have the first studies of probabilistic treatment for estimating damage to bridges in their retrofitted conditions been initiated, and the scope has been very limited. The following subsections detail the current state-of-the-art for development of fragility curves for highway bridges, the existing applications to retrofitted bridges, and the advantages or shortcomings for potential application of the methodologies to retrofitted bridges in the CSUS.

2.2.1 Expert Based Fragility Curves

The Applied Technology Council (ATC-13) (ATC, 1985) project funded by the Federal Emergency Management Agency in the mid-1980s was a pioneering effort to collect large

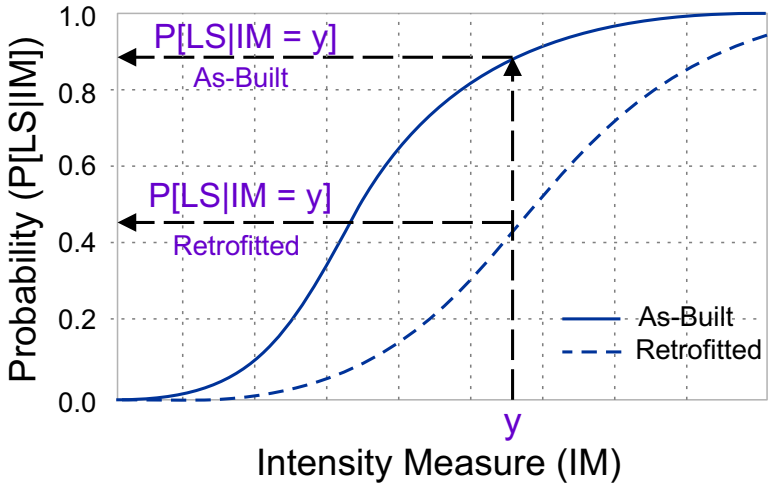

Figure 2-15: Example fragility curve for a retrofitted bridge

amounts of data on earthquake damage to California-type facilities. Due to the limited amount of data available, opinions from experts were solicited in order to estimate the damage to facilities due to earthquakes. A survey was executed following the Delphi method, in which several rounds, or iterations, of questionnaires were distributed. The participants were queried as to the probability of a facility being in a particular damage state for different levels of ground shaking using the Modified Mercalli Intensity scale. Seventy-one experts participated at some point of the questionnaire process. However, only 5 people were bridge experts and offered responses for the expected level of damage for two main classes of California bridges, conventional (less than 152.4 m spans) and major (greater than 152.4 m spans) (ATC, 1985).

Damage probability matrices were presented as a representation of the responses, in which the Beta distribution was used for their development. This data was later presented

in the form of a damage curve in the ATC-25 report (ATC, 1991), which indicated a continuous functional form relating bridge damage to ground motion, as shown in Figure 2-16.

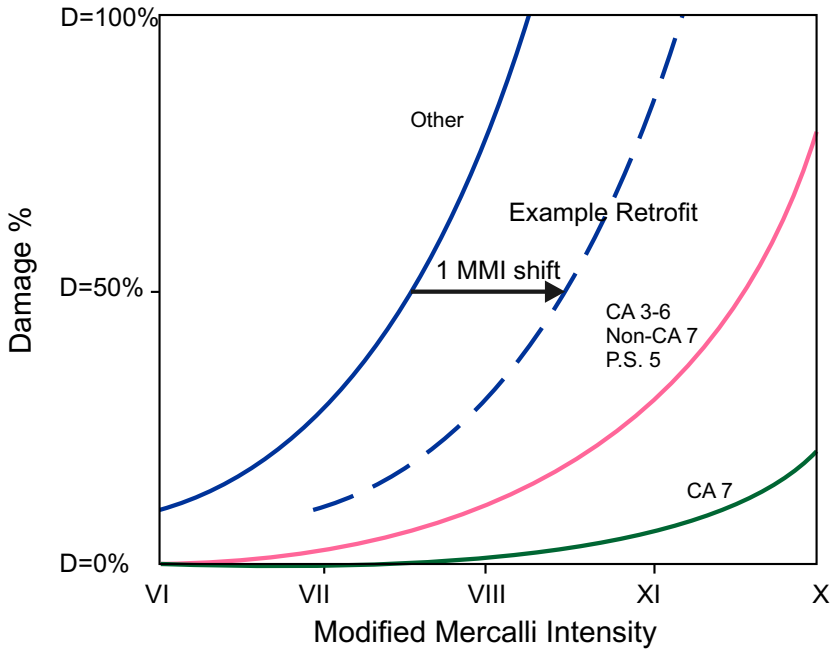

Figure 2-16: Expert-based fragility curves adapted from ATC-25 (ATC, 1991)

There are a number of limitations of the ATC-25 study which have been identified. Some indicate that these approaches are highly subjective, but even more concerning is the low response rate to the questionnaire that was used to develop the relationships. Other limitations include the vast generalization of bridge classes and regional dependence of the damage-motion relationships due to the assumption of California bridge types in the survey. The data collection did not specifically address or separate retrofitted bridges from as-built, as the bridge types were considered to represent a composite of bridges under

standard construction and present conditions (ATC, 1985). Authors of ATC-25 have indicated the need to consider a modified version of the bridge damage curves for facilities that have been upgraded, and in the absence of relevant data they have suggested a single unit MMI intensity shift to account for the anticipated improved performance (ATC, 1991), as indicated in Figure 2-16. Their suggestions highlight the need for further investigation of the effect of retrofit on the fragility of bridges.

2.2.2 Empirical Fragility Curves

Empirical fragility curves are those that offer the expected level of damage given a ground motion intensity based on past damage to bridges from earthquake events. The development of these fragility curves requires the utilization of actual bridge damage data that is often derived from post-earthquake inspection reports, as well as spatial distribution of ground motion information that is often collected from shake maps. Correlation of the two data sets allows for a presentation of the fragility curves for given damage states and bridge types in a region.

A number of researchers have presented methodologies and developed empirical fragility curves as a result of the increased amount of available data from recent earthquake events. Basoz et al. (1999) and Basoz and Kiremidjian (1999) have developed empirical fragility curves for bridges damaged in the Northridge (M_w=6.7) and Loma Prieta (M_w=6.9) earthquakes. Shinozuka et al. (2000, 2003) have presented empirical fragility curves based on Caltrans report data for the Northridge earthquake damage, and for the Kobe (M_w=6.9) earthquake from the Hanshin Expressway Public Corporation's bridge column damage data

(Figure 2-17). Yamazaki et al. (1999) have also developed empirical fragility curves for expressway bridges in Japan based on Kobe earthquake damage data. These methodologies are all quite similar in the approach of binning observed damage into ground motion intensity ranges, often peak ground acceleration, and assigning probabilities to the different damage levels. These are often referred to as damage probability matrices (Basoz and Kiremidjian, 1999). However, the subsequent fragility curve development varies slightly. Shinozuka (Shinozuka et al., 2000, 2003) uses the maximum likelihood method to derive the parameters of a lognormal distribution, Yamazaki et al. (1999) uses the least squares method for deriving lognormal parameters, and Basoz and Kiremidjian (1999) use logistic regression analysis for fitting curves to the data.

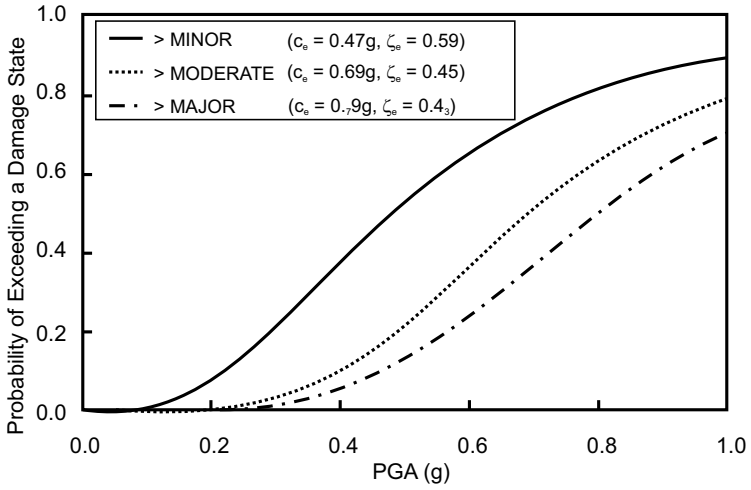

Figure 2-17: Empirical fragility curves based on bridge column damage data from Kobe (Shinozuka et al., 2003)

As a result of the limited available empirical data, fragility curves for bridges in their retrofitted conditions have not been presented in these studies. Basoz et al. note that only nine of the 233 damaged bridges in the Northridge earthquake had been retrofitted, with two sustaining major damage and seven sustaining minor damage (Basoz et al., 1999). A major limitation of this method, even for bridges in their un-retrofitted condition has been the lack of sufficient damage data for different bridge types and levels of damage, which has resulted in several groups of bridges without derived curves (Basoz and Kiremidjian, 1999). Alternatively, bridges from different classes are grouped together which poses a problem with homogeneity of the data and reduces the reliability of the fragility curves. This highlights a major shortcoming of applying such a method to typical CSUS bridges as there has been no damage from earthquakes in this region or for these bridge types, and underscores the necessity of an alternate approach for the development of fragility curves for bridges in their retrofitted condition.

2.2.3 Analytical Fragility Curves

In the absence of adequate empirical data, fragility curves have been developed through a number of analytical methods. Recalling that a fragility curve offers the probability of meeting or exceeding a level of damage given an input ground motion intensity parameter, we observe that the level of damage (damage state) can be related to the structural capacity and that the ground motion intensity relates to the structural demand. Thus an appropriate model for assessing the fragility of a structural system, such as a bridge, is to determine the probability that the structural demand exceeds the structural capacity, as shown in Equation 2.2

$$P_f = P\left[\frac{D}{C} \geq 1\right] \tag{2.2}$$

where P_f is the probability of meeting or exceeding a specific damage state, D is the structural demand and C is the structural capacity.

A fragility is often modeled by a lognormal cumulative distribution function where the structural demand and capacity are assumed to be lognormally or normally distributed (Hwang and Jaw, 1990). Thus a closed form solution for the fragility may be presented as given in Equation 2.3 (Melchers, 1999)

$$P_f = \Phi\left(\frac{\ln S_D/S_C}{\sqrt{\beta_D^2 + \beta_C^2}}\right) \tag{2.3}$$

where $\Phi[\cdot]$ is the standard normal probability integral, S_C is the median value of the structural capacity, β_C is its associated logarithmic standard deviation of structural capacity, S_D is the seismic demand, and β_D is the associated logarithmic standard deviation for the demand.

Several methods have been used to evaluate the structural capacity and demand, shown above as necessary quantities for analytical fragility curve development. These methods cover a range of levels of complexity and computational intensity. An elastic spectral method has been used by Jernigan and Hwang (2002) and by Hwang et al. (2000) to develop fragility curves for bridges in Memphis. Specifically, the seismic demand was determined through elastic spectral analysis, capacities of components were determined according to the FHWA 1995 edition of the *Seismic Retrofitting Manual for Highway Bridges* (FHWA,

1995), and damage states were determined by evaluating the Capacity/Demand (C/D) ratio. An alternate approach has been to use non-linear static methods, often referred to as capacity spectrum methods. This method has been utilized to develop fragility curves by Mander and Basoz (1999), Dutta and Mander (1998), Shinozuka et al. (2000), and Mander (1999). Though the application has been to different bridge types or with varying levels of information on bridge characteristics, they followed a similar methodology that uses the intersection of a capacity spectrum found through nonlinear static pushover analysis, and a demand spectrum found through reduction of the elastic response spectrum.

The most rigorous method for developing analytical fragility curves for bridges is through the utilization of non-linear time history analysis (THA) for determining the seismic demand. This method has been identified as the most time consuming, yet most reliable analytical method (Shinozuka et al., 2000). The non-linear THA method has been developed and adopted in various forms for bridge fragility assessment by Hwang and Huo (1998), Shinozuka et al. (2000), Hwang et al. (2000), Mackie (2004), Karim and Yamazaki (2003), Elnashai et al. (2004), and Choi et al. (2004). While there are some differences in methodology, the general procedure for developing analytical fragility curves by use of non-linear time history analysis is illustrated in Figure 2-18.

The initial step is to select a suite of ground motions representative of the region of interest. The ability of this suite to capture such inherent uncertainties as the earthquake source, wave propagation, and soil conditions dictates the ability of the fragility curve development procedure to propagate these aleatoric uncertainties. In regions with recorded strong ground motion, such as Japan, Greece, or California, earthquake ground motion

records from past events have been used, and in some cases scaled to various levels of excitation when employed in an incremental dynamic analysis (Elnashai et al., 2004; Karim and Yamazaki, 2003; Mackie and Stojadinovic, 2003). In regions of moderate seismicity, such as the Central and Southeast US, there may likely be little or no available strong ground motion records, so synthetic ground motions are often adopted. Hwang and Huo developed 50 histories for each of eight combinations of earthquake magnitude and epicentral distance based on their methodology for considering seismic source, path attenuation, and local soil condition (Hwang and Huo, 1994). Shinozuka et al. (2000) utilized these time histories in developing fragility curves for Memphis, and Choi et al. (2004) used them for developing fragility curves for the Central and Southeastern US. Wen and Wu (2001) have also simulated ground motions for three cities in mid-America for seismic performance assessment of structures, such that the median of the response spectra for the suite match the uniform hazard response spectra for 10% and 2% probability of exceedance in 50 years. More recently, Rix and Fernandez (2004) have developed scenario earthquake ground motions for Memphis for various earthquake magnitudes and hypocentral distances in which the nonlinear site response is considered. These suites will be discussed in further detail in Chapter 4.

Once an appropriate suite of ground motions is selected, a base bridge model must be developed and may be sampled. The probabilistic sampling of the bridge model allows for consideration of uncertainty in the structural characteristics of the bridge, such as material or geometric properties. Uncertainty in concrete compressive strength and in yield strength of steel have been common considerations for contributors to uncertainty due to material

properties. In developing fragility curves for classes of bridges, Choi et al. (2004) considered the uncertainty due to the size of gap between bridge decks , and Nielson (2005a) considered the effect of column height and span length. The set of nominally identical but statistically different bridge samples is paired with the earthquake ground motion set, and then a non-linear time history analysis is performed for each earthquake-bridge sample. Maximum responses for critical components are monitored. Often researchers have monitored only the response of the bridge columns, in terms of a displacement or curvature ductility, or column drift. However, previous research has found other bridge components of typical bridges in the CSUS to also be vulnerable (such as the bearings and abutments), and therefore should be considered (DesRoches et al., 2004). Following the

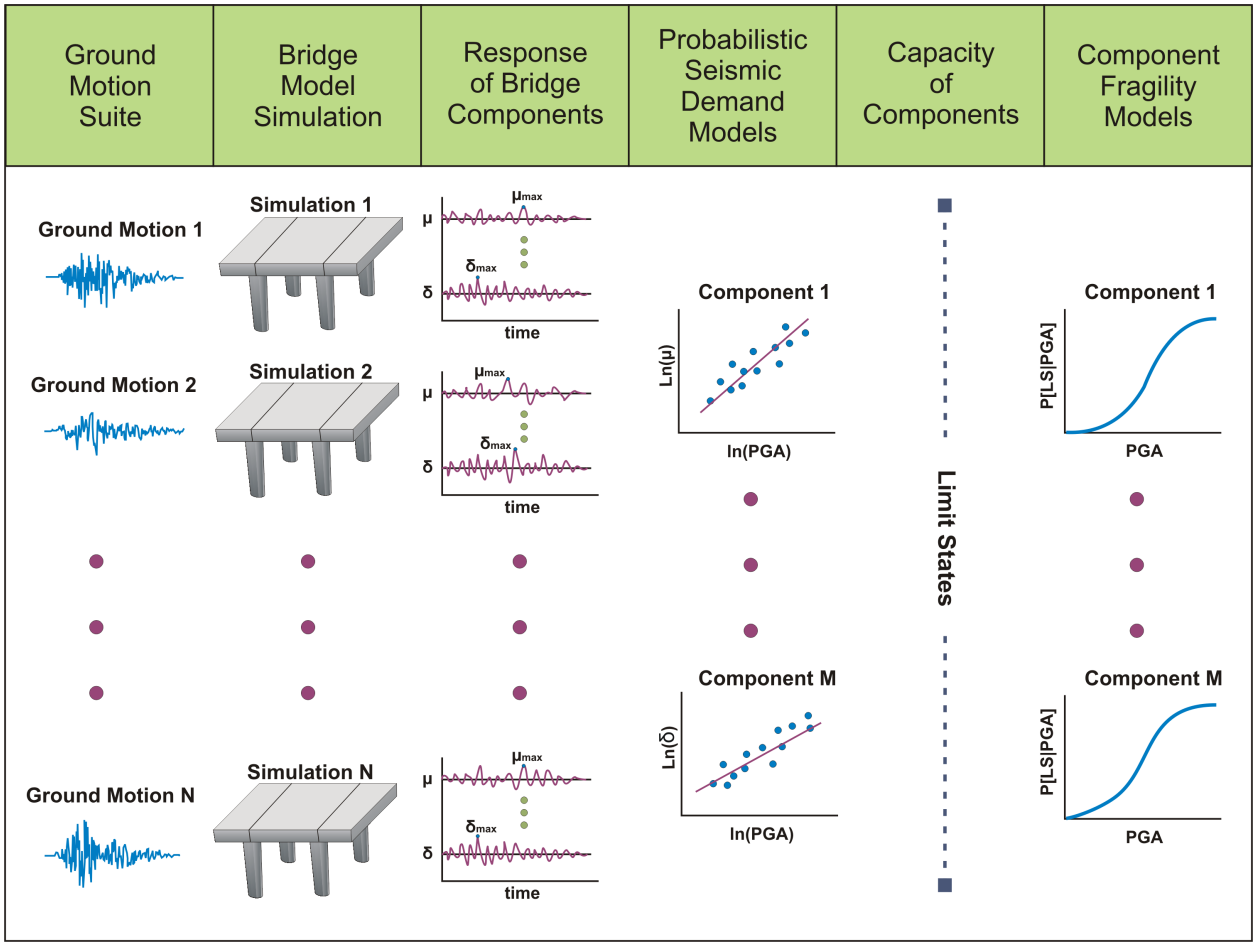

Figure 2-18: Fragility curve development through non-linear time history analysis.

work by Cornell et al. (2002), a linear regression of the logarithms of the intensity measure and response quantity establishes the probabilistic seismic demand model in the form of Equation 2.4.

$$\ln S_D = b \cdot \ln IM + \ln a \tag{2.4}$$

where a and b are the unknown regression coefficients and IM is the chosen ground motion intensity parameter. Another parameter estimation method is the use of the Maximum Likelihood method, as used by Shinozuka et al. (2000) for estimating column demands.

The structural capacity, often referred to as the limit state, of each component must be defined, as is often based on expert judgement, experimental data, or analytical methods. Recent advances and work by Mackie (2004) have recognized the importance of defining limit states in terms of meaningful quantities for bridge performance. They assert that limit states where the load carrying capacity could be associated with remaining traffic capacity should be considered. This gap has also been echoed by Werner and Taylor (2002). Finally, the capacity and demand are coupled assuming a lognormal distribution through the use of Equation 2.3, to determine the probability of failure (meeting or exceeding a level of damage) for the various levels of input ground motion intensity. Choi et al. (2004) have built upon this method by then combining the component fragilities for an overall bridge system fragility curve through first order reliability theory, and Nielson and DesRoches (2007a) have proposed a methodology for directly evaluating the bridge system fragility.

The effect of retrofit on the fragility of bridges has been considered in a very limited number of studies and with a limited scope. Studies have been performed by Kim and

Shinozuka (2004) which consider the effect of steel jacket retrofit on the column's ductility capacity (Figure 2-19). Fragility curves for two sample bridges were developed based solely on the demand placed on the columns, and preliminary results indicated that for some damage states the retrofit improved the performance by up to three times based on the median value PGA. Enhancement factors were proposed based on the ratio of the median value of the fragility curve for the retrofitted column to the un-retrofitted column. The enhancement is meant to be applied to empirical fragility curves in order to obtain the retrofitted fragility curves. While this study was pioneering in its efforts to consider the effect of retrofit on bridge fragility, the number of retrofits, bridge types, and components considered were limited. The development of the enhancement factors was targeted at California-type bridges and developed for two specific bridges. Thus the specific results of the study and enhancement factors derived may not be relevant for CSUS type bridge classes. A major drawback of this methodology for analytical fragility curve development of CSUS-type bridges is its consideration of the column as the only component contributing to the fragility of the bridge system. Shinozuka and colleagues (Kim and Shinozuka, 2003; Shinozuka et al., 2004) have also performed preliminary studies of the effect of restrainers and seat extenders on the bridge fragility using the same methodology. However, given that the details provided indicate that only the vulnerability of the columns are considered, it is unclear whether these curves or methodology capture the full impact of such retrofits.

Khan et al. (2005) have evaluated the fragility of a cable stayed bridge. Work by Cimellaro and Domaneschi (2006) has subsequently evaluated the seismic performance of a specific cable-stayed bridge over the Mississippi river with and without different passive control devices. They assessed the impact on the probability of exceeding different levels of

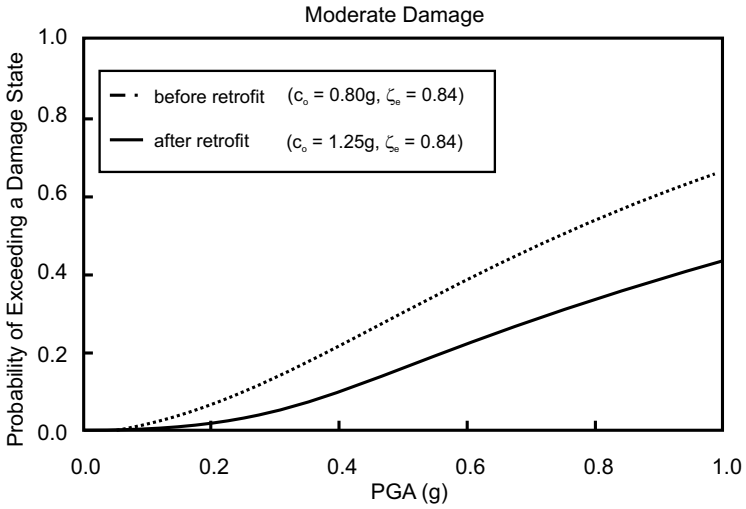

Figure 2-19: Analytical fragility curve for a sample multi-frame concrete bridge with steel jackets by Kim and Shinozuka (2004)

shear and moment in the piers and tension in the cables. While this study offered advances by evaluating the impact of retrofit on multiple components, system fragilities were not derived and the scope of the study was very focused. Thus a critical assessment of the state-of-the art reveals that there is a significant body of work on fragility development to build upon; however, neither the existing retrofitted bridge fragility curves nor methodology for their generation are appropriate for CSUS retrofitted bridges.

2.3 Closure

A review of the current state-of-the-art has provided insight into the current practice and research gaps relating to seismic evaluation of retrofitted bridges in the Central and Southeastern United States. States in the CSUS are in the early stages of developing seismic retrofit programs and assessing potential retrofit for deficient bridges. Due to limited funds,

the resources allocated for bridge retrofit must be carefully spent, and guidance on appropriate retrofit measures for different classes of common bridges would be timely. The impact of retrofit on seismic response, bridge vulnerability, and network performance could support such retrofit decisions and investment in seismic upgrade of CSUS bridges. While there are a number of different retrofit measures that are being considered or implemented in the field, there have not been any systematic evaluations of various retrofit measures for classes of bridges typical to the CSUS. Deterministic evaluation of CSUS bridges retrofit with different measures would provide insight into the impact of retrofit on bridge components' responses and identification of likely critical components. This would enhance the understanding of how various retrofit measures affect the seismic response of typical CSUS bridges, which has not sufficiently been addressed to date.

Fragility curves for a range of retrofit measures applied to CSUS bridges currently do not exist. Such curves would not only provide valuable information regarding the relative vulnerability of as-built and retrofitted bridges and the effectiveness of different retrofit measures, but they also would serve as key components for seismic risk assessments of transportation networks. The methodologies that currently exist for developing retrofitted bridge fragility curves are not appropriate for development of curves for the CSUS. Expert-based methods have been identified as particularly limited in scope and responses, and empirical methods are not an option because sufficient bridge damage data is not available in the CSUS. The analytical methods that have been applied for development of retrofitted bridge fragility curves have often focused solely on the vulnerability of the columns, and have addressed limited sources of uncertainty. Therefore there is a need for development

of an appropriate methodology to analytically derive fragility curves for CSUS retrofitted bridge classes.

CHAPTER III

RETROFIT MEASURES FOR BRIDGES

3.1 Overview

Chapter 2 has revealed the need to assess the performance of typical CSUS bridges under various retrofit measures. The impact of potential bridge retrofits on the performance of typical CSUS type bridges will be evaluated in subsequent chapters to illustrate the effect of retrofit strategies on the response of various bridge components. These results will be the first comprehensive and systematic look at typical CSUS bridges and the effect of different retrofit measures on the component responses. Chapter 2 presented common retrofit measures that are being used or considered by states in the Central and Southeastern US through a review of the current state-of-practice, as well as indicated in the literature to be potentially viable measures for some bridge types that are common in the region. The five retrofit measures that will be evaluated as a part of this study will be detailed below including the overall objective, past experimental testing, typical details, and analytical modeling. The models proposed will be used throughout the remainder of the work. The retrofit measures include steel jackets, elastomeric isolation bearings, restrainer cables, seat extenders, and shear keys.

3.2 Retrofit Measures for CSUS Bridges

3.2.1 Steel Jackets

As indicated in Chapter 2, concrete columns may be encased in steel jackets to help overcome typical CSUS column deficiencies. CSUS columns have been found to be particularly vulnerable due to insufficient lap splices and inadequate transverse reinforcement, leading to limited ductility capacity and low shear strength (DesRoches et al., 2000). Steel jacketing has been used as a retrofit measure to enhance the flexural ductility, shear strength, or performance of lap splices in reinforced concrete bridge columns. Extensive proof of concept testing of steel jacketed bridge columns was performed at the University of California, San Diego in the early 1990s, and Priestley et al. (1996) cite that several hundred bridges in the US had been retrofit with this technology by 1996. A review of the state-of-practice in the CSUS has revealed that this is the most common column retrofit in the CSUS, as well.

Figure 3-1 details a typical cross section of a circular column retrofit by a steel jacket, and the full height configuration which is assumed for this study. The steel jackets are typically A36 steel casings and a space of about 50.8 mm is provided at the ends of the column to prevent the jacket from bearing on adjacent members. This serves to avoid undesirable flexural strength enhancement in which larger shears and moments may be transferred to the footings and cap beams under seismic loading (Priestley et al., 1996). While the effect is not intended, experimental testing by Chai et al. has revealed that the steel jacket increases column stiffness by approximately 10 to 15% for partial height (Chai et al., 1991) and 20 to 40% for full height jackets (Priestley et al., 1996). This could

undesirably impact the imposed forces and performance of other bridge components, and is thus a critical consideration for analytical assessment of this retrofit.

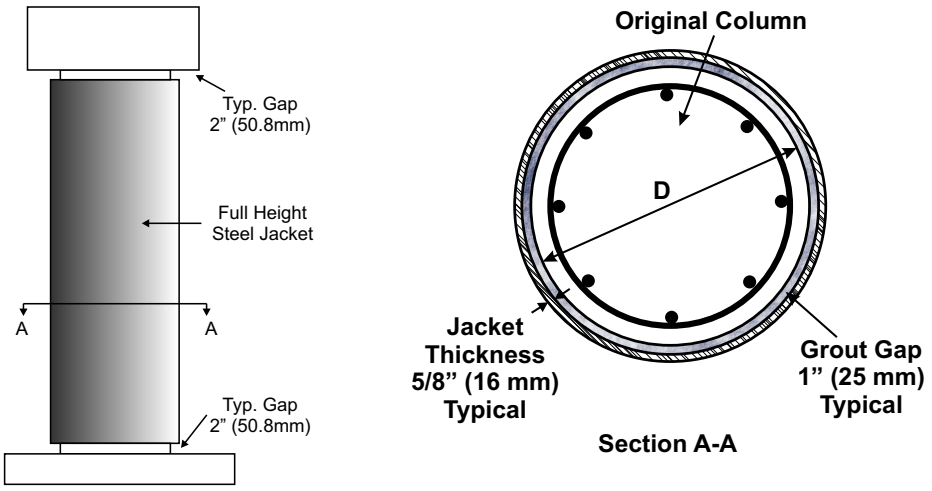

Figure 3-1: Typical steel jacket retrofit details: (a) full height, (b) typical section.

The steel jackets are designed according to the *Seismic Retrofitting Manual for Highway Structures* (FHWA, 1995), which considers the increase in compressive strength and ultimate strain in the concrete due to steel jacket confinement. The minimum recommended shell thickness for steel jackets is 10 mm for handling of the shells during construction. For the typical 91 cm diameter concrete columns found in many CSUS bridges (Nielson, 2005a), the minimum jacket thickness is adequate to provide for confinement of the lap splices and enhanced flexural confinement, with a significant increase in ductility capacity (ultimate curvature ductility demand of over μ_ϕ=30).

The steel jackets are modeled by altering the fiber section for the concrete column. In a fiber model, composite sections are created with fibers representing the unique stress-strain

relationships for the longitudinal steel reinforcement, unconfined concrete, and confined concrete. Thus the concrete fibers now have enhanced compressive strength and ultimate strain due to the confinement caused by jacketing. This effect is illustrated in Figure 3-2, adapted from Priestley et al. (1996). The compressive strength of concrete, $f'cc$, is estimated from Chai et al. (1991) following

$$f'cc = f'c(2.254\sqrt{1 + \frac{7.94f'l}{f'c}} - \frac{2f'l}{f'c} - 1.254) \tag{3.1}$$

where $f'l$ is the radial confining stress in the steel jacket at yield given by

$$f'l = \frac{2f_{yj}t_j}{(D_j - 2t_j)} \tag{3.2}$$

and f_{yj} is the yield stress of the jacket, D_j is the jacket diameter, and t_j is the jacket thickness. The corresponding conservative estimate of ultimate concrete strain capacity, ϵ_{cu}, following the *Seismic Retrofitting Manual for Highway Structures* (FHWA, 1995) is estimated by

$$\epsilon_{cu} = 0.004 + \frac{5.6f_{ys}\epsilon_{su}}{D_j f'cc} \tag{3.3}$$

where f_{ys} is the yield strength of the steel jacket and ϵ_{su} is the ultimate strain of the steel jacket, assumed as 0.10 for A36 steel.

In addition to the above modeling, the elastic modulus of the jacketed column section is increased such that there is a 20 to 40% increase in stiffness of the column based on Priestley's (Priestley et al., 1994a) test results of jacketed columns. In general, while the

analytical model is slightly affected by the use of steel jacketing, the primary impact of the retrofit is to increase the column ductility capacity.

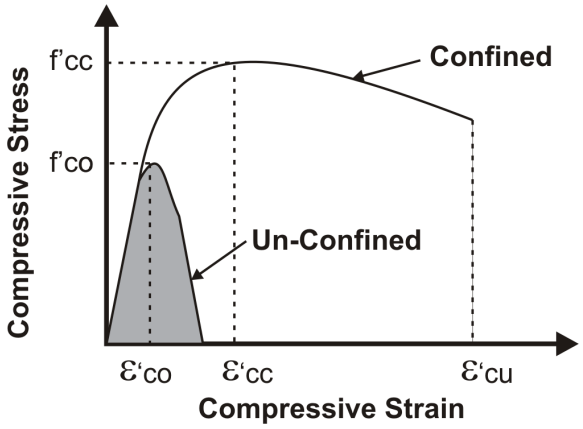

Figure 3-2: Effect of confinement on concrete, adapted from Priestley et al. (1996).

3.2.2 Elastomeric Isolation Bearings

Elastomeric bearings (or laminated-rubber bearings) are a form of isolation bearings that have been used in bridge and building construction for over 35 years (Stanton and Roeder, 1992), and have been used in some CSUS retrofit projects as noted in Chapter 2. The general concept of isolation is to shift the natural period of the structure out of the region of dominant earthquake energy, to increase the damping, and to limit the forces transferred from the superstructure to the substructure (Wendichansky et al., 1995). It is often adopted as a retrofit scheme because isolation systems tend to reduce the need for costly retrofit of deficient pier and foundation elements. Koh and Kelly (1989) have identified these elastomeric bearings as the simplest method of isolation, making them prime candidates

for retrofit of typical CSUS bridges. Elastomeric bearings are composed of horizontal layers of elastomer separated and reinforced by thin layers of steel (steel shims) as shown in Figure 3-3.

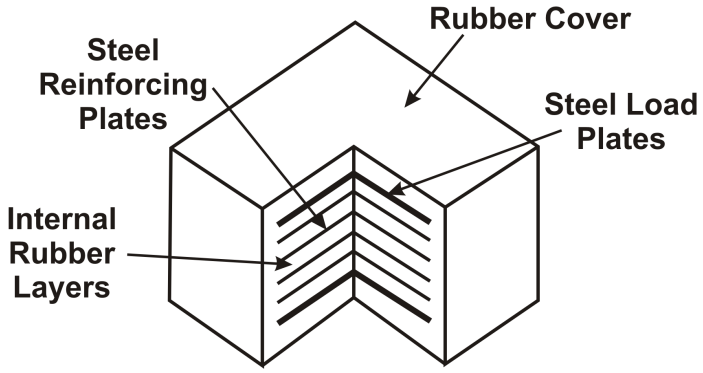

Figure 3-3: Elastomeric bearing adapted from Priestley et al. (1996).

The elastomeric isolation bearings used in this study are designed by targeting an estimated 2-3 times increase in the fundamental period of the bridge. The required isolation stiffness is backed out following the methodology in the *Guide Specifications for Seismic Isolation Design* by AASHTO (1999). Given an approximate target effective period, T_{eff}, and weight, W, the desired effective stiffness of the bridge system was estimated solving for K_{eff} in

$$T_{eff} = 2\pi \sqrt{\frac{W}{K_{eff} g}} \tag{3.4}$$

Subsequently, given the desired effective stiffness for the bridge system, K_{eff}, the required elastomeric bearing stiffness, k_{eff}, can be computed as recommended in the *Manual* by

$$K_{eff} = \Sigma(\frac{k_{sub}k_{eff}}{k_{sub} + k_{eff}}) \tag{3.5}$$

which essentially approximates the total stiffness by combining each isolator-substructure unit as a series of springs and then summing the resultants in parallel to approximate a single degree of freedom system. The elastomeric bearings selected for the retrofit target the desired effective elastomeric bearing stiffness such that

$$k_{eff} = \frac{AG}{h} \tag{3.6}$$

where the shear modulus of a typical elastomer is G=0.69 MPa (Skinner et al., 1993), h is the total height of the elastomer, and A is the plan area of the bearing assumed to be square (Kelly, 1997).

Kelly (1998) showed that elastomeric bearings can be modeled bi-linearly and that the equations for characterizing the elastomeric bearings are

$$k_{eff} = K_2 + \frac{Q}{h} \tag{3.7}$$

$$D_y = \frac{Q}{(K_1 - K_2)} \tag{3.8}$$

where Q is the characteristic strength, h is the total height of elastomer, D_y is the yield displacement, and K_1 and K_2 are the initial and secondary bearing stiffness. Assuming a yield displacement of 10% of the total elastomer height and that K_1=3K_2 based on characteristic tests of laminated elastomeric rubber bearings (HITEC, 1998), the properties Q, K_1, and K_2 which define the bi-linear model may be calculated for each elastomeric bearing retrofit.

The bearings used in the study have shape factors, S, that range from nearly 8 to 12 based on recommendations by Stanton (1997). The shape factor is defined as

$$S = \frac{ab}{2t_l(a+b)} \tag{3.9}$$

where a and b are the bearing dimensional length and width (assumed the same for this study), and t_l is the layer thickness which is on the order of 6.3 mm.

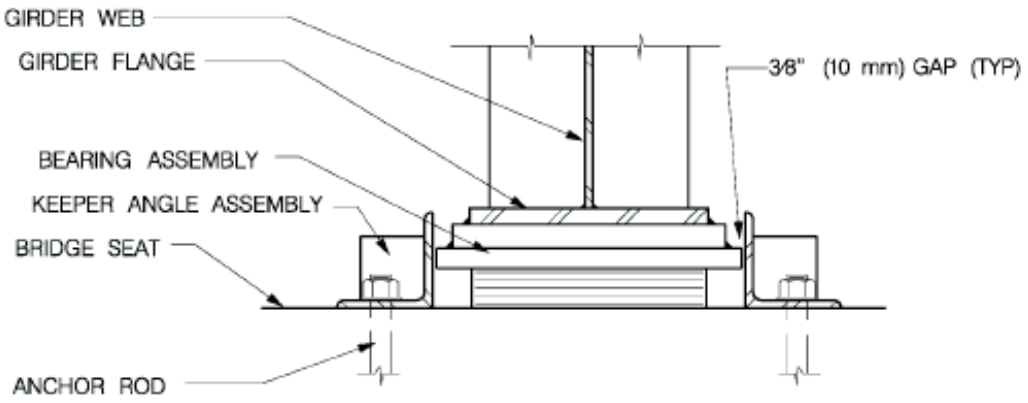

Figure 3-4: Typical elastomeric bearing with keeper detail (Collaboration, 2005).

Keeper plates (keeper angles) have been found to be common details in isolation bearings in the CSUS through a review of plans for retrofits performed in the region, and are posed as a viable detail for elastomeric bearings (Collaboration, 2005). The elastomeric bearing detail adopted for this study includes a keeper plate to restrict excessive transverse displacements with a gap between the keeper plate and bearing (see Figure 3-4). This tends to minimize any impacts or need for bi-directional dependence modeling of the bearings,

which have been noted by past researchers (Fenves et al., 1998). The bi-linear model is implemented in *OpenSees* using a uniaxial *Hardening* material. The bearing exhibits similar response in both the longitudinal and transverse directions because it is assumed to be square, and hence the model shown in Figure 3-5(a) is used in both principle directions. The keeper plate is modeled as a stiff element which yields at 270 kN, as approximated from typical details, and hardens. The gap between the bearing in the transverse direction before engaging the keeper may range from 6.4 mm to 19 mm, and is captured by the analytical model shown in Figure 3-5(b).

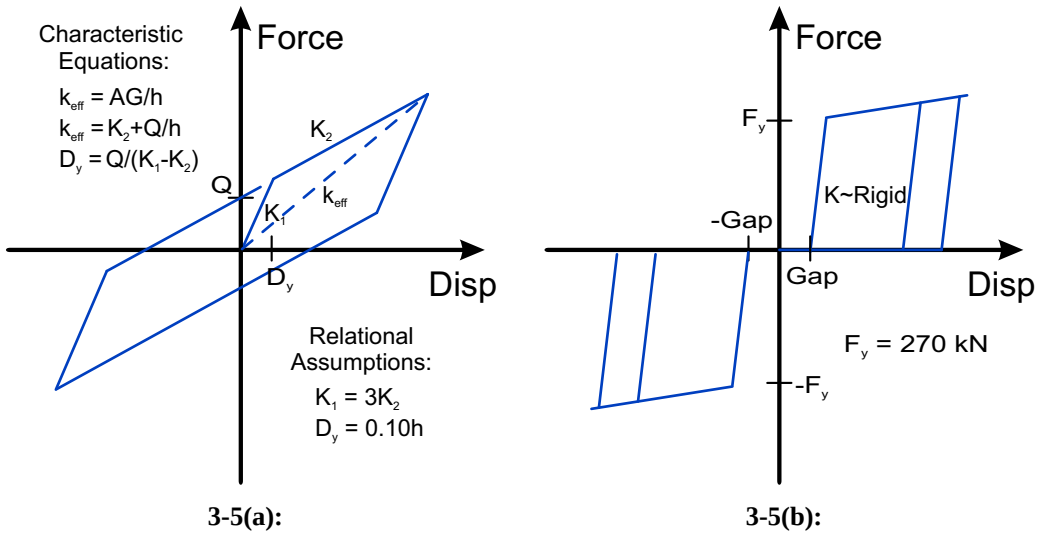

Figure 3-5: Analytical model for (a) elastomeric isolation bearings and (b) transverse keeper plates.

3.2.3 Restrainer Cables

This study will evaluate restrainer cables as one potential device for unseating prevention, which serves to limit relative hinge displacement and prevents collapse of a bridge

span. They are often employed in bridges with insufficient seat widths (such as those in the CSUS) between decks or between a deck and abutment. The use of restrainer cable retrofits has been a common approach on the West Coast since the 1970s following the 1971 San Fernando earthquake, and has been found to be a relatively simple and inexpensive retrofit measure to reduce the vulnerability to unseating (Priestley et al., 1996). Experience from previously installed retrofits in the Los Angeles area has shown that despite some pull-through failure, most restrainer cables performed adequately in the 1994 Northridge earthquake (Cooper et al., 1994; Housner and Thiel, 1995), as did most of those in the Oakland area in the 1989 Loma Prieta earthquake (Moehle et al., 1995).

The cable configuration considered for this study provides a connection between the deck and abutment, as well as the deck and bent cap for the simply supported bridges. There may be some variation in the geometric properties of the cables, though restrainer cables are often designed as 19 mm diameter cables with an effective area of 143 sq. mm, and a length between 1.52 m and 3.05 m. Due to ambient temperature conditions, the slack may also vary between 0 mm and 19 mm, which could significantly effect the response of the bridge (Saiidi et al., 1996). Testing by the California Department of Transportation (Caltrans, 1997) has revealed that the elastic modulus of these high strength steel cables is E=69000 MPa and that the yield force is approximately F_y=174 kN, corresponding to a stress of 1210 MPa. Figure 3-6 shows the test data for one typical restrainer cable.

As is commonly done in the CSUS, the restrainer cables in this study are designed such that they can support W/2 of their adjacent span, a viable design technique that produces similar results as other methods that require knowledge of local acceleration and site coefficients according to Saiidi et al. (2001). For the continuous bridges, restrainers are only

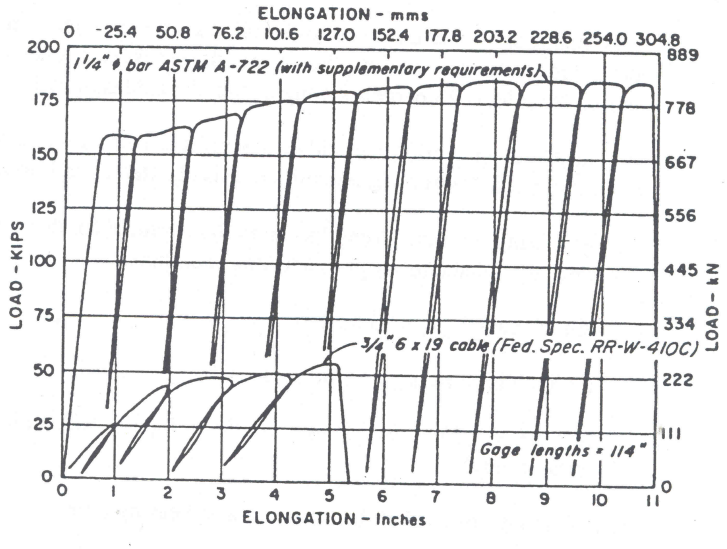

Figure 3-6: Load-deformation from Caltrans restrainer cable testing (Caltrans, 1997).

provided at the end of the continuous span between the abutment and girders, and hence are designed to have an area sufficient to carry W/2 of the entire deck. The restrainer cables are modeled as nonlinear, tension-only elements with an initial slack following the model as shown in Figure 3-7. The strain hardening is considered negligible, and the plastic deformations accumulate.

3.2.4 Seat Extenders

Seat extenders are an alternate method of preventing unseating of spans by providing an extended effective seat length, and have been found to be fairly common retrofits in the CSUS. Hipley (1997) has deemed them the simplest and least expensive means of preventing unseating and allowing the superstructure to float over the substructure. Thus they will also be evaluated as a part of this study. As a retrofit measure, seat extenders serve primarily to increase the capacity of the bridge to sustain longitudinal displacement without collapse

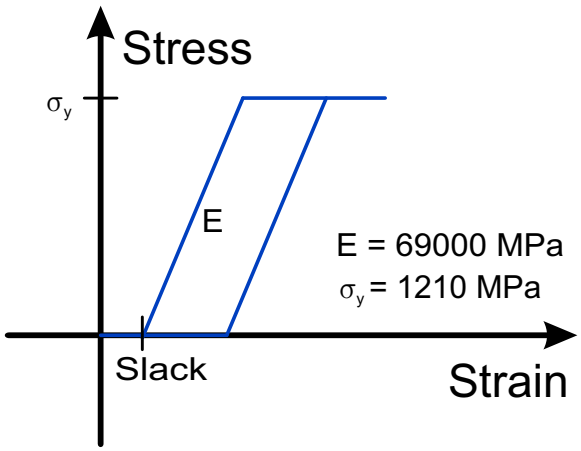

Figure 3-7: Analytical model for restrainer cables.

due to unseating. They do not protect other bridge components from damage. Assuming that the seat extender is designed to sustain the loading from the girders given excessive deck displacement, this retrofit measure does not require unique analytical modeling; however, the effect of the seat extenders on the fragility of the bridge will be to increase the limit state for collapse due to excess longitudinal displacement. Hence the impact of seat extenders will be addressed in later chapters.

3.2.5 Shear Keys

Many of the retrofit measures indicated above that will be considered as a part of this work primarily impact the response and vulnerability of a bridge in the longitudinal direction. However, typical CSUS bridges may also suffer damage due to excessive motion or demands in the transverse direction. As such, the use of shear key retrofits will also be evaluated, and have been identified in Chapter 2 as being present in a number of CSUS bridges. The shear keys serve to restrain the deck motion when a bridge is excited in the

transverse direction and facilitate shear force transfer to the substructure. These devices are often concrete blocks provided at each bearing location. The assumed shear key design for this study follows a shear friction approach and limits the shear forces transferred to the substructure to less than half of the shear strength of the concrete columns, thus preventing excessive column demands. The shear strength of a typical column considering the contribution of the concrete and transverse reinforcement is approximately 950 kN. The design shear strength of the shear keys based on the shear friction approach is

$$V_{sk} = \phi_s \mu A_s f_y \tag{3.10}$$

where ϕ_s is the shear strength reduction factor, μ is the coefficient of friction taken as 1.4 for a natural crack, and A_s is the total area of reinforcement crossing the face (Priestley et al., 1996). The shear keys are presumed to have a geometry such that the each key will behave in a shear mode rather than fail in flexure. The total required area of steel is distributed symmetrically in shear keys across the bent cap, where 774 mm^2 of reinforcement is provided per column in the bent. The shear keys are represented by a Coloumb friction model as illustrated in Figure 3-8 with the reduction factor in Equation 3.10 omitted in the assessment of lateral strength. An initial gap is provided before the shear key engages in the transverse direction which may be on the order of 12.7 mm, and the initial stiffness of shear keys is assumed to be relatively rigid based on recommendations by Priestley et al. (1996).

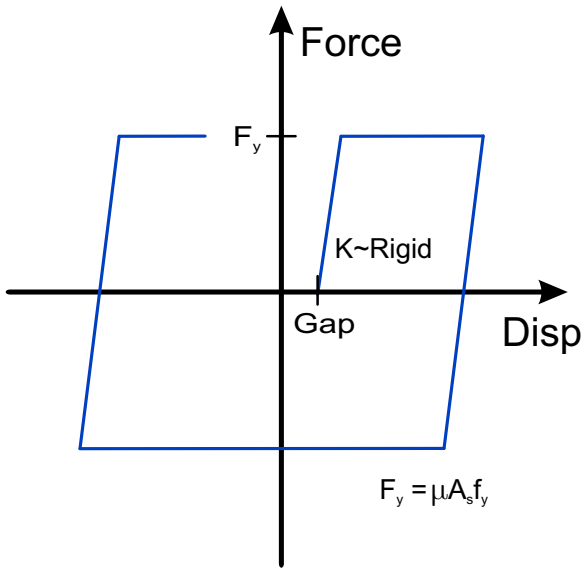

Figure 3-8: Coloumb friction model for shear keys in transverse direction.

3.3 Closure

Six potentially viable retrofit measures for CSUS bridges have been identified in this chapter. These measures target a number of different vulnerabilities of bridges common to the region and improve the response of different bridge components. These retrofits measures were found in the review of the state-of-practice in Chapter 2 to be common retrofits in CSUS projects, and typical details were identified. Findings from experimental tests of retrofitted components, recommendations from past researchers, along with common CSUS retrofit details were used to establish analytical models of the different retrofit measures. Potential uncertainties in the parameters defining these models will be further discussed in later chapters; however, the models presented form the basis for analytical assessment and performance evaluation of typical CSUS bridges under various retrofit measures.

CHAPTER IV

DETERMINISTIC ANALYSIS OF RETROFITTED BRIDGES

The impact of potential bridge retrofits on the performance of typical CSUS bridges is evaluated in this chapter to illustrate the effect of retrofit strategies on the response of various bridge components. These results will be the first comprehensive and systematic look at typical CSUS bridges and the effect of different retrofit measures on their components responses. This provides insight for decision makers on the impact of retrofit on the targeted response, as well as other components of the bridge. The intention is to highlight the improved or worsened component responses and serve as motivation for further evaluation of bridge system vulnerability through probabilistic measures.

4.1 Typical Bridges

A detailed inventory analysis of the 163,433 bridges in the 11 states in the Central and Southeastern US was performed by Nielson (2005a). The states included in the inventory study were Alabama, Arkansas, Georgia, Illinois, Indiana, Kentucky, Mississippi, Missouri, North Carolina, South Carolina, and Tennessee. Information presented in the National Bridge Inventory (NBI) was considered in order to assign the bridges to typical classes as listed in Table 4-1. Fragility curves for nine typical bridge classes which account for roughly 90% of the inventory were then derived in his work. The findings revealed

Table 4-1: CSUS Bridge Classes.

Bridge Type	Abbreviation	HAZUS Class
Multi-Span Continuous Concrete Girder	**MSC Concrete**	**HWB10, HWB22**
Multi-Span Continuous Steel Girder	**MSC Steel**	**HWB15, HWB26**
Multi-Span Continuous Slab	MSC Slab	HWB10, HWB22
Multi-Span Continuous Concrete Box Girder	MSC Concrete-Box	HWB10, HWB22
Multi-Span Simply Supported Concrete Girder	**MSSS Concrete**	**HWB5, HWB17**
Multi-Span Simply Supported Steel Girder	**MSSS Steel**	**HWB12, HWB24**
Multi-Span Simply Supported Slab	MSSS Slab	HWB5, HWB17
Multi-Span Simply Supported Concrete Box Girder	MSSS Concrete-Box	HWB5, HWB17
Single-Span Concrete Girder	SS Concrete	HWB3
Single-Span Steel Girder	SS Steel	HWB3

*boldface = bridge classes evaluated as a part of this study

that the MSC and MSSS steel girder bridges were among the most vulnerable to damage, followed by the MSC and MSSS concrete girder bridges, particularly at the higher damage states. These bridges are also among the most common classes of bridges found in the CSUS inventory (see bold-face bridge classes in Table 4-2). While the single span steel and concrete girder bridges account for a considerable percentage of the CSUS inventory, these bridge classes were found to be the least vulnerable and hence are less likely candidates for retrofit. As such, the four common and vulnerable classes of bridges (MSSS Steel, MSSS Concrete, MSC Steel, MSC Concrete) will be the focus of the work in this study. Retrofit of these classes of bridges will be evaluated and the results can then be assessed for extrapolation to other less common bridge classes for future studies.

An example bridge using typical geometric configurations and details is evaluated for each of the four bridge types. The details and geometry for the bridges are based on past studies which have examined bridge plans from over 150 bridges and presented typical representative configurations for MSSS and MSC steel and concrete girder bridges found in

Table 4-2: CSUS Bridge Inventory.

Bridge Type	Number	Percentage
MSC Concrete	**10,638**	**6.5**%
MSC Steel	**21,625**	**13.2**%
MSC Slab	5,955	3.6%
MSC Concrete-Box	916	0.6%
MSSS Concrete	**30,923**	**18.9**%
MSSS Steel	**18,477**	**11.3**%
MSSS Slab	9,981	6.1%
MSSS Concrete-Box	4,909	3.0%
SS Concrete	22,793	13.9%
SS Steel	18,281	11.2%
Other	18,945	11.7%
Total	163,433	100%

*boldface = bridge classes evaluated as a part of this study

the CSUS (Choi, 2002; Nielson, 2005a). The bridges examined in this study have characteristically non-seismic detailing, such as multi-column bents having approximately a 1% longitudinal reinforcement ratio in the columns with widely spaced transverse ties providing limited confinement, and high-type steel fixed and expansion (rocker) bearings. A brief overview of the typical bridge classes and an example geometry is presented in the following subsection. The bridges are characteristically non-skewed bridges, as found by Nielson (2005a) to be typical of the CSUS inventory, and are three-span bridges which was found to be the most common number of spans. Further details can be found in Nielson (2005a).

4.1.1 MSSS Steel Girder Bridge

MSSS Steel girder bridges, as shown in Figure 4-1, account for 11.3% of the CSUS inventory. The MSSS Steel girder bridge considered is a zero-skew, three-span concrete slab-on-girder bridge with 15 m wide decks consisting of eight steel plate girders. The spans are 12.2, 24.4, and 12.2 m in length. Each bridge is supported on three column bents, having

915 mm diameter circular columns that are 4.6 m tall, and seat type pile-bent abutments. For this layout, 2.44 m square, 1.09 m thick footings with eight piles having no positive connection are used, while the abutment utilizes ten driven vertical piles with a spacing of 1.45 m on-center. The average gap between the deck and abutment backwall is 25.4 mm and is 38.1 mm between adjacent decks. This class of bridges has characteristically seismically deficient bearings connecting the superstructure to the substructure, which are high-type steel bearings. Figure 4-2 shows the typical geometric configuration of a MSSS Steel girder bridge that is evaluated in this Chapter, while Figure 4-3 provides further illustration of the typical details of the steel bearings and concrete members. A notable feature is the 305 mm spacing between transverse reinforcement providing limited confinement in the columns.

Figure 4-1: Example multi-span simply supported (MSSS) slab-on-steel girder bridge.

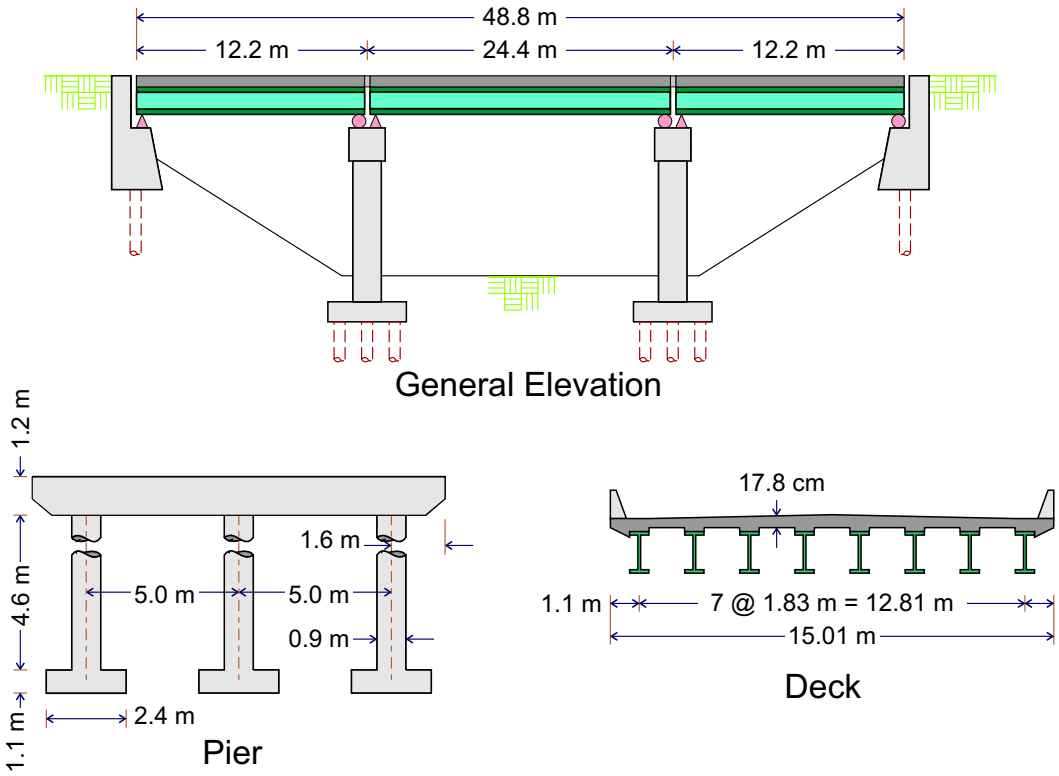

Figure 4-2: MSSS Steel girder bridge typical geometry.

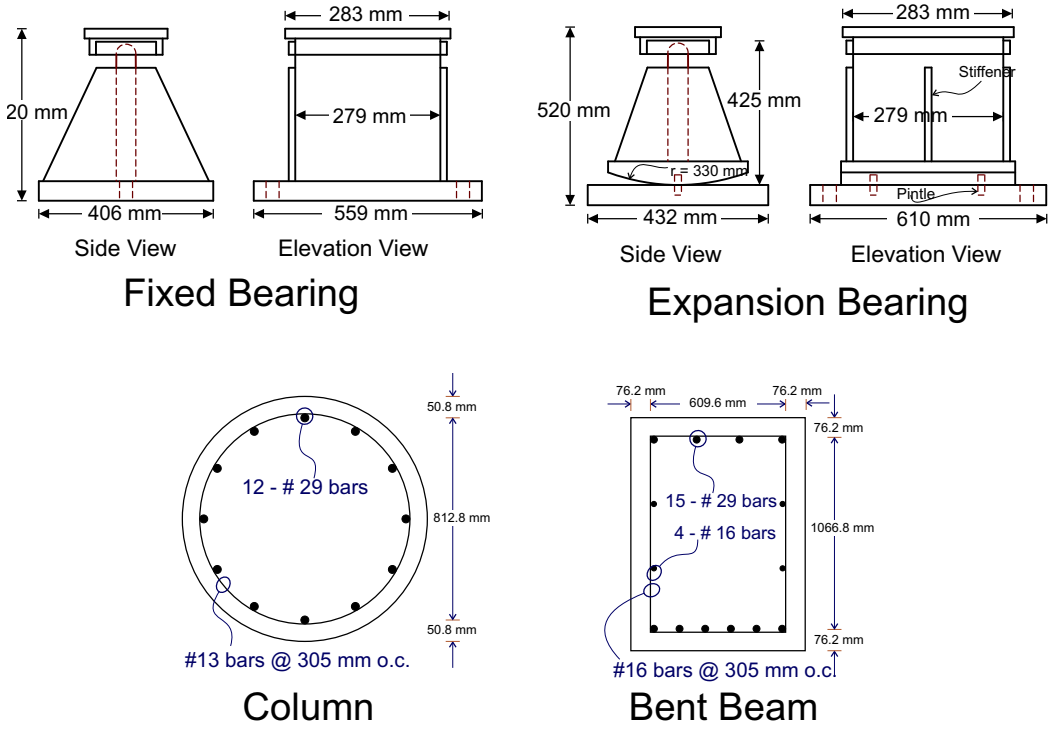

Figure 4-3: Steel fixed and expansion (rocker) bearings, and reinforced concrete column and bent beam details.

4.1.2 MSC Steel Girder Bridge

The photograph in Figure 4-4 shows a typical MSC Steel girder bridge found in Tennessee, which is one of the most vulnerable classes of bridges found in the CSUS. The multi-span continuous steel girder bridge has similar details as the MSSS Steel bridge, with like substructure assemblies, including the bent beam, column, and abutments. The primary distinction of this bridge type is the continuity of the deck provided over the bent beams. While the same type of steel bearings are employed in the MSC Steel bridge, the arrangement differs from the MSSS Steel bridge. As indicated in Figure 4-5, fixed bearings are provided at each girder along the bent beams, and expansion bearings are provided at the abutments. The span lengths, weights, and gaps, which are the primary differences in the representative bridges are listed in Table 4-3.

Figure 4-4: Example multi-span continuous (MSC) slab-on-steel girder bridge found in Tennessee.

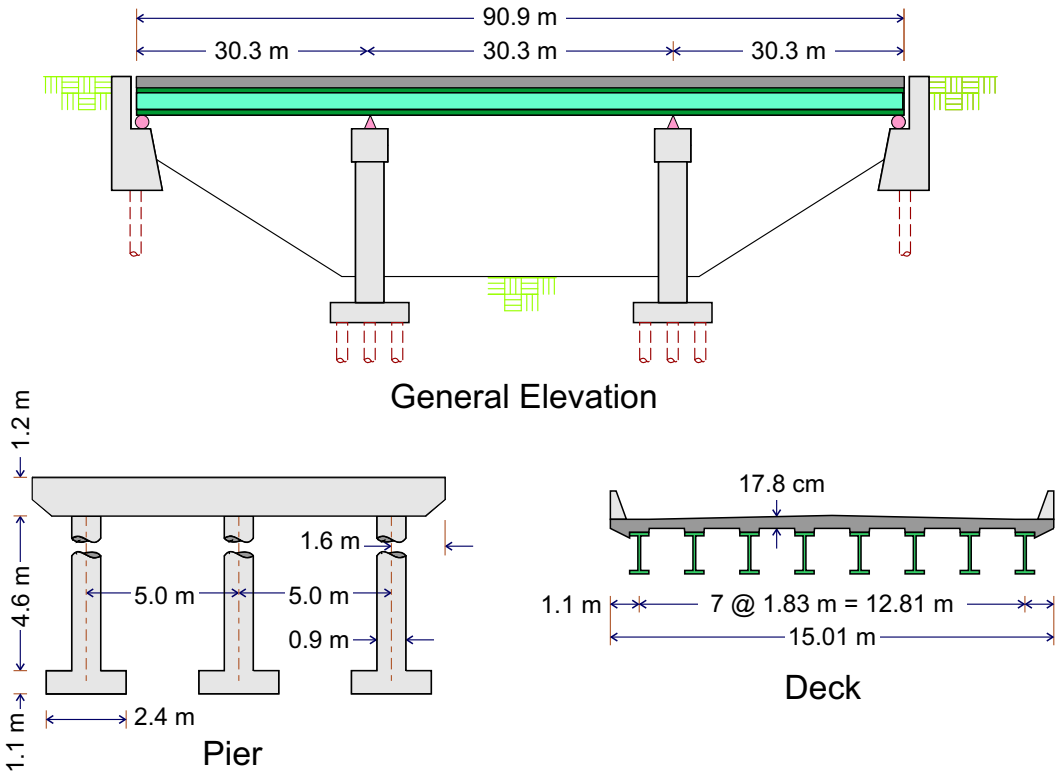

Figure 4-5: MSC Steel girder bridge typical geometry.

Table 4-3: Span properties for different bridge types.

Bridge	Span	Length (m)	Weight (kN/m)	Gap (mm)
MSSS Steel	End Span	12.2	39	38.1
	Mid Span	24.4	52	25.4
MSC Steel	End Span	30.3	68.3	76.2
	Mid Span	30.3	68.3	N/A
MSSS Concrete	End Span	12.2	92.8	38.1
	Mid Span	24.4	127.3	25.4
MSC Concrete	End Span	12.2	92.8	38.1
	Mid Span	24.4	127.3	N/A

4.1.3 MSSS Concrete Girder Bridge

Figure 4-6 shows an example MSSS Concrete girder bridge found in South Carolina. The multi-span simply supported concrete girder bridge examined in this study is also a three-span bridge with fixed and expansion supports at the end of each span, yet the superstructure is composed of a concrete deck supported by AASHTO-Type concrete girders. The typical configuration for this bridge class is illustrated in Figure 4-7, with spans of 12.2, 24.4, and 12.2 m long like the MSSS Steel bridge. However, with eight AASHTO Type I prestressed girders at the end spans and Type III girders at the midspan, the deck is heavier than the steel bridge. The MSSS Concrete bridge utilizes elastomeric pads as bearings, which have been found to be considerably less vulnerable than the steel bearings typically found in the steel bridges (Nielson, 2005a). These bearings are assumed to have two 25.4 mm diameter dowels with differing gaps before the dowels are engaged in the fixed and expansion bearings. This bridge has a similar substructure to the previously detailed bridge classes, where two multi-column bents and seat type abutments are utilized. A 2.4 m tall backwall is assumed for the abutment along with ten piles and driven pile foundations.

4.1.4 MSC Concrete Girder Bridge

The typical geometry of the MSC Concrete girder bridge (Figure 4-8) is nearly identical to the MSSS concrete girder bridge previously described, including the bearing configuration, substructure, and span lengths. The average typical gaps between the abutments and deck ends are still 38.1 m, however, the gaps between the three spans are eliminated by casting of a concrete parapet between the deck and girders. This provision for continuity which distinguishes the MSC Concrete bridge is detailed in Figure 4-9. This bridge is unique in

Figure 4-6: Example multi-span simply supported (MSSS) concrete girder bridge found in Charleston, South Carolina.

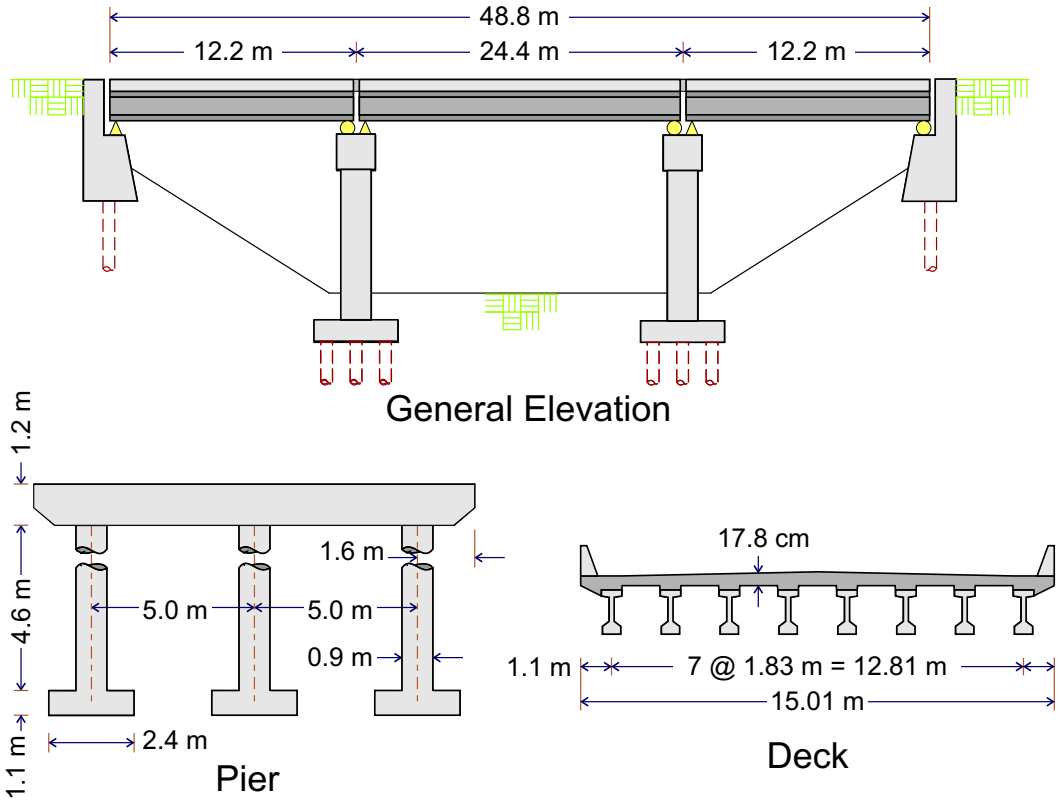

Figure 4-7: MSSS Concrete girder bridge typical geometry.

that it has the largest deck mass which would act in unison when excited by ground motion, because of the continuous nature of the superstructure and larger mass of the concrete girders.

Figure 4-8: Example multi-span continuous (MSC) concrete girder bridge.

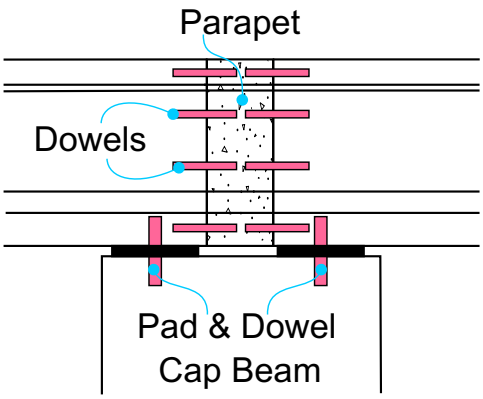

Figure 4-9: Provision for continuity in the MSC Concrete girder bridge.

Table 4-4: Deck Section Properties Adapted from Nielson (2005a).

Bridge Class	Span	E (MPa)	I_z (m^4)	I_y (m^4)	Area (m^2)	Weight (kN/m)
MSSS Steel	End Spans	2.00E+05	0.027	9.776	0.508	39.0
	Mid Span		0.113	12.992	0.676	52.0
MSC Steel	End Spans	2.00E+05	0.236	17.028	0.888	68.3
	Mid Span		0.236	17.028	0.888	68.3
MSSS Concrete	End Spans	2.78E+04	0.119	75.835	3.941	92.8
	Mid Span		1.102	103.760	5.407	127.3
MSC Concrete	End Spans	2.78E+04	0.119	75.835	3.941	92.8
	Mid Span		1.102	103.760	5.407	127.3

4.2 Analytical Modeling

The analytical modeling approach used for the retrofit measures themselves was detailed in Chapter 3. The intention of this section is to present a brief overview of the 3-dimensional modeling of the bridge structure and components. The bridge modeling in OpenSees (McKenna and Fenves, 2001) is performed consistent with Nielson's findings on typical bridge properties and modeling assumptions. Only general modeling approaches will be presented, while further details can be found elsewhere (Nielson, 2005a). An example of the modeling appraoch is presented in Figure 4-10 for the MSSS Steel bridge.

The composite slab and girders are modeled using linear elastic beam-column elements, since the superstructure is expected to remain elastic during seismic excitation. The section properties are presented in Table 4-4. Pounding between the decks or the deck and abutment are captured in the model by use of a bi-linear contact element. The model follows the recommendations of Muthukumar (2003) who proposed a hysteretic model to reflect the energy dissipated during pounding.

The high-type steel fixed and expansion bearings are modeled using non-linear translational springs in the longitudinal and transverse directions, based on tests of similar bearings performed by Mander et al. (1996). The model is intended to capture the prying action, rocking, and stiffness degradation observed in the tests. It is noted that the yield force of the bearings is a function of the coefficient of friction due to debris and wear of the bearing. The analytical models for the elastomeric pad and dowel utilized in the concrete bridges is characterized by both the elastomer stiffness, sliding of the bearing, and stiffness and yield of the steel dowels. Following the analytical modeling of Choi (2002) and Nielson (2005a), the elastomeric pad is modeled bi-linearly and the steel dowels engage beyond at longitudinal displacements 6.4 mm in the fixed bearings and 25.4 mm in the expansion bearing.

The concrete bent beams are represented by rectangular fiber sections and beam-column elements. The discretized fiber section permits the assignment of unique constitutive models for the confined, unconfined concrete, and steel reinforcement. In a similar fashion, the concrete columns are modeled with circular fiber sections and beam-column elements. The abutment model presented by Nielson (2005a) assimilates the findings of a number of past studies (Caltrans, 1990, 1999; Maroney et al., 1994, 1993; Martin and Yan, 1995). For the longitudinal model, the active (positive/tension) action of the abutment is dictated by the pile stiffness, while in passive action, the contribution of the piles and passive pressure of the soil against the abutment backwall are considered. The passive action reflecting the soil contribution uses a quadrilinear model, and the pile stiffness degrading from its initial stiffness before reaching its ultimate strength of 119 kN/pile. The pile contribution is the only component considered in the transverse abutment response.

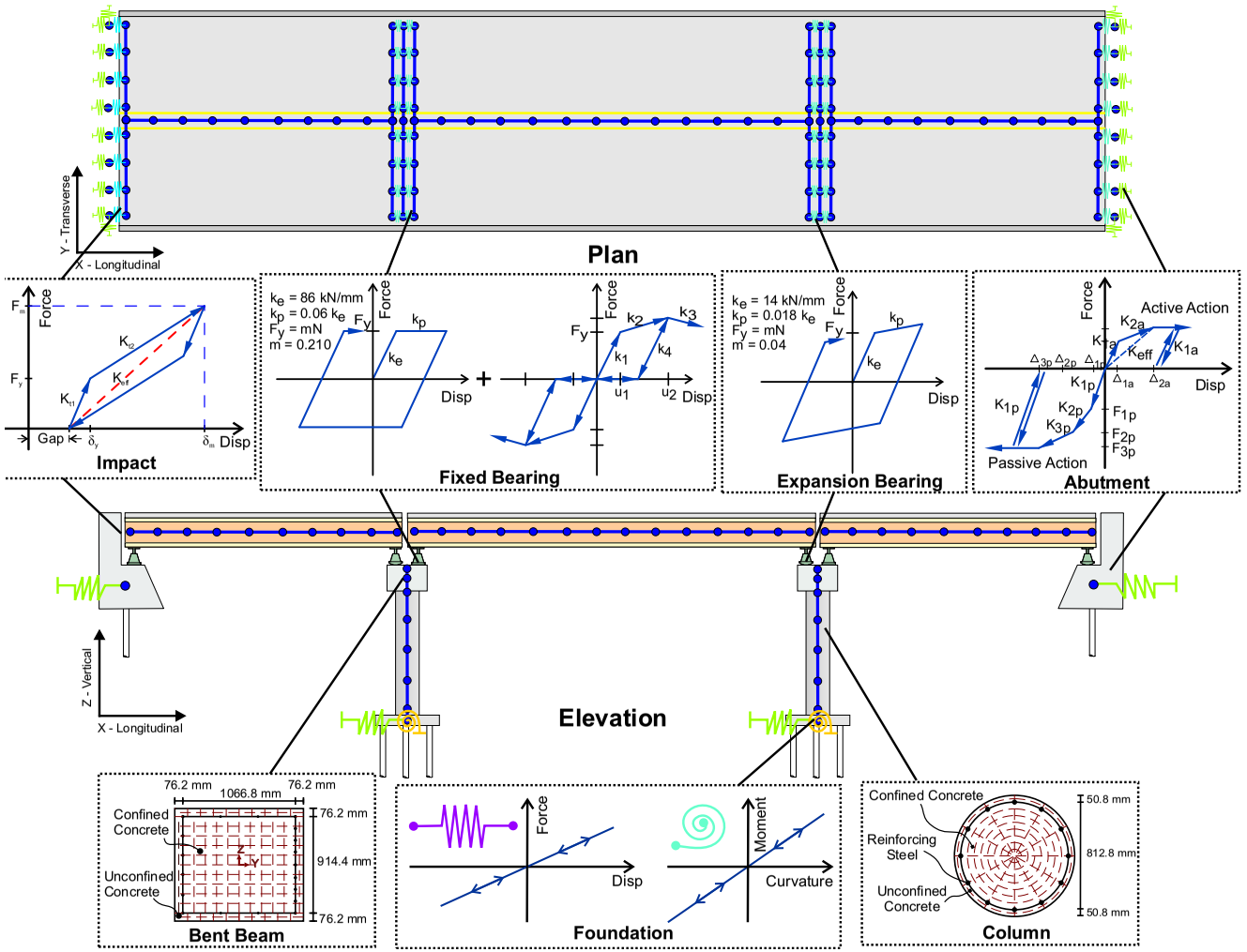

Figure 4-10: 3-d nonlinear analytical model of MSSS Steel bridge.

The pile foundations are modeled with simplified linear translational and rotational springs. The vertical and horizontal stiffness, and pile grouping, are considered in deriving the aggregate horizontal and rotational pile group stiffnesses.

4.3 Ground Motions

In performing analytical evaluations of bridge performance or deriving analytical fragility curves for regions with recorded strong ground motion, such as Japan, Greece, or California, earthquake ground motion records from past events have often been used, and in some cases scaled to various levels of excitation when employed in an incremental dynamic analysis (Elnashai et al., 2004; Karim and Yamazaki, 2003; Mackie and Stojadinovic, 2003). In regions of moderate seismicity, such as the Central and Southeast US, there may likely be little or no available strong ground motion records, so synthetic ground motions are often adopted. Two synthetic suites of ground motions will be used throughout this study. The ability of these suites to capture such inherent uncertainties as the earthquake source, wave propagation, and soil conditions dictates the ability of the fragility curve development procedure to propagate these aleatoric uncertainties.

4.3.1 Wen and Wu

Wen and Wu (2001) have simulated ground motions for three cities in Mid-America for seismic performance assessment of structures, such that the median of the response spectra for the suite matches the uniform hazard response spectra for 10% and 2% probability of exceedance in 50 years. Ten ground motions for each hazard level were presented for the cities of Memphis, TN; Carbondale, IL; and St. Louis, MO. Various magnitudes and

source locations were considered in the construction of the uniform hazard response spectra. The 10 ground motions representative of 2% in 50 year events in Memphis are used in the deterministic retrofit evaluation presented in this chapter. Figure 4-11 shows the acceleration response spectra for each ground motion in the suite along with a plot of the mean and mean plus or minus one standard deviation response spectra. Later probabilistic performance analyses of the bridges will also use 48 of the ground motions developed by Wen and Wu, as detailed in Chapter 7.

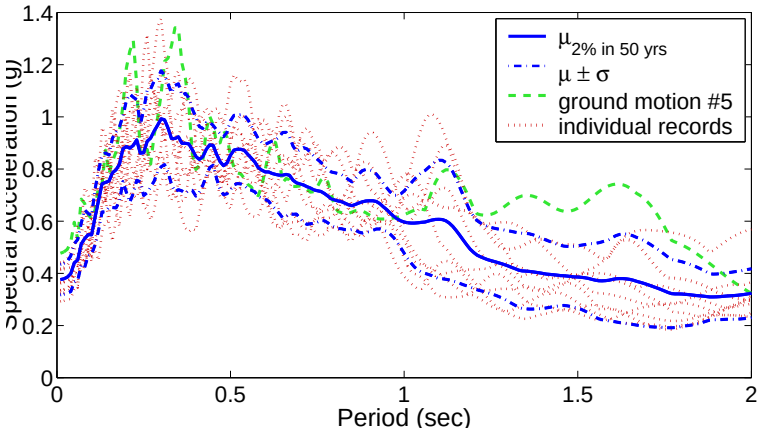

Figure 4-11: Response spectra for the 2% in 50 year Memphis ground motion suite used in the deterministic analysis. Ground motion #5 is used to illustrate typical component responses.

4.3.2 Rix and Fernandez

Rix and Fernandez (2004) developed a suite of scenario-based sythetic ground motions for Memphis, TN that will also be used in later studies in this work. These scenario ground motions were developed based on stochastic methods, considering nonlinear site response, and

the influence of the deep soil column of the Upper Mississippi Embayment. The simulation was based on a stochastic method proposed by Boore (1983), and following the work by Drosos (2003). Care was taken to capture uncertainties in the source, path, and site. The ground motions used in this work employ the source model by Frankel et al. (1996). Twenty ground motions were simulated for each of 11 different magnitude-distance pairs with Mw=5.5, 6.5, 7.5 and R=10 km, 20 km, 50 km, 100 km. Forty-eight of the 220 ground motions were identified by Nielson (2005a) for use in the fragility analysis, and will be discussed further in Chapter 7.

4.4 Deterministic Retrofit Evaluation

An example deterministic retrofit evaluation is performed herein for an example bridge class–the MSC Steel bridge. Nonlinear time history analysis using detailed three-dimensional models of the previously presented typical multi-span continuous steel girder bridge is used to evaluate the effectiveness of various retrofit strategies. Restrainer cables, steel jackets, shear keys, and elastomeric isolation bearings are assessed for their influence on the variability and peak longitudinal and transverse response of critical components in the bridge. Following the detailed retrofit evaluation for this bridge class, a summary of the findings is presented from similar evaluations for all four common classes of bridges under the different retrofit strategies.

4.4.1 Example with MSC Steel Bridge

4.4.1.1 Typical Component Responses

In order to illustrate the impact of the retrofit measures on the performance of various components in the bridge, typical nonlinear responses are shown for the as-built and retrofitted

MSC steel girder bridges subjected to ground motion #5, which has a peak ground acceleration of 0.47 g (see Figure 4-12). Note that the acceleration response spectrum for this ground motion is highlighted in Figure 4-11. The ground motion is applied separately along each of the principal orthogonal axes of the bridge to facilitate a comparison of how the retrofits affect both longitudinal and transverse motion. This is for illustration purposes of the responses. However, in the later fragility assessment, both orthogonal comonents of the ground motion are applied simultaneously for dynamic excitation of the 3-d analytical model.

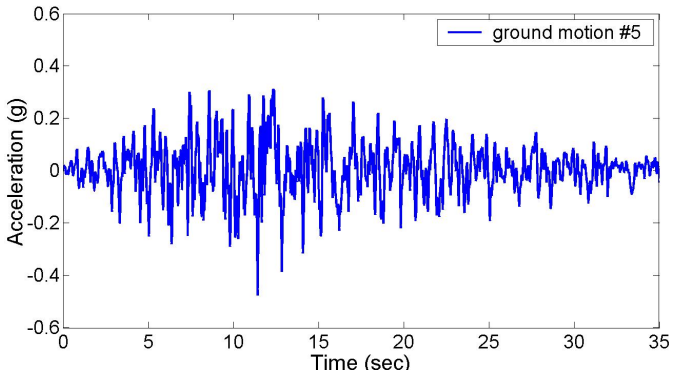

Figure 4-12: Time history for ground motion used in deterministic analyses.

The typical MSC Steel bridge evalauted has a fundamental mode at a period of 0.44 seconds, characterized by longitudinal motion, with roughly 96% mass participation. The second mode is predominately transverse action at a 0.31 second period. As indicated in past studies and earthquake reconnaissance (Bruneau, 1998; Nielson and DesRoches, 2006; Ranf et al., 2001), the ductility demands placed on the columns under earthquake loading

could be expected to result in considerable damage to the columns in the form of cracking, spalling, and lap splice failure. Figure 4-13 shows a plot of the moment-curvature response at a base section of the left column in the MSC Steel bridge when loaded longitudinally with this example ground motion. It is seen that through the use of elastomeric isolation bearings, the peak curvature ductility demands reduce from μ=2.7 to μ=0.6, and that with restrainer cables the column curvature ductility demands reduce to μ=1.8. The steel jackets tend to slightly reduce these demands (μ=2.4), but, more importantly, they considerably increase the capacity of the columns.

The expansion bearing deformations are a direct result of the motion of the bridge decks, and the relative displacement between the bridge decks and abutments in the MSC Steel bridge. The longitudinal response of the steel rocker bearings in the MSC Steel girder bridge are shown in Figure 4-14. The restrainer cables reduce the peak deformations from 103.3 mm to 80.4 mm for the case examined. The restrainers have yielded at this level, thereby inhibiting their ability to more significantly reduce the bearing demands. It is noted that the elastomeric isolation bearing at this location has a 115.5 mm deformation, though this is an altogether different component. The rocker bearing transverse deformations are initially 47.7 mm, which are considerably reduced by the shear keys to a level of 13.5 mm (see Figure 4-15). The elastomeric bearings that replace this bearing reaches a peak deformation of 14.3 mm, which is limited by the keeper plate detail as shown in Figure 4-15 (c) and (d).

The fixed bearings also exhibit nonlinear behavior in the transverse direction for the MSC Steel girder bridge, with deformations of 16.6 mm. Other than the elastomeric bearings, which replace these steel fixed bearings, the primary retrofit measure that affects the

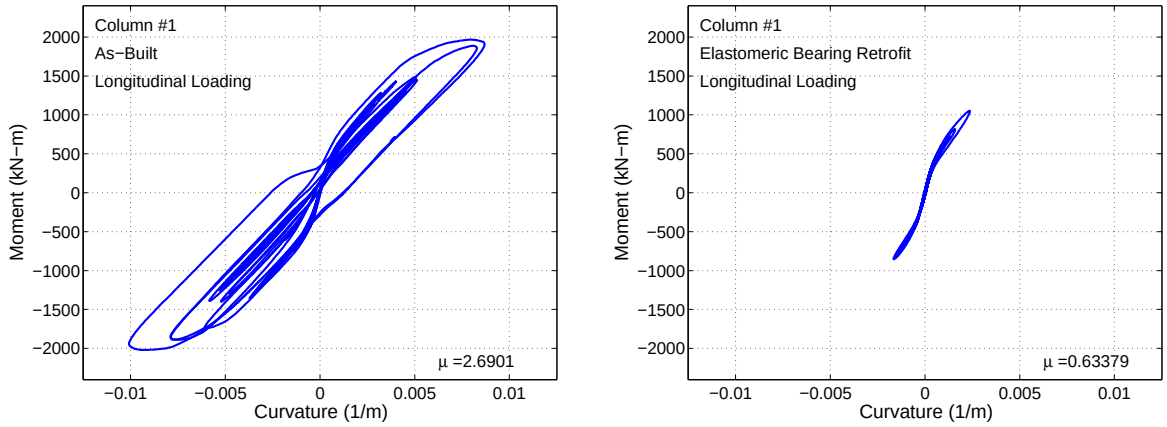

4-13(a): **4-13(b):**

4-13(c): **4-13(d):**

Figure 4-13: Curvature ductility demands placed on the columns in the (a) as-built MSC Steel bridge compared to the bridge retrofit with (b) elastomeric isolation bearings, (c) restrainer cables, and (d) steel jackets.

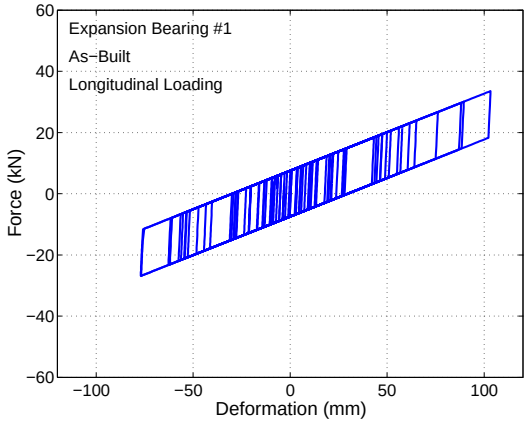

4-14(a):

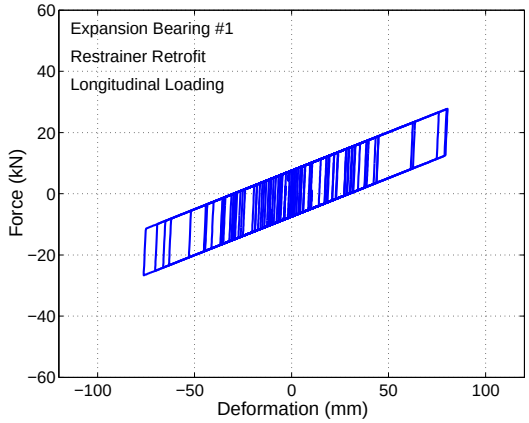

4-14(b):

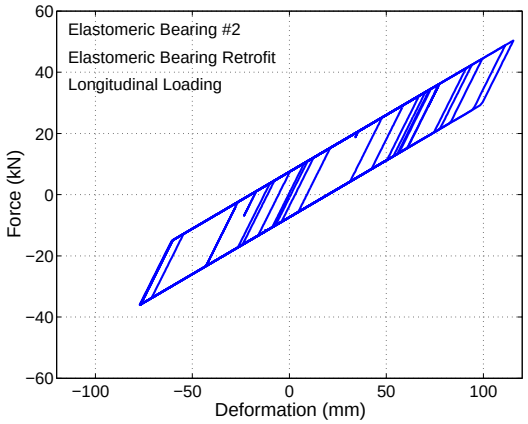

4-14(c):

Figure 4-14: Expansion bearing deformations under longitudinal loading in the (a) as-built MSC Steel bridge, (b) bridge retrofit with restrainers, as well as the (c) elastomeric bearing at the same location (note scale).

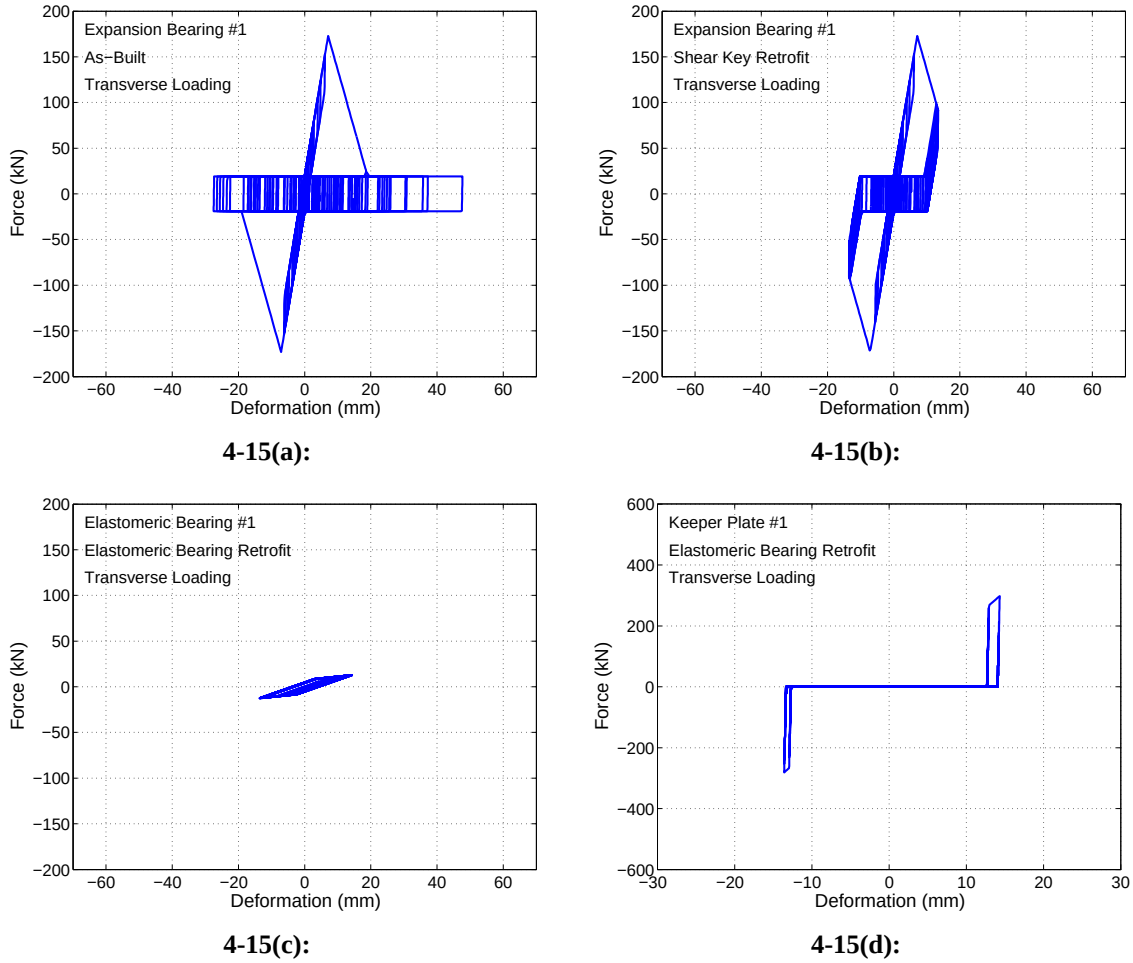

4-15(a): **4-15(b):**

4-15(c): **4-15(d):**

Figure 4-15: Transverse expansion bearing responses under transverse loading in the (a) as-built MSC Steel bridge, (b) bridge retrofit with shear keys, as well as the (c) elastomeric bearing at the same location with (d) its associated keeper plate.

transverse response of the bridge is the use of shear keys, which reduce the deformations to 5.3 mm. It is noted that the shear keys engage at the locations of the expansion bearings and that due to their gaps of 12.5 mm, have not actually engaged at the locations of the fixed bearings. The transverse fixed bearing response with and without the shear key retrofit are shown in Figure 4-16. In the longitudinal direction, the fixed bearings on the MSC Steel bridge have minimal deformations, as the bridge deck, fixed bearings, and columns tends to respond like a single degree of freedom system. The effect of retrofitting the columns with steel jackets on the response of the fixed and expansion bearings is negligible for this ground motion.

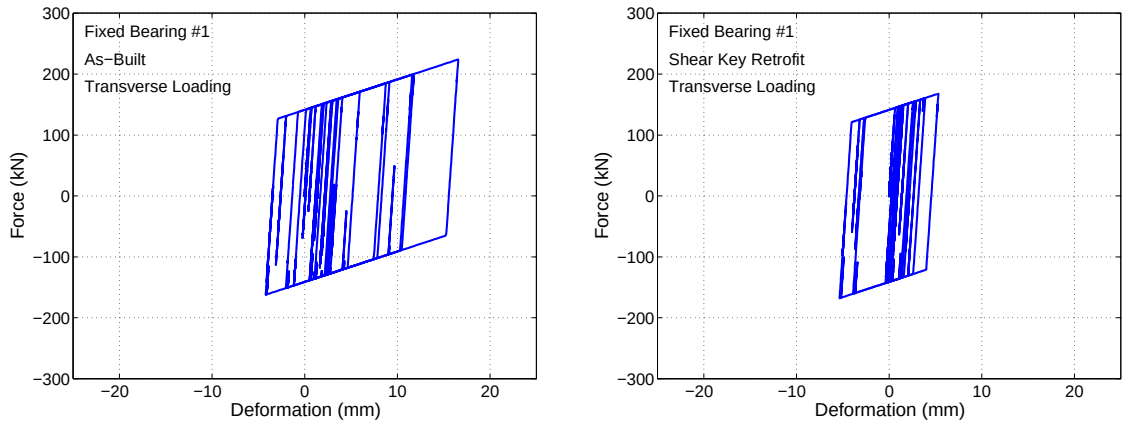

4-16(a): **4-16(b):**

Figure 4-16: Fixed bearing response in the transverse direction for the (a) as-built bridge and (b) bridge retrofit with shear keys.

The deformations of the abutment in active action (tension), passive action (compression), and in the transverse direction are relatively low for the as-built MSC Steel bridge. However, the use of elastomeric isolation bearing retrofit in the MSC bridge increases the

passive deformations (compression) from 17.4 mm to 29.0 mm due to pounding, while the restrainers reduce them to 1.0 mm (see Figure 4-17). Figure 4-18 illustrates that the initial transverse deformations are 6.0 mm, yet they increase to 10.0 mm with shear keys and 34.0 mm with elastomeric bearings having the keeper plate detail. These results are intuitive since both of these retrofits provide a means of transferring lateral loads to the abutment in this direction. The steel jacket retrofit has relatively little impact on the response of this component.

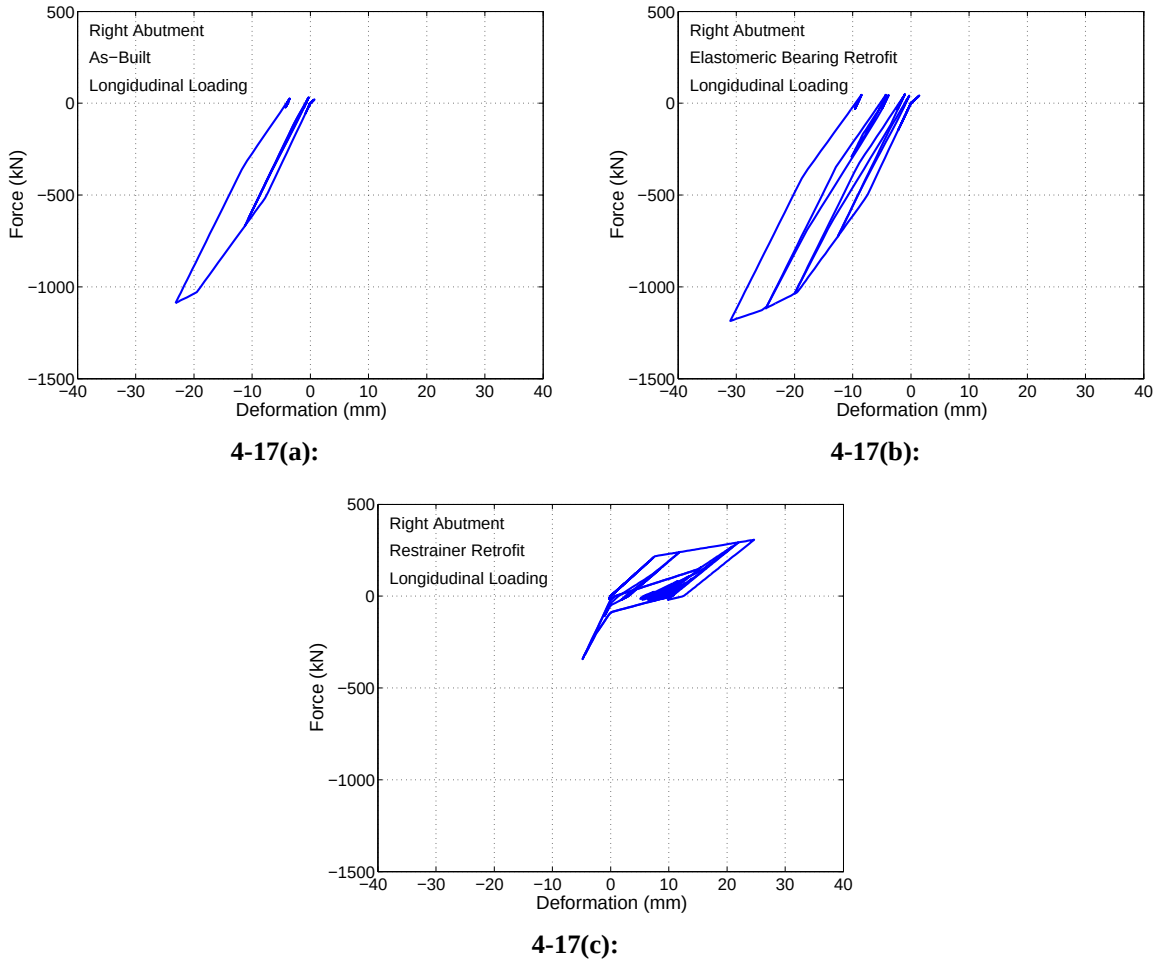

4-17(a): **4-17(b):**

4-17(c):

Figure 4-17: Longitudinal deformation of abutment for the (a) as-built MSC Steel bridge, bridge retrofit with (b) elastomeric bearings, and (c) restrainer cables.

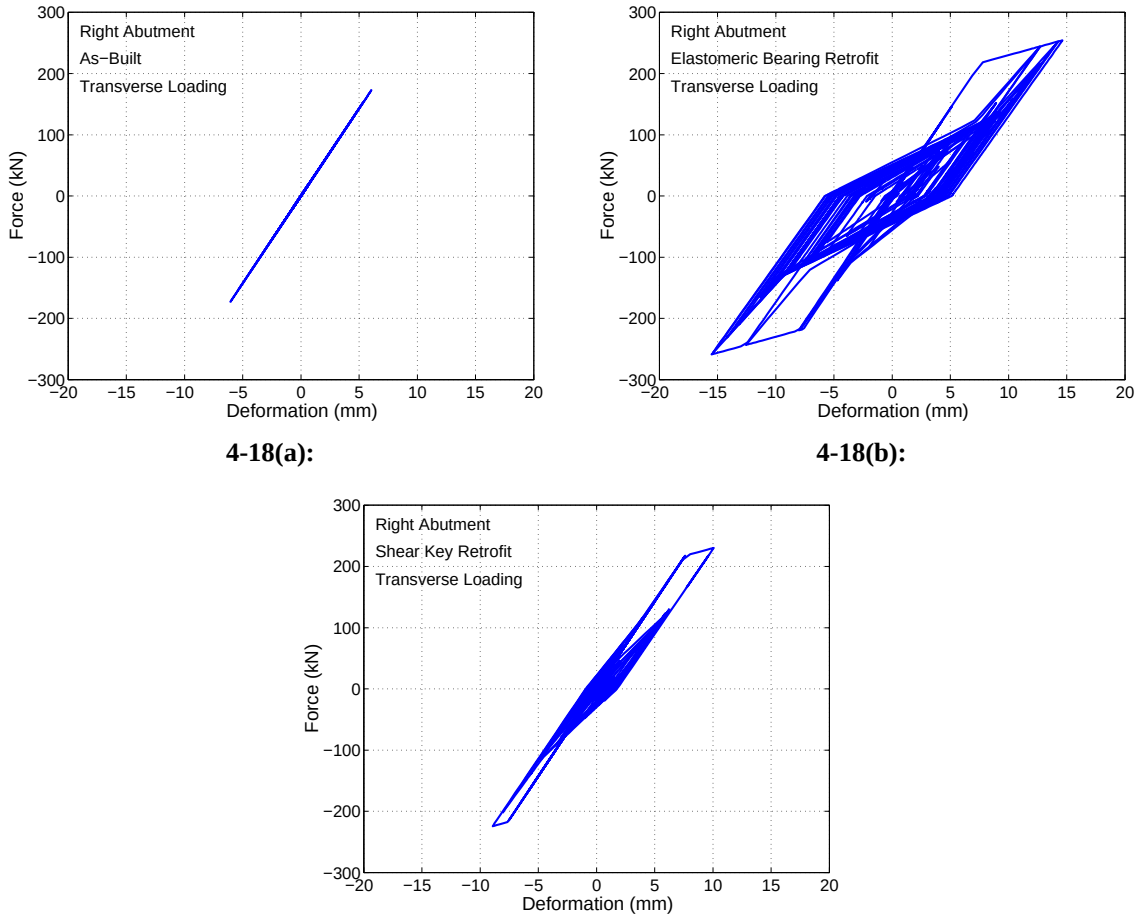

Figure 4-18: Force-deformation of right abutment in transverse direction: (a) as-built, (b) elastomeric bearing retrofit, and (c) shear key retrofit.

4.4.1.2 Retrofit Impact for Suite of Ground Motions

Composite results of the peak component responses (bearing deformations, abutments deformations, column ductility demands) using the suite of 10 ground motions provide further insight on the effect of retrofit on the response statistics for the MSC Steel bridge. Figure 4-19 provides box plots of the peak component responses for the bridge in its as-built condition, and retrofit with restrainer cables, steel jackets, elastomeric bearings, and shear keys.

A box plot presents a visual summary of several key statistical quantities of the responses and allows for comparison of how retrofitting the bridges affects the distribution of the peak component responses (Wu and Hamada, 2000). The boundary of the box plots represents the 25th and 75th percentiles of the peak component responses, while the whiskers plotted above and below the box represent the 5th and 95th percentile with outliers indicated. A black line is plotted in the box at the 50th percentile, or median value, and the dashed white line indicates the mean of the peak responses for the suite of time history analyses.

The mean peak transverse deformations of the steel fixed and expansion bearings in the MSC Steel bridge reach levels of potential damage, at 13.1 mm and 41.7 mm respectively. At these levels, the shear keys become effective in restricting transverse motion and reducing the bearing deformations. Toppling of the rocker bearings in the longitudinal direction is a particular concern for this bridge type, since past studies (Nielson and DesRoches, 2006; Saadeghvaziri and Rashidi, 1998) have indicated potential instability at a level of 94 mm, which is exceeded on average for the suite of ground motions. While the restrainers tend to reduce the deformation and variability in response, the mean peak deformations are only decreased to 82.8 mm because the restrainers often yield at such levels. This indicates that seat extenders may be a viable option to provide additional support length at the abutments in the case that the deck falls off of the supporting bearings. Alternatively, the use of elastomeric bearings is a feasible approach, since there is less potential for bearing damage.

As seen in Figure 4-19, the demands placed on the columns of the MSC Steel girder bridge are excessive, particularly in the longitudinal direction. The elastomeric bearings effectively decrease the ductility demands to well below μ=0.8, even at the 95th percentile,

and reduce the variability in column demands. Additionally, the peak curvature ductility demands placed on the columns retrofit with steel jackets are within an acceptable level, ranging from roughly μ_ϕ=1.6 to μ_ϕ=2.6 at the 5th and 95th percentiles, which are well below the ultimate capacity estimated at over μ_ϕ=30. In passive action, the use of elastomeric bearings increases the mean peak abutment deformations by nearly 64% from 16.0 mm to 26.3 mm again a result of pounding between the continuous deck and the abutments. The variability in response is also increased, with some responses exceeding 50 mm. The passive deformations are actually decreased through the use of the restrainer cable retrofit. The elastomeric bearings also increase the transverse deformations significantly to a mean of 20.4 mm, and the shear keys nearly double the deformations to 9.0 mm. Both increases can be attributed to the load transfer from the deck to the abutment through contact with either the shear key or bearing keeper plate.

4.4.2 Summary for All Bridges

The component responses that are evaluated as a part of the deterministic performance analysis are presented in Table 4-5, along with their abbreviations. The results of the deterministic seismic performance evaluation for the MSSS Steel, MSC Steel, MSSS Concrete, and MSC Concrete are summarized in Tables 4-6, 4-7, 4-8, and 4-9 respectively. These tables indicate the initial level of component response from time history analysis using the suite of Wen and Wu ground motions for the as-built bridge of each type. The impact of the different retrofit measures on the component response is identified based on whether the response was increased, decreased, or if the retrofit had a negligible effect. These summaries are anticipated to provide insight on the impact of different retrofit measures on the seismic

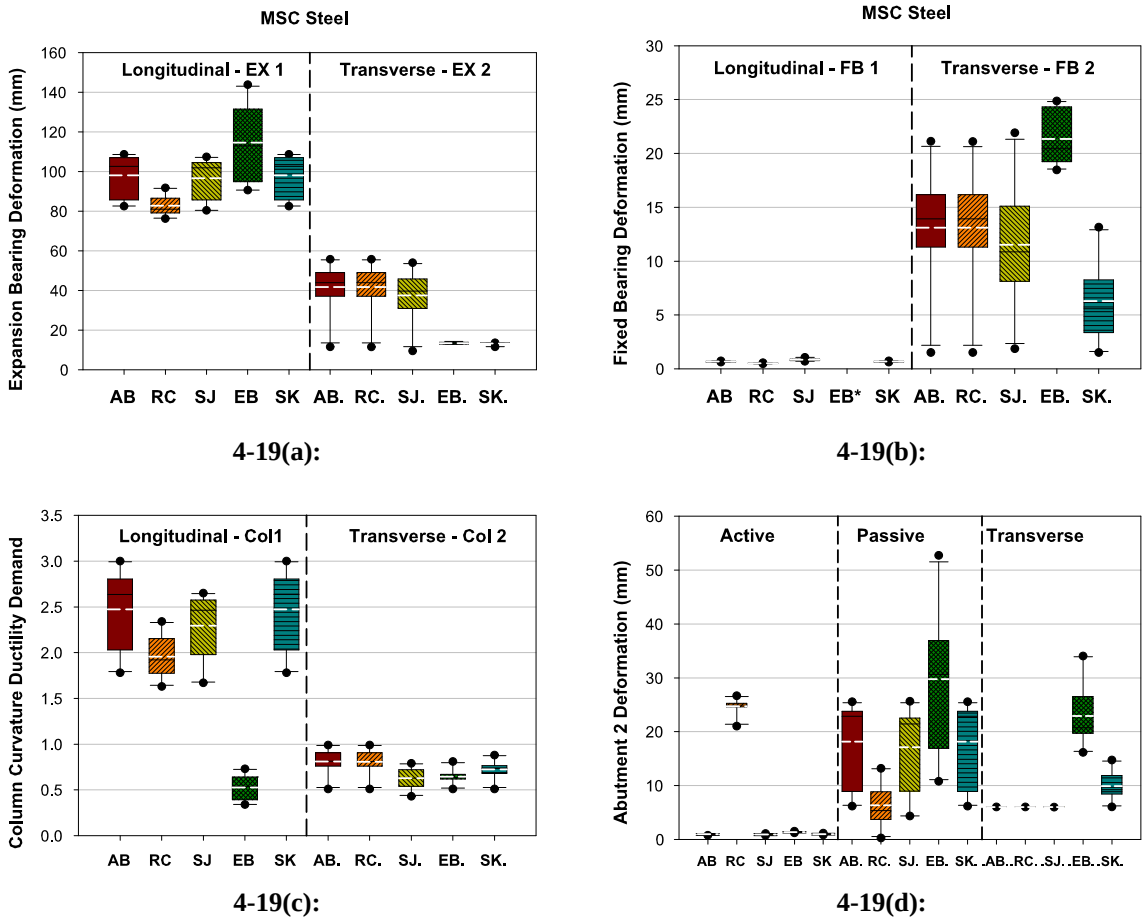

Figure 4-19: Box plot of component responses for retrofitted MSC steel girder bridge. (Note: The longitudinal Elastomeric Bearing (EB) deformations at the location of FB 1 are not shown for scaling purposes but are the same as those plotted at EX 1.)

Table 4-5: Abbreviations for Component Responses.

Component Response	Abbreviation
Longitudinal Deformation of Expansion Bearing	Exp-Long
Transverse Deformation of Expansion Bearing	Exp-Tran
Longitudinal Deformation of Fixed Bearing	Fb-Long
Transverse Deformation of Fixed Bearing	Fb-Tran
Column Curvature Ductility Demands under Longitudinal Loading	Col-Ductility-Long
Column Curvature Ductility Demands under Transverse Loading	Col-Ductility-Tran
Abutment Active Deformations	Ab-Act
Abutment Passive Deformations	Ab-Pass
Transverse Deformation of Abutment	Ab-Tran

response of each bridge type and their component response levels. It is noted, however, that these results are for a specific uniform hazard level (2% in 50 years) using ground motions developed for Memphis, TN.

Details on the seismic response of the retrofitted MSC Steel girder bridge were presented above in Section 4.4.1 and will not be revisited to avoid redundancy. However, summaries of the other bridge types follow.

The MSSS Steel girder bridge tends to have relatively high demands placed on the fixed and expansion bearings in the longitudinal direction and column demands indicative of potential damage. Since the typical MSSS Steel girder bridge exhibits predominant response and vulnerability in the longitudinal direction, the shear keys have little impact. The steel jackets provide ample capacity improvement in the columns and significantly reduce the likelihood for column damage in the MSSS Steel girder bridge, yet do not impact the response of other vulnerable components, such as the bearings. The restrainer cables reduce the rocker bearing deformations yet have little effect on the fixed bearings because of the initial slack in the cables. The column demands are slightly reduced by use of the cables

yet increase the active deformation of the abutments. The elastomeric bearings are highly effective in reducing potential component damage, and offer a potentially viable retrofit option. They considerably reduce the column demands by isolating the superstructure, and diminish the likelihood for bearing damage by replacing the vulnerable steel bearings with flexible isolation bearings. However, there are issues with increased pounding at the abutments.

The MSC Concrete girder bridge is heavier than the steel bridge and has relatively large deck displacements, bearing, and column demands. It is noted, however, that the bearings used in this bridge are more flexible than the steel bearings and can sustain larger deformations before damage is expected to occur. The mean peak expansion bearing deformations are reduced by roughly 20% with the restrainer cables and fixed bearings by only about 10%, because of the large inertial deck loads that tend to yield the restrainer cables and limit their effectiveness. The fairly high transverse bearing deformations are considerably reduced by use of the shear keys, yet this retrofit leads to an increase in abutment deformations in the transverse direction. It is interesting to note that the use of steel jackets in the MSC Concrete bridge slightly increases the transverse bearing deformations, which is attributed to the redistribution of forces due to slight stiffening of the columns from jacketing. Isolation of the superstructure by use of the elastomeric isolation bearings reduces the active deformations of the abutments considerably, and the demands placed on the columns (particularly in the longitudinal direction), yet still leads to an increase in the passive and transverse abutment deformations.

Table 4-6: MSSS Steel Retrofit Impact Summary.

	Response Level	Impact of Retrofit on Response			
Component	**As-Built**	**Restrainer Cable**	**Elastomeric Bearing**	**Steel Jacket**	**Shear Key**
Exp-Long	High	-	N/A	=	=
Exp-Tran	Low	=	N/A	=	=
Fb-Long	High	=	N/A	=	=
Fb-Tran	Medium	=	N/A	=	=
Col-Ductility-Long	Medium	-	-	=	=
Col-Ductility-Tran	Medium	=	=	=	=
Ab-Act	Low	+	-	=	=
Ab-Pass	Low	=	+	=	=
Ab-Tran	Low	=	+	=	=

* Increased (+), Reduced (-), Negligible impact (=)

Table 4-7: MSC Steel Retrofit Impact Summary.

	Response Level	Impact of Retrofit on Response			
Component	**As-Built**	**Restrainer Cable**	**Elastomeric Bearing**	**Steel Jacket**	**Shear Key**
Exp-Long	High	-	N/A	=	=
Exp-Tran	High	=	N/A	=	-
Fb-Long	Low	=	N/A	=	=
Fb-Tran	Medium	=	N/A	=	-
Col-Ductility-Long	High	-	-	=	=
Col-Ductility-Tran	Medium	=	-	-	=
Ab-Act	Low	+	=	=	=
Ab-Pass	Medium	=	+	=	=
Ab-Tran	Low	=	+	=	+

* Increased (+), Reduced (-), Negligible impact (=)

Table 4-8: MSSS Concrete Retrofit Impact Summary.

	Response Level	Impact of Retrofit on Response			
Component	**As-Built**	**Restrainer Cable**	**Elastomeric Bearing**	**Steel Jacket**	**Shear Key**
Exp-Long	Medium	-	N/A	=	=
Exp-Tran	High	=	N/A	+	-
Fb-Long	Medium	=	N/A	=	=
Fb-Tran	High	=	N/A	=	-
Col-Ductility-Long	Medium	+	-	-	=
Col-Ductility-Tran	Low	=	+	-	+
Ab-Act	Low	=	-	=	=
Ab-Pass	Low	=	+	=	=
Ab-Tran	Low	=	+	=	=

* Increased (+), Reduced (-), Negligible impact (=)

Table 4-9: MSC Concrete Retrofit Impact Summary.

	Response Level	Impact of Retrofit on Response			
Component	**As-Built**	**Restrainer Cable**	**Elastomeric Bearing**	**Steel Jacket**	**Shear Key**
Exp-Long	Medium	-	N/A	=	=
Exp-Tran	Medium	=	N/A	+	-
Fb-Long	Medium	=	N/A	=	=
Fb-Tran	Medium	=	N/A	+	-
Col-Ductility-Long	Medium	=	-	=	=
Col-Ductility-Tran	Medium	=	-	=	-
Ab-Act	Low	=	-	=	=
Ab-Pass	Low	-	+	=	=
Ab-Tran	Low	=	+	=	+

* Increased (+), Reduced (-), Negligible impact (=)

The MSSS Concrete girder bridge has particularly large deck and bearing displacements when excited in the transverse direction. The shear keys are effective in reducing these demands, yet result in transfer of forces to the columns and increase the column demands when excited in the transverse direction. The primary impact of the steel jacket is to increase the capacity of the columns, but for this bridge it actually leads to a slight increase in the transverse expansion bearing deformation and reduced curvature ductility demands on the columns themselves. The elastomeric isolation bearings do reduce the column demands in the longitudinal direction, yet due to the keeper plate detail, increased loading is actually transferred to the substructure when the earthquake has predominant motion in the transverse direction. While the active abutment deformations are reduced, the passive and transverse demands are increased. The restrainer cables have a slight impact on the response of the MSSS Concrete girder bridge by reducing the expansion bearing deformation in the longitudinal direction. However, the fixed bearing deformations are not significantly impacted, and it is noted that the fixed bearings located at the abutment still tends to have the largest deformations when the deck moves toward the abutment. The column supporting the left deck also has occasionally increased demands when the restrainer cables are employed.

4.5 Closure

Four typical bridge classes, common to the Central and Southeastern United States and found to have considerable vulnerability to earthquake damage, have been identified for retrofit evaluation. These include the MSSS Steel, MSC Steel, MSSS Concrete, and MSC Concrete girder bridges. Detailed three-dimensional analytical models were developed and

presented as a part of this Chapter and will be used in further studies. It is noted that the component models were validated against past test data in work by Nielson (2005a) and that the retrofitted components were modeled with a similar level of fidelity as a part of this work. Details on the retrofit measures evaluated can be found in Chapter 3.

This Chapter presented a deterministic evaluation of the impact of different retrofits on the seismic response of typical bridges using a suite of uniform hazard ground motions for the Memphis, TN region. The analyses highlighted the retrofits' impact on the response of various critical components within the bridge system. Traditional retrofit targets the improvement of individual components or response quantities, however may result in damage to other components. For example the use of the elastomeric isolation bearings reduces the column demands in the MSC Steel bridge, but increases the passive deformation demands placed on the abutments. The deterministic analyses pose critical considerations that should be made when adopting a retrofit strategy or designing a particular retrofit measure, such as which other components may be affected, and also provide an enhanced understanding of the seismic response of typical classes of retrofitted bridges. While valuable insights can be gained from these deterministic evaluations, conclusions on the overall impact of retrofit on the vulnerability of bridge classes are difficult to make. Probabilistic evaluation would allow for a depiction of the uncertainty in the ability of the retrofitted bridge to achieve a particular level of performance at a given seismic intensity level. The findings from this study illustrate the importance of considering multiple component performance measures when assessing and comparing retrofit strategies, and lend support to system-wide vulnerability assessments which consider the contribution of multiple components when assessing

retrofit impact. Such conclusions shall be considered and incorporated in the work of forth-coming chapters.

CHAPTER V

SENSITIVITY OF RETROFITTED BRIDGES TO MODELING PARAMETERS

A number of parameters that dictate the response of the 3-dimensional retrofitted bridges must be specified in the analytical models. Such parameters include bearing stiffness, concrete strength, deck-abutment gaps, incident angle of the earthquake, among others. Uncertainties such as geometric, material, or component response parameters of representative bridges in a portfolio likely exist due to structure-to-structure variation or variation over time.

There have been a number of studies which have evaluated the sensitivity of the seismic response of various components in bridges (such as bearing or column demands) to parameter variation through simplistic or robustly designed experiments (Jangid, 2004; Nielson and DesRoches, 2006; Saiidi et al., 1996). However, there is still a lack of overall understanding of the significance of a number of parameters in general classes of retrofitted bridges. A sensitivity study reveals how different levels of modeling parameters, in turn, affect the seismic response of the retrofitted bridge. Moreover, analysts are challenged with selecting a prudent level of uncertainty treatment while balancing the simulation and computational effort. Knowledge of the significance of each modeling parameter will provide insight as to whether its variation should be treated explicitly or may perhaps be neglected.

5.1 Uncertainty in Modeling Parameters

A number of sources of uncertainty are present in the modeling and performance assessment of portfolios of retrofitted bridges. Sources of uncertainty affecting structural performance are often characterized as either aleatoric or epistemic in nature. Aleatoric uncertainty refers to that which is inherently random, or stems from the unpredictable nature of events, whereas epistemic uncertainty is that which is due to a lack of knowledge, and stems from incomplete data, ignorance, or modeling assumptions. While the nature and sources of uncertainty are not always self-evident, many analytical modeling parameters can be attributed to a lack of knowledge of the actual bridge parameters (bearing stiffness, column height, etc.) and are epistemic in nature. Yet other parameters may stem from aleatoric uncertainty, including the inherent variability in material properties, such as the steel strength.

There are a number of analytical modeling parameters which are potentially variable in portfolios of retrofitted bridges. These parameters may be attributed to material strength, such as the yield strength of concrete or steel, which are the uncertain parameters that are often considered in vulnerability assessments. Other modeling parameters define the response of the bridge components, such as the stiffness of the bearings, coefficient of friction in the bearings, or stiffness of the foundations. Another group of uncertain modeling parameters can be attributed to the geometry of the bridges which are not included in the gross geometric properties such as the span length and column height. These additional geometric variables include such parameters as the gap between the decks, or between the

bridge deck and abutment. Each retrofit measure has a number of potentially variable parameters associated with it due to uncertainty in the retrofit design or realization of the material properties or component response parameters. As an example, for a bridge retrofit with restrainer cables, there is uncertainty in the yield strength of the restrainers, slack in the cables, and length of the cables.

Nielson (2005a) has identified probabilistic models and likely ranges in the realized values for approximately 14 modeling parameters associated with each class of as-built bridges. In addition to these parameters, uncertainties which are associated with each retrofit measure will be evaluated in this study. Details on the uncertainties associated with each retrofit measure will be presented, while the modeling parameters associated with the as-built structure can be found elsewhere (Nielson, 2005a).

5.1.1 Steel Jacket Modeling Parameters

As indicated in Chapter 3, past experimental tests have revealed that full height steel jackets can lead to a stiffness increase of the columns ranging from 20 to 40% (Priestley et al., 1996). With little further information on the probability distribution, a uniform distribution is assumed for the imposed additional column stiffness due to jacketing, $K_j \sim$ U(20, 40)%. This assumption is made throughout the study when sufficient information on the probability distribution is not available to roughly account for uncertainty in the parameter realization. The A36 steel jackets have a lognormal distribution for the jacket yield strength based on the work by Hess et al. (2002) and Galambos and Ravindra (1978), with parameters f_{yj} (MPa) $\sim$ LN($\lambda = 5.60, \zeta = 0.078$). The final uncertain parameter considered is the gap between the steel jacket and existing column. This gap variation affects the

total diameter of the steel jacket, radial confining stress, and compressive strength of the confined concrete, as shown in Equations 3.2 and 3.1 from Chapter 3. Typical designs have gaps ranging from 12.7 to 25.4 mm (Priestley et al., 1996), and the parameter is assumed to have a uniform distribution, $Gap_j \sim$ U(12.7, 25.4) mm.

5.1.2 Elastomeric Isolation Bearing Modeling Parameters

The gap between the keeper plate and elastomeric bearing may vary from design to design, yet potentially have a large impact on the transverse response of the isolated bridge. Based on a review of current practice, this gap tends to be on the order of 6.4 to 19.1 mm and is modeled with a uniform distribution ($Gap_{keeper} \sim$ U(6.4,19.1)mm). The stiffness of the elastomeric bearing is influenced by temperature among other parameters, which leads to a range of stiffness values that a given bearing may assume under field conditions (Hwang et al., 2002). For example, data from the HITEC (1998) testing program has revealed that for typical elastomeric bearings tested at low (-26 °C) and high (48.9 °C) temperatures, the corresponding change in bearing stiffness is -9% and +23%. Coupled with this is uncertainty in the actual bearing design dimensions which could in turn affect the effective bearing stiffness, K_{eff-eb}. Recalling that Stanton (1997) recommended that typical bridge isolation bearing shape factors range from 8 to 12, and to account for variation due to temperature and field conditions, a uniformly distributed range of effective bearing stiffnesses are assumed for each bridge class. The K_{eff-eb} parameter models for the MSSS Steel, MSC Steel, MSSS Concrete, and MSC Concrete bridges are U(420.3, 840.6)N/mm, U(367.8, 648.0)N/mm, U(175.1, 245.2)N/mm, and U(157.6, 227.7)N/mm respectively.

5.1.3 Restrainer Cable Modeling Parameters

The primary parameters which affect the performance of the restrainer cables are the cable slack, length, and yield strength. Work by Saiidi et al. (1996) indicates that the extreme low and high ambient temperatures may lead to restrainer cable slack between 0 and 19.1 mm, which is modeled by a uniform distribution, $Slack \sim$ U(0, 19.1)mm. A review of current Central and Southeastern US practice has revealed that the typical restrainer cable lengths are on the order of 1.52 m to 3.05 m ($L_{cab} \sim$ U(1.52,3.05)m). Uncertainty in this geometric property, in turn, affects the stiffness of the cable. It is presumed that the yield stress of the high strength steel cable reported by Caltrans (1997) of f_{ycab}=1214 MPa is the median value and that the strength can be modeled by a lognormal distribution with a COV=0.10 (Hess et al., 2002). This results in a probabilistic model of f_{ycab} (MPa) $\sim$ LN($\lambda = 7.10, \zeta = 0.10$).

5.1.4 Shear Key Modeling Parameters

Two uncertain parameters associated with the shear keys are considered. This includes the yield strength of the reinforcement steel, which building upon past work is modeled f_{ys-sk} (MPa) $\sim$ LN($\lambda = 6.13, \zeta = 0.08$) (Nielson, 2005a). Variation in the reinforcement steel strength of the shear key alters the force at which it is expected to yield when loaded transversely. The final parameter considered is the uncertainty in the realized gap before the shear key engages. Based on current practice (Yashinsky, 2006), the gap is considered to range from 6.4 to 19.1 mm ($Gap_{sk} \sim$ U(6.4,19.1)mm).

5.2 Parameter Screening of Retrofitted Bridges

Since there are a considerable number of uncertain modeling parameters, a screening study using design of experiments (DOE) principles is performed to assess which modeling parameters significantly affect component responses in each type of retrofitted bridge. The primary objective of the study is to identify critical modeling parameters whose variability has a significant impact on the seismic response of the bridge. A secondary benefit of the study is enhanced understanding of how different levels of the parameters influence the retrofitted bridge response. For example, how might using a longer restrainer cable affect the peak bearing deformations? The retrofitted multi-span continuous concrete girder bridge (MSC Concrete) is used as an example for the study, and a summary of the findings for each bridge will be presented. Identified significant parameters will later be tested in Chapter 7 to evaluate the impact of propagating these sources of uncertainty through the fragility assessment. The responses considered in the study include the longitudinal and transverse deformations of the fixed and expansion bearings, the curvature ductility demands on the columns, and the passive, active, and transverse deformations of the abutments. The study examines the significance of varying the modeling parameters over their range of potential realizations for each of the eight critical bridge responses.

A two level fractional factorial design where no main effects are aliased with one another is used for the experiment. The design pattern is generated with the aid of the statistical analysis program JMP (SAS, 2004). For our study, this requires 32 runs with various combinations of high and low levels of the bridge and retrofit parameters (factors). The high and low levels are set to encompass a reasonable range that the random variable may

assume based on its probabilistic model. For the experiments performed as a part of this work, this results in resolution III or IV designs, as is typical for screening experiments. An example of the screening design matrix for the MSC Concrete girder bridge retrofit with shear keys is shown in Table 5-1. Table 5-2 lists the high and low levels for of the parameters considered in the screening studies of all retrofitted bridge classes. This includes parameters associated with the existing bridge structures (Nielson, 2005a), as well as the retrofitted parameters whose probabilistic models are detailed above in Section 5.1. The 5^{th} and 95^{th} percentiles of the lognormally distributed retrofitted parameters are taken to be the lower (-) and upper (+) levels.

There are inherently heterogeneous qualities of bridges within a given class–most notably the variation in macroscopic characteristics such as span length, column height, and deck width. These gross geometric parameters are accounted for by the use of a blocking scheme in which eight different base bridge geometries are treated as separate blocks in the experiment. The blocks are intended to group the runs into homogeneous units and compare the treatments within blocks, as well as examine the differences between the blocks (Wu and Hamada, 2000). The eight base bridge geometries, or geometric samples, for each bridge class were proposed by (Nielson, 2005a) based on an assessment of the distribution of geometric properties and detailed CSUS inventory analysis. These geometric samples are shown for each of the four bridge types in Table 5-3. It is noted that all of the bridges examined in this study have three spans, which is the most commonly occurring number of spans in the CSUS inventory.

Additionally, the experiment is replicated two times using a total of three different earthquake time histories, resulting in 96 simulations for each retrofit type. Thus, we are trying

Table 5-1: Example Design Matrix for MSC Concrete with Shear Keys.

Run	Block	Parameter Level															
		1	**2**	**3**	**4**	**5**	**6**	**7**	**8**	**9**	**10**	**11**	**12**	**13**	**14**	**15***	**16***
1	8	-	-	-	-	-	-	-	-	-	-	-	-	-	-	-	-
2	1	-	-	-	-	+	+	+	+	+	+	+	+	-	-	-	-
3	1	-	-	-	+	-	+	+	+	+	-	-	-	+	+	+	-
4	8	-	-	-	+	+	-	-	-	-	+	+	+	+	+	+	-
5	5	-	-	+	-	-	+	+	-	-	+	+	-	+	+	-	+
6	4	-	-	+	-	+	-	-	+	+	-	-	+	+	+	-	+
7	4	-	-	+	+	-	-	-	+	+	+	+	-	-	-	+	+
8	5	-	-	+	+	+	+	+	-	-	-	-	+	-	-	+	+
9	3	-	+	-	-	-	+	-	+	-	+	-	+	+	-	+	+
10	6	-	+	-	-	+	-	+	-	+	-	+	-	+	-	+	+
11	6	-	+	-	+	-	-	+	-	+	+	-	+	-	+	-	+
12	3	-	+	-	+	+	+	-	+	-	-	+	-	-	+	-	+
13	2	-	+	+	-	-	-	+	+	-	-	+	+	-	+	+	-
14	7	-	+	+	-	+	+	-	-	+	+	-	-	-	+	+	-
15	7	-	+	+	+	-	+	-	-	+	-	+	+	+	-	-	-
16	2	-	+	+	+	+	-	+	+	-	+	-	-	+	-	-	-
17	2	+	-	-	-	-	+	-	-	+	-	+	+	-	+	+	+
18	7	+	-	-	-	+	-	+	+	-	+	-	-	-	+	+	+
19	7	+	-	-	+	-	-	+	+	-	-	+	+	+	-	-	+
20	2	+	-	-	+	+	+	-	-	+	+	-	-	+	-	-	+
21	3	+	-	+	-	-	-	+	-	+	+	-	+	+	-	+	-
22	6	+	-	+	-	+	+	-	+	-	-	+	-	+	-	+	-
23	6	+	-	+	+	-	+	-	+	-	+	-	+	-	+	-	-
24	3	+	-	+	+	+	-	+	-	+	-	+	-	-	+	-	-
25	5	+	+	-	-	-	-	-	+	+	+	+	-	+	+	-	-
26	4	+	+	-	-	+	+	+	-	-	-	-	+	+	+	-	-
27	4	+	+	-	+	-	+	+	-	-	+	+	-	-	-	+	-
28	5	+	+	-	+	+	-	-	+	+	-	-	+	-	-	+	-
29	8	+	+	+	-	-	+	+	+	+	-	-	-	-	-	-	+
30	1	+	+	+	-	+	-	-	-	-	+	+	+	-	-	-	+
31	1	+	+	+	+	-	-	-	-	-	-	-	-	+	+	+	+
32	8	+	+	+	+	+	+	+	+	+	+	+	+	+	+	+	+

*=retrofit parameter

Table 5-2: Parameters in the Screening Study of Retrofitted Bridges.

Description	Abbreviation	Lower Level	Upper Level	Units
Existing/As-Built Parameters				
Concrete strength	Conc Str	26.4	40.6	MPa
Steel strength	Steel Str	438	555	MPa
Coefficient of friction for elastomeric pads	Pad Frict	50	150	%
Initial stiffness of elastomeric pads	Pad Stiff	50	150	%
Dowel strength	Dowel Str	80	120	%
Gap at dowels for expansion bearing only	Dowel Gap	0	50.8	mm
Coefficient of friction for steel expansion bearing	Exp Frict	50	150	%
Coefficient of friction for steel fixed bearing	Fxd Frict	50	150	%
Initial stiffness of steel fixed bearing	Fxd Stiff	80	120	%
Initial stiffness of passive abutment	Ab-Pas Stf	50	150	%
Initial Stiffness of active abutment	Ab-Act Stf	50	150	%
Rotational stiffness of foundations	Fnd-Rot Stf	50	150	%
Translational stiffness of foundations	Fnd-Hor Stf	50	150	%
Mass	Mass	90	110	%
Damping ratio	Damp Ratio	0.02	0.08	ratio
Gap between abutments and decks (MSSS Concrete)	Abut Gap	36	40	mm
Gap between abutments and decks (MSSS Steel)	Abut Gap	28	48	mm
Gap between abutments and decks (MSC Conc & Steel)	Abut Gap	37	116	mm
Gap between adjacent decks (MSSS Concrete)	Deck Gap	20	31	mm
Gap between adjacent decks (MSSS Steel)	Hinge Gap	18	33	mm
Loading direction (Long or Trans)	Load Dir	L	T	
Steel Jacket Parameters				
Yield strength of jacket	Jacket Str	237.9	307.5	MPa
Gap between column and jacket	Jacket Gap	12.7	25.4	mm
Stiffness increase due to jacket	Jacket Stiff	20	40	%
Elastomeric Isolation Bearing Parameters				
Gap to keeper plate	Keeper Gap	6.4	19.1	mm
Elastomeric bearing stiffness (MSSS Steel)	Elasto Stf	420.3	840.6	N/mm
Elastomeric bearing stiffness (MSC Steel)	Elasto Stf	367.8	648.0	N/mm
Elastomeric bearing stiffness (MSSS Concrete)	Elasto Stf	175.1	245.2	N/mm
Elastomeric bearing stiffness (MSC Concrete)	Elasto Stf	157.6	227.7	N/mm
Restrainer Cable Parameters				
Yield strength of cable	Cable Str	149.5	207.5	MPa
Slack in restrainer cable	Slack Cab	0	19.1	MPa
Restrainer cable length	Length Cab	1.52	3.05	m
Shear Key Parameters				
Shear key steel reinforcement strength	SK Reinf Str	438.5	555.7	MPa
Gap to shear key	Gap to SK	6.4	19.1	mm

Table 5-3: Geometric Bridge Samples for Each Bridge Class from Nielson (2005a).

Bridge No.	Spans	Max Span Length (m)	Deck Width (m)	Column Height (m)
MSSS Steel Girder Bridge				
1	3	18.30	8.70	5.10
2	3	20.40	8.00	3.62
3	3	15.50	4.90	5.95
4	3	13.70	10.50	4.02
5	3	25.60	29.70	3.54
6	3	7.30	5.50	3.90
7	3	8.80	7.40	4.26
8	3	10.40	12.80	6.62
MSC Steel Girder Bridge				
1	3	13.40	13.00	3.72
2	3	39.00	12.90	3.49
3	3	25.10	10.20	3.93
4	3	29.90	14.50	5.42
5	3	18.20	20.10	4.20
6	3	19.80	5.50	5.76
7	3	22.30	10.30	4.08
8	3	40.80	7.90	6.74
MSSS Concrete Girder Bridge				
1	3	7.60	8.20	4.43
2	3	9.10	7.50	3.34
3	3	10.70	12.60	3.74
4	3	20.10	8.60	4.00
5	3	13.40	10.40	4.23
6	3	9.40	9.20	6.01
7	3	12.20	18.60	6.06
8	3	27.40	6.60	3.88
MSC Concrete Girder Bridge				
1	3	39.60	21.20	4.00
2	3	22.60	12.80	3.93
3	3	18.90	10.80	6.29
4	3	21.00	8.00	3.19
5	3	26.20	13.10	4.20
6	3	10.40	14.10	3.64
7	3	14.50	8.70	4.46
8	3	15.20	9.80	5.93

to reduce the impact of a single ground motion's characteristics such as peak ground acceleration, frequency content, or strong motion duration on the response. The records used in this sensitivity study are the same records selected by Nielson and DesRoches (2006) for evaluation of as-built bridge sensitivity. These are three synthetic ground motion records that were developed for Memphis, TN by Rix and Fernandez (2004), with magnitudes of 5.5, 6.5 and 7.5 and epicentral distances of 10 km, 10 km and 20 km respectively. The peak ground accelerations are 0.217g, 0.484g and 0.646g and durations are 8.06, 13.45 and 25.09 seconds. It is noted that loading direction itself is also considered as a potentially variable parameter, and the sensitivity study evaluates if bridge response is significantly impacted by loading the bridge in the longitudinal or transverse direction.

A run of the experiment consists of performing a nonlinear time history analysis in *OpenSees* of the bridge sample generated with the above specified parameter levels (treatments) for a defined input ground motion. Since this is an analytical experiment, randomization and repetition are not necessary. The eight different peak component responses are monitored in each run in order to facilitate statistical analysis of the importance of each modeling parameter.

A separate analysis of variance (ANOVA) is performed to evaluate the sensitivity of each component response to variation in the modeling parameters. Through this analysis of variance, a null hypothesis is tested which states that the coefficient of regression for the multiple linear regression model of our experiment is zero (or the effect of varying the parameter is insignificant). In this assessment $p-values$ are computed in order to interpret the results of the hypothesis test. A $p-value$ is defined as the probability of rejecting the null hypothesis, or the probability that the variation between conditions occurred by chance

(Wu and Hamada, 2000). The formulation for calculation of ANOVA tables including $p-values$ can be found in most statistical analysis texts (Hines et al., 2003), and the general form of an ANOVA table for a fractional factorial design with blocking is presented in Nielson (2005a). Smaller $p-values$ indicate stronger evidence for rejecting the null hypothesis (higher statistical significance). For this study, parameters with a $p-value$ less than a cut-off of α=0.05 are considered significant.

5.2.1 Example with MSSS Concrete Bridge

The results of the sensitivity study for the multi-span simply supported concrete girder bridge with the four different retrofit measures having uncertain modeling parameters is detailed below. This is intended to provide insight on the screening of modeling parameters for a single class of bridges, while the composite results for all bridge types will follow.

5.2.1.1 Steel Jackets

The $p-values$ from an ANOVA of the MSSS Concrete bridge retrofit with Steel Jackets are presented in Table 5-4. Boldface values indicate that the modeling parameter has a significant effect ($p-value < \alpha$=0.05) on the component response of interest. Those parameters that have a significant effect on at least three responses are shown above the horizontal line, and are identified as the *most* significant modeling parameters. Boldface modeling parameters are those which are associated with the retrofit measure. The significance of the blocking (difference in base bridge geometry) is also indicated at the bottom of the Table. For this particular bridge type, the gap between the steel jacket and column was found to be the most significant of the modeling parameters associated with the retrofit itself. As one would intuitively expect, loading in the transverse or longitudinal direction significantly

Table 5-4: P-Values for MSSS Concrete with Steel Jackets.

Parameter	P-Value							
	Ab-Act	**Ab-Pass**	**Ab-Tran**	**Ductility**	**Exp-Long**	**Exp-Tran**	**Fb-Long**	**Fb-Tran**
Load Dir	**0.000**	**0.000**	**0.000**	**0.000**	**0.000**	**0.000**	**0.000**	**0.000**
Jacket Gap	**0.000**	0.320	**0.000**	0.554	**0.011**	0.736	**0.002**	0.762
Ab-Act Stf	**0.000**	0.269	**0.000**	0.594	0.093	0.741	**0.024**	0.772
Dowel Str	**0.008**	0.802	**0.004**	0.677	0.899	0.625	0.858	0.495
Pad Frict	0.626	0.593	0.569	0.082	0.098	**0.008**	0.064	**0.006**
Mass	0.132	0.118	**0.000**	0.671	0.893	**0.036**	0.975	0.110
Ab-Pas Stf	**0.017**	**0.015**	0.634	0.373	0.968	0.937	0.980	0.763
Fnd-Rot Stf	0.101	0.549	**0.000**	**0.016**	0.937	0.636	0.998	0.706
Jacket Str	**0.016**	0.350	**0.026**	0.751	0.248	0.626	0.319	0.495
Damp Ratio	0.192	0.365	**0.000**	0.064	0.307	0.059	0.283	0.186
Conc Str	0.219	0.692	**0.002**	0.264	0.471	0.630	0.620	0.710
Pad Stiff	0.432	0.358	**0.001**	0.205	0.277	0.308	0.276	0.194
Dowel Gap	**0.004**	0.970	0.791	0.529	0.209	0.591	0.301	0.685
Steel Str	0.699	0.680	0.830	**0.016**	0.465	0.681	0.299	0.644
Jackt Stiff	**0.029**	0.477	0.655	0.505	0.600	0.805	0.344	0.866
Fnd-hor Stf	0.515	0.897	0.258	0.751	0.864	0.566	0.919	0.748
Abut Gap	0.217	0.866	0.053	0.305	0.680	0.583	0.823	0.782
Hinge Gap	0.184	0.962	0.062	0.786	0.409	0.675	0.488	0.636
Block	**0.000**	**0.002**	**0.000**	**0.000**	**0.001**	**0.048**	**0.001**	**0.009**

affects the response of most bridge components, as does the blocking. It is interesting to note that the parameters that are found to be the most significant in this screening study (other than the one retrofit parameter), are the same as those that Nielson (2005a) identified for the as-built bridge. This can be explained by the fact that the MSSS Concrete bridge responds very similarly with and without the steel jackets, as illustrated in Chapter 4. This retrofit measure primarily affects the column capacity.

5.2.1.2 Elastomeric Bearings

When elastomeric isolation bearings are used to replace the existing bearings, any parameters associated with the elastomeric pads are eliminated. Thus this experiment has the fewest number of parameters to examine, and the responses monitored are limited. While several parameters affect at least one component response, such as the damping for column

Table 5-5: P-Values for MSSS Concrete with Elastomeric Bearings.

Parameter	P-Value					
	Ab-Act	**Ab-Pass**	**Ab-Tran**	**Ductility**	**EB-Long**	**EB-Tran**
Load Dir	**0.000**	**0.000**	**0.000**	**0.000**	**0.000**	0.076
Keeper Gap	0.995	0.958	**0.030**	**0.032**	**0.000**	0.869
Ab-Act Stf	**0.000**	0.781	**0.000**	0.096	0.391	0.934
Abut Gap	**0.000**	0.486	0.789	**0.001**	0.891	0.564
Conc Str	0.956	0.928	0.721	0.444	0.973	**0.000**
Steel Str	0.956	0.797	0.488	**0.000**	0.784	0.392
Fnd-Rot Stf	0.927	0.926	0.167	0.155	0.593	**0.000**
Mass	0.664	0.527	0.149	0.102	0.458	**0.000**
Elasto Stf	0.079	0.919	0.707	0.075	0.746	**0.000**
Damp Ratio	0.561	0.619	0.241	**0.001**	0.504	0.668
Ab-Pas Stf	0.396	0.340	0.502	0.198	0.899	0.767
Fnd-hor Stf	0.646	0.895	0.559	0.692	0.845	0.244
Block	**0.000**	**0.002**	**0.001**	**0.000**	1.000	**0.000**

demands, mass for transverse bearing deformations, or abutment gap for the active abutment deformations and column demands, only one parameter other than the loading and blocking is significant for at least three responses. This is the gap between the keeper plate and elastomeric bearing, as shown in Table 5-5.

5.2.1.3 Restrainer Cables

Table 5-6 shows the $p-values$ calculated in the ANOVA of the MSSS Concrete bridge retrofit with Restrainer Cables. As found with the other retrofits and as-built bridge, variation in the loading direction, abutment active stiffness, and blocking are significant considerations. The slack in the restrainer cables has a considerable influence on the response of the abutments and bearings in the longitudinal direction. Though variation in the other restrainer parameters do not affect the components, further evidence is revealed in the study that the restrainers considerably alter the seismic response of the as-built bridge system.

Table 5-6: P-Values for MSSS Concrete with Restrainer Cables.

Parameter	P-Value							
	Ab-Act	**Ab-Pass**	**Ab-Tran**	**Ductility**	**Exp-Long**	**Exp-Tran**	**Fb-Long**	**Fb-Tran**
Load Dir	**0.000**	**0.000**	**0.000**	**0.000**	**0.000**	0.065	**0.000**	0.065
Ab-Act Stf	**0.000**	**0.014**	**0.000**	**0.001**	**0.002**	0.406	**0.000**	0.402
Slack Cab	**0.000**	0.113	**0.000**	0.131	**0.030**	0.405	**0.002**	0.402
Pad Stiff	0.898	**0.001**	0.595	**0.004**	**0.023**	0.574	**0.047**	0.579
Fnd-Rot Stf	0.148	**0.072**	**0.000**	**0.011**	**0.027**	0.495	0.230	0.476
Damp Ratio	**0.040**	0.065	**0.033**	**0.018**	**0.008**	0.159	0.083	0.173
Pad Frict	0.642	**0.012**	0.890	0.060	**0.002**	0.252	**0.004**	0.252
Conc Str	0.108	0.010	**0.001**	0.141	**0.048**	0.124	**0.030**	0.135
Mass	0.284	0.667	**0.001**	**0.006**	0.347	0.183	0.422	0.171
Ab-Pas Stf	**0.002**	**0.048**	0.230	0.794	0.984	0.186	0.135	0.187
Dowel Gap	**0.000**	0.082	0.363	0.872	0.767	0.485	0.168	0.491
Steel Str	0.939	0.143	0.262	**0.000**	0.658	0.586	0.544	0.563
Abut Gap	0.117	0.282	**0.012**	0.359	0.843	0.417	0.608	0.438
Dowel Str	0.328	0.552	0.929	0.160	0.407	0.166	**0.028**	0.163
Hinge Gap	**0.037**	0.356	0.066	0.486	0.498	0.515	0.976	0.538
Fnd-hor Stf	0.575	0.347	0.058	0.633	0.427	0.241	0.348	0.223
Cable Str	0.270	0.747	0.837	0.490	0.950	0.163	0.207	0.160
Length Cab	0.5673	0.8688	0.2273	0.573	0.6913	0.5192	0.8789	0.5139
Block	**0.000**	**0.000**	**0.000**	**0.000**	**0.000**	0.470	**0.000**	0.470

This is illustrated by the fact that new parameters are now found to be significant in affecting the response, including the bearing pad stiffness, rotational stiffness of the foundation, damping ratio, bearing pad friction, and concrete strength.

5.2.1.4 Shear Keys

The final retrofit measure which affects the analytical modeling of the MSSS Concrete bridge is the use of shear keys, which has two potentially variable modeling parameters. It is noted that with the shear keys installed, which considerably alter the transverse response of the bridge, a number of modeling parameters are now found to significantly impact the transverse component responses, such as the transverse fixed and expansion bearing deformations. The gap to the shear key are found to have a significant effect on these transverse bearing deformations. While variation in the shear key modeling parameters are

Table 5-7: P-Values for MSSS Concrete with Shear Keys.

Parameter	P-Value							
	Ab-Act	**Ab-Pass**	**Ab-Tran**	**Ductility**	**Exp-Long**	**Exp-Tran**	**Fb-Long**	**Fb-Tran**
Load Dir	**0.000**	**0.000**	**0.000**	**0.000**	**0.000**	**0.000**	**0.000**	**0.000**
Fnd-Rot Stf	0.468	**0.001**	0.231	**0.010**	**0.009**	0.079	0.098	0.100
Mass	0.971	0.482	**0.017**	0.797	0.962	**0.003**	0.804	**0.002**
Steel Str	0.339	0.267	0.325	**0.015**	0.954	**0.026**	0.596	**0.032**
Pad Frict	0.080	0.379	0.535	0.969	**0.042**	0.054	**0.046**	**0.044**
Ab-Act Stf	**0.000**	0.305	**0.000**	0.502	0.105	0.774	0.110	0.820
Pad Stiff	0.369	0.147	0.881	0.523	0.452	**0.002**	0.181	**0.002**
Gap to SK	0.530	0.397	0.234	0.462	0.703	**0.006**	0.892	**0.008**
Abut Gap	0.893	0.745	0.433	0.650	0.684	**0.009**	0.803	**0.013**
Damp Ratio	0.068	**0.026**	0.282	**0.001**	0.179	0.972	0.438	0.994
Dowel Str	0.503	0.821	0.571	0.722	0.338	**0.028**	0.174	**0.033**
Ab-Pas Stf	0.301	**0.016**	0.806	0.316	0.742	0.109	0.410	0.126
Dowel Gap	0.195	0.174	0.474	0.519	0.375	0.191	0.934	0.306
Fnd-hor Stf	0.730	0.243	0.373	0.449	0.471	0.975	0.978	0.803
Conc Str	0.467	0.510	0.416	0.227	0.447	0.351	0.451	0.287
Hinge Gap	0.368	0.892	0.266	0.349	0.326	0.964	0.379	0.779
SK Reinf St	0.286	0.094	0.795	0.101	0.672	0.361	0.311	0.403
Block	0.499	**0.000**	0.234	**0.000**	**0.001**	**0.010**	**0.006**	**0.007**

not found to be among the most significant parameters, a number of other parameters affect the response of at least three responses. These are indicated in Table 5-7.

5.2.1.5 Comparison of Select Main Effects

The ANOVA provided a robust approach for evaluating the significance of varying uncertain modeling parameters and screening important parameters. Another approach for assessing the sensitivity of the bridge response quantities to the various parameters is to analyze the main effects of the factors considered. In general terms, the main effects are computed by

$$ME(B) = \bar{y}(B+) - \bar{y}(B-) \tag{5.1}$$

where $ME(B)$ denotes the main effect of parameter B, $\bar{y}(B+)$ is the mean of the y responses when parameter B is at its high level, and $\bar{y}(B-)$ is the mean of the y responses when B is at its low level. In order to visually screen those parameters which significantly affect the responses, we can examine the main effects plots. The values of $\bar{y}(B+)$ and $\bar{y}(B-)$ are plotted on the y-axis, with $B+$ and $B-$ on the x-axis. For rapid parameter screening, the main effects plots with the steepest slopes indicate the most significant parameters influencing a given response. The primary reason for presenting some select main effects plots is not to be redundant in parameter screening, but to provide further insight as to how varying parameters influences the bridge response. The main effects plots indicate whether the high or low value of a modeling parameter tends to increase or decrease the response quantity of interest.

A sample set of main effects plots are shown in Figure 5-1 that compare the impacts of varying select modeling parameters on the column curvature ductility demands and the expansion bearing deformations in the longitudinal direction for the MSSS Concrete girder bridge. The main effects are shown for the as-built bridge and retrofit with steel jackets, restrainer cables, elastomeric bearings, and shear keys in order to examine the difference in modeling parameter significance. When the MSSS Concrete bridge is loaded in the transverse direction (+) for all of the retrofitted bridges except the elastomeric bearings, the column ductility demands tend to be larger. When retrofit with steel jackets, the column demands tend to be more sensitive to variation in the loading direction than for the other retrofits. Figure 5-1 indicates that the column demands are not as sensitive to the variation in mass as they are to loading direction. However, the bridge retrofit with restrainer cables is most sensitive to this potential change in realized mass.

The main effects plots in Figure 5-1(c) reveal that the sensitivity of the expansion bearing deformations in the different retrofitted bridges to abutment active stiffness does not vary much from one retrofit type to another. This is indicated by a fairly consistent slope, despite the change in the magnitude of deformation demands. Figure 5-1(d) illustrates the impact that the retrofits have on the as-built bridge response and sensitivity to parameter variation. For example, the elastomeric bearings are no longer sensitive to variation in the hinge gap (deck-to-deck gap), and the use of restrainers change the trend in expansion bearing response for given high and low levels of gap relative to the as-built bridge.

5.2.2 Summary for All Bridges

Table 5-8 summarizes the findings of the ANOVA for each retrofitted bridge type. Any modeling parameter which significantly affects at least three component responses for the given retrofitted bridge is shown in the table. Interpretation of the ANOVA tables presented by Nielson (2005a) permits the most significant parameters for the bridge in its as-built condition to be presented for comparison. The sensitivity to blocking is not listed in the table, as it is not truly a factor, or modeling parameter, from the DOE. However, the results of the study reveal that for every bridge type and retrofit measure, the blocking effect is significant. Thus the difference in gross geometric properties of the bridges has a considerable impact on the bridge response, as one might expect. Additionally, the difference in loading the bridge primarily in the longitudinal or transverse direction has a significant impact on the response of the bridge, regardless of bridge or retrofit type. Other bridge modeling parameters that tend to be important for a range of bridge and retrofit measures include the

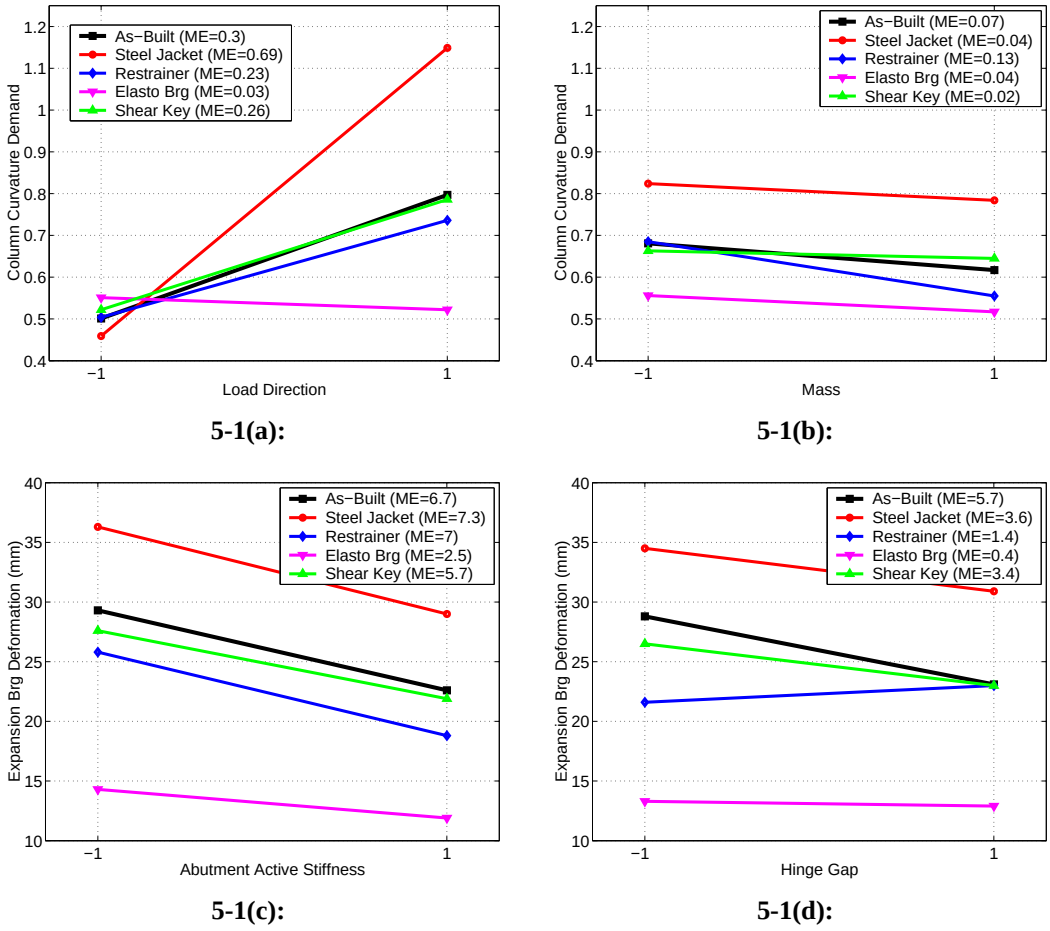

Figure 5-1: Main effects plots revealing how variation in modeling parameters affects the (a,b) column demands or (c,b) longitudinal expansion bearing deformations in the as-built and retrofitted MSSS Concrete bridge.

active stiffness of the abutments, the deck-abutment gaps (particularly for the continuous bridges), followed by the damping ratio.

For many of the retrofitted bridges, the list of most significant parameters tends to include one parameter associated with the retrofit measure itself. For a given retrofit measure, the important modeling parameter is not necessarily consistent from bridge type to bridge type. For example, when looking at restrainer cable retrofits, it is found that for the MSSS Steel bridge the length of the restrainer cable is important, while for the MSC Steel and MSSS Concrete bridges the slack in the cable is most significant. In some cases, the findings from the screening study reveal the considerable change in seismic response of the as-built and retrofitted bridge, because of the stark difference in modeling parameters that are important in influencing the response. The MSSS Concrete bridge retrofit with restrainer cables has six more significant parameters than the as-built of its type; while the number of significant parameters in the MSC Steel bridge reduces from four to two when the elastomeric bearings are used.

5.3 Closure

This Chapter highlighted a number of potential uncertainties in the modeling parameters associated with common classes of retrofitted bridges. Probabilistic models for potentially variable retrofit parameters stemming from design, material, or geometric uncertainties were established based on a review of current retrofit practice, experimental studies, and past work.

Table 5-8: Most Significant Parameters from Screening Study of each Retrofitted Bridge Type.

Most Significant Parameters				
As-Built	**Restrainer Cable**	**Elastomeric Bearing**	**Steel Jacket**	**Shear Key**
MSSS Steel				
Load Dir	Load Dir	Load Dir	Load Dir	Load Dir
Damp Ratio	Ab-Act Stf	Elasto Stf	Ab-Act Stf	Damp Ratio
Fxd Stiff	Length Cab	Fnd-Rot Stf	Damp Ratio	Fxd Frict
Fxd Frict	Damp Ratio	Keeper Gap	Jackt Stiff	Ab-Act Stf
Mass				Mass
Ab-Act Stf				Hinge Gap
MSC Steel				
Load Dir	Load Dir	Load Dir	Load Dir	Load Dir
Abut Gap	Abut Gap	Ab-Act Stf	Jacket Gap	Abut Gap
Ab-Act Stf	Slack Cab		Abut Gap	Gap to SK
Fxd Stiff	Fxd Frict		Ab-Act Stf	Ab-Act Stf
	Ab-Act Stf			
MSSS Concrete				
Load Dir	Load Dir	Load Dir	Load Dir	Load Dir
Ab-Act Stf	Ab-Act Stf	Ab-Act Stf	Jacket Gap	Fnd-Rot Stf
	Slack Cab	Elasto Stf	Ab-Act Stf	Mass
	Pad Stiff	Fnd-Rot Stf		Steel Str
	Fnd-Rot Stf			Pad Frict
	Damp Ratio			
	Pad Frict			
	Conc Str			
MSC Concrete				
Load Dir	Load Dir	Load Dir	Load Dir	Load Dir
Ab-Act Stf	Ab-Act Stf	Keeper Gap	Ab-Act Stf	Ab-Act Stf
Abut Gap	Damp Ratio		Abut Gap	Abut Gap
	Abut Gap			

The screening study presented utilizes design of experiments principles to identify which modeling parameters significantly impact the seismic response of a number of different component responses in retrofitted bridges. The results of the study provide insight on the potentially uncertain modeling parameters that most significantly affect the seismic response of the retrofitted systems, which to date has not been thoroughly assessed. In addition to loading direction and blocking scheme (gross geometry), the most important parameters include those associated with the bridge itself (abutment stiffness, damping ratio, mass) as well as parameters associated with each retrofit measure (restrainer length, elastomeric bearing stiffness, steel jacket stiffness). However, the most significant modeling parameters varied from bridge type and retrofit measure employed.

In general, some of the modeling parameters which were consistently insignificant include the dowel strength, gap at the dowels, and coefficient of friction for the steel expansion bearings, the initial stiffness of the abutments in passive action, the translational stiffness of the foundations, the yield strength of the steel jackets, and the yield strength of the restrainer cables. The variation in these parameters over their identified range was not found to have a statistically significant impact on the component responses, and therefore may not be of a concern for future studies. Efforts may be better spent in defining or characterizing the significant modeling parameters identified as a part of this work.

While these results indicate which uncertain parameters affect the seismic response of the retrofitted bridge, the propagation of these sources of uncertainty and influence on the fragility estimates are yet to be determined. Their influence on the seismic fragility curves for the different types of retrofitted bridges will be discussed in Chapter 7.

CHAPTER VI

BRIDGE DAMAGE-FUNCTIONALITY RELATIONSHIPS FOR REFINEMENT OF LIMIT STATE CAPACITIES AND DAMAGE STATE DEFINITIONS

Previous chapters have revealed that the potential seismic response of as-built and retrofitted bridges can be examined through high-fidelity analytical modeling and time history analysis. Through careful treatment of uncertainty and computational simulation, the seismic demand and propagation of sources of uncertainty can be assessed. As indicated in Chapter 2, this is one of the critical stages of a fragility analysis for bridge structures. However, an assessment of the capacity of various components is essential in assessing the overall potential for exceeding different limit states, or being in a given damage state.

These damage states are often related to performance objectives for the structure, and Ellingwood and Wen (2005) indicate the need for these objectives to be related to economic losses or opportunity losses for some systems. Key objectives for bridges, as critical nodes in the transportation network, are their states of functionality following an event. Thus, appropriate damage states for bridges may be defined such that the component damage for each damage state is indicative of a level of bridge functionality.

The limit states, or structural capacities, C, for estimating bridge fragility are quantitative measures of bridge or component performance, and should have a relation to the functionality or overall operation and performance of the bridge, referred to here as the damage state. These limit states should be mappable to the level of response or demand (D) placed on the structure, often referred to as an engineering demand parameter (EDP), in order to facilitate evaluation of the fragility as expressed in 6.1.

$$Fragility = P\,[D \geq C] \tag{6.1}$$

Traditionally, researchers have considered the demand placed on a single bridge component, such as the columns, using engineering demand parameters of drift or column ductility (Hwang et al., 2000; Shinozuka et al., 2000). As analytical methods for evaluation of the bridge fragility are maturing, the contribution of other vulnerable components (ie. bearings, abutments) to the bridge fragility have been recognized and considered (Choi et al., 2004), as will be an essential part of this work. However, it is critical that the limit states for different components have a similar meaning in terms of the overall bridge performance, expressed as its functionality. The challenge is to assess, for example, the limit states that result in slight damage to the columns and slight damage to the bearings affecting the performance of the bridge in an analogous way. One approach for doing so is to scale the component limit states such that their achievement has an equivalent meaning in terms of the impact on bridge functionality resulting from inspection and closure decisions. These functionally consistent limit states may be derived through evaluation of judgmental data

to assess the limits that bridge inspectors and officials place on damage before the functionality is expected to be affected. This can only be achieved with an enhanced understanding of the relationships between bridge damage and functionality.

Hence, the objective of this chapter is to develop bridge damage-functionality relationships. This information is intended to be used for refinement of limit state capacities in fragility analysis, such that they have functional consistency, and to provide definitions of damage states for bridges which are indicative of meaningful performance objectives for bridges (traffic carrying capacity and anticipated restoration of functionality). As seismic risk assessment is becoming a more prevalent approach for estimating the potential impact of an earthquake event on an affected region, both information on bridge vulnerability and expected functionality are essential. One of the critical data needs is the relationship between extent of damage to a bridge and the resulting loss-of-functionality.

6.1 Previous Studies and Approaches

Functionality is often a result of closure decisions made by post-earthquake inspectors, as well as the procedures for repair of the bridge. While there has been limited previous research in the area, relationships between bridge damage and functionality provide essential data for various components of the seismic risk assessment framework. Such relationships are essential for modeling potential decisions of bridge inspectors following an event and the anticipated allowable traffic carrying capacity of bridges and roadways, as well as for refining the limit states for bridge fragility curve development such that these limit states for different components have a similar implication in terms of overall bridge system functionality and allowable traffic carrying capacity.

Currently, very little information linking bridge damage and subsequent functionality exists. These relationships may be developed through assimilation of empirical data from past earthquake events; however this information is limited even in regions of high seismicity, such as parts of the West Coast, and is altogether lacking for the Central and Southeastern United States (CSUS) region. Analytical approaches to developing these relationships have been investigated for bridges that are typical in California (Mackie and Stojadinovic, 2006), and are more prescriptive in the fact that they serve to indicate the available load carrying capacity of the bridge. While this is valuable information, the intent of this research is to capture the anticipated decisions by inspectors that would be expected to affect the traffic carrying capacity, and to investigate damage to various components of typical CSUS bridges.

An alternate approach to gathering information relating bridge damage to functionality is the use of expert opinion. The FEMA funded ATC-13 project recognized the need for this data in California and attempted to gather data on loss of function and restoration time for lifeline facilities (ATC, 1985). The survey participants were queried as to the number of days elapsed before restoring 30%, 60%, and 100% functionality for a given damage state. Although there were only four respondents to the bridge survey, HAZUS uses this data to provide discrete and continuous curve fits to the ATC-13 responses (FEMA, 2005). Hwang et al. (2000) performed an initial study on bridge repair sequencing and downtime in Mid-America through a survey of DOT and consulting engineers. They presented four descriptive damage states for a continuous multi-span concrete girder bridge supported on multi-column bents and reported potential repair strategies, estimated percent replacement

costs, and stepwise functionality restoration curves. Their expert opinion survey received nine responses and indicated the need for follow up investigation.

6.2 Survey Methodology

The advantage of the expert opinion method for developing bridge damage-functionality relationships is its ability to capture the subjective nature of bridge functionality and closure decisions. While significant uncertainty exists in the closure and repair decisions following an earthquake event, eliciting the opinions of those who will be called upon to make those subjective decisions helps to most appropriately model potential decision making and estimate allowable levels of bridge traffic carrying capacity. Targeting respondents in the region of interest (Central and Southeastern US) provides results indicative of the regional dependence of the relationships. For the above stated reasons, the expert opinion method has been adopted for this study. This research addresses the need for development of relationships between bridge damage and functionality by use of a web-based survey which elicits expert opinion data on the expected levels of allowable traffic carrying capacity and repair measures for various types and levels of bridge damage.

6.2.1 Web-Based Survey Design

The survey has been devised considering the technical language and approach common to CSUS inspectors, using recommended principles for web survey development by researchers in the field, and through iteration in coordination with officials from the Central US Earthquake Consortium (CUSEC) Transportation Task Force. Key considerations included, but are not limited to, the following:

- Using visuals to relate bridge damage descriptions to physical and meaningful events
- Balancing the need for comprehensive data collection with reasonable survey response length
- Careful utilization of the capabilities of internet technologies and web survey formats such that convenience, understanding, and response accuracy are maximized

Dillman has performed extensive research in the field of survey development, expert opinion solicitation, and web survey design. Many of the findings from Dillman and Smyth's research and the principles recommended for construction of web surveys have been implemented. Some examples include effective use of fonts, spacing, and grouping; providing instructions on necessary computer actions; and allowing respondents to skip questions and allowing them to answer out of order (Dillman et al., 1998; Smyth et al., 2004). In general, implementation of these among other principles has helped to produce a more respondent-friendly web survey regarding bridge damage-functionality.

Post-earthquake inspection manuals from CSUS DOTs, namely the *Indiana Handbook for the Post-Earthquake Safety Evaluation of Bridges and Roads* (INDOT, 2000) and the *Missouri Post Incident Bridge Inspection Training Manual* (MODOT, 2004) were reviewed for consistent terminology and organization of the survey. The component damage questions were posed in the same sequence as a bridge inspector is instructed to evaluate a bridge and using similar quantitative and visual descriptions as are presented in inspection training and field guides. The clarity and comprehensibility of instructions and question format were refined with CUSEC members input, and the length of the survey was revised to achieve an anticipated increased level of response.

6.2.2 Responses Elicited

The web-based survey queried DOT officials and consulting engineers as to the expected level of traffic carrying capacity of a bridge over time, given a level of bridge component damage. Multi-span continuous and multi-span simply supported bridges were addressed and the results are expected to be extracted to single span bridges through consideration of the appropriate components. Damage considered includes the approach and abutments, superstructure/bearings, columns in single and multi-column bents, and footings. For each component, various levels of damage were presented in quantitative or qualitative terms, and photos from past earthquake damage that correspond with the given level of damage were offered as an illustrative example. The respondents were asked to provide the expected traffic carrying capacity at time 0, 1, 3, 7, and 30 days following an event that may result from closure decisions, traffic restrictions, repair and restoration. The respondents were also asked to select a potential repair measure that would be executed for the given level of component damage. A screen shot from the web-based survey is shown in Figure 6-1(a), with an example of a completed table for one section of the survey (Figure 6-1(b)).

As with previous expert opinion surveys, the respondents were asked to assume a given set of conditions. The assumptions for this response data are as follows:

- Assume the typical post-disaster level of funding and resources are available for repair.
- Consider current best practices for repair procedures.
- Consider only the effect of the component of interest on the traffic restrictions and resulting bridge functionality.

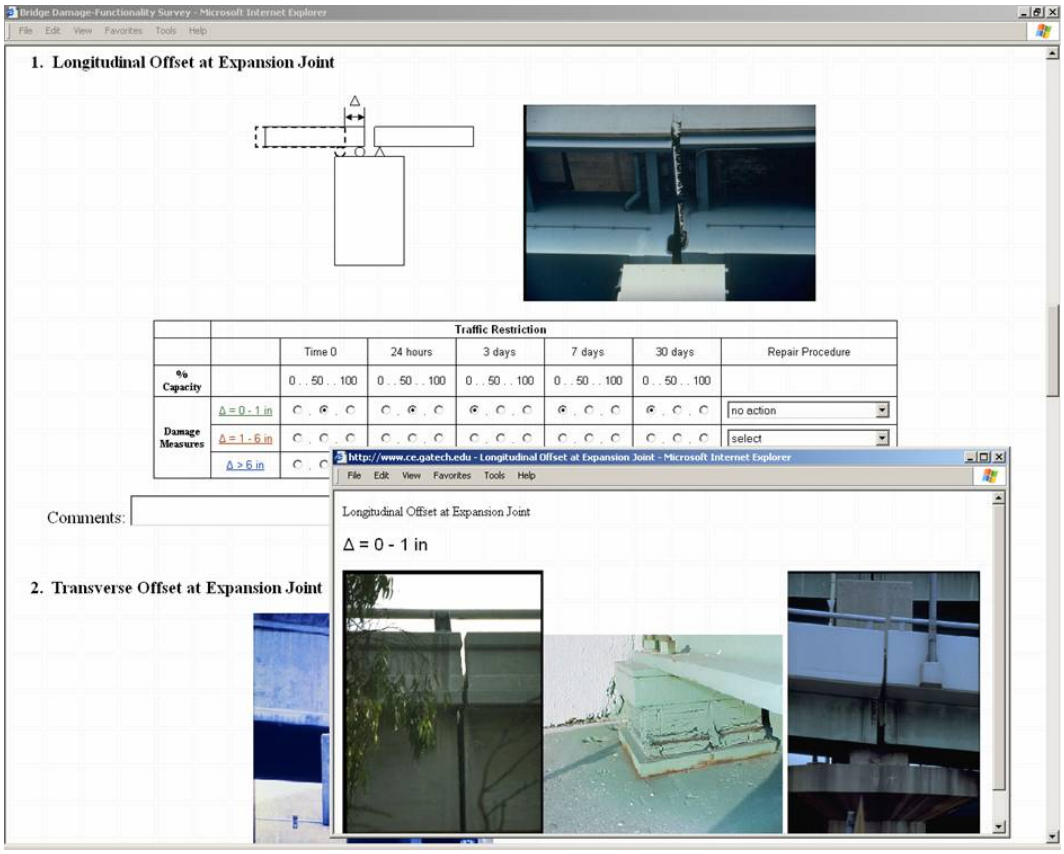

6-1(a):

		Traffic Restriction					
		Time 0	24 hours	3 days	7 days	30 days	Repair Procedure
% Capacity		0 . . 50 . . 100	0 . . 50 . . 100	0 . . 50 . . 100	0 . . 50 . . 100	0 . . 50 . . 100	
Damage Measures	Δ = 0 - 1 in	○ . ○ . ●	○ . ○ . ●	○ . ○ . ●	○ . ○ . ●	○ . ○ . ●	no action
	Δ = 1 - 6 in	● . ○ . ○	● . ○ . ○	● . ○ . ○	○ . ● . ○	○ . ○ . ●	replace bearing
	Δ > 6 in	● . ○ . ○	● . ○ . ○	● . ○ . ○	● . ○ . ○	● . ○ . ○	demolish and replace bridge

6-1(b):

Figure 6-1: Web-based damage-functionality survey screen capture of (a) survey with hyperlink opened for examples from past earthquake events, and (b) sample responses of expected level of allowable traffic carrying capacity.

6.3 Results of Web-Based Survey

A contact person was identified at nine Central and Southeastern US DOTs and asked to distribute the survey to 3-5 persons in the bridge engineering, maintenance, and operations departments. Two consultants that were identified as close collaborators in post event inspection and repair were also included. Twenty-eight respondents from nine states in the CSUS region participated in the web-survey. The states represented include Arkansas, Georgia, Illinois, Indiana, Kentucky, Mississippi, Missouri, South Carolina, and Tennessee. While the overall response rate may not be directly computed because the exact number of total recipients is unknown, an estimate is determined based on knowledge of the response rate from a subset of the sample. For a two states, the number of recipients were known and compared to the number of respondents, indicating that the response rate for the survey is on the order of 75%.

6.3.1 Probable Allowable Traffic Carrying Capacity

The results of the bridge damage-functionality survey may be presented in the form of functionality probability matrices (FPM). The matrices directly represent the results of the survey and provide the percent of respondents that indicate a given level of component damage would result in a specific level of allowable traffic carrying capacity over time:

$$P[X = x|Dg = dg \cap T = t] \tag{6.2}$$

where X is the allowable traffic carrying capacity, Dg is the level of damage to the component of interest, and T is the time following the earthquake event. Examples of the FPMs are listed in Table 6-1 for settlement of the approach at the approach/abutment interface,

transverse offset of the deck at the expansion joint, and column damage in a single column bent. The survey results in the form of FMPs for the other types and levels of damage are presented in Appendix A.

As evidenced by Table 6-1, the trends parallel what one might deduce from intuitive reasoning. Increased damage to a component often leads to a higher probability of reduced functionality, and the probability for full (100%) capacity increases over time. In general, the results showed that the variance in responses decreased over time for the lower levels of damage and increased over time for the higher levels of damage. This indicates that for a larger level of component damage, there is more uncertainty in the expected level of allowable traffic carrying capacity of the bridge as time progresses following the event, while for smaller levels of damage the uncertainty in capacity is at its highest level immediately following the event and decreases over time.

Table 6-1: Example Functionality Probability Matrices for Various Types of Bridge Damage.

Settlement of Approach at Approach/Abutment Interface															
Damage, dg	**0-1 inch**					**1-6 inch**					**≥ 6 inch**				
Time, t (days)	**0**	**1**	**3**	**7**	**30**	**0**	**1**	**3**	**7**	**30**	**0**	**1**	**3**	**7**	**30**
P[X=0%| Dg=dg ∩ T=t]	0.107	0.036	0.036	0.036	0.036	0.357	0.185	0.036	0	0	0.857	0.5	0.25	0.071	0.036
P[X=50%|Dg=dg ∩ T=t]	0.179	0.071	0.036	0.036	0.036	0.5	0.37	0.286	0.036	0.036	0.143	0.25	0.357	0.321	0.071
P[X=100%|Dg=dg ∩ T=t]	0.714	0.893	0.929	0.929	0.929	0.143	0.444	0.679	0.964	0.964	0	0.25	0.393	0.607	0.893
Transverse Offset at Expansion Joint															
Damage, dg	**0-1 inch**					**1-6 inch**					**≥ 6 inch**				
Time, t (days)	**0**	**1**	**3**	**7**	**30**	**0**	**1**	**3**	**7**	**30**	**0**	**1**	**3**	**7**	**30**
P[X=0%|Dg=dg ∩ T=t]	0.107	0.036	0	0	0	0.571	0.464	0.286	0.107	0.036	0.857	0.75	0.643	0.464	0.286
P[X=50%|Dg=dg ∩ T=t]	0.214	0.179	0.179	0.107	0.071	0.179	0.214	0.321	0.286	0.25	0.071	0.143	0.107	0.179	0.036
P[X=100%|Dg=dg ∩ T=t]	0.679	0.786	0.821	0.893	0.929	0.25	0.321	0.393	0.607	0.714	0.071	0.107	0.25	0.357	0.679
Damage to Column (Single Column Bent)															
Damage, dg	**Cracking**					**Spalling**					**Rebar Buckle/Fracture/Pullout**				
Time, t (days)	**0**	**1**	**3**	**7**	**30**	**0**	**1**	**3**	**7**	**30**	**0**	**1**	**3**	**7**	**30**
P[X=0%|Dg=dg ∩ T=t]	0.37	0.222	0.148	0.148	0.074	0.75	0.607	0.429	0.25	0.143	0.964	0.929	0.821	0.75	0.5
P[X=50%|Dg=dg ∩ T=t]	0.148	0.259	0.259	0.185	0.074	0.179	0.25	0.393	0.25	0.143	0	0	0.143	0.107	0.036
P[X=100%|Dg=dg ∩ T=t]	0.482	0.519	0.593	0.667	0.852	0.071	0.143	0.179	0.5	0.714	0.036	0.071	0.036	0.143	0.464

6.3.2 Damage State Definititions and Probability of Exceedance

One application of the results of the damage-functionality survey is in quantifying the probability of having a given anticipated restoration function, or capacity over time. In essence, the restoration functions themselves become definitions of various damage states, where, for example, slight damage corresponds to a particular restoration. The definitions of damage states for slight, moderate, extensive, and complete damage used in this analysis are those types and levels of damage that correspond to the step-wise restorations shown in Figure 6-2. For example, slight damage indicates damage resulting in capacity reduced to 50% following the earthquake event, yet fully restored in approximately 1 day. This might often be likened to limited visible damage which may be inspected but requires no closure of the bridge. Complete damage, however, refers to damage leading to closure of the bridge, and still having 0% capacity 30 days after the event. The probability of having a capacity that is less than or equal to the damage state definition for a given type and level of damage can then be assessed through analysis of the damage-functionality survey results. This results in an assessment of whether or not the damage state definitions were exceeded, by evaluating the functionality over time. These damage state exceedance probabilities are found as the probability of an intersection of events along the restoration timeline, as shown in Equation 6.3

$$P[DS \geq ds_i | Dg = dg] = P\left[\bigcap_t X_T \leq x_{t,i}\right] \tag{6.3}$$

where DS is the damage state, ds_i is the damage state of interest, Dg is the level of component damage, dg is the realization of that component damage expressed as a range of values

for our data set, X_T is the allowable traffic carrying capacity at time t, where t= {0,1,3,7,30} days, and $x_{t,i}$ is the definition of capacity at time t for damage state i. For example, this conditional probability would be expressed as shown in Equation 6.4 for moderate damage given transverse offset at the expansion joints of 0-1 in.

$$P[DS \geq Moderate | Dg = 0 - 1in]$$

$$= P[X_{t=0} \leq 0\% \cap X_{t=1} \leq 50\% \cap X_{t=3} \leq 50\% \cap X_{t=7} \leq 100\% \cap X_{t=30} \leq 100\%] \quad (6.4)$$

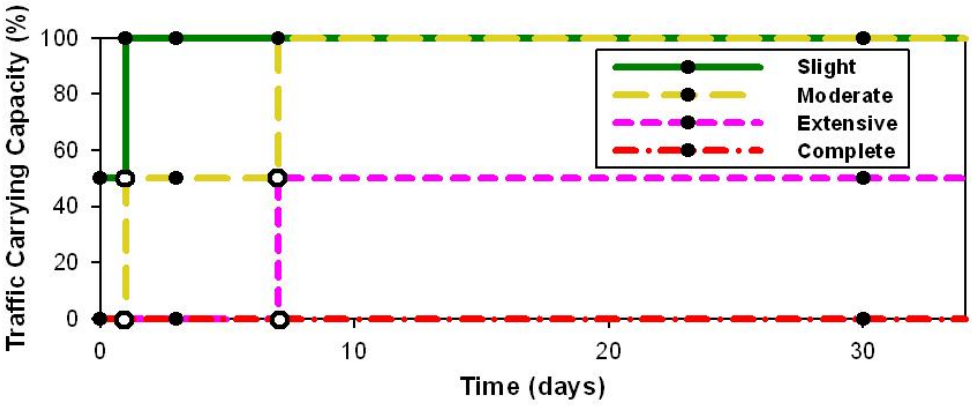

Figure 6-2: Step-wise restorations functions for slight through complete damage.

Analysis of the twenty-eight survey responses allows for an estimation of the probability of meeting or exceeding a given damage state, where the intersection of events expressed in Equation 6.3 is evaluated for each survey respondent in order to assess the damage state exceedance probability. Example conditional probabilities for the potential of meeting or exceeding a damage state as defined in Figure 6-2, given a level of damage to the bridge, are

shown in Table 6-2. Appendix A (Table A-2) contains the set of damage state exceedance probabilities for the remaining types of damage investigated in the survey. These conditional damage state probabilities represent the cumulative distributions over the levels of damage investigated. The results of this analysis offer a critical link between the level of damage to bridge components and the damage states defined in terms of allowable traffic carrying capacity. In deriving the exceedance probabilities, an assumption is made that the survey responses reflect the expected post-earthquake decisions affecting bridge functionality. The author acknowledges that other social, political, or economic factors may indeed impact the restoration as well. For example, such issues as the availability and allocation of resources, pressure to more rapidly restore routes in various neighborhoods or near critical facilities, or the ability of organizations to mobilize after an event are all examples of additional external factors affecting the functional restoration of bridges. However, these results provide excellent insight on the relative limits that inspectors place on the capacity of bridge components and the anticipated functionality. The application of these damage state exceedance probabilities for evaluating and refining component capacity limit states are discussed below.

6.4 Refinement of Limit States and Damage State Definitions

The survey data collected and analyzed above relating bridge damage to functionality is used to refine the limit state capacities for various bridge components evaluated as a part of the fragility analysis. The aim is to derive limit states that have functional consistency among components, and that are related to meaningful performance objectives for bridges.

Table 6-2: Damage State Exceedance Probabilities for Different Levels and Types of Damage.

Settlement of Approach at Approach/Abutment Interface				
	P[DS≥ds|Dg=dg]			
Damage, dg	**Slight**	**Moderate**	**Extensive**	**Complete**
0-1 in	0.286	0.036	0.036	0.036
1-6 in	0.889	0.148	0.000	0.000
≥6 in	1.000	0.464	0.214	0.071
Transverse Offset at Expansion Joint				
	P[DS≥ds|Dg=dg]			
Damage, dg	**Slight**	**Moderate**	**Extensive**	**Complete**
0-1 in	0.321	0.036	0.000	0.000
1-6 in	0.750	0.429	0.214	0.107
≥6 in	0.929	0.714	0.536	0.464
Damage to Column (Single Column Bent)				
	P[DS≥ds|Dg=dg]			
Damage, dg	**Slight**	**Moderate**	**Extensive**	**Complete**
Cracking	0.519	0.185	0.148	0.148
Spalling	0.929	0.607	0.286	0.250
Rebar buckle/fracture/pullout	0.964	0.929	0.786	0.750

This measure of performance is an anticipated level of traffic carrying capacity, including such subjective decision making as inspection decisions and recommendations for closure, repair, and restoration as captured by the survey. It is recognized that the use of such data introduces subjectivity into the assessment of structural capacity, along with significant uncertainty; however, this type of approach attempts to model what may actually occur following an event and the impacts of human decisions regarding closure and repair.

It is apparent that the damage state exceedance probabilities derived above are synonymous with the percentiles of the cumulative distributions for the capacity limit states (slight through complete) at various levels of damage to components. However, some mapping is necessary between quantitative or qualitative damage descriptions presented in the survey and analytically measurable quantities. For example, the transverse offset at the expansion joint may be mapped by either monitoring the transverse offset as the engineering demand

parameter, or the deformation of the bearings at the expansion joint. However, some mapping is more abstract, as in the case with the columns, where the survey data and percentiles of the cumulative distribution function correspond to cracking, spalling, and bar buckling. The mapping of such physical phenomena to engineering demand parameters is dependent upon the seismic detailing, geometry, and parameters specific to the bridge of interest, and may be strengthened through assessment of empirical data from experimental testing of similar components, as discussed by Mackie (2004).

Mapping between the survey damage levels and EDPs evaluated as a part of this work may be found in Nielson (2005a). The limit state capacities are derived by Nielson using the exceedance probabilities presented above in a Bayesian updating process. So called prescriptive, or physics based limit states, were identified based on the constitutive models for the components. For example, at a steel fixed bearing deformation of 6 mm, cracking in the concrete pier became evident (Mander et al., 1996), hence the prescriptive limit for slight damage was placed at this level. The new knowledge acquired from the Damage-Functionality survey provided as a part of this work offer descriptive limits based on judgement. The probability distributions for the capacity limit states were then updated through a Bayesian approach to incorporate this new information regarding the limit state distributions. Details may be found elsewhere (Nielson, 2005a), and an example of the updated capacity distribution of curvature ductility demand for moderate damage to the columns is shown in Figure 6-3. The resulting capacity limit states will be presented in Chapter 7, along with the assessment of limits placed on retrofitted components.

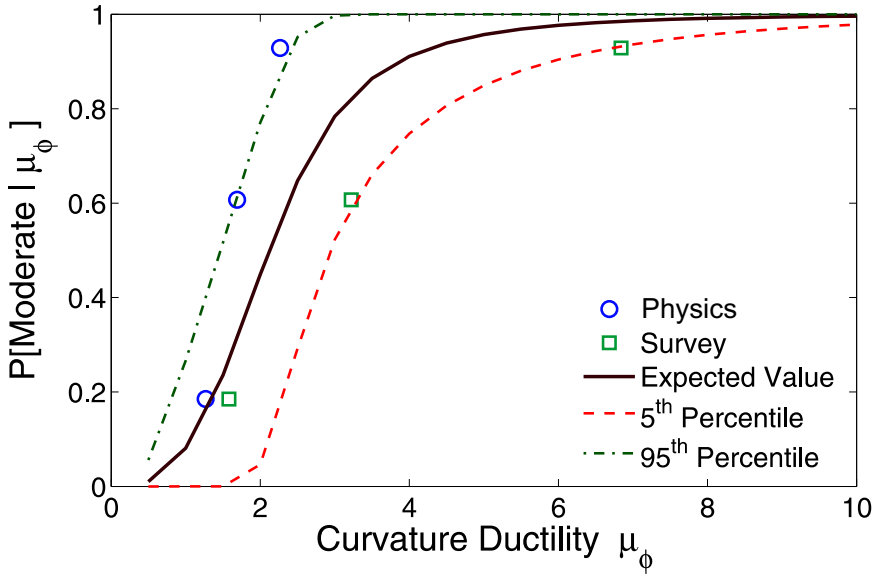

Figure 6-3: Update of capacity limit states for column (Nielson, 2005a).

CHAPTER VII

RETROFITTED BRIDGE FRAGILITY CURVE DEVELOPMENT

7.1 Introduction

This chapter synthesizes the work from previous sections. Included is the proposed methodology and resulting fragility curves for classes of retrofitted bridges in the Central and Southeastern US. The approach, however, is extendible to other bridge types and retrofit measures. The retrofit measures identified in Chapters 2 and 3, as well as the 3-d analytical models (Chapter 4), are used in the time history analysis for the vulnerability assessment. In addition, the results of the probabilistic modeling and parameter screening from Chapter 5 are used in the simulation for estimating the demand and fragility estimate. This chapter will include a focused study on the sensitivity of the fragility estimate to various levels of uncertainty treatment, building upon the previous screening study. The limit state capacities presented in this chapter will incorporate the findings of the damage-functionality survey and refined damage state definitions from Chapter 6.

The following sections detail the analytical methodology for developing retrofitted bridge fragility curves, as well as some of the research challenges and insights that can

be gained at various stages of their development. The effect of retrofit on demand models, capacities, component fragilities, and ultimately on bridge system fragility is assessed. Proposed retrofitted bridge fragility curves will be presented at the end of the Chapter.

7.2 Ground Motions

As indicated in Section 4.3, two different suites of ground motions will be used in the generation of probabilistic seismic demand models and fragility estimation of 48 ground motions from Wen and Wu (2001) and 48 ground motions from Rix and Fernandez (2004). These ground motions were identified by Nielson (2005a), consisting of a range of *PGA* and S_a values and representative of CSUS ground motion characteristics. Forty-eight were selected because of the ease of use with the 8 bridge samples used in the study. The mean response spectra of the Wen and Wu and the Rix and Fernandez ground motion suite are shown in Figure 7-1. Some of the differences in these are attributed of the different soil profiles for locations considered in deriving the ground motion suites, the source models used, and the fact that the Rix and Fernandez are deterministic, while the Wen and Wu are probabilistic. The response spectra shown in Figure 7-1 actually represent the spectral accelerations for the geometric mean of ground motion pairs. Because the fragility analysis as a part of this work considers 3-d response, it is necessary to simulate the time history analyses with orthogonal ground motion components. The suites of ground motions used as a part of this work are simulated suites of orthogonal ground motion components developed by Nielson (2005a) for the seed Wen and Wu and the Rix and Fernandez motions. The procedure for generating the ground motion components from the original suites of geometric mean motions can be found elsewhere, and follows the work by Baker and

Cornell (2006) for simulating response spectra for orthogonal components, then spectrally matching the seed motion, and tapering the duration to the original motion using a cosine window following Rix and Fernandez (2004).

A composite suite of the synthetic ground motions from Wen and Wu and Rix and Fernandez are used for the fragility analysis. By using both suites of ground motions, the uncertainty captured and modeled by the fragility includes epistemic uncertainty in different ground motion modeling approaches. Additionally, these researchers produced the ground motion suites with an effort to capture various sources of uncertainty in the source, path, and site characteristics which are then propagated through the fragility analysis. The ground motion uncertainty reflected in the fragilities also includes the unknown incident angle of the earthquake, recalling that this was identified in Chapter 5 as a parameter which could significantly affect the structural response. Figure 7-2 illustrates the simultaneous application of orthogonal ground motion components, as well as the variable incident angle of the earthquake which is considered in the fragility development.

7.3 Probabilistic Seismic Demand Models

A probabilistic seismic demand model (PSDM) offers the relationship between ground motion intensity and demand (or a response measure of demand) specific to the class of structure evaluated. This is a common approach for describing the demand placed on the structure, or structural components, particularly when fragility assessment is performed through analytical methods using nonlinear time history analysis. The development of PSDMs for this methodology includes simulation of suites of analytical bridge models reflecting various sources of uncertainty affecting the demand placed on the retrofitted bridge, and

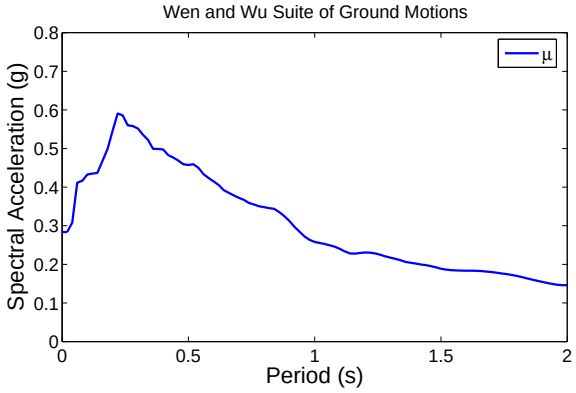

7-1(a):

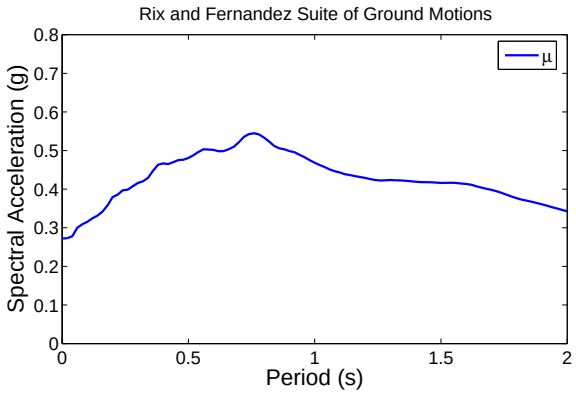

7-1(b):

Figure 7-1: Mean response spectra for suites of 48 ground motions from (a) Wen and Wu and (b) Rix and Fernandez.

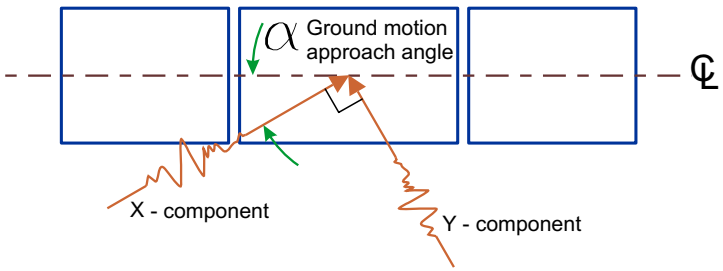

Figure 7-2: Loading direction and orthogonal ground motion components for time history analysis (Nielson, 2005a).

potential realizations of the analytical modeling parameters. The simulation for this study uses the 3-d modeling approach detailed in Chapters 3 and 4, and samples upon the uncertain modeling parameters identified in Chapter 5 as most significantly affecting the bridge response. Latin hypercube sampling is used to augment the base bridge models by sampling upon the various significant modeling parameters to generate *N* statistically different yet nominally identical bridge samples. For each bridge type, eight different base bridge geometries (previously presented) are used to reflect variation in gross geometric properties. Bridge model-ground motion pairs are subjected to nonlinear time history analysis and peak component responses are monitored for various critical components. While other works have often monitored only column demands, the component demands considered as a part of this study include column curvature ductility demands, longitudinal fixed bearing deformations, transverse fixed bearing deformations, longitudinal expansion bearing deformations, transverse expansion bearing deformations, active abutment deformations, passive abutment deformations, and transverse abutment deformations. The column demands are taken as

$$\mu_\phi = \sqrt{\mu^2_{\phi-longitudidal} + \mu^2_{\phi-transverse}} \tag{7.1}$$

Work by Cornell et al. (2002) has suggested that an estimate of the median of the seismic demand, S_D, follows a power law as shown in Equation 7.2

$$S_D = aIM^b \tag{7.2}$$

where a and b are the unknown coefficients and IM is the ground motion intensity. As indicated in Chapter 2, transforming this relationship into lognormal space simplifies the parameter estimation to a linear regression following Equation 7.3.

$$\ln S_D = b \cdot \ln IM + \ln a \tag{7.3}$$

Figure 7-3 illustrates this regression in transformed space. From this regression an estimate of the median of the demand, S_D, is obtained as well as the variation of the demand about this quantity. The demand can be probabilistically modeled with a lognormal distribution (Mackie and Stojadinovic, 2005; Shinozuka et al., 2000); thus in the transformed space the residual is modeled by a normal distribution with mean zero and standard deviation, σ. This permits an estimate of the conditional dispersion of the demand, or lognormal standard deviation, $\beta_{D|IM}$. The choice of intensity measure for bridge fragilities has been investigated by various researchers (Hwang et al., 2000; Mackie and Stojadinovic, 2001; Nielson, 2005a). However, this study will use peak ground acceleration, PGA, as the intensity measure for developing PSDMs and retrofitted bridge fragility curves. Work by Nielson (2005a) and follow up study by the author have evaluated and compared IMs for classes of CSUS bridges and found PGA to be an appropriate choice based on the criteria of practicality, efficiency, sufficiency, and hazard computability. This IM will facilitate incorporation of the fragilities developed herein into regional risk assessment packages.

Each key component demand is represented by a probabilistic seismic demand model. The parameters of the lognormal distribution of demand are estimated through regression,

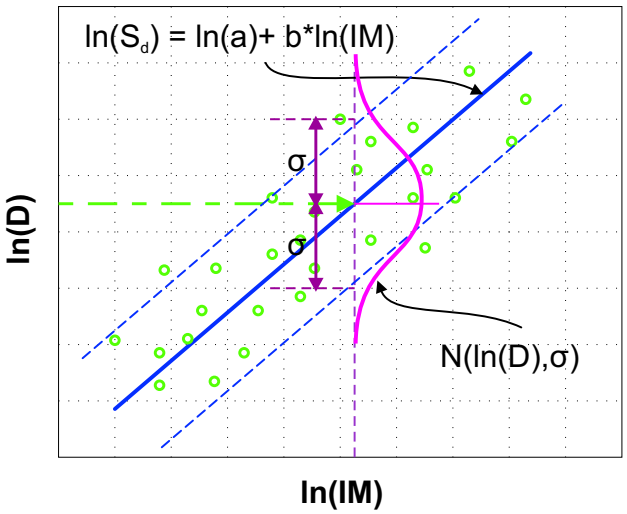

Figure 7-3: PSDM illustration in lognormal space.

as indicated above. Hence, the form of the PSDM relating the peak component demand, *D*, to the ground motion intensity in lognormal form is shown in Equation 7.4.

$$P[D \geq d|IM] = 1 - \Phi\left(\frac{\ln(d) - \ln(S_D)}{\beta_{D|IM}}\right) \tag{7.4}$$

Equation 7.4 could alternately be written as shown in Equation 7.5 for ease of substitution of the regression parameters.

$$P[D \geq d|IM] = \Phi\left(\frac{\ln(IM) - \frac{\ln(d)-\ln(a)}{b}}{\frac{\beta_{D|IM}}{b}}\right) \tag{7.5}$$

7.3.1 PSDMs for Retrofitted Bridges

The demand models for the components are altered by the use of retrofit in some cases. This is consistent with the findings of the deterministic analyses which revealed that the response of the component may be increased, decreased, or unaffected by various retrofits.

An example of the regression and PSDMs for select components of the multi-span continuous concrete (MSC Concrete) bridge retrofit with shear keys is shown in Figure 7-4. The PSDM for the as-built bridge is shown relative to the retrofitted bridge for visual comparison of the demand model before and after retrofit. It is evident from this figure that the shear keys alter the PSDMs by decreasing the demands placed on the fixed bearings and increase the demands place on the abutments in the transverse direction. The decrease in σ for the fixed bearing deformations also indicates that the shear keys have affected the dispersion about the demand estimate. Similar findings are revealed for the various bridge types, retrofit measures, and component demand models. Appendix B presents the component PSDMs for all retrofitted bridges in tabular form.

7.3.2 Joint PSDMs

While the component probabilistic seismic demand models will be useful for developing component fragility curves to assess the impact of retrofit on the variability of different critical components within the bridge, there is a need to derive system fragility curves. These system fragilities permit an evaluation of the impact of retrofit on the overall bridge system vulnerability, considering the contribution of multiple critical components. For the methodology used in this work, system demand models (joint PSDMs) are developed following Nielson (2005a). The component PSDMs presented above are actually marginals for the joint probability distribution of demand. In this case, a joint probability density function describes the demand placed on a number of components within the bridge system, such as the bearings, abutments, and columns.

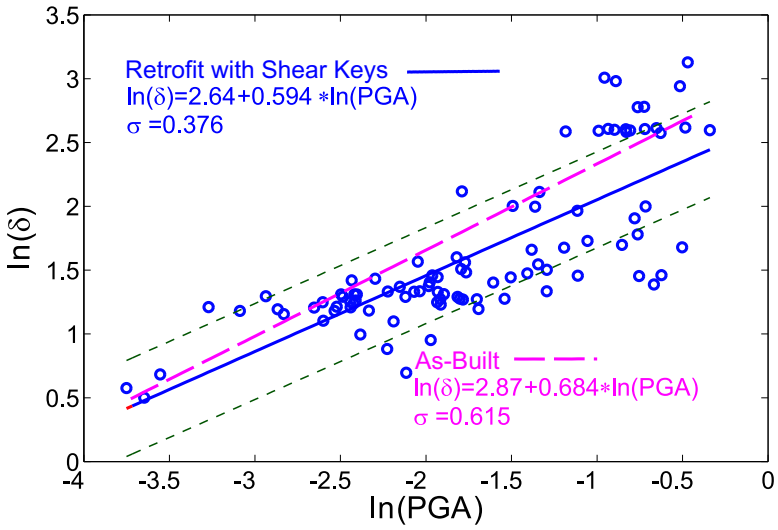

7-4(a):

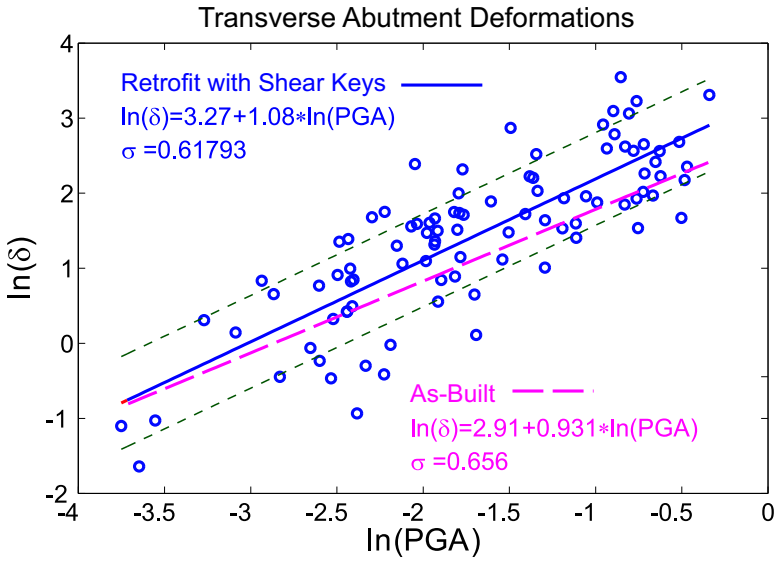

7-4(b):

Figure 7-4: Impact of Shear Key retrofit on the MSC Concrete PSDMs for (a) transverse fixed bearing deformations and (b) transverse abutment deformations.

The joint PSDMs are derived in lognormal space, where each component demand is transformed ($y_i = \ln(x_i)$), and as illustrated above the demands placed on the n components are then normally distributed. For such a joint normal distribution, a vector of means, μ_y, and the covariance matrix, Σ_y, are needed to fully describe it. The correlation coefficients are actually calculated from the transformed demands, y_i. Estimation of μ_y is calculated by $\bar{y} = \frac{1}{n}\sum_{i=1}^{n}\ln(x_i)$ and ${\sigma_y}^2$ is estimated by $s^2 = \frac{1}{n-1}\sum_{i=1}^{n}(\ln(x_i) - \overline{\ln(x)})^2$. All operations are performed on the jointly normal PDF. Realizations of this joint normal distribution for demand are transformed back into the original system through a simple operation, $x_i = \exp(y_i)$. Nielson (2005a) found that the correlation between demands did not vary significantly across a range of different earthquake intensities, and hence this study assumes constant correlation coefficients for the demand models. The correlation matrices (for the transformed demands) of the retrofitted bridges are presented in Appendix B along with the PSDMs.

7.4 Limit State Capacities

The limit states for various bridge components offer a quantitative measure of capacity which correspond to a damage state definition. The limit states for the as-built components are those presented in Nielson (2005a). These limit states are intended to correspond to the qualitative damage state descriptions presented in the FEMA loss assessment package HAZUS-MH (FEMA, 2005). The qualitative description of the four damage states (Slight, Moderate, Extensive and Complete) are given in Table 7-1. Similar to the restoration functions presented in HAZUS, the damage state definitions for this study have a corresponding

level of anticipated functionality (Figure 6-2). This provides meaningful measures of performance for bridge structures. However, the quantitative limit states for the component capacities are carefully derived to be consistent with this level of functionality. Details on the survey data and limit state refinement were presented in Chapter 3. The limit state capacities for the retrofitted component are assigned with consideration for the functional implications.

Table 7-1: Qualitative Damage State Descriptions from HAZUS (FEMA, 2005).

Limit State	**Description**
Slight	Minor cracking and spalling to the abutment, cracks in shear keys at abutments, minor spalling and cracks at hinges, minor spalling at the column (damage requires no more than cosmetic repair) or minor cracking to the deck.
Moderate	Any column experiencing moderate (shear cracks) cracking and spalling (column structurally still sound), moderate movement of the abutment (<2”), extensive cracking and spalling of shear keys, any connection having cracked shear keys or bent bolts, keeper bar failure without unseating, rocker bearing failure or moderate settlement of the approach.
Extensive	any column degrading without collapse – shear failure – (column structurally unsafe), significant residual movement at connections, or major settlement approach, vertical offset of the abutment, differential settlement at connections, shear key failure at abutments.
Complete	any column collapsing and connection losing all bearing support, which may lead to imminent deck collapse, tilting of substructure due to foundation failure.

7.4.1 As-Built Component Capacities

The resulting capacity limit states from Nielson (2005a) for the as-built components used in this study are presented in Table 7-2.

Table 7-2: As-Built Limit States for Bridge Components (Nielson, 2005a).

	Slight		Moderate		Extensive		Complete	
Component	S_c	β_c	S_c	β_c	S_c	β_c	S_c	β_c
Concrete Column (μ_ϕ)	1.29	0.59	2.10	0.51	3.52	0.64	5.24	0.65
Steel Bearing Fixed-Long (mm)	6.00	0.25	20.0	0.25	40.0	0.47	187	0.65
Steel Bearing Fixed-Tran (mm)	6.00	0.25	20.0	0.25	40.0	0.47	187	0.65
Steel Bearing Rocker-Long (mm)	37.4	0.60	104	0.55	136	0.59	187	0.65
Steel Bearing Rocker-Tran (mm)	6.00	0.25	20.0	0.25	40.0	0.47	187	0.65
Elastomeric Bearing Fixed-Long (mm)	28.9	0.60	104	0.55	136	0.59	187	0.65
Elastomeric Bearing Fixed-Tran (mm)	28.8	0.79	90.9	0.68	142	0.73	195	0.66
Elastomeric Bearing Expan-Long (mm)	28.9	0.60	104	0.55	136	0.59	187	0.65
Elastomeric Bearing Expan-Tran (mm)	28.8	0.79	90.9	0.68	142	0.73	195	0.66
Abutment-Passive (mm)	37.0	0.46	146	0.46	N/A	N/A	N/A	N/A
Abutment-Active (mm)	9.80	0.70	37.9	0.90	77.2	0.85	N/A	N/A
Abutment-Tran (mm)	9.80	0.70	37.9	0.90	77.2	0.85	N/A	N/A

7.4.2 Retrofitted Component Capacities

It has been previously illustrated that various retrofits affect the seismic response and demand. However, the use of retrofit may also alter the capacity of some components, including the retrofitted component itself. For example, new limit states must be defined for the steel jacketed columns, elastomeric isolation bearings, and steel bearings when seat extenders are present. The limit states for these components are defined with an effort to maintain the functional implications of each damage state, and at limits where visual damage may be apparent to inspectors. The median values of the retrofitted component limit states are assigned in most cases based on past experimental tests of the retrofits. With little additional information on the dispersion about the median, judgement is often used along with knowledge of the uncertainty in the capacity of the as-built component.

The steel jacketed columns provide considerable enhanced ductility capacity as indicated in Chapter 3. Limit states for slight through complete damage are assessed based on tests of steel jacketed circular columns by Chai et al. (1991) and Priestley et al. (1994b).

The visual damage and findings of tests for similar columns have often been reported in displacement ductility demands, μ_Δ, and are converted to a corresponding curvature ductility based on (FHWA, 1995)

$$\mu_\phi = 1 + \frac{\mu_\Delta - 1}{3 \cdot \frac{l_p}{l} \cdot (1 - 0.5 \cdot \frac{l_p}{l})} \tag{7.6}$$

where l is the column height (5.5 m on average), and the plastic hinge region, l_p, is approximated from Priestley et al. (1994b)

$$l_p = 2 \cdot X \cdot d_{bl} + g \tag{7.7}$$

where X is taken as 9 for grade 60 steel, g is the jacket gap taken as 19 mm, and the longitudinal bar diameter is approximated as d_{bl} = 25.4 mm.

The tests indicated that at μ_ϕ = 9.35, considerable shear cracking at the connection between the jacketed column and footing may form, or spalling of concrete cover may occur, particularly with non-seismically detailed footings lacking a top reinforcement map. This has been identified as the limit state for slight damage. Moderate damage is presumed to correspond to a level of μ_ϕ = 17.7, where permanent concrete dilation resulted in yielding of the jacket and visual bulging on the tension side. Extensive damage is triggered at a curvature ductility demand of 26.1, where stable hysteretic response of the jacketed columns is no longer observed and tension reinforcement may potentially fracture. At μ_ϕ = 30.2, the complete limit state is defined as the point where rapid strength degradation occurs along with potential jacket buckling and longitudinal reinforcement fracture. This

also roughly corresponds to the estimated ultimate curvature ductility demand of a typical jacketed column based on Priestley et al. (1996).

$$\mu_{\phi_u} = \frac{\phi_m}{\phi_y} = \frac{\epsilon_{cu}/c}{\phi_y} \tag{7.8}$$

where c is the neutral axis depth, ϵ_{cu} is the ultimate concrete strain from Equation 3.3, and ϕ_y is the yield curvature. The lognormal standard deviation associated with the capacity of the steel jacketed columns is presumed to be the same level as that of the original columns for slight through complete damage.

The use of elastomeric isolation bearings replaces more vulnerable bearings; yet these isolation bearings also have limits on their peak displacements. Each bridge type has different size elastomeric bearings, designed as discussed in Chapter 7. Therefore, the limit states for horizontal displacement demands are discussed in terms of shear strains and then transformed appropriately based on each bearing's dimension. At shear strains of approximately 100%, tests of typical CSUS bearings and pedestals have revealed potential yielding of anchor bolts and cracking of the pedestals. This first visible indicator of damage is considered the slight limit state (DesRoches et al., 2004). Moderate damage is associated with initial visible damage to the bearings themselves. At a level of 150% shear strain in the bearings, past analytical and experimental investigations by Mori et al. (1997) have indicated that the steel shims would yield. Test have revealed, however, that at a 200% shear strain significant uplift and rocking of the bearing occurs and the steel shims become severely bent (Mori et al., 1999). At this level of damage, the bearing would require replacement and hence is indicative of extensive damage. The complete damage state is associated with ultimate

failure of the bearings, which may lead to potential span unseating. Tests of laminated elastomeric bearings by Kelly and Quiroz (1992) have indicated that this may occur by tearing of the elastomer at the bearing center at a bearing shear strain of approximately 350%. The dispersions are assumed to be similar to those from the elastomeric bearing pads.

The restrainer cables and shear keys do not affect the limit states for the component capacities, but influence the seismic demand placed on them. The seat extenders, however, have not yet been considered to alter the response of the bridge. Their impact is captured by altering the limit on the longitudinal bearing displacements permissible at the highest damage state. The seat extenders are assumed to provide an additional 152 mm of support for the superstructure before unseating is expected to occur. For each bearing type (steel or elastomeric, fixed or expansion) the original median value for complete damage is 187 mm. This is increased to 339 mm when the seat extenders are employed. All other parameters remain the same.

Table 7-3 lists the lognormal parameters of the limit state for the component capacities which are affected by retrofit.

7.5 Retrofitted Bridge Component Fragility Curves

With knowledge of both the seismic demand and capacity placed on each component within the retrofitted bridge, fragility curves for the components can be developed. These component fragilities offer insight on the impact of different retrofit measures on the component vulnerability. As previously indicated with a lognormal distribution of the component capacity and demand, the fragility can be evaluated as shown in Equation 7.9.

Table 7-3: Limit State Parameters for Retrofitted Bridge Components.

	Slight		Moderate		Extensive		Complete	
Component	S_c	β_c	S_c	β_c	S_c	β_c	S_c	β_c
Elastomeric Isolation Bearings								
MSSS Steel Bridge-Long (mm)	76.2	0.60	114	0.55	152	0.59	267	0.65
MSSS Steel Bridge-Trans (mm)	76.2	0.79	114	0.68	152	0.73	267	0.66
MSC Steel Bridge-Long (mm)	82.6	0.60	124	0.55	165	0.59	289	0.65
MSC Steel Bridge-Trans (mm)	82.6	0.79	124	0.68	165	0.73	289	0.66
MSSS Conc Bridge-Long (mm)	146	0.60	219	0.55	292	0.59	511	0.65
MSSS Conc Bridge-Trans (mm)	146	0.79	219	0.68	292	0.73	511	0.66
MSC Conc Bridge-Long (mm)	140	0.60	210	0.55	279	0.59	489	0.65
MSC Conc Bridge-Trans (mm)	140	0.79	210	0.68	279	0.73	489	0.66
Steel Jacketed Column (μ_ϕ)	9.35	0.59	17.7	0.51	26.1	0.64	30.2	0.65
Steel Bearing Fixed-Long w/**SE** (mm)	6.00	0.25	20.0	0.25	40.0	0.47	339	0.65
Steel Bearing Rocker-Long w/**SE** (mm)	37.4	0.60	104	0.55	136	0.59	339	0.65
Elast Brg Fixed-Long w/**SE** (mm)	28.9	0.60	104	0.55	136	0.59	339	0.65
Elast Brg Expan-Long w/**SE** (mm)	28.9	0.60	104	0.55	136	0.59	339	0.65

Elast Brg = Elastomeric Bearing Pad
SE = **Seat Extender**

$$P[LS|IM] = P[D \geq C|IM] = \Phi\left(\frac{\ln(S_D/S_C)}{\sqrt{\beta_{D|IM}^2 + \beta_C^2}}\right) \tag{7.9}$$

This fragility can be directly evaluated from the capacity estimates for each damage state, S_C and β_C, presented in Section 7.4, as well as the parameters for the probabilistic seismic demand models (a, b, $\beta_{D|IM}$) from Section 7.3. These parameters can be utilized for fragility estimation by rearranging Equation 7.9 in the following form

$$P[LS|IM] = \Phi\left(\frac{\ln(IM) - \frac{\ln(S_c)-\ln(a)}{b}}{\frac{\sqrt{\beta_{D|IM}^2+\beta_C^2}}{b}}\right) \tag{7.10}$$

This component fragility is lognormally distributed, $Fragility \sim \text{LN}(\ln(med_{comp}),\beta_{comp})$, as indicated in Equation 7.11.

$$P[LS|IM] = \Phi\left(\frac{\ln(IM) - \ln(med_{comp})}{\beta_{comp}}\right) \tag{7.11}$$

The median of the lognormal distribution for the component fragility is in units of gravitational acceleration g, and is defined as $med_{comp} = exp(\frac{\ln(S_C)-\ln(a)}{b})$. The dispersion for the component fragility is $\beta_{comp}=\frac{\sqrt{\beta_{D|IM}^2+\beta_C^2}}{b}$. The fragility of the component is evaluated for each damage state (slight, moderate, extensive, complete), and can be compared for the components in the as-built and retrofitted bridges.

The component fragility curves for the as-built bridge can offer insight on the most vulnerable components within the bridge system, and indicate which components may be in need of retrofit. For example, Figure 7-5 reveals that the columns, followed by fixed and expansion bearings in the longitudinal direction, are the components most susceptible to Moderate damage. An example of the retrofitted fragility curves for select components is shown in Figure 7-6 for the moderate damage state of the MSC Concrete bridge. This Figure compares the vulnerability of the component before and after the bridge is retrofit with different measures. The system fragility curves will be discussed in the following section. Table 7-4 defines the legend labels (abbreviations) for the various retrofit measures. These will be used throughout the Chapter when presenting fragility curves. Comparing the component vulnerabilities with different retrofits (Figure 7-6) provides insights on the retrofit's impact on different critical components.

Observations from Figure 7-6 reveal how the retrofit measures may decrease the vulnerability of some components, while increasing the vulnerability of others, or not affect them at all. For example, the column vulnerability is considerably reduced with the steel jackets, but this retrofit measure doesn't affect any other components. The use of elastomeric isolation bearings lead to a reduction in the bearing vulnerabilities as well as the active abutment demands, yet do increase the passive vulnerability of the abutments (not

shown). The restrainer cables slightly reduce the expansion bearing fragility, yet lead to a higher potential for moderate damage of the abutments in active action as seen in Figure 7-6(d).

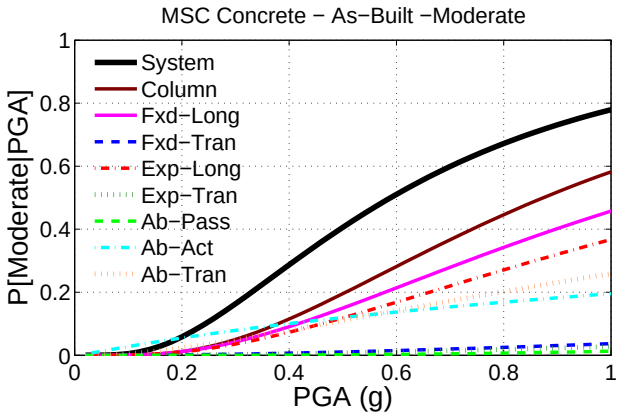

Figure 7-5: Relative vulnerability of the MSC Concrete as-built components for the moderate damage state.

Table 7-4: Retrofit Abbreviations for Fragility Curves.

Abbreviation	Description
As-Built	As-Built Bridge
Seat Extender	Retrofit with Seat Extenders
Restrainer	Retrofit with Restrainer Cables
Steel Jacket	Retrofit with Steel Jackets
Elasto Brg	Retrofit with Elastomeric Isolation Bearings
Shear Key	Retrofit with Shear Keys
RC & SK	Retrofit with Restrainer Cables and Shear Keys
SE & SK	Retrofit with Seat Extenders and Shear Keys

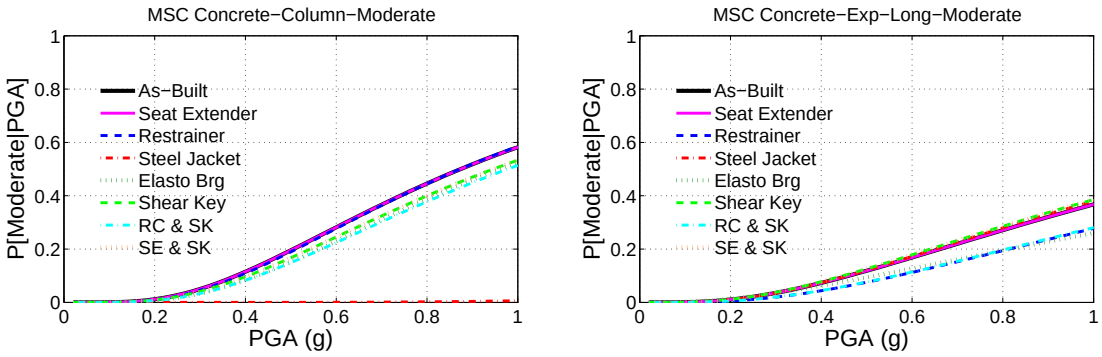

7-6(a):

7-6(b):

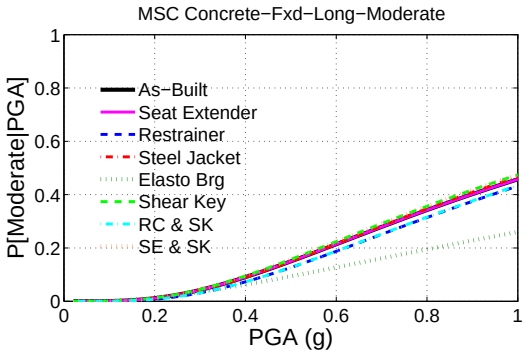

7-6(c):

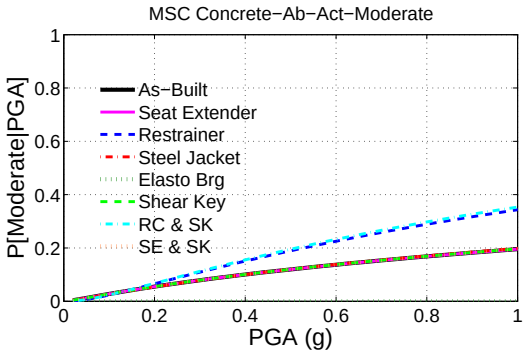

7-6(d):

Figure 7-6: Select component fragility curves for retrofitted MSC Concrete Girder bridge.

Similar trends are observed for the other bridge types in terms of retrofit having varying positive or negative effect on different components. The component fragility curves for all of the retrofitted bridge types are found in Appendix C.

7.6 Retrofitted Bridge System Fragility Curves

The insight gained from the component fragility curves leads to a need to evaluate the overall system vulnerability and impact of retrofit. A bridge system fragility curve serves to depict the overall bridge vulnerability and relative impact of various retrofits on the performance of the system. The system fragility curves are developed by convolving the joint probabilistic seismic demand models (or joint PDFs) with the limit states which describe the failure domain for each damage state. The integration is performed numerically through Monte Carlo simulation to estimate the failure probabilities across a range of intensities (PGAs). Figure 7-7 illustrates the intersection of a bi-variate joint probability density function with its failure domain. An example of one of the *N* simulations is shown.

For each Monte Carlo simulation, a sample of the system demand from the joint PSDMs and the limit state capacities for each component are simulated. Correlation between the demand placed on each component assessed in Section 7.3 is captured in the sampling. As recommended by Nielson (2005a), 100% correlation between the limit states for slight, moderate, extensive, and complete damage is assumed to ensure that the samples are in rank order ($c_{slight} < c_{moderate} < c_{extensive} < c_{complete}$). An indicator function is used to monitor the number of failed capacity-demand simulation pairs and numerically estimate the failure probability at each level of intensity across a reasonable range of peak ground accelerations. These failure probabilities are representative of estimates of the cumulative distribution

function (CDF) for the bridge system fragility. The parameters of the lognormal fragility distribution for each damage state are estimated through regression analysis. The form of the fragility is the same as shown in Equation 7.11, where the system fragility parameters are now termed med_{sys} and β_{sys}.

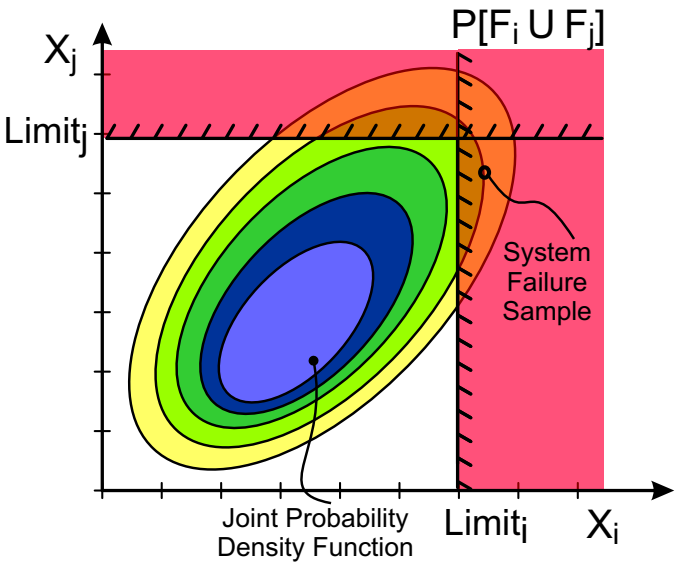

Figure 7-7: Example simulation for bi-variate PDF and failure domain.

7.7 Effect of Uncertainty Treatment on Fragility Estimates

Before presenting a detailed comparison of the system fragility curves for various bridge types and retrofit measures, a study is performed to assess the appropriate level of uncertainty treatment for fragility analysis of classess of retrofitted bridges. The results will be incorporated in the development and proposal of the new system fragility curves.

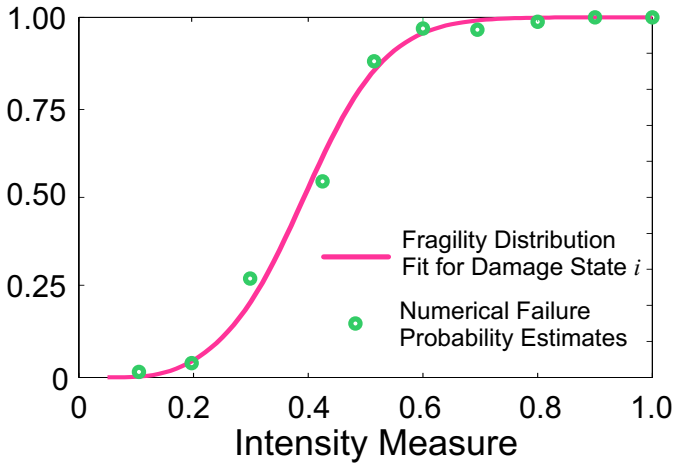

Figure 7-8: Illustration of system fragility estimation adapted from Nielson (2005a).

Analysts of the fragility of portfolios of structures have utilized a range of fidelity of uncertainty treatment, from considering only ground motion uncertainty (Karim and Yamazaki, 2001) to statistically varying over a dozen parameters (Nielson and DesRoches, 2007b) in simulations used to estimate the seismic demand. Without knowledge of the sensitivity of the failure estimate to various uncertainties it is difficult to know what level of uncertainty treatment is necessary to assess the fragility of these portfolios of structures. One may either be disregarding significant parameters which could lead to unreliable fragility estimates; or conversely may exhaust efforts unnecessarily on time-intensive and computationally expensive statistical sampling and simulation which has minimal influence on the resulting fragility estimates.

The ultimate objective of this study is to assess the impact of statistical treatment of the uncertain parameters relative to deterministic treatment on the resulting failure probability estimates. The goal is to assess the relative importance of ground motion uncertainty, gross

geometric uncertainty, and modeling parameter uncertainty on the fragility of classes of retrofitted bridges. The study is illustrated with one specific bridge type (multi-span simply supported steel girder). However, the general results have been found to be applicable to other common retrofitted bridge types.

7.7.1 Sensitivity of Fragility Curves

The parametric study presented in Chapter 5 revealed that the seismic response of various components in the retrofitted bridges are sensitive to a number of different modeling parameters, and the most significant parameters for each type of retrofitted bridges have been identified. The study also revealed the importance of considering the potential variation in loading direction and in the base geometries for portfolio analysis of retrofitted bridges (examined through a blocking analysis). The influence of capturing these different sources of uncertainty on the resulting fragility curves developed using the above outlined approach are assessed, by incrementally increasing the level of uncertainty treatment. Four sets of fragility curves with different levels of uncertainty treatment are considered as follows:

1. only the uncertainty in the ground motion (*Ground Motion*)
2. uncertainty in the ground motion and gross geometry (+*Geometry*)
3. uncertainty in the ground motion, geometry, and most important modeling parameters identified in the sensitivity study (+$Significant\ Parameters$)
4. considering all of the identified potential sources of uncertainty (+*All Parameters*)

The ground motion uncertainty captured and modeled by the fragility includes epistemic uncertainty in different ground motion modeling approaches by including the previously discussed suites of synthetic ground motions developed by Wen and Wu (2001) and Rix and Fernandez (2004). These researchers produced the ground motion suites with an effort to capture various sources of uncertainty in the source, path, and site characteristics which are then propagated through the fragility analysis. The ground motion uncertainty reflected in the fragilities also includes the unknown incident angle of the earthquake. The fragility curves developed considering only ground motion uncertainty (1) assume a single base bridge geometry (# 4 from Table 5-3 for the MSSS Steel bridge), and all other potentially uncertain modeling parameters previously discussed, such as the bearing stiffness, concrete strength, etc. are set to their median values. In addition to the ground motion uncertainty, the next level of uncertainty treatment (2) evaluated for fragility estimation considers the potential variation in base bridge geometry which is inherent to an assessment of portfolios of retrofitted bridges. The eight base bridge geometry samples previously discussed and listed in Table 5-3 are used in this simulation.

The other two sets of fragility estimates (3,4) developed also include uncertainties due to the modeling parameters discussed previously in the sensitivity study, such as steel strength, bearing stiffness, etc. The set of fragility curves named *+Significant Parameters* includes the variation only in the modeling parameters identified in Table 5-8 as the most significant parameters in the sensitivity study, in addition to the ground motion and gross geometric uncertainty. The fragility curves corresponding to *+All Parameters* are generated with all potentially uncertain modeling parameters (Table 5-2) as random variables, as well as ground motion and gross geometric uncertainties. A total of 12-16 parameters

are varied in these analyses for the MSSS Steel bridge, depending on the retrofit measure. These fragility curves represent the highest level of uncertainty treatment addressed in the study, and will be used as a basis of comparison for the other cases.

7.7.2 Example Using MSSS Steel Girder Bridge Retrofit with Restrainer Cables

Assessment of the fragility estimates for the MSSS steel bridge retrofit with restrainers (Figure 7-9) reveals that the fragilities developed considering the variation only in those modeling parameters identified as most important in the sensitivity study are nearly the same as those considering all potentially variable modeling parameters. The median values differ by only 0.3-2.4% for the slight through complete damage states. This is intuitive, since we have only varied those which significantly affect the seismic response of the critical components and thus impact the system vulnerability. These results reveal that we can save time and effort in simulating bridge models for the probabilistic seismic demand analysis by considering the variability only in those significant parameters identified in the sensitivity study.

It is interesting to note that there is relatively little difference between these fragilities and those developed considering only the uncertainty in the ground motion and base bridge geometry. Compared to the bridge considering all variable parameters, there is a 4.3-5.9% increase in the median values and a 2.0-6.1% decrease in the dispersion for the slight-complete damage states. In general, the uncertainty in the significant modeling parameters does not have a large affect on the fragility estimates, and the inclusion of only ground motion and geometric uncertainties may be adequate. It is evident in Figure 7-9, however, that there is a notable difference in the fragilities when the variation in gross geometric

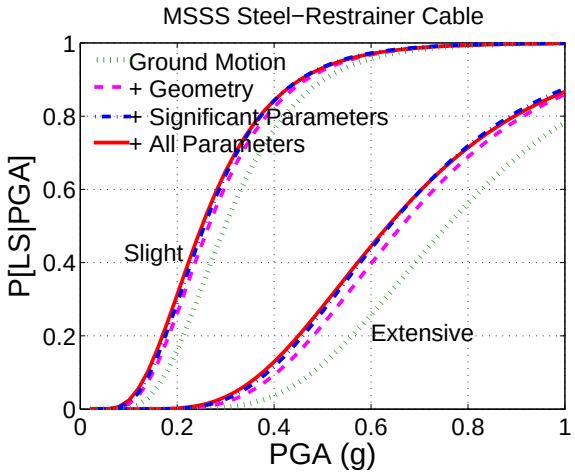

Figure 7-9: Comparison of different levels of uncertainty treatment for the MSSS Steel girder bridge retrofit with Restrainer Cables (showing fragility estimates for the slight and extensive damage state).

properties is neglected and only ground motion uncertainty is considered. The median values are 18.4-20.6% higher and dispersions 4.0-15.0% lower compared to the estimates with the highest level of uncertainty treatment. Without including the gross geometric variation in typical three-span steel girder bridges, the fragility for this portfolio may have been considerably underestimated, particularly at the higher damage states. Similar results were observed for the other retrofit measures.

In general, the uncertainty in the ground motion and gross geometry overshadows the contribution of other sources of uncertainty attributed to the bridge modeling itself. These findings underscore the importance of carefully characterizing the range in base geometric configurations in developing fragility estimates for portfolios of structures, as well as the

significant contribution of ground motion uncertainty that stems from the unknown incident angle of the earthquake, the random nature of ground motion, and the ground motion models (or synthetic suites) themselves which are used in the analysis.

The impact of increasing the level of uncertainty treatment in the development of fragility curves for the MSSS steel bridge retrofit with other measures is similar to the findings presented above for the restrainer retrofit. The difference in the fragility estimates with the other retrofits and the as-built bridge were of a similar magnitude, and reveal the significance of incorporating not only ground motion uncertainty but also variation in base geometry. Additionally they show the similarity between the fragilities considering all parameters as variable and only those identified in the sensitivity study. Lastly, they indicate that incorporating the uncertainty in these modeling parameters often has little effect on the resulting fragility estimate. The only exception is the elastomeric bearing retrofit. Including only the significant parameters relative to the fragilities with all variable parameters still yields little difference. However, assuming the median value for all parameters leads to a greater difference in the estimated lognormal parameters than observed in the other retrofitted bridges: 4.4-9.8% difference in the median values and 25.6-32.8% difference in the dispersion. Such a large difference in dispersion could have significant impacts on the conclusions, particularly if the fragilities are convolved with a seismic hazard. Evaluation of other classes of retrofitted bridges also indicates that the difference in dispersion could be considerable if only median values are assumed for the significant modeling parameters rather than probabilistic treatment.

The findings indicate that savings in simulation and computational effort may be achieved through a preliminary screening of parameters. However, this does not minimize the importance of carefully characterizing the potential range of modeling parameters in order to assign an assumed median value to these otherwise random variables. Additionally, the potential variation in both the ground motion and base geometry are critical considerations for developing seismic fragility curves for these classes of structures. Moreover, these sources of uncertainty tend to overshadow the others associated with modeling parameter variation, such as the damping ratio, elastomeric bearing stiffness, and length of restrainer cables. Careful definition of these modeling parameters could allow for deterministic treatment of a number of parameters whose variation has little effect on the overall fragility estimate. Efforts may be better spent in characterizing gross geometric configurations of the structure and addressing a number of factors which contribute to the ground motion uncertainty, such as loading direction, ground motion model, among others, and how to capture and propagate these sources through the fragility analysis. However, complete abandonment of probabilistic treatment of the modeling parameters identified as significant in the preliminary screening study would not be recommended. The findings of this study have revealed that the fragility estimate for some retrofitted bridge types is sensitive to incorporating the uncertainty in these modeling parameters, particularly in defining the lognormal standard deviation.

While this approach and the findings are presented for one class of bridges, the multi-span simply supported steel girder bridge, assessment of other bridge classes and retrofit measures yield similar results.

7.8 Developed Retrofitted Bridge Fragility Curves

Based on the findings above, the fragility curves proposed in this section are developed with an intermediate level of uncertainty treatment. In addition to ground motion and base geometric variation, uncertainty in only those parameters identified as the most significant parameters from the screening study will be incorporated. The resulting fragility curves derived for each bridge type and retrofit measure are presented below. The units for the median (med_{sys}) of the fragility is PGA.

7.8.1 Retrofitted MSSS Steel Girder Bridge

The fragility curves for the MSSS Steel Girder bridge are presented in Figure 7-10 for the slight, moderate, extensive, and complete damage states. These figures compare the as-built fragility to the fragility curves for the retrofit measures listed in Table 7-4. The derived system median, med_{sys}, and dispersion, β_{sys}, from this analysis are listed in Table 7-5.

Visual screening of the fragilities for the MSSS Steel bridge indicate that for the slight through extensive damage state, the elastomeric isolation bearing retrofit is the only measure that has a considerable impact on the system vulnerability. For this bridge type, while the columns had notable initial vulnerability, the steel fixed bearings followed by the expansion bearings tended to dominate the bridge vulnerability at the lower damage states. This is illustrated for the moderate damage state in Figure 7-11 which provides the component and system fragilities for the as-built bridge. It is noted that the relative vulnerability of the components does vary by damage state. By replacing the vulnerable steel bearings with isolation bearings, the fragility is significantly reduced. At these damage states, the

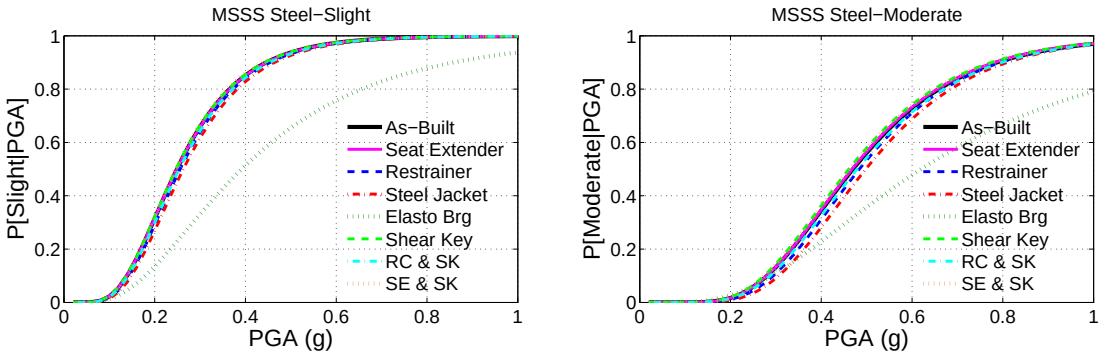

7-10(a):

7-10(b):

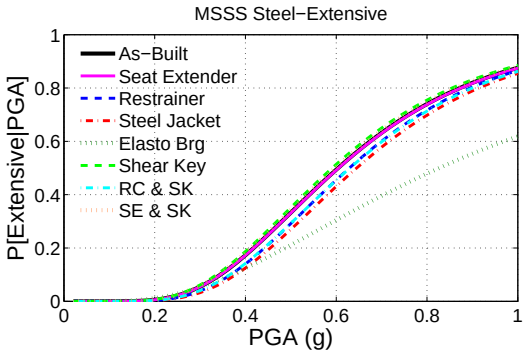

7-10(c):

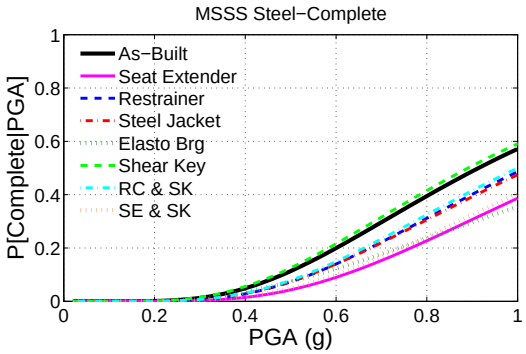

7-10(d):

Figure 7-10: Fragility curves for retrofitted MSSS Steel Girder bridge.

other retrofit measures are not particularly effective in reducing the system vulnerability, primarily because of the impact of the bearings. The restrainer cables have little impact at the lower damage states because of the low levels of displacement required to induce damage in the fixed bearings and relative slack in the cables, and for the higher damage states were not particularly effective in limiting deformations because of cable yielding. For the complete damage state, the seat extenders are effective due to the considerable increase in the limit state for complete damage of the bearings because of the lengthened support before collapse (152.4 mm of additional seat width).

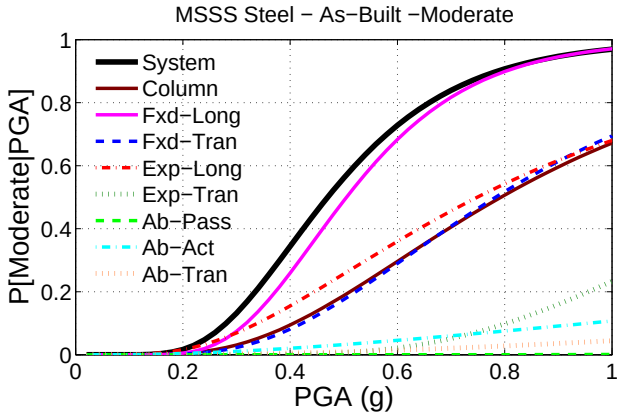

Figure 7-11: Relative vulnerability of the MSSS Steel as-built components for the moderate damage state.

7.8.2 Retrofitted MSC Steel Girder Bridge

The MSC Steel Girder Bridge is the most vulerable bridge type in the CSUS inventory. The relative vulnerability of the bridge with various retrofit measures is shown in Figure 7-12, and Table 7-6 lists the fragility parameters.

Table 7-5: System Fragility Curves for Retrofitted MSSS Steel Bridge.

Retrofit Condition	Slight		Moderate		Extensive		Complete	
	med_{sys}	β_{sys}	med_{sys}	β_{sys}	med_{sys}	β_{sys}	med_{sys}	β_{sys}
As-Built	0.25	0.45	0.47	0.40	0.60	0.44	0.91	0.50
Steel Jackets	0.26	0.44	0.50	0.38	0.65	0.42	1.03	0.50
Elastomeric Isolation Bearings	0.39	0.61	0.62	0.59	0.83	0.63	1.27	0.64
Restrainer Cables	0.26	0.45	0.48	0.39	0.63	0.42	1.02	0.49
Seat Extenders	0.25	0.46	0.47	0.40	0.61	0.44	1.15	0.49
Shear Keys	0.25	0.46	0.46	0.41	0.59	0.44	0.89	0.50
Restrainer Cables and Shear Keys	0.25	0.45	0.48	0.40	0.63	0.42	1.00	0.49
Seat Extenders and Shear Keys	0.25	0.45	0.46	0.40	0.60	0.44	1.13	0.49

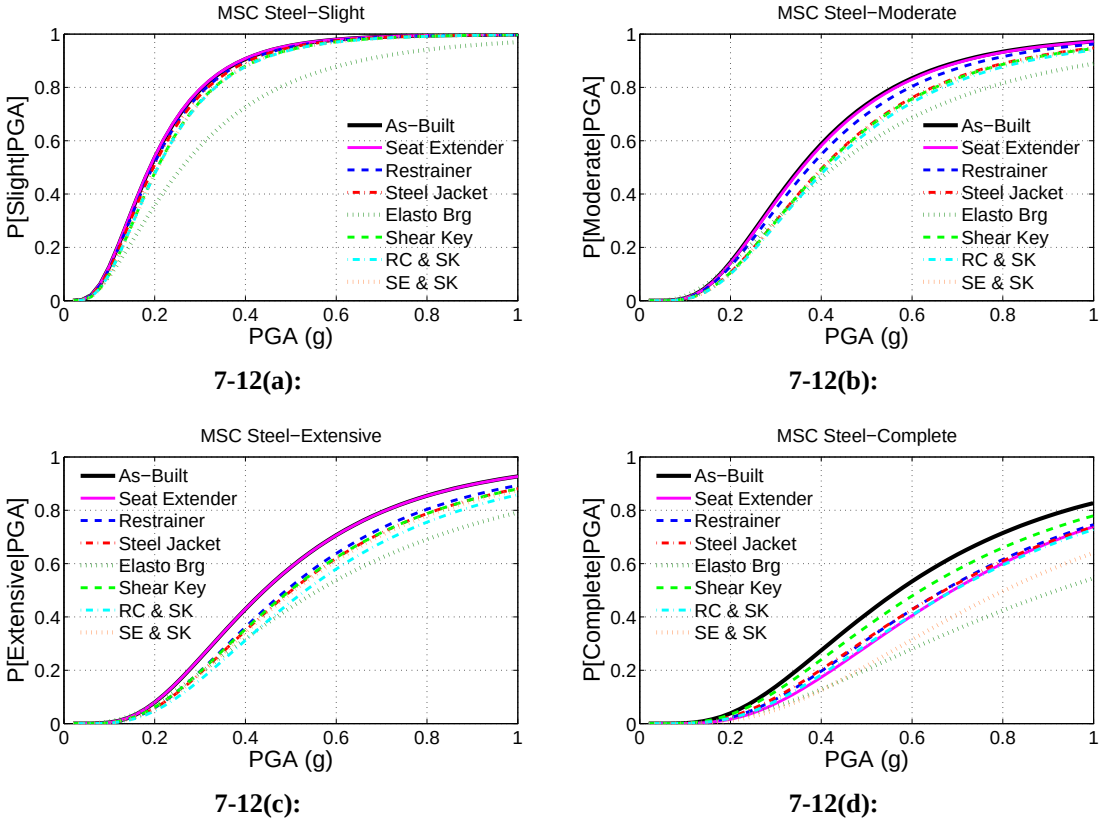

7-12(a): **7-12(b):** **7-12(c):** **7-12(d):**

Figure 7-12: Fragility curves for retrofitted MSC Steel Girder bridge.

The steel bearings in this bridge are still a primary concern, but for the continuous steel girder bridge which tends to respond like a single degree of freedom system, the fixed bearings above the columns are not as vulnerable as the expansion bearings at the far ends of the continuous bridge deck. The fixed bearings deform very little and the columns, deck, and bearings move together, facilitated by deformation of the expansion bearings and relatively large expansion joint at the deck ends. In addition, larger demands are placed on the columns of this bridge because of the inertial loads of the continuous deck acting in unison. The elastomeric bearings, therefore, are effective in replacing the more vulnerable steel expansion bearings. However, because all of the bearings act similarly in order to isolate the superstructure from the substructure, the demands are fairly high causing them to be slightly more vulnerable than the original fixed bearings (which are not required to deform considerably). This is not intuitive, but explains why the elastomeric bearings are not as effective as one may have presumed.

The expansion bearings are also vulnerable to damage in the transverse direction which is part of the explanation for the synergistic improvement of the performance of the MSC Steel bridge with seat extenders and shear keys. While the steel jackets have a significant impact on reducing the column vulnerability, their inability to affect other components results in limited improvement for the system fragility. The restrainer cables offer a slight improvement in the vulnerability of the expansion bearings, yet do not considerably reduce the system vulnerability because of the introduction of a new vulnerability. While the abutments initially had a low level of vulnerability, the large transfer of forces from the cable considerably increases their vulnerability and hence the system vulnerability.

Table 7-6: System Fragility Curves for Retrofitted MSC Steel Bridge.

	Slight		Moderate		Extensive		Complete	
Retrofit Condition	med_{sys}	β_{sys}	med_{sys}	β_{sys}	med_{sys}	β_{sys}	med_{sys}	β_{sys}
As-Built	0.19	0.56	0.36	0.54	0.44	0.56	0.57	0.59
Steel Jackets	0.20	0.57	0.40	0.56	0.50	0.58	0.67	0.62
Elastomeric Isolation Bearings	0.26	0.72	0.43	0.70	0.56	0.71	0.92	0.73
Restrainer Cables	0.20	0.57	0.37	0.55	0.49	0.57	0.67	0.60
Seat Extenders	0.19	0.56	0.36	0.54	0.44	0.56	0.69	0.58
Shear Keys	0.21	0.56	0.41	0.56	0.50	0.59	0.62	0.62
Restrainer Cables and Shear Keys	0.21	0.57	0.41	0.57	0.53	0.59	0.69	0.61
Seat Extenders and Shear Keys	0.21	0.56	0.41	0.56	0.51	0.59	0.80	0.61

7.8.3 Retrofitted MSSS Concrete Girder Bridge

Figure 7-13 shows the relative vulnerability of the as-built and retrofitted MSSS Concrete girder bridge. This concrete girder bridge has considerably less vulnerable bearings than its steel counterpart, yet has a larger mass. The relative vulnerability of various components in this as-built bridge varies considerably depending on the damage state. This helps to explain why different retrofits have a varying effect at the different damage states. For example, at the slight damage state, the longitudinal fixed and expansion bearings as well as the abutments in active action are the most susceptible to damage. Hence, the elastomeric bearings are particularly effective because they both replace the bearings and reduce the active demands placed on the abutments.

Beyond the limit of moderate damage, the columns tend to become more vulnerable and the steel jacketing becomes particularly effective. However, this retrofit does not improve the bearing or active abutment performance which both still contribute to the system fragility. The elastomeric bearings are not as effective beyond the slight damage state as one might have expected, because of the increased vulnerability of the abutments in the transverse direction. When this heavier bridge is on isolators which have transverse keepers

or allow pounding of the deck and wingwall, large forces can be transferred to this substructure element. It is also interesting to note that the use of shear keys actually increases the system vulnerability at the higher damage states. This is because the bearings of the bridge are not particularly susceptible to the higher levels of damage in the transverse direction, so there is negligible positive effect realized. Instead the shear keys actually result in more vulnerable columns due to the inertial loads transferred when the bridge is excited in the transverse direction. The parameters of these retrofitted bridge fragility curves can be found in Table 7-7.

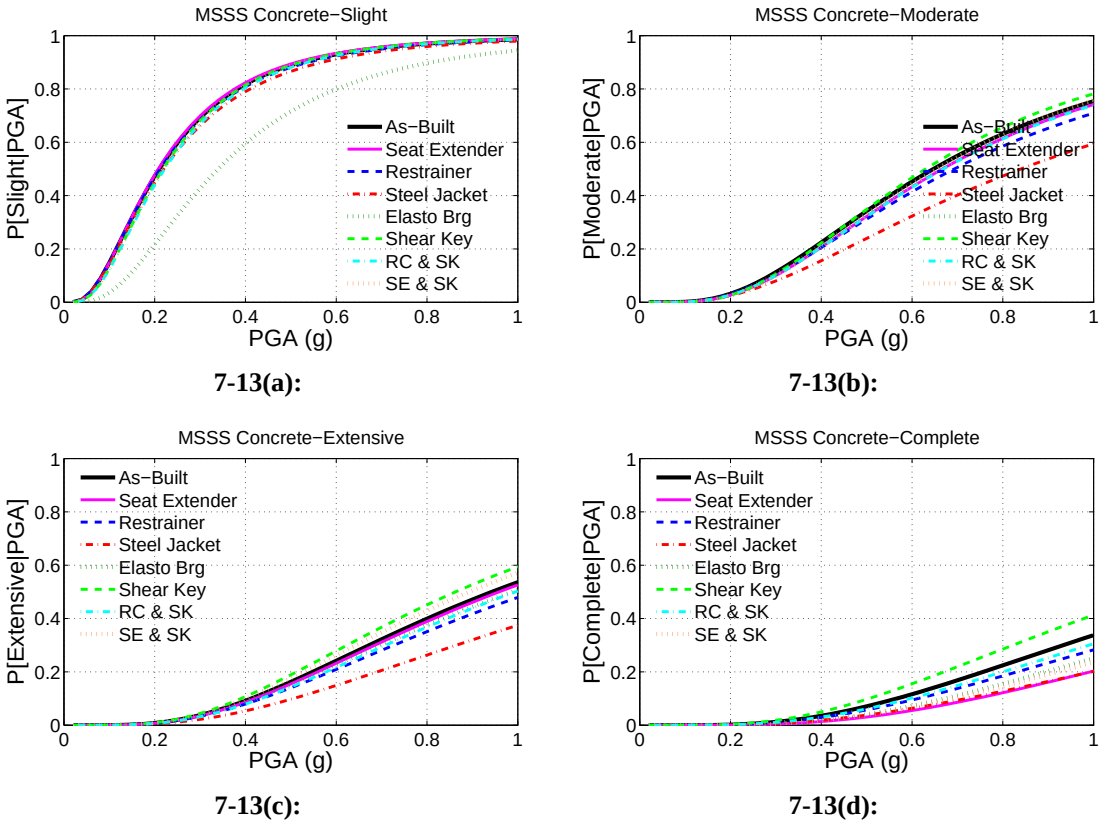

7-13(a): **7-13(b):** **7-13(c):** **7-13(d):**

Figure 7-13: Fragility curves for retrofitted MSSS Concrete Girder bridge.

Table 7-7: System Fragility Curves for Retrofitted MSSS Concrete Bridge.

	Slight		Moderate		Extensive		Complete	
Retrofit Condition	med_{sys}	β_{sys}	med_{sys}	β_{sys}	med_{sys}	β_{sys}	med_{sys}	β_{sys}
As-Built	0.21	0.71	0.65	0.63	0.94	0.65	1.32	0.66
Steel Jackets	0.22	0.74	0.84	0.73	1.25	0.71	1.85	0.74
Elastomeric Isolation Bearings	0.34	0.68	0.65	0.62	0.99	0.66	1.54	0.65
Restrainer Cables	0.21	0.73	0.69	0.67	1.04	0.68	1.49	0.69
Seat Extenders	0.21	0.70	0.67	0.62	0.96	0.64	1.74	0.67
Shear Keys	0.22	0.68	0.63	0.59	0.86	0.62	1.15	0.64
Restrainer Cables and Shear Keys	0.22	0.69	0.67	0.63	1.00	0.65	1.41	0.67
Seat Extenders and Shear Keys	0.22	0.68	0.66	0.60	0.89	0.63	1.60	0.66

7.8.4 Retrofitted MSC Concrete Girder Bridge

The as-built MSC Concrete girder bridge system and component fragilities at the slight and complete damage state are shown in Figure 7-14 to facilitate an assessment of the reason for different retrofit measures' impact on the bridge vulnerability. The fragility curves for the retrofitted bridge system is shown in Figure 7-15 with parameters listed in Table 7-8. It is evident that the elastomeric bearings are very effective at the slight damage state for the MSC Concrete bridge, though no other measures impact the system fragility. The steel jackets are effective in reducing the column vulnerability at the slight damage state, but the other vulnerable components shown in Figure 7-14(a) are not improved. The slight improvement in transverse bearing vulnerability (though not a particularly vulnerable component) using the shear keys is offset by the increased vulnerability of the transverse demands on the abutments. As seen with the MSSS Concrete bridge, the steel jackets tend to be more effective at limiting the higher levels of damage where the columns contribute more to the vulnerability. The restrainer cables, however, are not effective for this bridge because their effectiveness on improving bearing performance is limited by the yielding of the cables induced by the large inertial loads. Additionally, any positive benefit they have is negated

by the negative impact on the abutments in active action. The seat extenders become effective at the complete damage state because they virtually remove any contribution of the bearings to the system's potential for complete damage.

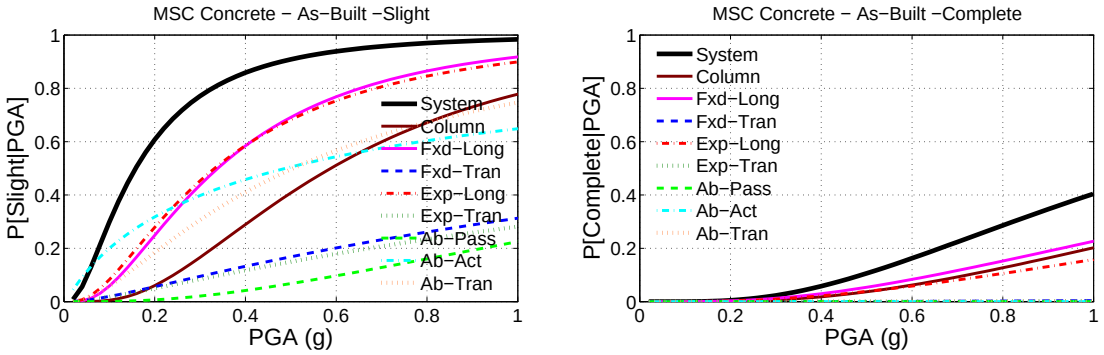

7-14(a): **7-14(b):**

Figure 7-14: Relative vulnerability of the MSC Concrete as-built components for the (a) slight and (b) complete damage states.

Table 7-8: System Fragility Curves for Retrofitted MSC Concrete Bridge.

	Slight		Moderate		Extensive		Complete	
Retrofit Condition	med_{sys}	β_{sys}	med_{sys}	β_{sys}	med_{sys}	β_{sys}	med_{sys}	β_{sys}
As-Built	0.16	0.86	0.59	0.69	0.85	0.69	1.18	0.69
Steel Jackets	0.16	0.88	0.69	0.78	0.99	0.73	1.42	0.74
Elastomeric Isolation Bearings	0.47	0.66	0.77	0.64	1.03	0.70	1.38	0.70
Restrainer Cables	0.16	0.79	0.57	0.69	0.86	0.67	1.24	0.66
Seat Extenders	0.16	0.86	0.59	0.69	0.85	0.68	1.54	0.68
Shear Keys	0.16	0.82	0.58	0.69	0.84	0.67	1.19	0.69
Restrainer Cables and Shear Keys	0.16	0.76	0.57	0.69	0.88	0.67	1.33	0.67
Seat Extenders and Shear Keys	0.16	0.84	0.57	0.69	0.84	0.67	1.62	0.69

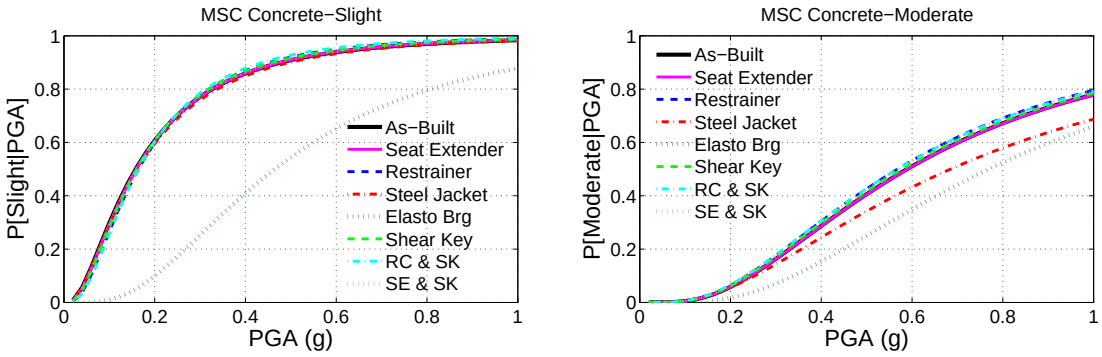

7-15(a):

7-15(b):

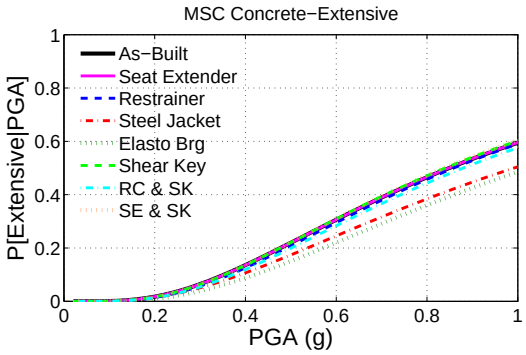

7-15(c):

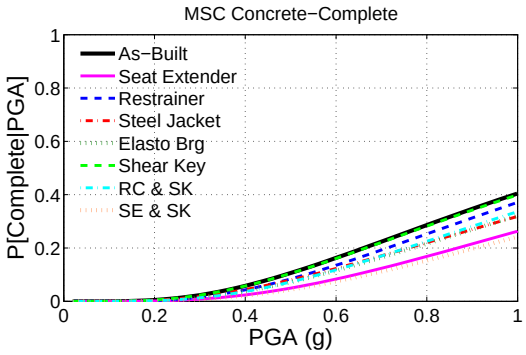

7-15(d):

Figure 7-15: Fragility curves for retrofitted MSC Concrete Girder bridge.

7.9 Closure

This Chapter has presented the methodology for analytically deriving system fragility curves for general classes of retrofit bridges, as well as the developed retrofitted bridge fragilities for common bridge classes in the Central and Southeastern United States. Four different bridge types and five retrofit measures were considered, as well as common combinations of some superstructure retrofits. The retrofits considered include elastomeric isolation bearings, restrainer cables, steel jackets, shear keys, and seat extenders.

The fragilities developed utilize a total of 96 ground motions that have been synthesize by other researchers for the CSUS region (Rix and Fernandez, 2004; Wen and Wu, 2001). The impact of retrofit on the demand placed on multiple components was captured through the development of joint probabilistic seismic demand models (PSDMs), or joint probability distributions. Capacity estimates for the various bridge components were presented such that they have functional consistency, and the alteration of these limit state capacities due to the retrofits was also assessed. The impact of retrofit on the fragility of different components was presented to illustrate that retrofits may reduce the vulnerability of some components, have negligible impact on others, and increase the vulnerability of some. Retrofitted bridge system fragility curves are developed by convolving the joint PDFs for demand with the failure domain across all components through Monte Carlo simulation. These fragility curves were developed including ground motion uncertainty, variation in base bridge geometry, and variation in those modeling parameters which were identified in the screening study from Chapter 5. This level of uncertainty treatment was identified as appropriate in the study in this Chapter.

The fragility curves developed as a part of this work reveal that the retrofit measure which most effectively reduces the vulnerability of the bridge system is a function of the bridge type and damage state of interest. In general, the elastomeric bearings are particularly effective retrofit measures for the Steel girder bridges. This attributed more to the fact that they replace the highly vulnerable steel bearings with less vulnerable isolation bearings than the improved column performance. The seat extenders are effective for the complete damage state because of their ability to limit unseating and reduce bearing vulnerability. For the continuous steel and concrete girder bridges the column vulnerability contributes more to the system fragility and hence the steel jackets show more of an impact than in their MSSS counterpart. This retrofit measure does not improve the vulnerability of other components, though. The shear keys actually lead to increased vulnerability of the MSSS Concrete bridge because of the increased forces transferred to the abutments in the transverse direction. Overall, the restrainer cables are not particularly effective. In some cases this is because of the small deformations indicative of steel bearing damage and relative cable slack, or because of the increased demands placed on the abutments in active action, or in other cases because of the yielding of the cables (particularly for the heavier concrete bridges).

It is evident that overarching statements regarding the most viable retrofit measure are difficult to make. This is because the ability of a retrofit measure to reduce the potential for meeting a level of damage is dependent upon the class of bridge and damage state. Also, the objectives of the decision maker could factor heavily into the recommendation, such as targeting a specified level of bridge performance or considering the cost-effectiveness of the investment in retrofit. Selection of viable retrofit measures for general classes of bridges

common to the CSUS using these developed fragility curves is presented in the next chapter. Their application in various frameworks for risk mitigation activities is highlighted.

CHAPTER VIII

APPLICATIONS OF RETROFITTED BRIDGE FRAGILITY CURVES

This chapter presents approaches for implementing fragility curves for retrofitted bridges, including proposed fragilities and potential simplifications, modification factors describing the scaling of fragility parameters for various retrofit measures, and the potential extension and application for other bridge types. In addition, applications of the retrofitted bridge fragility curves developed in the thesis are highlighted, including selecting viable retrofit strategies based on a range of techniques (median value fragility improvement, performance-based retrofit, or cost-benefit analyses). The chapter concludes with a discussion of the application of the retrofitted bridge fragility curves in a regional seismic risk assessment.

8.1 Implementation and Proposed Retrofitted Bridge Fragility Curves

The retrofitted bridge fragility curves developed in Chapter 7 can be adopted with the log-normal parameters directly evaluated as a part of this work. The as-built bridge fragilities developed by Nielson and DesRoches (2007b) for common classes of retrofitted bridges are presented in Table 8-1. As evidenced in the Table, these as-built fragilities have been simplified to have similar dispersions for each damage state across a given bridge type.

Table 8-1: Simplified Fragility Curves for As-Built CSUS Bridges Proposed by Nielson and DesRoches (2007b).

	Median PGA Value (g), med_{sys}				
Bridge Type	**Slight**	**Moderate**	**Extensive**	**Complete**	β_{sys}
MSC Concrete	0.15	0.52	0.75	1.03	0.70
MSC Slab	0.17	0.45	0.78	1.73	0.70
MSC Steel	0.18	0.31	0.39	0.5	0.55
MSSS Concrete	0.2	0.57	0.83	1.17	0.65
MSSS Conc Box	0.21	0.65	1.19	2.92	0.75
MSSS Slab	0.18	0.52	0.94	1.92	0.75
MSSS Steel	0.24	0.44	0.56	0.82	0.50
SS Concrete	0.41	1.84	2.62	3.64	0.90
SS Steel	0.63	1.14	1.52	2.49	0.55

8.1.1 Simplified Fragility Parameters

Users may choose to use the more specific retrofitted bridge fragility curves presented in Chapter 7 with unique median and dispersions for each damage state. As previously indicated, simplified fragility curves with a single dispersion for each as-built bridge type have been presented by Nielson and DesRoches (2007b) as well as in HAZUS (FEMA, 2005). This simplification is intended to facilitate the dissemination of information and incorporation into software packages or studies. The simplified fragility curves for the retrofitted bridges are listed in Table 8-2 - Table 8-5.

Table 8-2: Proposed Simplified Fragility Curves for Retrofitted MSSS Steel Girder Bridge.

	Median PGA Value (g), med_{sys}				
Retrofit Measure	**Slight**	**Moderate**	**Extensive**	**Complete**	β_{sys}
Steel Jackets	0.26	0.50	0.65	1.03	0.45
Elastomeric Isolation Bearings	0.39	0.62	0.83	1.27	0.60
Restrainer Cables	0.26	0.48	0.63	1.02	0.45
Seat Extenders	0.25	0.47	0.61	1.15	0.45
Shear Keys	0.25	0.46	0.59	0.89	0.45
Restrainer Cables and Shear Keys	0.25	0.48	0.63	1.00	0.45
Seat Extenders and Shear Keys	0.25	0.46	0.60	1.13	0.45

Table 8-3: Proposed Simplified Fragility Curves for Retrofitted MSC Steel Girder Bridge.

	Median PGA Value (g), med_{sys}				
Retrofit Measure	**Slight**	**Moderate**	**Extensive**	**Complete**	β_{sys}
Steel Jackets	0.20	0.40	0.50	0.67	0.60
Elastomeric Isolation Bearings	0.26	0.43	0.56	0.92	0.70
Restrainer Cables	0.20	0.37	0.49	0.67	0.60
Seat Extenders	0.19	0.36	0.44	0.69	0.60
Shear Keys	0.21	0.41	0.50	0.62	0.60
Restrainer Cables and Shear Keys	0.21	0.41	0.53	0.69	0.60
Seat Extenders and Shear Keys	0.21	0.41	0.51	0.80	0.60

Table 8-4: Proposed Simplified Fragility Curves for Retrofitted MSSS Concrete Girder Bridge.

	Median PGA Value (g), med_{sys}				
Retrofit Measure	**Slight**	**Moderate**	**Extensive**	**Complete**	β_{sys}
Steel Jackets	0.22	0.84	1.25	1.85	0.70
Elastomeric Isolation Bearings	0.34	0.65	0.99	1.54	0.65
Restrainer Cables	0.21	0.69	1.04	1.49	0.70
Seat Extenders	0.21	0.67	0.96	1.74	0.65
Shear Keys	0.22	0.63	0.86	1.15	0.65
Restrainer Cables and Shear Keys	0.22	0.67	1.00	1.41	0.65
Seat Extenders and Shear Keys	0.22	0.66	0.89	1.60	0.65

8.1.2 Modification Factors and Extension to Other Bridge Types

The most significant change between the as-built and retrofitted fragility parameters is in the variation in the median values. Modification factors are derived that can be applied to as-built fragility curves to account for the impact of retrofit on the bridge system vulnerability. These modification factors may be applied as scalars on the median values to refined fragility curves developed in the future, or empirical fragility curves should sufficient data allow for their development for these bridge types. The modification is calculated using the

Table 8-5: Proposed Simplified Fragility Curves for Retrofitted MSC Concrete Girder Bridge.

	Median PGA Value (g), med_{sys}				
Retrofit Measure	**Slight**	**Moderate**	**Extensive**	**Complete**	β_{sys}
Steel Jackets	0.16	0.69	0.99	1.42	0.80
Elastomeric Isolation Bearings	0.47	0.77	1.03	1.38	0.65
Restrainer Cables	0.16	0.57	0.86	1.24	0.70
Seat Extenders	0.16	0.59	0.85	1.54	0.75
Shear Keys	0.16	0.58	0.84	1.19	0.75
Restrainer Cables and Shear Keys	0.16	0.57	0.88	1.33	0.70
Seat Extenders and Shear Keys	0.16	0.57	0.84	1.62	0.75

fragility curves from Chapter 7, for consistency in the methodology and level of uncertainty treatment between the as-built and retrofitted bridges, as shown in Equation 8.1.

$$Modification = \frac{med_{sys(retrofitted)}}{med_{sys(as-built)}} \tag{8.1}$$

The resulting modification factors for the median values are indicated in Table 8-6 - Table 8-9 for the four bridge types.

Table 8-6: Modification Factors for Retrofitted MSSS Steel Girder Bridge.

	Modification Factor for Median Value			
Retrofit Measure	**Slight**	**Moderate**	**Extensive**	**Complete**
Steel Jackets	1.06	1.06	1.07	1.13
Elastomeric Isolation Bearings	1.57	1.32	1.37	1.39
Restrainer Cables	1.03	1.03	1.04	1.11
Seat Extenders	1.00	1.00	1.00	1.26
Shear Keys	0.99	0.98	0.98	0.97
Restrainer Cables and Shear Keys	1.02	1.02	1.04	1.09
Seat Extenders and Shear Keys	0.99	0.98	0.99	1.23

Table 8-7: Modification Factors for Retrofitted MSC Steel Girder Bridge.

	Modification Factor for Median Value			
Retrofit Measure	**Slight**	**Moderate**	**Extensive**	**Complete**
Steel Jackets	1.04	1.14	1.14	1.18
Elastomeric Isolation Bearings	1.37	1.21	1.27	1.61
Restrainer Cables	1.03	1.05	1.11	1.17
Seat Extenders	1.00	1.00	1.00	1.21
Shear Keys	1.08	1.14	1.13	1.09
Restrainer Cables and Shear Keys	1.09	1.17	1.21	1.21
Seat Extenders and Shear Keys	1.09	1.15	1.15	1.41

Table 8-8: Modification Factors for Retrofitted MSSS Concrete Girder Bridge.

	Modification Factor for Median Value			
Retrofit Measure	**Slight**	**Moderate**	**Extensive**	**Complete**
Steel Jackets	1.05	1.30	1.33	1.41
Elastomeric Isolation Bearings	1.62	1.01	1.05	1.17
Restrainer Cables	1.01	1.07	1.10	1.13
Seat Extenders	0.99	1.03	1.02	1.32
Shear Keys	1.04	0.97	0.92	0.87
Restrainer Cables and Shear Keys	1.06	1.03	1.06	1.07
Seat Extenders and Shear Keys	1.04	1.01	0.95	1.22

Table 8-9: Modification Factors for Retrofitted MSC Concrete Girder Bridge.

	Modification Factor for Median Value			
Retrofit Measure	**Slight**	**Moderate**	**Extensive**	**Complete**
Steel Jackets	1.03	1.16	1.17	1.20
Elastomeric Isolation Bearings	2.94	1.31	1.21	1.17
Restrainer Cables	1.04	0.96	1.01	1.05
Seat Extenders	1.00	1.00	1.00	1.31
Shear Keys	1.01	0.98	0.99	1.01
Restrainer Cables and Shear Keys	1.04	0.96	1.04	1.12
Seat Extenders and Shear Keys	1.01	0.97	0.99	1.37

This work focused on evaluating the impact of seven different retrofit approaches on the four most common and potentially vulnerable bridges in the Central and Southeastern US. However, as indicated in Table 8-1, Nielson and DesRoches have developed as-built fragility curves for other common classes of bridges. The modification factors could be applied to these additional as-built bridge fragilities to obtain an estimate of the potential impact of retrofit on the fragility. However appropriate mapping of the modification factors must be identified so that they are applicable to as-built structures which have similar response and vulnerabilities. Table 8-10 presents recommendations for which retrofit modification factors should be applied to a given as-built fragility. It is noted that the resulting retrofitted bridge fragility estimates for classes not directly evaluated as a part of this work are estimates and representative of the likely influence of retrofit on the bridge system performance. The mapping is based on judgement from evaluation of the work by Nielson (2005a) which allows for comparison of the relative vulnerability of the as-built bridges and which classes respond similarly or have similar component vulnerabilities within the system.

The single span bridges are more unique from those evaluated for retrofit as a part of this work since the column vulnerabilities do not contribute to these systems. Therefore, direct mapping to the median value modification factors listed in Table 8-6 - Table 8-9 are not appropriate. Simplified approximations are proposed in Tables 8-11 and 8-12. For the singe span (SS) bridges, the components which tend to dominate the vulnerability of the system are the bearings. The most vulnerable bearing response quantity for each damage

Table 8-10: Recommendations for Mapping of Modification Factors for Other Bridge Types.

As-Built Bridge Type	Recommended Modification Factors
MSC Concrete	MSC Concrete
MSC Slab	MSC Concrete
MSC Steel	MSC Steel
MSSS Concrete	MSSS Concrete
MSSS Conc Box	MSSS Concrete
MSSS Slab	MSSS Concrete
MSSS Steel	MSSS Steel
SS Concrete	Approx SS Concrete*
SS Steel	Approx SS Steel*

* = see approximations for single span (SS) bridges presented below

state for the SS Steel and SS Concrete girder bridges are identified and modification factors are approximated based on the impact of retrofit on these components in the MSSS counterparts. Any modification factor greater than ten is assigned a value of 10.00.

In general for both of these bridge types the seat extenders are the most effective at the complete damage state because this level of damage tends to be controlled by the longitudinal bearing vulnerability, and the seat extenders considerably increase the capacity of these components. The restrainer cables are not expected to be effective for the SS Steel bridge at the lower damage states because of the limited impact they have for the steel fixed bearings relative to the cable slack. The isolation bearings are particularly effective for the lower damage states because they replace the vulnerable existing bearings with ones of higher capacity. For the SS Concrete bridge with larger deck mass, it is expected that the effect of the restrainers at limiting higher levels of damage may be diminished because of cable yielding. It is also noted that because the longitudinal bearing deformations tend

to dominate the bridge vulnerability, the transverse shear keys actually result in the limiting transverse deformations but increasing longitudinal bearing deformations. Hence, the effect of the shear keys on this bridge may actually be negative, as evidenced in Table 8-12.

Table 8-11: Approximate Modification Factors for Retrofitted SS Steel Girder Bridge.

	Modification Factor for Median Value			
Retrofit Measure	**Slight**	**Moderate**	**Extensive**	**Complete**
Steel Jackets	N/A	N/A	N/A	N/A
Elastomeric Isolation Bearings	6.92	1.63	1.58	1.53
Restrainer Cables	1.04	1.01	1.02	1.30
Seat Extenders	1.00	1.00	1.00	1.61
Shear Keys	0.96	0.99	0.99	0.98
Restrainer Cables and Shear Keys	0.99	1.02	1.02	1.25
Seat Extenders and Shear Keys	0.96	0.99	0.99	1.57

Table 8-12: Approximate Modification Factors for Retrofitted SS Concrete Girder Bridge.

	Modification Factor for Median Value			
Retrofit Measure	**Slight**	**Moderate**	**Extensive**	**Complete**
Steel Jackets	N/A	N/A	N/A	N/A
Elastomeric Isolation Bearings	2.58	1.07	1.12	1.39
Restrainer Cables	1.12	1.30	1.34	1.01
Seat Extenders	1.00	1.00	1.00	10.00
Shear Keys	0.92	0.85	0.83	0.83
Restrainer Cables and Shear Keys	1.07	1.14	1.16	1.02
Seat Extenders and Shear Keys	0.92	0.85	0.83	1.36

8.2 Retrofit Selection for Typical Bridges

The fragility curves developed as a part of this work provide insight on appropriate retrofit measures for different bridge types and damage states. Evaluation of the fragilities provides

insight for designers and decision makers on viable retrofit selections. Three approaches to using these retrofitted bridge fragility curves to identify and select a retrofit measure are presented below to provide guidance for future studies and retrofit of bridges in the CSUS.

8.2.1 Median Value Improvement

One of the simplest ways of comparing the different retrofit measures is to evaluate the relative change in the median value of the fragility estimate. While the modification factors themselves provide insight, directly computing the percent change in the median value relative to the as-built median allows for quick screening and comparison of the retrofits. A positive percent change in the median indicates a shift of the median value indicative of a less vulnerable structure, while a negative change in the median value indicates a more vulnerable structure (Figure 8-1).

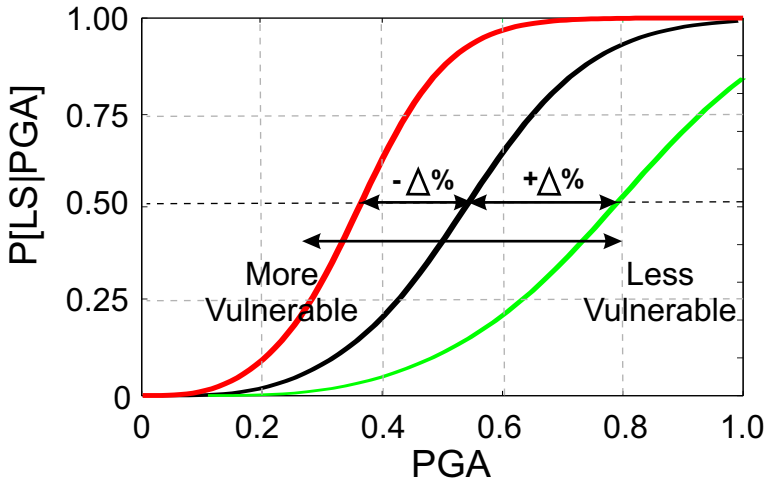

Figure 8-1: Illustration of percent change in median value relative to as-built system vulnerability.

The percent change in the median values for the system fragility curves are listed in Appendix D for the four typical classes of bridges evaluated as a part of this work. The table for the MSSS Concrete bridge is listed in Table 8-13. The retrofit with the largest positive percent difference in the median value is indicative of the most favorable retrofit selection, based on the criteria of median value shift of the vulnerability. In the Tables, the retrofit measure with the largest median value improvement for each bridge type and damage state is presented in boldface type. Screening of these median value changes indicates for the MSSS Concrete girder bridge, for example, that the elastomeric bearings are the most effective for the slight damage state, while the steel jackets are the most effective for the other damage states.

Table 8-13: Percent Difference in Fragility Medians for Retrofitted MSSS Concrete Relative to As-Built Bridge.

	% Difference in med_{sys} from As-Built			
Retrofit Measure	**Slight**	**Moderate**	**Extensive**	**Complete**
Steel Jackets	+5%	**+30%**	**+33%**	**+41%**
Elastomeric Isolation Bearings	**+62%**	+1%	+5%	+17%
Restrainer Cables	+1%	+7%	+10%	+13%
Seat Extenders	-1%	+3%	+2%	+32%
Shear Keys	+4%	-3%	-8%	-13%
Restrainer Cables and Shear Keys	+6%	+3%	+6%	+7%
Seat Extenders and Shear Keys	+4%	+1%	-5%	+22%

8.2.1.1 Fragility Comparison at Other Percentiles

While comparing median values of the fragility for the as-built bridge with various retrofit measure provides a quick approach for screening retrofits, there are some noted limitations.

This does not capture the impact of different retrofits on the dispersion, which could affect the failure probability, and the likely impact of retrofit for higher probability events. It may therefore be desirable to evaluate other percentiles (in addition to the 50th percentile represented by comparing median values). For example entering at the 5th percentile would provide insight as to what level of earthquake could be experienced to avoid damage 95% of the time, with and without retrofit. Such lower percentiles as the 5th or 10th percentiles are often used for screening structural vulnerability (Ellingwood and Wen, 2005), and could offer viable levels for comparison of retrofit.

The comparison at alternate percentiles is accomplished by the following

$$\Phi\left(\frac{\ln(PGA_{x\%}) - \ln(med_{sys})}{\beta_{sys}}\right) = x\% \tag{8.2}$$

$$\frac{\ln(PGA_{x\%}) - \ln(med_{sys})}{\beta_{sys}} = \Phi^{-1}(x\%) \tag{8.3}$$

$$\ln(PGA_{x\%}) = \ln(med_{sys}) + \beta_{sys} \cdot \Phi^{-1}(x\%) \tag{8.4}$$

$$PGA_{x\%} = med_{sys} \cdot exp\left(\beta_{sys} \cdot \Phi^{-1}(x\%)\right) \tag{8.5}$$

Comparison of the 5th percentile values will be illustrated herein, where the $PGA_{0.05}$ is found as shown in Equation 8.6.

$$PGA_{0.05} = med_{sys} \cdot exp\left(\beta_{sys} \cdot (-1.645)\right) \tag{8.6}$$

This percentile is illustrated in Figure 8-2 comparing the value of the fragility for the as-built and retrofitted bridge.

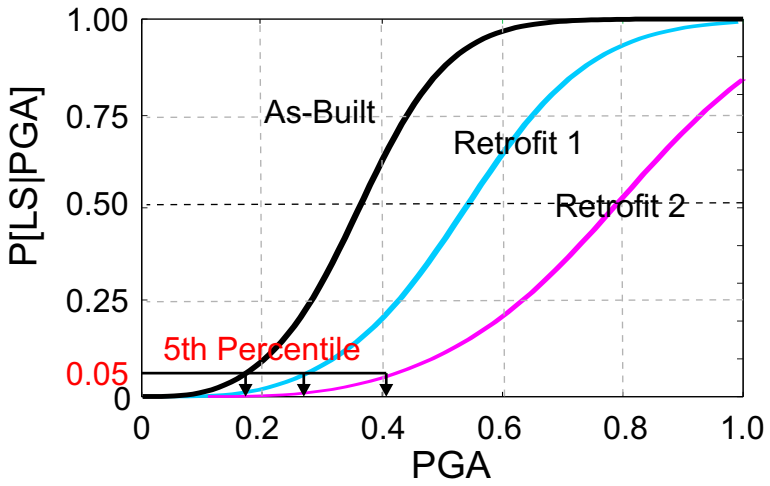

Figure 8-2: Illustration of 5th percentile for the as-built and retrofitted bridge.

The 5th percentile values of the fragility for the as-built and retrofitted MSC Concrete bridge are listed in Table 8-14 based on Equation 8.6. A comparison of these values reveals that 95% of the time, the as-built bridge would be completely damaged following an earthquake having a peak ground acceleration (PGA) of 0.38 g. However, the bridge retrofit with seat extenders and shear keys would require an earthquake with a PGA of 0.52 g. This corresponds to a 37% increase in the 5th percentile value of the fragility. From Equation 8.5, decision-makers can select alternate percentiles for comparison of other classes of as-built and retrofitted bridge fragilities.

Table 8-14: 5th Percentile Values of As-Built and Retrofitted Fragility for the MSC Concrete Bridge.

	PGA (g) for the 5th Percentile			
Retrofit Measure	**Slight**	**Moderate**	**Extensive**	**Complete**
As-Built	0.038	0.190	0.275	0.380
Steel Jackets	0.038	0.191	0.299	0.418
Elastomeric Isolation Bearings	0.158	0.269	0.327	0.440
Restrainer Cables	0.044	0.184	0.287	0.419
Seat Extenders	0.039	0.190	0.276	0.501
Shear Keys	0.041	0.185	0.277	0.381
Restrainer Cables and Shear Keys	0.047	0.181	0.293	0.441
Seat Extenders and Shear Keys	0.040	0.184	0.277	0.522

8.2.2 Performance-Based Retrofit Assessment

In recent years, performance-based design has gained support and is a paradigm that has been recommended for bridge retrofit. The benefits of this approach include the ability to design to a target level of performance, and to assess and predict the bridge response and performance within an interval of confidence. The recent draft edition of the *Seismic Retrofitting Manual for Highway Bridges* (FHWA, 2006) has encouraged a performance-based approach to seismic retrofitting, including the use of fragility curves for assessing potential bridge damage, prioritizing bridges for retrofit, and performing seismic risk assessments.

Building upon the existing performance-based approach outlined in the *Seismic Retrofitting Manual*, fragility curves for retrofitted bridges could provide an opportunity to assess potential bridge retrofit measures. The recommended retrofit process for bridges in the Seismic Retrofitting Manual has two stages, including a dual-level performance evaluation where the acceptable level of performance is determined based on the bridge importance

and remaining service life. Retrofitted bridge fragility curves could be utilized to assess the probability of meeting the dual-level performance objectives identified in the retrofit process framework. The retrofitted bridge fragilities developed as a part of this work can be used to identify which retrofit measures might be most appropriate for achieving a set of performance objectives for a given bridge type. As evidenced by the fragility curves shown in Chapter 7, some retrofits tend to reduce the potential for achieving a given state of damage. Identification of the retrofit measure which most effectively reduces this probability is dependent on the bridge type, the performance objectives in terms of the realization of the design level earthquake, and the damage state of interest.

8.2.2.1 Dual Level Retrofit Evaluation

The *Seismic Retrofit Manual for Highway Bridges* (FHWA, 2006) recommends minimum performance levels for retrofitted bridges for two levels of seismic hazard. These design performance levels are intended to help achieve a target level of bridge operation (or functionality) and an acceptable level of damage following the earthquake event. Table 8-15 presents the minimum performance levels for the upper and lower level hazards recommended in the Retrofit Manual. As evidenced in the Table, the performance objectives for each hazard are dependent upon the years of anticipated service life remaining and the importance level of the bridge.

The performance levels defined in the dual-level assessment must be mapped to the fragility damage states in order to utilize the fragilities in a performance assessment of the bridge with various retrofit strategies. This is facilitated by the fact that the fragilities in this work were developed with limit states and damage state definitions that correspond to an

anticipated level of functionality (allowable traffic carrying capacity). For a $PL1$, life safety performance level, the objective is to reduce the probability of achieving the complete damage state. The $PL2$ performance level, defined by the ability to provide service for emergency vehicles after inspection and eventually restore full functionality after repair, is assumed to coincide with the moderate damage state which has a restoration function as shown in Figure 6-2 from Chapter 6. Finally, if the fully operational $PL3$ is the objective, it is desirable to reduce the probability of even slight damage. Because the fragility limit states have been associated with an expected level of functionality, mapping to operational performance objectives as stated above is facilitated. A summary of the mapping between performance levels presented in the Retrofit Manual and the damage state definitions from Chapter 6 are presented in Table 8-16.

8.2.2.2 Example Performance-Based Retrofit Assessment

The retrofitted bridge fragility curves coupled with the dual-level framework will be used in an example preliminary retrofit screening for a multi-span simply supported steel girder bridge. The fragilities in this work are being developed for general classes of bridges that are common to the CSUS and are not intended to be structure-specific. Thus, the conclusions drawn are intended to serve as the starting point in the preliminary retrofit selection or alternative identification phase. However, the methodology could be applied for the evaluation of a specific structure.

It is assumed that the bridge of interest is a standard MSSS Steel bridge located in Caruthersville, MO with an anticipated remaining service life of over fifty years ($ASL3$).

Table 8-15: Minimum Performance Levels for Retrofitted Bridges Adapted from the *Seismic Retrofitting Manual for Highway Bridges* (FHWA, 2006).

	Bridge Importance and Service Life Category					
	Standard			Essential		
Earthquake Ground Motion	**ASL 1**	**ASL 2**	**ASL 3**	**ASL 1**	**ASL 2**	**ASL 3**
Lower Level Ground Motion	PL0	PL3	PL3	PL0	PL3	PL3
Upper Level Ground Motion	PL0	PL1	PL1	PL0	PL1	PL2

1. *Ground Motion Levels*
    - **Lower Level Ground Motion:** 50% probability of exceedance in 50 years; return period is about 100 years
    - **Upper Level Ground Motion:** 7% probability of exceedance in 75 years; return period is about 1,000 years
2. *Anticipated Service Life*
    - **ASL 1:** 0-15 years
    - **ASL 2:** 16-50 years
    - **ASL 3:** >50 years
3. *Performance Levels*
    - **PL0: No minimum** level of performance is recommended.
    - **PL1: Life safety.** Significant damage is sustained and service is significantly disrupted, but life safety is preserved. The bridge may need to be replaced after a large earthquake.
    - **PL2: Operational.** Damage sustained is minimal and service for emergency vehicles should be available after inspection and clearance of debris. Bridge should be reparable with or without restrictions on traffic flow.
    - **PL3: Fully operational.** No damage is sustained and full service is available for all vehicles immediately after the earthquake. No repairs are required.

Table 8-16: Mapping from Minimum Performance Level to Fragility Damage State.

Performance Levels	Summary	Fragility Damage State
PL0	No minimum objective	No Evaluation
PL1	Life safety	Complete
PL2	Emergency vehicles permitted; repairable	Moderate
PL3	Fully operational for all vehicles	Slight

It may be common for bridges in this region to have a lengthy anticipated remaining service life yet still require retrofit, because many states in the CSUS did not begin designing bridges for seismic forces until after 1990 (Gupta and Hartnagel, 2003). As shown in Table 8-15, this bridge would be required to remain fully operational ($PL3$) following a Lower Level design event. In order to meet this performance objective, it is desired to reduce the probability of exceeding slight damage. As evidenced in the fragility curves presented in Figure 7-10, the elastomeric bearings are the only retrofit which effectively reduces the probability of achieving slight damage, and meeting the $PL3$ objective. However, following an Upper Level design event, the standard $ASL3$ bridge would be required to meet a minimum performance level of $PL1$, where life safety is preserved. In this case, the fragility curves corresponding to complete damage are utilized for the assessment. It is evident that nearly all of the retrofit measures considered reduce the probability of achieving complete damage, with the elastomeric bearings, seat extenders, and shear key-seat extender combo all being particularly effective measures.

While this assessment has presented the use of the fragility curves for assisting in evaluating the effectiveness of different retrofit measures in helping to achieve a particular level of performance, it is also noted that the framework presented in the *Retrofit Manual* specifies a design level earthquake at which the performance levels must be achieved. The lower level ground motion corresponds to a design event with 50% probability of being exceeded in 50 years, and the upper level corresponds to an event with 7% probability of being exceeded in 75 years. Recalling that earthquake occurrence is often modeled using a Poisson probability model, the probability of exceeding a ground motion amplitude (ie. pga) is expressed as

$$P_E = 1 - e^{-\nu t} \tag{8.7}$$

where t is the lifetime of the bridge and ν is the annual frequency of exceeding the ground motion amplitude. Therefore, the mean occurrance rate can be calculated as follows

$$\nu = \frac{-ln(1 - P_E)}{t} \tag{8.8}$$

The annual frequency of exceeding a pga having 50% probability of being exceeded in 50 years (lower level) is 0.013863 and is 0.000968 for a pga with 7% probability of being exceeded in 75 years (upper level). From the seismic hazard curve for the site of interest, which offers the relationship between peak ground acceleration and its annual probability of exceedance, the pga associated with each design level can be determined. The seismic hazard curve for Caruthersville, MO provided by the USGS (Frankel and Leyendecker, 2001) is shown in Figure 8-3. From this hazard curve it is estimated that the peak ground accelerations associated with the lower and upper ground motions are 0.03g and 0.64g respectively.

While achieving the operational performance level *PL*3 for the Lower Level design event is facilitated by the use of elastomeric bearings, as previously stated, retrofit may not be necessary since the probability of damage at this design event is very low. At an acceleration of 0.03g, the probability of meeting or exceeding slight damage for the bridge in its as-built condition is nearly zero, and retrofit may not be justified for this performance objective alone. However, for the Upper Level design event with a pga of 0.64g, the performance objective is to reduce the probability of complete damage. As shown in Figure

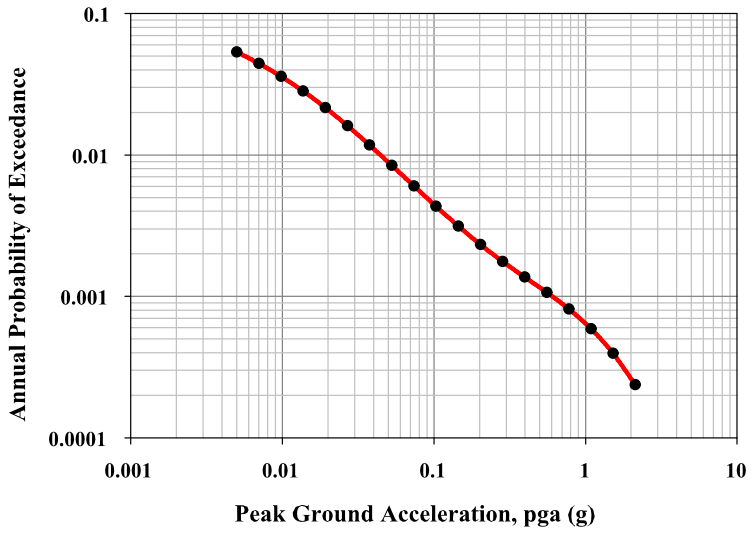

Figure 8-3: Seismic hazard curve for Caruthersville, MO adapted from Frankel and Leyendecker (2001).

8-4, all of the retrofit measures, with the exception of shear keys, are viable strategies for reducing the probability of complete damage at a pga of 0.64g. However, seat extenders are the most effective measure and lower this probability from 24% to 10%, reducing the vulnerability by more than a half. While the combined use of shear keys and seat extenders results in an analogous reduction, this combination is not chosen because of the lack of improved performance beyond the use of seat extenders alone.

This dual-level performance-based evaluation using the retrofitted fragility curves results in the identification of seat extenders as a viable retrofit strategy for the MSSS steel girder bridge. This retrofit measure should be carefully considered in the detailed retrofit assessment. It is recognized from the fragilities that several other retrofit strategies also help to reduce the potential for complete damage and help achieve the outlined performance objective for the upper level ground motion. Thus, other considerations such as cost

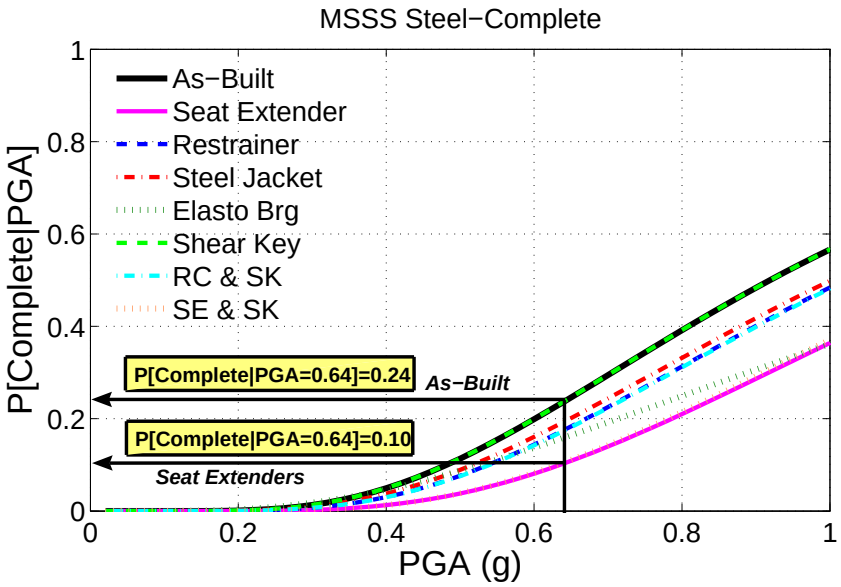

Figure 8-4: Assessment of the retrofitted fragilities for the complete damage state to identify strategies that help achieve the upper level ground motion performance objective for the MSSS Steel Bridge.

and constructability may also be a factor in weighing the relative benefits of these measures and play a role in the final retrofit selection.

While the example illustrates the use of fragility curves in a retrofit assessment applied to a dual-level performance evaluation and targets achieving only the minimum level of performance outlined in the *Seismic Retrofitting Manual for Highway Bridges* (FHWA, 2006), this framework could easily be extended. Additional performance objectives including a desired operation level and hazard level defined by the owner could also be considered.

8.2.3 Cost-Benefit Analysis

Due to the many competing needs for state transportation funding, there are often limited resources available for seismic upgrade of bridges. In particular, for regions of low-to-moderate seismicity, such as the CSUS, funds for seismic retrofit are scarce and require careful investment. The retrofitted bridge fragility curves developed as a part of this work can support such decision-making. In addition to offering a probabilistic framework for assessing the impact of retrofit on bridge system performance and treatment of uncertainty in performance evaluation, these fragility curves serve as critical components of loss assessments and cost-benefit analyses. Several researchers have indicated the potential use of such an approach for evaluating a new design or an upgrade of existing structures with a range of fidelity of uncertainty treatment, life-cycle costing, and loss modeling (Chang and Shinozuka, 1996; Smyth et al., 2004; Thiel and Hagen, 1998). The fragility curves developed as a part of this study provide the basis for making such risk-benefit-based decisions as proposed by Ellingwood and Wen (2005).

A number of researchers have proposed the use of cost-benefit analyses or probabilistic loss assessments for evaluating design alternatives or mitigation strategies. While there are still a number of gaps and refinements left to be addressed by the research community, the development of retrofitted bridge fragility curves fills a critical void in support of such analyses. The loss assessment requires information on the probable damage states, as provided by the retrofitted bridge fragility curves. This information coupled with probabilistic seismic hazard data and cost estimates associated with the bridge damage supports assessment of the direct economic losses incurred with and without the retrofit employed.

These estimates can be compared to assess the cost-effectiveness of the mitigation strategy through a traditional cost-benefit analysis, and may be estimated including various sources of aleatory and epistemic uncertainties. The approach presented herein does not address the need for improved cost-accounting, and considers the costs associated with damage to be deterministic values. However, it could be extended to include the uncertainty in such parameters and incorporate more robust estimation of losses if coupled with an appropriate network analysis and regional assessment. The methodology is presented to illustrate the criticality of the retrofitted bridge fragility curves in such a framework, and an example of a bridge retrofit cost-benefit analysis is presented for illustration purposes.

8.2.3.1 Loss Model

The bridge fragility information must be coupled with probabilistic seismic hazard curves in order to assess the annual probability of meeting or exceeding a particular state of damage

$$P[DS \geq ds] = \int_{a_{min}}^{a_{max}} P[DS \geq ds | PGA = pga] \cdot \left| \frac{dH(a)}{da} \right| \tag{8.9}$$

where the probability depicted in the first term is the fragility, and $H(a)$ is the seismic hazard curve, expressed as the annual probability of exceeding a peak ground acceleration (pga) in this study (Cornell et al., 2002). The distribution of these failures (or instances of being in or exceeding a damage state) is assumed to be a Poisson process as indicated by Nuti and Vanzi (2003), where the annual probability of a damage state is given in Equation 8.10.

$$P[DS_i(only)] = \begin{cases} P[DS \geq Slight] - P[DS \geq Moderate] & \text{for i=1} \\ P[DS \geq Moderate] - P[DS \geq Extensive] & \text{for i=2} \\ P[DS \geq Extensive] - P[DS \geq Complete] & \text{for i=3} \\ P[DS \geq Complete] & \text{for i=4} \end{cases} \tag{8.10}$$

Thus the present value of losses or costs incurred from bridge damage, PV, over a period of time, T, may be computed as (Wen et al., 2003)

$$PV = \sum_{t=1}^{T} \sum_{i=1}^{4} \lambda_i e^{-\lambda_i t} \cdot \frac{C_i}{(1+d)^{t-1}} \tag{8.11}$$

where i is the damage state, λ_i is the mean annual rate of failure, and C_i is the cost or losses associated with damage state i. For rare events such as earthquakes, it is often assumed that the annual probability of an event is equal to the mean annual rate of exceedance. Hence the mean annual rate of failure, λ_i, is approximated as $P[DS_i(only)]$. The inflation-adjusted discount rate, d, is used for converting future costs into present values (assumed to be stationary in time), which is based on the principal idea that costs and benefits incurred sooner are worth more to the investor and attempts to reflect some of the opportunity losses associated with investing in the present and realizing the returns later. This rate is adjusted for inflation such that the present day costs for repair can be used in Equation 8.11. There is debate over the most appropriate discount rate to use, and for the purposes of the example a d=3% is assumed (Smyth et al., 2004).

The benefit of a particular retrofit, r, is then evaluated as the difference between the present value of the losses without retrofit, $PV_{as-built}$, and the present value of the losses with retrofit, PV_r

$$Benefit_r = PV_{as-built} - PV_r \tag{8.12}$$

The difference in these present value terms stems from the reduction in vulnerability of the retrofitted bridge resulting in a reduced mean annual rate of failure. The cost-benefit ratio (CBR) is simply assessed as the ratio between the net present value of the investment in retrofit, $Benefit_r$, divided by the initial cost of the retrofit, $Cost_r$ as shown in Equation 8.13.

$$CBR_r = \frac{Benefit_r}{Cost_r} \tag{8.13}$$

The CBR is a measure of the financial return for each dollar invested in the seismic retrofit. It should be noted that the scope of this study does not include potential fatality, social losses, or intangible benefits, though with great care, they could be considered in an evaluation of earthquake consequences (Bostrom et al., 2006). A CBR greater than 1 indicates a positive return on investment, and the retrofit with the largest CBR has a larger savings in losses over the time period, T, per dollar of investment in mitigation. This type of analysis is meant to support decision making on investment in seismic retrofit by quantifying the cost effectiveness of a potential mitigation strategy. As indicated in the recent edition of the *Seismic Retrofitting Manual for Highway Structures* (FHWA, 2006), threshold values for acceptable cost-benefit ratios will be determined based on experience and judgment. There are other factors that would affect these decisions, such as the relative size of the initial investment, availability of funds, or other projects forgone in order to invest in seismic upgrade.

Table 8-17: Repair Cost Ratios from Basoz and Mander (1999) for Cost of Damage Estimate.

Damage State	Best Mean Repair Cost Ratio
Slight	0.03
Moderate	0.08
Extensive	0.25
Complete	1.0 (if n < 3)
	2.0/n (if n ≥ 3)

*n = number of spans

8.2.3.2 Example Cost-Benefit Study with MSC Steel Girder Bridge

The repair costs associated with each damage state are assumed to be a percentage of the replacement cost of the bridge utilizing the estimates from Basoz and Mander (1999) for the best mean repair cost ratio shown in Table 8-17. The replacement cost for the example 3-span MSC Steel bridge shown in Figure 4-5 is estimated to be $1,407,057, and the mean estimated repair costs for the slight, moderate, extensive, and complete damage states are $42,212, $112,564, $351,764, $938,038, respectively. These estimates include only the direct losses due to structural damage. The results of the ATC-25 (ATC, 1991) assessment of the seismic vulnerability of lifelines show that the total losses for highways, including both direct and indirect losses from increased travel time, are on the order of 5 to 20 times larger than the direct losses. As a simplistic approach for acknowledging and accounting for potential indirect losses due to bridge damage, the total cost of losses associated with each damage state is assumed to be 13 times the above estimated repair costs (roughly the average of the two extremes from ATC). A network analysis and further economic impact studies would improve the estimated total cost.

Following the method outlined above, the estimated realized losses for the as-built bridge are $273,000, over its remaining life of 50 years. The estimated retrofit costs and present value benefits for the seven retrofit measures are shown in Table 8-17. The retrofit measures, or combinations of retrofits, are ordered by *CBR*. While the elastomeric bearing retrofit is expected to result in the largest savings in potential losses, or $Benefit_{EB}$, its cost-benefit ratio is 1.16. The combined use of the shear keys and seat extenders result in savings of nearly $70,000 over the remaining life of the structure, yet due to their reduced cost have a cost-benefit ratio indicative of a more favorable investment at CBR_{SE-SK}=2.92. The cost-benefit analysis for the example bridge presented indicates that the seat extender-shear key retrofit is the most economically viable.

It is noted that these results may be highly sensitive to the cost data and repair cost ratios assumed, and that fatalities and socio-economic factors were not included in this study. There may be investments with a *CBR* less than one which are favorable because of non-monetary benefits and social responsibility, such as loss of life avoided. However, it is evident that this type of analysis is dependent upon the development of reliable retrofitted bridge fragility curves for a range of bridge types and potential retrofit measures, as provided by this research.

8.3 Regional Seismic Risk Assessment

Regional seismic risk assessments (SRAs) are becoming a popular tool for evaluating the performance of the transportation network under earthquake loading. The term seismic risk refers to the potential for damage or losses that may be associated with a seismic event. Such regional assessments provide a unique approach for estimating the risk to highway

Table 8-18: Cost-Benefit Analysis of Example Bridge with Different Retrofit Measures.

Retrofit Measure	Cost	Benefit	CBR
Steel Jackets	$36,000	$39,920	1.11
Elastomeric Bearings	$70,353	$81,760	1.16
Restrainer Cables and Shear Keys	$28,500	$52,900	1.86
Restrainer Cables	$16,500	$37,206	2.25
Shear Keys	$12,000	$27,610	2.30
Seat Extenders	$12,000	$33,110	2.76
Seat Extenders and Shear Keys	$24,000	$69,980	2.92

infrastructure by evaluating potential bridge damage and consequences of the seismic event, such as estimated losses incurred. This framework offers support to decision-makers for pre-event planning and risk mitigation, emergency route identification, retrofit selection and prioritization, among other critical tasks.

Methodologies for seismic risk assessment of transportation systems have been presented by many researchers in the field of lifeline earthquake engineering (Chang et al., 2000; Kiremidjian et al., 2002; Werner et al., 1997). These methodologies offer a potential framework for assessing likely bridge damage, direct losses due to repair and replacement of the structures, and some extend this evaluation to include an assessment of the impact of the event on network performance and the resulting indirect economic losses. Several researchers have indicated that such a highway system SRA could allow for relative comparison of different seismic retrofit strategies' impact on the regional consequences of an event, system-wide traffic flow disruptions, or associated losses (Werner et al., 2000; Zhou et al., 2004). While there have been initial studies that propose the viability of this framework, the results depend heavily on the availability and reliability of utilized tools and input models. These include such items as ground motion models, fragility information on the

bridge vulnerability, repair cost information, among others. Development of the first set of fragility curves for general classes of retrofitted bridges in the CSUS in this work provides an essential piece of the framework and permits such a retrofit evaluation.

The seismic risk assessment methods previously proposed by researchers vary in the extent to which hazards, damage, and losses are treated. However, the general methodologies have common threads. The general methodology for SRA of highway systems is presented in Figure 8-5. As illustrated in the Figure, the first phase of the SRA process for transportation networks is to define the regional inventory, including identifying the characteristics and locations of the bridges. Scenario earthquake events are often used, where the magnitude and location of the event must be specified. During the system analysis, fragility curves for classes of bridges common to the region are utilized, along with an estimate of the level of ground shaking at the location of each bridge in the spatially distributed region. This facilitates evaluation of the expected level of damage to each bridge, as illustrated in Figure 8-6. This Figure presents a fictitious depiction of relative bridge damage before and after retrofit. The bridge damage may be coupled with information on the repair cost ratio (or fraction of replacement cost) and replacement cost data for different bridge types permits an assessment of the losses. Alternatively, relationships between bridge damage and functionality may be used to evaluate the ability of the bridges to perform their function and continue to carry traffic. The consequence assessment may be further enhanced by the application of transportation network analyses and traffic flow simulations. These assessments facilitate evaluation of the consequences of the earthquake event and can be used to compare such consequences before and after retrofit. This includes comparing likely

bridge damage before and after retrofit (Figure 8-6), direct losses, travel time in the system, indirect losses, among others.

8.4 Closure

This Chapter has provided details to help promote the transfer of this work to application in general seismic risk evaluation and assessment of seismic risk reduction efforts. The first step of doing this was to provide simplified fragility models for the classes of retrofitted bridges for ease of implementation and dissemination of the information. Additionally, modification factors were derived that can be applied to scale as-built bridge system fragilities to estimate retrofit impact on the vulnerability. Recommendations for mapping of modification factors from bridge classes evaluated as a part of this study to other common classes of CSUS bridges evaluated by Nielson (2005a) are provided to permit a holistic evaluation of the CSUS inventory. These modification factors may also be valuable for assessing retrofit impact for future studies evaluating bridge fragility, or as information becomes available to assess empirical fragility relationships for these classes of as-built bridges.

Three frameworks for using the retrofitted bridge fragility curves for identifying viable retrofit measures are presented. These include simplified screening of the retrofits based on their impact on the median value of the fragility. Tables indicating the percent difference in as-built and retrofitted median values are presented to facilitate such an assessment. A performance-based approach to seismic retrofit is also proposed with the fragility curves forming the foundation for identifying a retrofit measure to achieve a given set of performance goals. This approach is tailored to support the performance objectives defined in

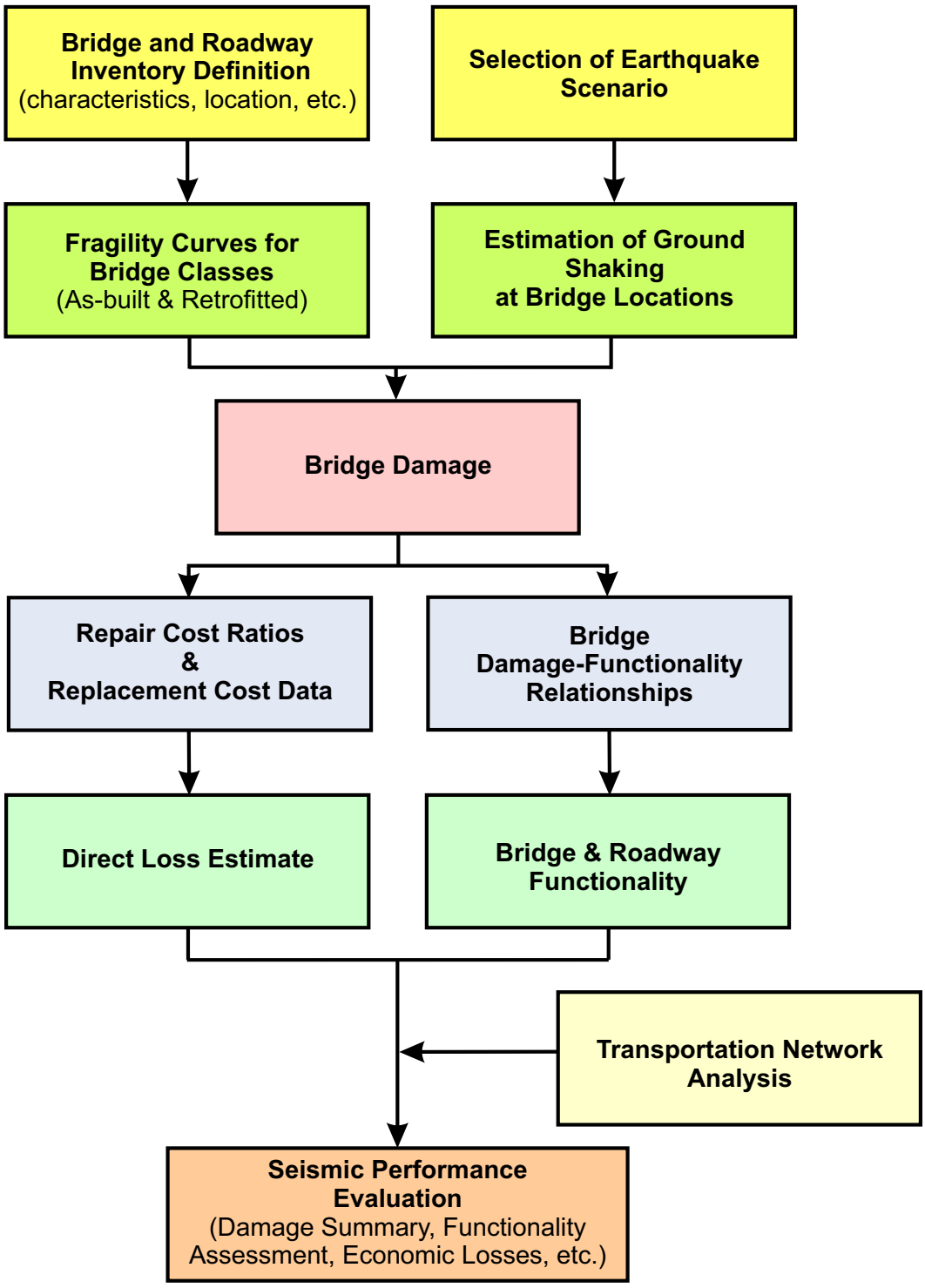

Figure 8-5: General Seismic Risk Assessment (SRA) method for highway systems.

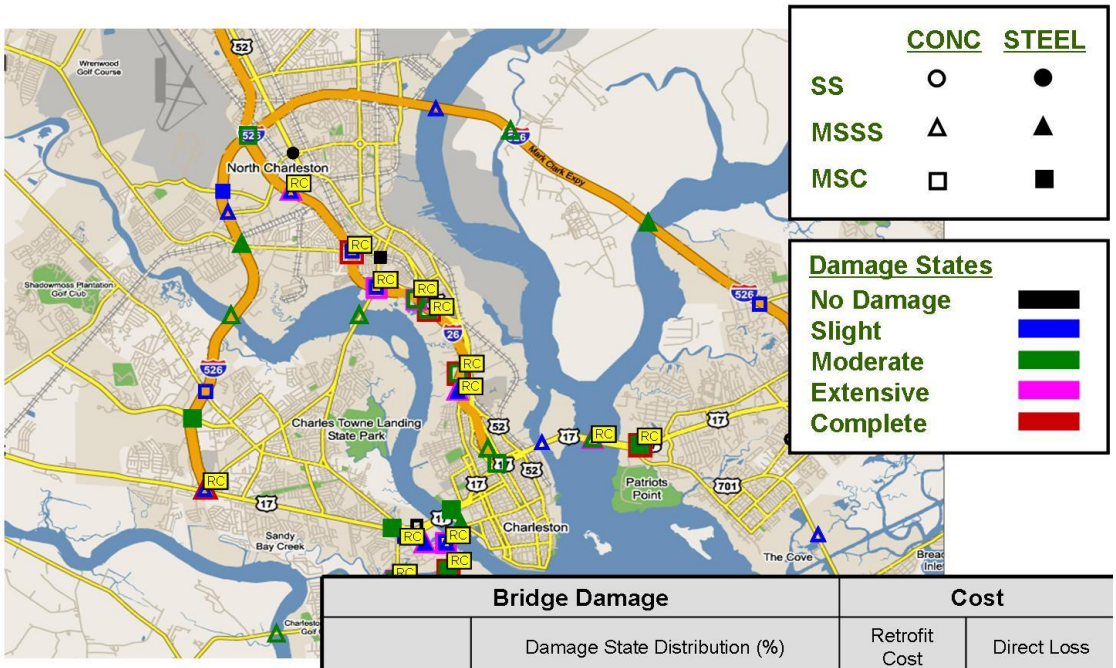

Bridge Damage						Cost	
	Damage State Distribution (%)					Retrofit Cost	Direct Loss
	No	Slight	Mod	Ext	Comp	($ M)	($ M)
Initial	2	12	33	41	12	--	$110 M
Retrofitted	2	26	38	30	4	$3	$62 M

Figure 8-6: Illustration of the assessment of retrofit on regional seismic risk to Charleston, SC.

the *Seismic Retrofitting Manual for Highway Bridges*, but could easily be applied to meet user specified objectives for a targeted level functional performance and design level event. The use of the retrofitted bridge fragility curves in a cost-benefit assessment is presented as an approach for weighing the financial viability of different retrofit measures in a probabilistic framework. Rather than evaluating the cost-effectiveness for a scenario event, the cost-benefit assessment considers the potential losses avoided over the remaining life of the structure, and provides an effective way to evaluate investment in seismic upgrade.

Additionally, the seismic risk assessment methodology is presented to indicate the gap in the framework that is filled by the developed retrofitted bridge fragility curves from this work. These tools provide an effective way to assess the impact of retrofit on regional consequences and transportation network performance. The availability of fragility curves for general classes of retrofitted bridges in the CSUS will permit a systems approach to seismic upgrade of this critical infrastructure.

CHAPTER IX

SUMMARY, CONCLUSIONS, AND FUTURE WORK

9.1 Summary and Conclusions

The infrequent nature of large earthquakes has led to uncertainty in the seismic hazard in the Central and Southeastern United States (CSUS), and has resulted in many of the bridges being designed with little or no seismic consideration. This lack of seismic detailing in much of the existing highway bridge inventory leaves the transportation network particularly vulnerable to earthquake damage, and indicates the potential for severe consequences from a future event. As awareness of the potential seismic threat to the CSUS rises, several states in this part of the country are beginning to establish bridge retrofit programs and are in the early stages of evaluating bridge vulnerability and potential retrofit strategies for their existing non-seismically designed bridges.

The main objective of this study was to provide reliable fragility curves for general classes of retrofitted bridges. This work is critical and timely as many of the states in the CSUS are beginning to initiate retrofit activities and require an understanding of the relative benefits of retrofits for the typical bridges in the CSUS. Unfortunately, to date, few studies have assessed retrofit for bridges common to this region or provided comparative assessment of different options. Moreover, the development of a methodology for analytical fragility curve development for bridges in their retrofitted condition has been very limited. Those that have evaluated retrofitted bridge vulnerabilities are not practical or

fully appropriate for portfolio analysis of general classes of retrofitted bridges typical to the CSUS.

From a review of retrofit practice coupled with past studies, five potentially viable or common retrofit measures were identified for examination in this work. The retrofit measures cover a range of approaches for seismic retrofit from response modification to capacity enhancement to partial replacement. Three-dimensional analytical models of the retrofit measures and bridge classes were established. Deterministic analyses revealed the impact of retrofit on the seismic response of various critical components. It was concluded that traditional retrofit targets the improvement of individual components or response quantities, however may result in damage to other components. This highlights the need to evaluate the impact of retrofit on system performance.

Sensitivity studies were conducted to identify the modeling parameters which significantly affect the seismic response of the different classes of retrofitted bridges. It was concluded that for nearly every response measure and type of retrofitted bridge, the potential variation in loading direction was important as well as the blocking scheme representative of the uncertainty in the bridge configurations (span length, column height, etc.). Hence, through the remainder of the study these eight geometric configurations were used to capture the variation in the inventory and the ground motions were applied as a coupled pair of orthogonal components with random incident angle. The additional most significant modeling parameters were identified for each type of retrofitted bridge, often consisting of at least one parameter associated with the retrofit measure and others due to as-built parameters. There was some consistency between the significant parameters for the as-built and retrofitted bridge of each class. The retrofit parameters which were significant for various

bridge classes included slack and length of the restrainer cables; stiffness of the elastomeric bearings and gap to the transverse keeper plate; additional stiffness imposed by steel jackets and the grout gap between the jacket and existing column; and the gap before the transverse shear keys engage.

Later studies evaluated the sensitivity of not only the bridge response quantities, but the fragility estimate to different sources of variability to help address the question of a prudent level of uncertainty treatment. The results of the study indicated that while the ground motions may overshadow some other sources of uncertainty, capturing the variation in base bridge geometry is critical for analyses of structural portfolios. Additionally, the use of preliminary screening studies can help to identify which modeling parameters should be treated probabilistically in fragility analyses.

Probabilistic methods were used to develop fragility curves for retrofitted bridges. Through careful treatment of uncertainty and computational simulation, the seismic demand was assessed, including the propagation of sources of uncertainty associated with the ground motions, significant analytical modeling parameters, and variation in geometric properties in the classes of bridges. Joint probabilistic seismic demand models (PSDMs) were established to characterize the impact of retrofit on the demand placed upon and dependency between various critical components in the bridge. A survey of bridge engineers and inspectors was conducted to provide insight on the relationship between component damage and anticipated closure or repair recommendations affecting the anticipated allowable traffic carrying capacity. The study provided descriptions of damage state definitions in terms of meaningful performance measures–anticipated post-event functionality. These damage-functionality relationships were used to refine limit state capacities to have more functional

consistency and incorporate uncertainties associated with such human subjectivity. Some of the retrofits tended to alter the component limit states and were defined with care to maintain the functional implications.

Fragility curves for components of retrofitted bridges were first developed to provide insight on the impact of retrofit on the vulnerability of different components within the system. Notable findings which were consistent with the deterministic analyses include the following:

- Elastomeric bearings led to increased vulnerability of the abutment in passive action. This became more prevalent for the continuous bridges and was magnified for the heavier concrete girder bridges.

- In general, the elastomeric bearings were effective in isolating the superstructure and substructure and reduced column demands. However, their effect was more considerably realized in reducing bearing vulnerability by replacing the existing bearings with less vulnerable bearings. This was more critical for the high-type steel bearings in the steel girder bridges

- The restrainer cables led to higher potential for damage to abutments in active action because of the forces transferred through the cables. Additionally, this retrofit was not as effective in reducing bearing vulnerability because of the low levels of deformation (particularly for steel bearings) indicative of damage and the slack in the cables, or the potential for cable yielding in larger events (particularly for the concrete bridges).

- The steel jackets considerably reduced the column vulnerability to the point that they were nearly negligible for most bridge types and damage states. No other component vulnerabilities were considerably impacted.

- The seat extenders effectively reduced the vulnerability of all longitudinal bearings at the complete damage state by providing an additional support length before risking unseating. Their impact was captured by altering these longitudinal bearing deformation limit states, however the bridge response is not otherwise affected.

- Transverse shear keys provided at the bents and abutments are effective in reducing the transverse vulnerability of the bearings in all of the bridges, with the exception of the MSSS Steel. However, they can lead to increased vulnerability of the abutments in the transverse direction or even the columns for the simply supported bridges.

These conclusions are not consistent across each damage state. The impact of retrofit on component vulnerability in each bridge type was found to be a function of the level of damage of interest. The use of different retrofit measures tended to alter the relative vulnerability of different components in the system.

Retrofitted bridge system fragility curves were developed by convolving the demands and capacities across all potential failure domains in order to capture the impact of retrofit on multiple components. These system-level fragilities provide insight on the relative vulnerability of the bridge classes before and after retrofit, and with different retrofit measures. The identification of the retrofit measure which most effectively reduces likely damage depends on the bridge type and damage state of interest. In particular, more retrofit measures

tended to become effective in reducing the potential for the higher levels of damage. In general the elastomeric isolation bearings were the most effective for the Steel girder bridges. At the complete damage state the combined use of the seat extender and shear key was effective for the MSC Steel bridge and the seat extender was effective for the MSSS Steel bridge. The steel jackets were more effective in reducing potential damage for the Concrete girder bridges.

Conclusions as to the most appropriate retrofit measure for a given bridge type depend upon the objectives of the decision-maker. The most viable retrofit may be that which has the greatest increase in median value of the fragility; helps to achieve a stated set of performance objectives (level of functionality for a design level event); or provides the most cost-effective investment in seismic upgrade, just to name a few. Thus, different frameworks were presented to support retrofit selection using the retrofitted bridge fragility curves. These include median value improvement, performance-based retrofit, and cost-benefit analysis. Additionally, to promote implementation of the developed fragilities and facilitate ease of transfer of these curves, simplified fragility estimates, as-built modification factors, and mapping to a broader range of CSUS inventory are proposed. This promotes incorporation of the retrofitted bridge fragility curves in regional seismic risk assessments.

9.2 Impact of Research

A rigorous approach to probabilistic assessment of the impact of retrofit on the seismic performance of typical CSUS bridges was used in this work to provide reliable fragility curves for general classes of retrofitted bridges. A primary contribution of the work is the

refinement and evaluation of a methodology for generation of retrofitted bridge fragility curves that would facilitate a comparison of bridge retrofits and would permit a network assessment for effective retrofit selection and prioritization based on transportation network performance. Additional benefits and contributions include the following:

- Examination of current and potential retrofit measures viable for the CSUS to date has been limited. This study provides the first systematic and comprehensive assessment of retrofit for CSUS bridges and offer insight for researchers and practitioners in the region. The three-dimensional analytical modeling and response evaluation provides enhanced understanding of the seismic response of typical classes of retrofitted bridges.

- The development and evaluation of a methodology for analytical fragility curve development for bridges in their retrofitted condition has been very limited, and offers a significant contribution to the research community that can be applied to other parts of the country, bridge types, and retrofit measures.

- An enhanced understanding of the sources of uncertainty whose variability most significantly effect the seismic response of the retrofitted bridges, as well as the sensitivity of the fragility estimate to different levels of uncertainty treatment is provided. This indicates areas for future study to try to reduce our uncertainty in the realization of some parameters (where appropriate) or to prudent levels of uncertainty treatment for future fragility assessments of structural portfolios.

- The development of fragility curves for bridges in their retrofitted states allows decision makers to examine the relative vulnerability of bridges in their as-built and

retrofitted conditions for various retrofit strategies. This will aid practitioners in the selection of appropriate bridge retrofit measures, including providing frameworks for their use in performance-based retrofit or weighing the cost-effectiveness of different measures in a probabilistic framework.

- The evaluation of relationships between bridge damage and functionality offers critical understanding between these subjective decisions. This enabled a new approach for the definition of damage states and limit state capacities on the basis of functional consistency, which were used in this study. However, this also provides a key link between structural response and consequence assessment of earthquake events. This promotes the integration of these fragility curves in regional risk assessments and traffic model simulations by implying an anticipated level of post-event functionality.

- Seismic risk assessment and loss estimation tools (and their users) will benefit from the incorporation of retrofitted bridge fragility curves. This will allow for evaluation of the impact of retrofit on network performance. It will also allow SRA packages to capture a class of bridges that have already been retrofit in the region, which could have a significant impact on the system vulnerability if key bridges have already been retrofit. These retrofitted bridge fragility curves permit a transportation system level approach to seismic risk mitigation and infrastructure upgrade.

9.3 Recommendations for Future Work

Areas in which this work can be extended through additional research include the following:

- The effect of retrofit was examined for typical geometries of CSUS highway overpass bridges as a part of this work. Future studies could evaluate the impact of skew, number of spans, curved girders, or additional retrofit measures on the fragility.

- As approaches for assessing and simulation the liquefaction hazard mature, the impact of this hazard on bridge response and vulnerability should be incorporated. This could have a particular impact on regional damage in such areas as Charleston, SC.

- Potential combinations of bridge retrofits may be virtually unlimited, yet may be an appropriate way to target bridge system upgrade. A simplified approach for assessing the impact of retrofit combination on system fragility would be a valuable extension of the research.

- Coupling evaluation of retrofit on bridge fragility and network reliability would further support decisions on investment in seismic upgrade, through an approach that maximizes the impact of financial input for retrofit and optimizes system performance.

- Since our infrastructure is subjected to numerous threats, extension of this bridge vulnerability and retrofit/rehabilitation assessment to other hazards is warranted. This could provide a more holistic examination of risk and permit the evaluation of multi-hazard mitigation strategies.

APPENDIX A

FUNCTIONALITY PROBABILITY MATRICES AND EXCEEDANCE PROBABILITIES FROM ANALYSIS OF DAMAGE-FUNCTIONALITY SURVEY DATA

This appendix includes tables of the additional functionality probability matrices (FPMs) which were not presented in 6. These FPMs provide the percent of respondents that indicate a given level of component damage would result in a specific level of allowable traffic carrying capacity over time. Damage state exceedance probabilities calculated as an analysis of the data collected from the Damage-Functionality survey presented in Chapter 6 are also presented herein. These exceedance probabilities are used to refine the limit state capacities for various components as discussed in the Chapter.

Table A-1: Functionality Probability Matrices for Additional Types of Bridge Damage.

Longitudinal Offset at Expansion Joint															
Damage, dg	**0-1 inch**					**1-6 inch**					**≥6 inch**				
Time, t (days)	**0**	**1**	**3**	**7**	**30**	**0**	**1**	**3**	**7**	**30**	**0**	**1**	**3**	**7**	**30**
P[X=0%|Dg=dg ∩ T=t]	0.036	0.000	0.000	0.000	0.000	0.500	0.321	0.179	0.143	0.000	0.929	0.786	0.679	0.536	0.321
P[X=50%|Dg=dg ∩ T=t]	0.143	0.071	0.036	0.036	0.036	0.393	0.429	0.321	0.286	0.286	0.071	0.179	0.071	0.143	0.071
P[X=100%|Dg=dg ∩ T=t]	0.821	0.929	0.964	0.964	0.964	0.107	0.250	0.500	0.571	0.714	0.000	0.036	0.250	0.321	0.607
Vertical Offset at Expansion Joint															
Damage, dg	**0-1 inch**					**1-6 inch**					**≥6 inch**				
Time, t (days)	**0**	**1**	**3**	**7**	**30**	**0**	**1**	**3**	**7**	**30**	**0**	**1**	**3**	**7**	**30**
P[X=0%|Dg=dg ∩ T=t]	0.214	0.071	0.036	0.036	0.000	0.704	0.519	0.296	0.222	0.111	1.000	0.889	0.667	0.407	0.259
P[X=50%|Dg=dg ∩ T=t]	0.214	0.214	0.143	0.107	0.107	0.296	0.333	0.370	0.259	0.111	0.000	0.074	0.148	0.259	0.037
P[X=100%|Dg=dg ∩ T=t]	0.571	0.714	0.821	0.857	0.893	0.000	0.148	0.333	0.519	0.778	0.000	0.037	0.185	0.333	0.704
Longitudinal Offset at Over Pier (MSC)															
Damage, dg	**0-1 inch**					**1-6 inch**					**≥6 inch**				
Time, t (days)	**0**	**1**	**3**	**7**	**30**	**0**	**1**	**3**	**7**	**30**	**0**	**1**	**3**	**7**	**30**
P[X=0%|Dg=dg ∩p T=t]	0.179	0.107	0.071	0.036	0.036	0.607	0.464	0.321	0.143	0.036	0.8571	0.8571	0.6429	0.4286	0.25
P[X=50%|Dg=dg ∩ T=t]	0.071	0.107	0.036	0.071	0.036	0.250	0.286	0.286	0.321	0.143	0.107	0.107	0.179	0.214	0.107
P[X=100%|Dg=dg ∩ T=t]	0.750	0.786	0.893	0.893	0.929	0.143	0.250	0.393	0.536	0.821	0.036	0.036	0.179	0.357	0.643
Damage to Column (one column in multi-column bent)															
Damage, dg	**Cracking**					**Spalling**					**Rebar Buckle/Fracture/Pullout**				
Time, t (days)	**0**	**1**	**3**	**7**	**30**	**0**	**1**	**3**	**7**	**30**	**0**	**1**	**3**	**7**	**30**
P[X=0%|Dg=dg ∩ T=t]	0.321	0.107	0.036	0.036	0.000	0.643	0.464	0.250	0.143	0.071	0.786	0.714	0.714	0.571	0.393
P[X=50%|Dg=dg ∩ T=t]	0.179	0.357	0.357	0.214	0.143	0.214	0.286	0.500	0.393	0.214	0.179	0.214	0.250	0.214	0.143
P[X=100%|Dg=dg ∩ T=t]	0.500	0.536	0.607	0.750	0.857	0.143	0.250	0.250	0.464	0.714	0.036	0.071	0.036	0.214	0.464

Damage to Abutment										
Damage, dg	**Cracking**					**Spalling and/or Rotation**				
Time, t (days)	**0**	**1**	**3**	**7**	**30**	**0**	**1**	**3**	**7**	**30**
P[X=0%|Dg=dg ∩ T=t]	0.214	0.071	0.071	0.000	0.000	0.500	0.393	0.286	0.107	0.036
P[X=50%|Dg=dg ∩ T=t]	0.321	0.286	0.179	0.107	0.036	0.321	0.357	0.286	0.357	0.179
P[X=100%|Dg=dg ∩ T=t]	0.464	0.643	0.750	0.893	0.964	0.179	0.250	0.429	0.536	0.786
Separation of Soil from Footing										
Damage, dg	**0-3 inch**					**≥3 inch**				
Time, t (days)	**0**	**1**	**3**	**7**	**30**	**0**	**1**	**3**	**7**	**30**
P[X=0%|Dg=dg ∩ T=t]	0.296	0.115	0.077	0.039	0.000	0.500	0.346	0.192	0.154	0.080
P[X=50%|Dg=dg ∩ T=t]	0.074	0.077	0.154	0.154	0.077	0.063	0.346	0.308	0.231	0.080
P[X=100%|Dg=dg ∩ T=t]	0.630	0.808	0.769	0.808	0.923	0.438	0.308	0.500	0.615	0.840

Table A-2: Damage State Exceedance Probabilities for All Levels and Types of Damage.

Settlement of Approach at Approach/Abutment Interface				
	P[DS≥ds|Dg=dg]			
Damage, dg	**Slight**	**Moderate**	**Extensive**	**Complete**
0-1 in	0.286	0.036	0.036	0.036
1-6 in	0.889	0.148	0.000	0.000
≥6 in	1.000	0.464	0.214	0.071
Transverse Offset at Expansion Joint				
	P[DS≥ds|Dg=dg]			
Damage, dg	**Slight**	**Moderate**	**Extensive**	**Complete**
0-1 in	0.321	0.036	0.000	0.000
1-6 in	0.750	0.429	0.214	0.107
≥6 in	0.929	0.714	0.536	0.464
Damage to Column (Single Column Bent)				
	P[DS≥ds|Dg=dg]			
Damage, dg	**Slight**	**Moderate**	**Extensive**	**Complete**
Cracking	0.519	0.185	0.148	0.148
Spalling	0.929	0.607	0.286	0.250
Rebar buckle/fracture/pullout	0.964	0.929	0.786	0.750

Settlement of Approach at Approach/Abutment Interface				
	P[DS≥ds|Dg=dg]			
Damage, dg	**Slight**	**Moderate**	**Extensive**	**Complete**
0-1 in	0.286	0.036	0.036	0.036
1-6 in	0.889	0.148	0	0
≥6 in	1	0.464	0.214	0.071
Damage to Abutment				
	P[DS≥ds|Dg=dg]			
Damage, dg	**Slight**	**Moderate**	**Extensive**	**Complete**
Cracking	0.536	0.071	0.036	0
Spalling and/or Rotation	0.821	0.393	0.25	0.107
Longitudinal Offset at Expansion Joint				
	P[DS≥ds|Dg=dg]			
Damage, dg	**Slight**	**Moderate**	**Extensive**	**Complete**
0-1 in	0.179	0	0	0
1-6 in	0.893	0.25	0.143	0.143
≥6 in	1	0.75	0.643	0.536
Vertical Offset at Expansion Joint				
	P[DS≥ds|Dg=dg]			
Damage, dg	**Slight**	**Moderate**	**Extensive**	**Complete**
0-1 in	0.429	0.036	0.036	0.036
1-6 in	1	0.482	0.259	0.222
≥6 in	1	0.778	0.593	0.407
Longitudinal Offset Over Pier				
	P[DS≥ds|Dg=dg]			
Damage, dg	**Slight**	**Moderate**	**Extensive**	**Complete**
0-1 in	0.25	0.071	0.071	0.036
1-6 in	0.857	0.393	0.286	0.143
≥6 in	0.964	0.714	0.536	0.429
Damage to Column (Multi-Column Bent - One Column Damaged)				
	P[DS≥ds|Dg=dg]			
Damage, dg	**Slight**	**Moderate**	**Extensive**	**Complete**
0-1 in	0.5	0.107	0.036	0.036
1-6 in	0.857	0.464	0.179	0.143
≥6 in	0.964	0.714	0.607	0.571
Separation of Soil from Footings				
	P[DS≥ds|Dg=dg]			
Damage, dg	**Slight**	**Moderate**	**Extensive**	**Complete**
0-3 in	0.346	0.115	0.077	0.039
≥3 in	0.692	0.308	0.192	0.154

APPENDIX B

PSDMS WITH CORRELATION MATRICES FOR RETROFITTED BRIDGES

The following tables (Table B-1 - Table B-4) show the PSDMs in the form presented in Chapter 7

$$\ln S_D = b \cdot \ln IM + \ln a \tag{B.1}$$

for each type of retrofitted bridge. Note that the demand models for the bridges retrofit with seat extenders are not listed, because they do not affect the seismic response and are the same as the as-built bridge. Additionally, while the combined use of seat extenders and shear keys will be assessed, the demand model is the same as that for shear keys alone.

The correlation matrices for each type of retrofitted bridge are shown in the following tables. Note that the correlation coefficients are actually for the lognormally transformed demand placed on the components.

Table B-1: MSSS Steel PSDMs.

Response	$\ln(S_D) = b \cdot \ln(PGA) + \ln(a)$ b	a	R^2	$\beta_{D\|IM}$
As-Built				
$\ln(\mu_\phi)$	0.958	1.387	0.83	0.50
$\ln(fx_L)$	4.551	2.276	0.84	0.78
$\ln(fx_T)$	3.494	2.039	0.75	0.95
$\ln(ex_L)$	5.008	1.251	0.77	0.55
$\ln(ex_T)$	2.587	1.423	0.83	0.51
$\ln(ab_P)$	2.712	1.336	0.78	0.57
$\ln(ab_A)$	2.403	0.865	0.73	0.41
$\ln(ab_T)$	1.919	0.952	0.74	0.45
Steel Jackets				
$\ln(\mu_\phi)$	0.839	1.385	0.81	0.53
$\ln(fx_L)$	4.465	2.250	0.86	0.73
$\ln(fx_T)$	3.734	2.198	0.80	0.88
$\ln(ex_L)$	4.962	1.246	0.77	0.54
$\ln(ex_T)$	2.529	1.404	0.84	0.50
$\ln(ab_P)$	2.536	1.259	0.78	0.53
$\ln(ab_A)$	2.201	0.775	0.77	0.33
$\ln(ab_T)$	1.894	0.954	0.77	0.42
Elastomeric Isolation Bearings				
$\ln(\mu_\phi)$	0.809	1.327	0.77	0.59
$\ln(eb_L)$	4.946	1.069	0.68	0.58
$\ln(eb_T)$	3.492	0.611	0.61	0.39
$\ln(ab_P)$	3.287	2.020	0.67	1.13
$\ln(ab_A)$	1.050	0.672	0.75	0.31
$\ln(ab_T)$	2.865	1.493	0.72	0.74

Response	$\ln(S_D) = b \cdot \ln(PGA) + \ln(a)$ b	a	R^2	$\beta_{D\|IM}$
Restrainer Cables				
$\ln(\mu_\phi)$	0.887	1.356	0.82	0.50
$\ln(fx_L)$	4.490	2.227	0.85	0.74
$\ln(fx_T)$	3.754	2.205	0.79	0.92
$\ln(ex_L)$	4.725	1.140	0.76	0.51
$\ln(ex_T)$	2.513	1.394	0.82	0.52
$\ln(ab_P)$	2.460	1.215	0.78	0.52
$\ln(ab_A)$	2.605	0.918	0.74	0.43
$\ln(ab_T)$	1.820	0.916	0.76	0.41
Shear Keys				
$\ln(\mu_\phi)$	1.006	1.405	0.82	0.52
$\ln(fx_L)$	4.567	2.275	0.84	0.78
$\ln(fx_T)$	3.397	1.990	0.72	1.00
$\ln(ex_L)$	5.038	1.262	0.77	0.54
$\ln(ex_T)$	2.669	1.459	0.79	0.60
$\ln(ab_P)$	2.832	1.371	0.76	0.61
$\ln(ab_A)$	2.479	0.885	0.75	0.40
$\ln(ab_T)$	1.897	0.942	0.75	0.43
Restrainer Cables and Shear Keys				
$\ln(\mu_\phi)$	0.932	1.377	0.82	0.51
$\ln(fx_L)$	4.492	2.242	0.85	0.75
$\ln(fx_T)$	3.331	1.967	0.71	1.01
$\ln(ex_L)$	4.769	1.158	0.77	0.51
$\ln(ex_T)$	2.597	1.428	0.78	0.61
$\ln(ab_P)$	2.674	1.310	0.78	0.56
$\ln(ab_A)$	2.750	0.983	0.76	0.45
$\ln(ab_T)$	1.827	0.911	0.75	0.41

Table B-2: MSC Steel PSDMs.

	$\ln(S_D) = b \cdot \ln(PGA) + \ln(a)$			
Response	**b**	**a**	R^2	$\beta_{D\|IM}$
As-Built				
$\ln(\mu_\phi)$	1.921	1.710	0.71	0.88
$\ln(fx_L)$	2.083	1.589	0.62	1.00
$\ln(fx_T)$	2.974	1.818	0.59	1.23
$\ln(ex_L)$	5.797	1.457	0.72	0.73
$\ln(ex_T)$	4.437	1.936	0.71	0.99
$\ln(ab_P)$	3.722	2.295	0.50	1.83
$\ln(ab_A)$	0.348	0.624	0.42	0.59
$\ln(ab_T)$	2.378	0.872	0.67	0.49
Steel Jackets				
$\ln(\mu_\phi)$	1.697	1.670	0.74	0.79
$\ln(fx_L)$	2.288	1.680	0.64	1.00
$\ln(fx_T)$	3.037	1.837	0.58	1.25
$\ln(ex_L)$	5.770	1.454	0.72	0.72
$\ln(ex_T)$	4.251	1.866	0.70	0.96
$\ln(ab_P)$	3.492	2.203	0.47	1.87
$\ln(ab_A)$	0.332	0.619	0.42	0.59
$\ln(ab_T)$	2.487	0.925	0.68	0.50
Elastomeric Isolation Bearings				
$\ln(\mu_\phi)$	0.890	1.379	0.69	0.74
$\ln(eb_L)$	5.616	1.152	0.64	0.69
$\ln(eb_T)$	3.189	0.313	0.51	0.24
$\ln(ab_P)$	4.289	2.367	0.55	1.71
$\ln(ab_A)$	0.917	0.658	0.49	0.54
$\ln(ab_T)$	4.000	1.644	0.59	1.10

Response	$\ln(S_D) = b \cdot \ln(PGA) + \ln(a)$ b	a	R^2	$\beta_{D\|IM}$
Restrainer Cables				
$\ln(\mu_\phi)$	1.625	1.597	0.68	0.88
$\ln(fx_L)$	1.436	1.382	0.60	0.90
$\ln(fx_T)$	2.928	1.793	0.59	1.19
$\ln(ex_L)$	5.449	1.343	0.73	0.65
$\ln(ex_T)$	4.413	1.927	0.71	0.98
$\ln(ab_P)$	2.799	1.968	0.45	1.76
$\ln(ab_A)$	3.953	1.830	0.56	1.30
$\ln(ab_T)$	2.429	0.894	0.66	0.52
Shear Keys				
$\ln(\mu_\phi)$	1.426	1.491	0.70	0.78
$\ln(fx_L)$	2.020	1.587	0.64	0.96
$\ln(fx_T)$	2.146	1.472	0.60	0.97
$\ln(ex_L)$	5.728	1.427	0.72	0.72
$\ln(ex_T)$	3.405	1.479	0.79	0.61
$\ln(ab_P)$	3.565	2.228	0.50	1.80
$\ln(ab_A)$	0.348	0.624	0.42	0.59
$\ln(ab_T)$	2.733	1.023	0.70	0.53
Restrainer Cables and Shear Keys				
$\ln(\mu_\phi)$	1.535	1.558	0.69	0.84
$\ln(fx_L)$	1.380	1.355	0.60	0.89
$\ln(fx_T)$	2.323	1.530	0.62	0.97
$\ln(ex_L)$	5.453	1.345	0.73	0.65
$\ln(ex_T)$	3.383	1.469	0.78	0.62
$\ln(ab_P)$	2.949	2.034	0.47	1.74
$\ln(ab_A)$	3.976	1.840	0.56	1.30
$\ln(ab_T)$	2.833	1.067	0.69	0.57

Table B-3: MSSS Concrete PSDMs.

Response	$\ln(S_D) = b \cdot \ln(PGA) + \ln(a)$ b	a	R^2	$\beta_{D\|IM}$
As-Built				
$\ln(\mu_\phi)$	0.776	1.191	0.77	0.52
$\ln(fx_L)$	4.147	1.162	0.67	0.66
$\ln(fx_T)$	3.012	0.742	0.40	0.73
$\ln(ex_L)$	4.420	0.961	0.73	0.47
$\ln(ex_T)$	3.119	0.783	0.38	0.79
$\ln(ab_P)$	2.465	1.001	0.67	0.57
$\ln(ab_A)$	2.899	0.876	0.55	0.63
$\ln(ab_T)$	2.540	1.035	0.74	0.49
Steel Jackets				
$\ln(\mu_\phi)$	0.642	1.184	0.76	0.53
$\ln(fx_L)$	4.028	1.112	0.66	0.63
$\ln(fx_T)$	2.781	0.639	0.35	0.69
$\ln(ex_L)$	4.354	0.945	0.73	0.46
$\ln(ex_T)$	2.752	0.634	0.35	0.68
$\ln(ab_P)$	2.475	1.029	0.66	0.59
$\ln(ab_A)$	2.963	0.910	0.58	0.62
$\ln(ab_T)$	2.410	0.994	0.69	0.54
Elastomeric Isolation Bearings				
$\ln(\mu_\phi)$	0.782	1.246	0.76	0.56
$\ln(eb_L)$	5.120	0.889	0.65	0.52
$\ln(eb_T)$	3.650	0.511	0.62	0.32
$\ln(ab_P)$	4.176	2.343	0.61	1.51
$\ln(ab_A)$	0.778	0.700	0.55	0.51
$\ln(ab_T)$	3.345	1.273	0.62	0.81

Response	$\ln(S_D) = b \cdot \ln(PGA) + \ln(a)$ b	a	R^2	$\beta_{D\|IM}$
Restrainer Cables				
$\ln(\mu_\phi)$	0.714	1.139	0.74	0.54
$\ln(fx_L)$	4.146	1.152	0.66	0.66
$\ln(fx_T)$	2.912	0.687	0.32	0.80
$\ln(ex_L)$	4.214	0.865	0.70	0.46
$\ln(ex_T)$	2.999	0.729	0.36	0.77
$\ln(ab_P)$	2.429	0.966	0.62	0.61
$\ln(ab_A)$	2.981	0.884	0.68	0.50
$\ln(ab_T)$	2.295	0.940	0.71	0.49
Shear Keys				
$\ln(\mu_\phi)$	0.833	1.213	0.74	0.58
$\ln(fx_L)$	4.312	1.224	0.66	0.71
$\ln(fx_T)$	2.579	0.559	0.55	0.41
$\ln(ex_L)$	4.578	1.026	0.75	0.48
$\ln(ex_T)$	2.492	0.521	0.53	0.39
$\ln(ab_P)$	2.650	1.085	0.67	0.62
$\ln(ab_A)$	2.593	0.728	0.66	0.43
$\ln(ab_T)$	2.438	1.009	0.74	0.49
Restrainer Cables and Shear Keys				
$\ln(\mu_\phi)$	0.807	1.188	0.73	0.59
$\ln(fx_L)$	4.136	1.148	0.66	0.66
$\ln(fx_T)$	2.535	0.535	0.51	0.42
$\ln(ex_L)$	4.311	0.915	0.73	0.44
$\ln(ex_T)$	2.532	0.538	0.53	0.41
$\ln(ab_P)$	2.574	1.038	0.64	0.63
$\ln(ab_A)$	3.088	0.946	0.71	0.49
$\ln(ab_T)$	2.417	0.998	0.72	0.50

Table B-4: MSC Concrete PSDMs.

Response	$\ln(S_D) = b \cdot \ln(PGA) + \ln(a)$ b	a	R^2	$\beta_{D\|IM}$
As-Built				
$\ln(\mu_\phi)$	0.829	1.217	0.72	0.61
$\ln(fx_L)$	4.558	1.105	0.68	0.61
$\ln(fx_T)$	2.873	0.684	0.44	0.62
$\ln(ex_L)$	4.388	0.928	0.66	0.53
$\ln(ex_T)$	2.793	0.651	0.44	0.59
$\ln(ab_P)$	2.907	0.991	0.49	0.81
$\ln(ab_A)$	2.655	0.525	0.26	0.70
$\ln(ab_T)$	2.913	0.931	0.57	0.66
Steel Jackets				
$\ln(\mu_\phi)$	0.792	1.266	0.74	0.60
$\ln(fx_L)$	4.578	1.122	0.69	0.60
$\ln(fx_T)$	2.827	0.663	0.43	0.60
$\ln(ex_L)$	4.413	0.950	0.68	0.53
$\ln(ex_T)$	2.758	0.643	0.43	0.59
$\ln(ab_P)$	3.004	1.035	0.53	0.78
$\ln(ab_A)$	2.667	0.541	0.27	0.70
$\ln(ab_T)$	2.906	0.938	0.58	0.65
Elastomeric Isolation Bearings				
$\ln(\mu_\phi)$	0.787	1.244	0.75	0.58
$\ln(eb_L)$	4.864	0.726	0.57	0.51
$\ln(eb_T)$	3.114	0.306	0.32	0.36
$\ln(ab_P)$	4.791	2.458	0.55	1.78
$\ln(ab_A)$	0.037	0.336	0.41	0.32
$\ln(ab_T)$	4.228	1.508	0.68	0.85

Response	$\ln(S_D) = b \cdot \ln(PGA) + \ln(a)$ b	a	R^2	$\beta_{D\|IM}$
Restrainer Cables				
$\ln(\mu_\phi)$	0.835	1.225	0.74	0.58
$\ln(fx_L)$	4.512	1.100	0.71	0.56
$\ln(fx_T)$	2.731	0.631	0.42	0.59
$\ln(ex_L)$	4.223	0.875	0.70	0.46
$\ln(ex_T)$	2.660	0.599	0.40	0.58
$\ln(ab_P)$	2.828	0.956	0.52	0.74
$\ln(ab_A)$	3.184	0.767	0.47	0.66
$\ln(ab_T)$	2.914	0.932	0.59	0.63
Shear Keys				
$\ln(\mu_\phi)$	0.709	1.169	0.72	0.58
$\ln(fx_L)$	4.593	1.119	0.68	0.62
$\ln(fx_T)$	2.646	0.595	0.62	0.38
$\ln(ex_L)$	4.424	0.943	0.67	0.53
$\ln(ex_T)$	2.569	0.565	0.59	0.38
$\ln(ab_P)$	3.041	1.042	0.54	0.77
$\ln(ab_A)$	2.658	0.526	0.26	0.70
$\ln(ab_T)$	3.275	1.085	0.67	0.62
Restrainer Cables and Shear Keys				
$\ln(\mu_\phi)$	0.683	1.161	0.74	0.55
$\ln(fx_L)$	4.515	1.101	0.71	0.56
$\ln(fx_T)$	2.469	0.520	0.57	0.36
$\ln(ex_L)$	4.229	0.877	0.70	0.46
$\ln(ex_T)$	2.434	0.509	0.58	0.35
$\ln(ab_P)$	2.880	0.978	0.55	0.72
$\ln(ab_A)$	3.213	0.780	0.47	0.66
$\ln(ab_T)$	3.274	1.087	0.69	0.59

Table B-5: MSSS Steel Correlation Matrices.

As-Built								
	$\ln(\mu_\phi)$	$\ln(fx_L)$	$\ln(fx_T)$	$\ln(ex_L)$	$\ln(ex_T)$	$\ln(ab_P)$	$\ln(ab_A)$	$\ln(ab_T)$
$\ln(\mu_\phi)$	1.000	0.917	0.913	0.834	0.932	0.863	0.854	0.874
$\ln(fx_L)$	0.917	1.000	0.886	0.900	0.898	0.934	0.872	0.890
$\ln(fx_T)$	0.913	0.886	1.000	0.806	0.909	0.827	0.805	0.861
$\ln(ex_L)$	0.834	0.900	0.806	1.000	0.800	0.887	0.800	0.807
$\ln(ex_T)$	0.932	0.898	0.909	0.800	1.000	0.845	0.836	0.903
$\ln(ab_P)$	0.863	0.934	0.827	0.887	0.845	1.000	0.914	0.900
$\ln(ab_A)$	0.854	0.872	0.805	0.800	0.836	0.914	1.000	0.924
$\ln(ab_T)$	0.874	0.890	0.861	0.807	0.903	0.900	0.924	1.000
Steel Jackets								
	$\ln(\mu_\phi)$	$\ln(fx_L)$	$\ln(fx_T)$	$\ln(ex_L)$	$\ln(ex_T)$	$\ln(ab_P)$	$\ln(ab_A)$	$\ln(ab_T)$
$\ln(\mu_\phi)$	1.000	0.909	0.939	0.831	0.928	0.844	0.866	0.876
$\ln(fx_L)$	0.909	1.000	0.920	0.912	0.890	0.948	0.890	0.894
$\ln(fx_T)$	0.939	0.920	1.000	0.831	0.939	0.852	0.847	0.896
$\ln(ex_L)$	0.831	0.912	0.831	1.000	0.797	0.892	0.802	0.816
$\ln(ex_T)$	0.928	0.890	0.939	0.797	1.000	0.837	0.847	0.899
$\ln(ab_P)$	0.844	0.948	0.852	0.892	0.837	1.000	0.899	0.906
$\ln(ab_A)$	0.866	0.890	0.847	0.802	0.847	0.899	1.000	0.934
$\ln(ab_T)$	0.876	0.894	0.896	0.816	0.899	0.906	0.934	1.000
Elastomeric Isolation Bearings								
	$\ln(\mu_\phi)$	$\ln(eb_L)$	$\ln(eb_T)$	$\ln(ab_P)$	$\ln(ab_A)$	$\ln(ab_T)$		
$\ln(\mu_\phi)$	1.000	0.868	0.857	0.833	0.875	0.906		
$\ln(eb_L)$	0.868	1.000	0.822	0.926	0.945	0.873		
$\ln(eb_T)$	0.857	0.822	1.000	0.755	0.789	0.828		
$\ln(ab_P)$	0.833	0.926	0.755	1.000	0.911	0.856		
$\ln(ab_A)$	0.875	0.945	0.789	0.911	1.000	0.857		
$\ln(ab_T)$	0.906	0.873	0.828	0.856	0.857	1.000		

Restrainer Cables								
	$\ln(\mu_\phi)$	$\ln(fx_L)$	$\ln(fx_T)$	$\ln(ex_L)$	$\ln(ex_T)$	$\ln(ab_P)$	$\ln(ab_A)$	$\ln(ab_T)$
$\ln(\mu_\phi)$	1.000	0.914	0.944	0.836	0.932	0.850	0.844	0.881
$\ln(fx_L)$	0.914	1.000	0.908	0.903	0.890	0.943	0.912	0.882
$\ln(fx_T)$	0.944	0.908	1.000	0.823	0.937	0.847	0.815	0.885
$\ln(ex_L)$	0.836	0.903	0.823	1.000	0.794	0.867	0.832	0.792
$\ln(ex_T)$	0.932	0.890	0.937	0.794	1.000	0.838	0.819	0.895
$\ln(ab_P)$	0.850	0.943	0.847	0.867	0.838	1.000	0.938	0.905
$\ln(ab_A)$	0.844	0.912	0.815	0.832	0.819	0.938	1.000	0.927
$\ln(ab_T)$	0.881	0.882	0.885	0.792	0.895	0.905	0.927	1.000
Shear Keys								
	$\ln(\mu_\phi)$	$\ln(fx_L)$	$\ln(fx_T)$	$\ln(ex_L)$	$\ln(ex_T)$	$\ln(ab_P)$	$\ln(ab_A)$	$\ln(ab_T)$
$\ln(\mu_\phi)$	1.000	0.918	0.906	0.837	0.933	0.872	0.862	0.871
$\ln(fx_L)$	0.918	1.000	0.887	0.908	0.898	0.948	0.890	0.890
$\ln(fx_T)$	0.906	0.887	1.000	0.800	0.908	0.820	0.802	0.845
$\ln(ex_L)$	0.837	0.908	0.800	1.000	0.794	0.889	0.803	0.802
$\ln(ex_T)$	0.933	0.898	0.908	0.794	1.000	0.842	0.833	0.885
$\ln(ab_P)$	0.872	0.948	0.820	0.889	0.842	1.000	0.912	0.897
$\ln(ab_A)$	0.862	0.890	0.802	0.803	0.833	0.912	1.000	0.919
$\ln(ab_T)$	0.871	0.890	0.845	0.802	0.885	0.897	0.919	1.000
Restrainer Cables and Shear Keys								
	$\ln(\mu_\phi)$	$\ln(fx_L)$	$\ln(fx_T)$	$\ln(ex_L)$	$\ln(ex_T)$	$\ln(ab_P)$	$\ln(ab_A)$	$\ln(ab_T)$
$\ln(\mu_\phi)$	1.000	0.918	0.906	0.839	0.934	0.871	0.849	0.877
$\ln(fx_L)$	0.918	1.000	0.872	0.904	0.894	0.951	0.914	0.891
$\ln(fx_T)$	0.906	0.872	1.000	0.789	0.902	0.813	0.780	0.837
$\ln(ex_L)$	0.839	0.904	0.789	1.000	0.790	0.875	0.829	0.793
$\ln(ex_T)$	0.934	0.894	0.902	0.790	1.000	0.845	0.819	0.884
$\ln(ab_P)$	0.871	0.951	0.813	0.875	0.845	1.000	0.941	0.908
$\ln(ab_A)$	0.849	0.914	0.780	0.829	0.819	0.941	1.000	0.923
$\ln(ab_T)$	0.877	0.891	0.837	0.793	0.884	0.908	0.923	1.000

Table B-6: MSC Steel Correlation Matrices.

As-Built								
	$\ln(\mu_\phi)$	$\ln(fx_L)$	$\ln(fx_T)$	$\ln(ex_L)$	$\ln(ex_T)$	$\ln(ab_P)$	$\ln(ab_A)$	$\ln(ab_T)$
$\ln(\mu_\phi)$	1.000	0.784	0.904	0.828	0.892	0.795	0.721	0.857
$\ln(fx_L)$	0.784	1.000	0.767	0.816	0.683	0.714	0.687	0.657
$\ln(fx_T)$	0.904	0.767	1.000	0.745	0.888	0.758	0.694	0.817
$\ln(ex_L)$	0.828	0.816	0.745	1.000	0.809	0.849	0.810	0.757
$\ln(ex_T)$	0.892	0.683	0.888	0.809	1.000	0.741	0.586	0.751
$\ln(ab_P)$	0.795	0.714	0.758	0.849	0.741	1.000	0.791	0.721
$\ln(ab_A)$	0.721	0.687	0.694	0.810	0.586	0.791	1.000	0.829
$\ln(ab_T)$	0.857	0.657	0.817	0.757	0.751	0.721	0.829	1.000
Steel Jackets								
	$\ln(\mu_\phi)$	$\ln(fx_L)$	$\ln(fx_T)$	$\ln(ex_L)$	$\ln(ex_T)$	$\ln(ab_P)$	$\ln(ab_A)$	$\ln(ab_T)$
$\ln(\mu_\phi)$	1.000	0.819	0.896	0.832	0.881	0.768	0.712	0.864
$\ln(fx_L)$	0.819	1.000	0.780	0.839	0.705	0.732	0.737	0.715
$\ln(fx_T)$	0.896	0.780	1.000	0.752	0.903	0.743	0.694	0.827
$\ln(ex_L)$	0.832	0.839	0.752	1.000	0.805	0.836	0.812	0.762
$\ln(ex_T)$	0.881	0.705	0.903	0.805	1.000	0.720	0.576	0.754
$\ln(ab_P)$	0.768	0.732	0.743	0.836	0.720	1.000	0.787	0.714
$\ln(ab_A)$	0.712	0.737	0.694	0.812	0.576	0.787	1.000	0.823
$\ln(ab_T)$	0.864	0.715	0.827	0.762	0.754	0.714	0.823	1.000
Elastomeric Isolation Bearings								
	$\ln(\mu_\phi)$	$\ln(eb_L)$	$\ln(eb_T)$	$\ln(ab_P)$	$\ln(ab_A)$	$\ln(ab_T)$		
$\ln(\mu_\phi)$	1.000	0.911	0.865	0.851	0.819	0.948		
$\ln(eb_L)$	0.911	1.000	0.814	0.907	0.887	0.902		
$\ln(eb_T)$	0.865	0.814	1.000	0.749	0.777	0.880		
$\ln(ab_P)$	0.851	0.907	0.749	1.000	0.817	0.846		
$\ln(ab_A)$	0.819	0.887	0.777	0.817	1.000	0.865		
$\ln(ab_T)$	0.948	0.902	0.880	0.846	0.865	1.000		

Restrainer Cables								
	$\ln(\mu_\phi)$	$\ln(fx_L)$	$\ln(fx_T)$	$\ln(ex_L)$	$\ln(ex_T)$	$\ln(ab_P)$	$\ln(ab_A)$	$\ln(ab_T)$
$\ln(\mu_\phi)$	1.000	0.815	0.876	0.829	0.880	0.797	0.798	0.858
$\ln(fx_L)$	0.815	1.000	0.826	0.830	0.737	0.769	0.769	0.741
$\ln(fx_T)$	0.876	0.826	1.000	0.766	0.866	0.753	0.768	0.834
$\ln(ex_L)$	0.829	0.830	0.766	1.000	0.816	0.801	0.907	0.778
$\ln(ex_T)$	0.880	0.737	0.866	0.816	1.000	0.705	0.737	0.749
$\ln(ab_P)$	0.797	0.769	0.753	0.801	0.705	1.000	0.841	0.717
$\ln(ab_A)$	0.798	0.769	0.768	0.907	0.737	0.841	1.000	0.793
$\ln(ab_T)$	0.858	0.741	0.834	0.778	0.749	0.717	0.793	1.000
Shear Keys								
	$\ln(\mu_\phi)$	$\ln(fx_L)$	$\ln(fx_T)$	$\ln(ex_L)$	$\ln(ex_T)$	$\ln(ab_P)$	$\ln(ab_A)$	$\ln(ab_T)$
$\ln(\mu_\phi)$	1.000	0.833	0.891	0.814	0.852	0.751	0.710	0.888
$\ln(fx_L)$	0.833	1.000	0.810	0.845	0.735	0.759	0.722	0.701
$\ln(fx_T)$	0.891	0.810	1.000	0.741	0.823	0.728	0.712	0.888
$\ln(ex_L)$	0.814	0.845	0.741	1.000	0.817	0.841	0.809	0.777
$\ln(ex_T)$	0.852	0.735	0.823	0.817	1.000	0.683	0.580	0.802
$\ln(ab_P)$	0.751	0.759	0.728	0.841	0.683	1.000	0.791	0.752
$\ln(ab_A)$	0.710	0.722	0.712	0.809	0.580	0.791	1.000	0.808
$\ln(ab_T)$	0.888	0.701	0.888	0.777	0.802	0.752	0.808	1.000
Restrainer Cables and Shear Keys								
	$\ln(\mu_\phi)$	$\ln(fx_L)$	$\ln(fx_T)$	$\ln(ex_L)$	$\ln(ex_T)$	$\ln(ab_P)$	$\ln(ab_A)$	$\ln(ab_T)$
$\ln(\mu_\phi)$	1.000	0.827	0.887	0.824	0.860	0.787	0.795	0.915
$\ln(fx_L)$	0.827	1.000	0.832	0.833	0.745	0.771	0.777	0.737
$\ln(fx_T)$	0.887	0.832	1.000	0.782	0.845	0.770	0.778	0.874
$\ln(ex_L)$	0.824	0.833	0.782	1.000	0.824	0.808	0.906	0.804
$\ln(ex_T)$	0.860	0.745	0.845	0.824	1.000	0.677	0.713	0.806
$\ln(ab_P)$	0.787	0.771	0.770	0.808	0.677	1.000	0.855	0.777
$\ln(ab_A)$	0.795	0.777	0.778	0.906	0.713	0.855	1.000	0.830
$\ln(ab_T)$	0.915	0.737	0.874	0.804	0.806	0.777	0.830	1.000

Table B-7: MSSS Concrete Correlation Matrices.

As-Built								
	$\ln(\mu_\phi)$	$\ln(fx_L)$	$\ln(fx_T)$	$\ln(ex_L)$	$\ln(ex_T)$	$\ln(ab_P)$	$\ln(ab_A)$	$\ln(ab_T)$
$\ln(\mu_\phi)$	1.000	0.815	0.688	0.883	0.717	0.861	0.810	0.920
$\ln(fx_L)$	0.815	1.000	0.752	0.831	0.757	0.819	0.630	0.722
$\ln(fx_T)$	0.688	0.752	1.000	0.666	0.885	0.688	0.498	0.642
$\ln(ex_L)$	0.883	0.831	0.666	1.000	0.677	0.925	0.836	0.833
$\ln(ex_T)$	0.717	0.757	0.885	0.677	1.000	0.697	0.520	0.680
$\ln(ab_P)$	0.861	0.819	0.688	0.925	0.697	1.000	0.849	0.825
$\ln(ab_A)$	0.810	0.630	0.498	0.836	0.520	0.849	1.000	0.850
$\ln(ab_T)$	0.920	0.722	0.642	0.833	0.680	0.825	0.850	1.000
Steel Jackets								
	$\ln(\mu_\phi)$	$\ln(fx_L)$	$\ln(fx_T)$	$\ln(ex_L)$	$\ln(ex_T)$	$\ln(ab_P)$	$\ln(ab_A)$	$\ln(ab_T)$
$\ln(\mu_\phi)$	1.000	0.792	0.690	0.874	0.689	0.854	0.790	0.906
$\ln(fx_L)$	0.792	1.000	0.697	0.827	0.706	0.826	0.661	0.713
$\ln(fx_T)$	0.690	0.697	1.000	0.611	0.982	0.643	0.511	0.654
$\ln(ex_L)$	0.874	0.827	0.611	1.000	0.617	0.927	0.842	0.817
$\ln(ex_T)$	0.689	0.706	0.982	0.617	1.000	0.650	0.501	0.647
$\ln(ab_P)$	0.854	0.826	0.643	0.927	0.650	1.000	0.842	0.811
$\ln(ab_A)$	0.790	0.661	0.511	0.842	0.501	0.842	1.000	0.843
$\ln(ab_T)$	0.906	0.713	0.654	0.817	0.647	0.811	0.843	1.000
Elastomeric Isolation Bearings								
	$\ln(\mu_\phi)$	$\ln(eb_L)$	$\ln(eb_T)$	$\ln(ab_P)$	$\ln(ab_A)$	$\ln(ab_T)$		
$\ln(\mu_\phi)$	1.000	0.899	0.872	0.843	0.803	0.871		
$\ln(eb_L)$	0.899	1.000	0.823	0.939	0.909	0.881		
$\ln(eb_T)$	0.872	0.823	1.000	0.786	0.774	0.820		
$\ln(ab_P)$	0.843	0.939	0.786	1.000	0.867	0.801		
$\ln(ab_A)$	0.803	0.909	0.774	0.867	1.000	0.852		
$\ln(ab_T)$	0.871	0.881	0.820	0.801	0.852	1.000		

Restrainer Cables								
	$\ln(\mu_\phi)$	$\ln(fx_L)$	$\ln(fx_T)$	$\ln(ex_L)$	$\ln(ex_T)$	$\ln(ab_P)$	$\ln(ab_A)$	$\ln(ab_T)$
$\ln(\mu_\phi)$	1.000	0.817	0.695	0.897	0.715	0.886	0.905	0.956
$\ln(fx_L)$	0.817	1.000	0.742	0.806	0.762	0.835	0.746	0.748
$\ln(fx_T)$	0.695	0.742	1.000	0.615	0.968	0.679	0.604	0.662
$\ln(ex_L)$	0.897	0.806	0.615	1.000	0.631	0.927	0.957	0.877
$\ln(ex_T)$	0.715	0.762	0.968	0.631	1.000	0.684	0.627	0.679
$\ln(ab_P)$	0.886	0.835	0.679	0.927	0.684	1.000	0.934	0.844
$\ln(ab_A)$	0.905	0.746	0.604	0.957	0.627	0.934	1.000	0.877
$\ln(ab_T)$	0.956	0.748	0.662	0.877	0.679	0.844	0.877	1.000
Shear Keys								
	$\ln(\mu_\phi)$	$\ln(fx_L)$	$\ln(fx_T)$	$\ln(ex_L)$	$\ln(ex_T)$	$\ln(ab_P)$	$\ln(ab_A)$	$\ln(ab_T)$
$\ln(\mu_\phi)$	1.000	0.824	0.860	0.886	0.867	0.883	0.840	0.950
$\ln(fx_L)$	0.824	1.000	0.798	0.849	0.787	0.852	0.642	0.757
$\ln(fx_T)$	0.860	0.798	1.000	0.758	0.968	0.778	0.634	0.814
$\ln(ex_L)$	0.886	0.849	0.758	1.000	0.766	0.947	0.892	0.868
$\ln(ex_T)$	0.867	0.787	0.968	0.766	1.000	0.775	0.640	0.824
$\ln(ab_P)$	0.883	0.852	0.778	0.947	0.775	1.000	0.873	0.854
$\ln(ab_A)$	0.840	0.642	0.634	0.892	0.640	0.873	1.000	0.844
$\ln(ab_T)$	0.950	0.757	0.814	0.868	0.824	0.854	0.844	1.000
Restrainer Cables and Shear Keys								
	$\ln(\mu_\phi)$	$\ln(fx_L)$	$\ln(fx_T)$	$\ln(ex_L)$	$\ln(ex_T)$	$\ln(ab_P)$	$\ln(ab_A)$	$\ln(ab_T)$
$\ln(\mu_\phi)$	1.000	0.832	0.866	0.886	0.868	0.891	0.910	0.957
$\ln(fx_L)$	0.832	1.000	0.790	0.816	0.802	0.847	0.774	0.759
$\ln(fx_T)$	0.866	0.790	1.000	0.718	0.970	0.767	0.742	0.824
$\ln(ex_L)$	0.886	0.816	0.718	1.000	0.729	0.932	0.954	0.875
$\ln(ex_T)$	0.868	0.802	0.970	0.729	1.000	0.777	0.750	0.827
$\ln(ab_P)$	0.891	0.847	0.767	0.932	0.777	1.000	0.937	0.855
$\ln(ab_A)$	0.910	0.774	0.742	0.954	0.750	0.937	1.000	0.892
$\ln(ab_T)$	0.957	0.759	0.824	0.875	0.827	0.855	0.892	1.000

Table B-8: MSC Concrete Correlation Matrices.

As-Built								
	$\ln(\mu_\phi)$	$\ln(fx_L)$	$\ln(fx_T)$	$\ln(ex_L)$	$\ln(ex_T)$	$\ln(ab_P)$	$\ln(ab_A)$	$\ln(ab_T)$
$\ln(\mu_\phi)$	1.000	0.867	0.787	0.871	0.789	0.755	0.630	0.828
$\ln(fx_L)$	0.867	1.000	0.697	0.977	0.697	0.841	0.656	0.742
$\ln(fx_T)$	0.787	0.697	1.000	0.703	0.990	0.627	0.292	0.500
$\ln(ex_L)$	0.871	0.977	0.703	1.000	0.704	0.897	0.695	0.739
$\ln(ex_T)$	0.789	0.697	0.990	0.704	1.000	0.643	0.297	0.501
$\ln(ab_P)$	0.755	0.841	0.627	0.897	0.643	1.000	0.659	0.640
$\ln(ab_A)$	0.630	0.656	0.292	0.695	0.297	0.659	1.000	0.825
$\ln(ab_T)$	0.828	0.742	0.500	0.739	0.501	0.640	0.825	1.000
Steel Jackets								
	$\ln(\mu_\phi)$	$\ln(fx_L)$	$\ln(fx_T)$	$\ln(ex_L)$	$\ln(ex_T)$	$\ln(ab_P)$	$\ln(ab_A)$	$\ln(ab_T)$
$\ln(\mu_\phi)$	1.000	0.882	0.786	0.881	0.783	0.769	0.633	0.827
$\ln(fx_L)$	0.882	1.000	0.712	0.977	0.705	0.845	0.651	0.750
$\ln(fx_T)$	0.786	0.712	1.000	0.712	0.960	0.644	0.318	0.525
$\ln(ex_L)$	0.881	0.977	0.712	1.000	0.706	0.904	0.698	0.748
$\ln(ex_T)$	0.783	0.705	0.960	0.706	1.000	0.653	0.281	0.480
$\ln(ab_P)$	0.769	0.845	0.644	0.904	0.653	1.000	0.637	0.642
$\ln(ab_A)$	0.633	0.651	0.318	0.698	0.281	0.637	1.000	0.835
$\ln(ab_T)$	0.827	0.750	0.525	0.748	0.480	0.642	0.835	1.000
Elastomeric Isolation Bearings								
	$\ln(\mu_\phi)$	$\ln(eb_L)$	$\ln(eb_T)$	$\ln(ab_P)$	$\ln(ab_A)$	$\ln(ab_T)$		
$\ln(\mu_\phi)$	1.000	0.871	0.717	0.817	0.770	0.927		
$\ln(eb_L)$	0.871	1.000	0.712	0.907	0.929	0.870		
$\ln(eb_T)$	0.717	0.712	1.000	0.583	0.658	0.723		
$\ln(ab_P)$	0.817	0.907	0.583	1.000	0.792	0.815		
$\ln(ab_A)$	0.770	0.929	0.658	0.792	1.000	0.803		
$\ln(ab_T)$	0.927	0.870	0.723	0.815	0.803	1.000		

Restrainer Cables								
	$\ln(\mu_\phi)$	$\ln(fx_L)$	$\ln(fx_T)$	$\ln(ex_L)$	$\ln(ex_T)$	$\ln(ab_P)$	$\ln(ab_A)$	$\ln(ab_T)$
$\ln(\mu_\phi)$	1.000	0.861	0.781	0.860	0.782	0.747	0.721	0.818
$\ln(fx_L)$	0.861	1.000	0.684	0.975	0.681	0.825	0.778	0.736
$\ln(fx_T)$	0.781	0.684	1.000	0.683	0.986	0.621	0.388	0.466
$\ln(ex_L)$	0.860	0.975	0.683	1.000	0.681	0.874	0.838	0.744
$\ln(ex_T)$	0.782	0.681	0.986	0.681	1.000	0.632	0.389	0.462
$\ln(ab_P)$	0.747	0.825	0.621	0.874	0.632	1.000	0.773	0.618
$\ln(ab_A)$	0.721	0.778	0.388	0.838	0.389	0.773	1.000	0.821
$\ln(ab_T)$	0.818	0.736	0.466	0.744	0.462	0.618	0.821	1.000
Shear Keys								
	$\ln(\mu_\phi)$	$\ln(fx_L)$	$\ln(fx_T)$	$\ln(ex_L)$	$\ln(ex_T)$	$\ln(ab_P)$	$\ln(ab_A)$	$\ln(ab_T)$
$\ln(\mu_\phi)$	1.000	0.866	0.855	0.870	0.854	0.771	0.660	0.901
$\ln(fx_L)$	0.866	1.000	0.791	0.978	0.786	0.851	0.654	0.796
$\ln(fx_T)$	0.855	0.791	1.000	0.791	0.985	0.704	0.464	0.790
$\ln(ex_L)$	0.870	0.978	0.791	1.000	0.788	0.905	0.694	0.800
$\ln(ex_T)$	0.854	0.786	0.985	0.788	1.000	0.706	0.454	0.786
$\ln(ab_P)$	0.771	0.851	0.704	0.905	0.706	1.000	0.666	0.715
$\ln(ab_A)$	0.660	0.654	0.464	0.694	0.454	0.666	1.000	0.789
$\ln(ab_T)$	0.901	0.796	0.790	0.800	0.786	0.715	0.789	1.000
Restrainer Cables and Shear Keys								
	$\ln(\mu_\phi)$	$\ln(fx_L)$	$\ln(fx_T)$	$\ln(ex_L)$	$\ln(ex_T)$	$\ln(ab_P)$	$\ln(ab_A)$	$\ln(ab_T)$
$\ln(\mu_\phi)$	1.000	0.860	0.846	0.855	0.844	0.761	0.748	0.902
$\ln(fx_L)$	0.860	1.000	0.772	0.976	0.767	0.835	0.782	0.795
$\ln(fx_T)$	0.846	0.772	1.000	0.766	0.988	0.693	0.535	0.764
$\ln(ex_L)$	0.855	0.976	0.766	1.000	0.762	0.885	0.839	0.805
$\ln(ex_T)$	0.844	0.767	0.988	0.762	1.000	0.695	0.532	0.760
$\ln(ab_P)$	0.761	0.835	0.693	0.885	0.695	1.000	0.790	0.705
$\ln(ab_A)$	0.748	0.782	0.535	0.839	0.532	0.790	1.000	0.817
$\ln(ab_T)$	0.902	0.795	0.764	0.805	0.760	0.705	0.817	1.000

APPENDIX C

COMPONENT FRAGILITY MODELS FOR RETROFITTED BRIDGES

Section 7.5 presented the approach for developing fragility curves for the critical components of the retrofitted bridge systems. This appendix presents tables of the parameters for the component fragility models, where the median value, med_{comp}, is in units of g PGA and β_{comp} is the lognormal standard deviation. As done by (Nielson, 2005a) for the as-built bridges, when any component median value is greater than 4.0, the median and dispersions are replaced by 99.00 and 0.00 respectively, to indicate that this component is not significantly vulnerable for that damage state.

Table C-1: Retrofitted MSSS Steel Component Fragility Curves.

As-built								
	Slight		**Moderate**		**Extensive**		**Complete**	
Component	med_{comp}	β_{comp}	med_{comp}	β_{comp}	med_{comp}	β_{comp}	med_{comp}	β_{comp}
Column	0.56	0.56	0.79	0.52	1.14	0.59	1.52	0.59
Fxd-Long	0.30	0.36	0.51	0.36	0.69	0.40	1.35	0.45
Fxd-Tran	0.43	0.48	0.78	0.48	1.10	0.52	2.34	0.57
Exp-Long	0.33	0.65	0.75	0.62	0.93	0.64	1.19	0.68
Exp-Tran	0.57	0.40	1.33	0.40	2.17	0.49	99.00	0.00
Ab-Pass	1.96	0.55	99.00	0.00	99.00	0.00	99.00	0.00
Ab-Act	0.87	0.94	99.00	0.00	99.00	0.00	99.00	0.00
Ab-Tran	1.46	0.87	99.00	0.00	99.00	0.00	99.00	0.00
Steel Jacket								
	Slight		**Moderate**		**Extensive**		**Complete**	
Component	med_{comp}	β_{comp}	med_{comp}	β_{comp}	med_{comp}	β_{comp}	med_{comp}	β_{comp}
Column	2.48	0.58	3.90	0.54	5.13	0.60	5.70	0.61
Fxd-Long	0.31	0.34	0.52	0.34	0.71	0.39	1.40	0.43
Fxd-Tran	0.41	0.42	0.72	0.42	0.98	0.46	1.97	0.50
Exp-Long	0.34	0.65	0.78	0.62	0.96	0.64	1.24	0.68
Exp-Tran	0.59	0.40	1.39	0.40	2.28	0.49	6.84	0.58
Ab-Pass	2.35	0.56	99.00	0.00	99.00	0.00	99.00	0.00
Ab-Act	1.10	1.00	99.00	0.00	99.00	0.00	99.00	0.00
Ab-Tran	1.50	0.85	99.00	0.00	99.00	0.00	99.00	0.00
Elastomeric Isolation Bearing								
	Slight		**Moderate**		**Extensive**		**Complete**	
Component	med_{comp}	β_{comp}	med_{comp}	β_{comp}	med_{comp}	β_{comp}	med_{comp}	β_{comp}
Column	0.60	0.60	0.86	0.56	1.25	0.63	1.68	0.63
EB-Long	0.56	0.78	0.82	0.75	1.08	0.78	1.82	0.82
EB-Tran	3.96	1.44	99.00	0.00	99.00	0.00	99.00	0.00
Ab-Pass	1.17	0.60	2.32	0.60	6.00	0.56	6.00	0.56
Ab-Act	99.00	0.00	99.00	0.00	99.00	0.00	99.00	0.00
Ab-Tran	0.68	0.68	1.67	0.78	2.70	0.76	14.98	0.50
Restrainer Cables								
	Slight		**Moderate**		**Extensive**		**Complete**	
Component	med_{comp}	β_{comp}	med_{comp}	β_{comp}	med_{comp}	β_{comp}	med_{comp}	β_{comp}
Column	0.58	0.58	0.83	0.54	1.20	0.60	1.60	0.61
Fxd-Long	0.30	0.35	0.51	0.35	0.70	0.39	1.39	0.44
Fxd-Tran	0.41	0.43	0.71	0.43	0.97	0.47	1.95	0.51
Exp-Long	0.38	0.69	0.93	0.66	1.18	0.68	1.56	0.73
Exp-Tran	0.60	0.41	1.41	0.41	2.33	0.50	99.00	0.00
Ab-Pass	2.58	0.58	99.00	0.00	99.00	0.00	99.00	0.00
Ab-Act	0.70	0.89	3.07	1.09	99.00	0.00	99.00	0.00
Ab-Tran	1.65	0.88	99.00	0.00	99.00	0.00	99.00	0.00

Seat Extenders								
	Slight		Moderate		Extensive		Complete	
Component	med_{comp}	β_{comp}	med_{comp}	β_{comp}	med_{comp}	β_{comp}	med_{comp}	β_{comp}
Column	0.56	0.56	0.79	0.52	1.14	0.59	1.52	0.59
Fxd-Long	0.30	0.36	0.51	0.36	0.69	0.40	1.75	0.45
Fxd-Tran	0.43	0.48	0.78	0.48	1.10	0.52	2.34	0.57
Exp-Long	0.33	0.65	0.75	0.62	0.93	0.64	1.92	0.68
Exp-Tran	0.57	0.40	1.33	0.40	2.17	0.49	99.00	0.00
Ab-Pass	1.96	0.55	99.00	0.00	99.00	0.00	99.00	0.00
Ab-Act	0.87	0.94	99.00	0.00	99.00	0.00	99.00	0.00
Ab-Tran	1.46	0.87	99.00	0.00	99.00	0.00	99.00	0.00
Shear Keys								
	Slight		Moderate		Extensive		Complete	
Component	med_{comp}	β_{comp}	med_{comp}	β_{comp}	med_{comp}	β_{comp}	med_{comp}	β_{comp}
Column	0.55	0.57	0.77	0.53	1.10	0.59	1.45	0.60
Fxd-Long	0.30	0.36	0.50	0.36	0.68	0.40	1.34	0.45
Fxd-Tran	0.45	0.52	0.82	0.52	1.16	0.56	2.51	0.60
Exp-Long	0.33	0.64	0.73	0.61	0.91	0.63	1.16	0.67
Exp-Tran	0.55	0.44	1.25	0.44	2.01	0.52	5.78	0.61
Ab-Pass	1.77	0.56	4.81	0.56	19.55	0.44	19.55	0.44
Ab-Act	0.80	0.91	3.69	1.12	8.25	1.06	148.98	0.46
Ab-Tran	1.50	0.87	6.32	1.06	13.46	1.01	203.99	0.46
Restrainer Cables and Shear Keys								
	Slight		Moderate		Extensive		Complete	
Component	med_{comp}	β_{comp}	med_{comp}	β_{comp}	med_{comp}	β_{comp}	med_{comp}	β_{comp}
Column	0.57	0.57	0.80	0.53	1.16	0.60	1.54	0.60
Fxd-Long	0.30	0.35	0.51	0.35	0.70	0.40	1.39	0.44
Fxd-Tran	0.46	0.53	0.84	0.53	1.20	0.57	2.63	0.61
Exp-Long	0.37	0.68	0.90	0.64	1.13	0.67	1.49	0.71
Exp-Tran	0.57	0.46	1.32	0.46	2.15	0.54	99.00	0.00
Ab-Pass	2.05	0.56	99.00	0.00	99.00	0.00	99.00	0.00
Ab-Act	0.62	0.84	2.46	1.03	99.00	0.00	99.00	0.00
Ab-Tran	1.64	0.89	99.00	0.00	99.00	0.00	99.00	0.00
Seat Extenders and Shear Keys								
	Slight		Moderate		Extensive		Complete	
Component	med_{comp}	β_{comp}	med_{comp}	β_{comp}	med_{comp}	β_{comp}	med_{comp}	β_{comp}
Column	0.55	0.57	0.77	0.53	1.10	0.59	1.45	0.60
Fxd-Long	0.30	0.36	0.50	0.36	0.68	0.40	1.74	0.45
Fxd-Tran	0.45	0.52	0.82	0.52	1.16	0.56	2.51	0.60
Exp-Long	0.33	0.64	0.73	0.61	0.91	0.63	1.87	0.67
Exp-Tran	0.55	0.44	1.25	0.44	2.01	0.52	99.00	0.00
Ab-Pass	1.77	0.56	99.00	0.00	99.00	0.00	99.00	0.00
Ab-Act	0.80	0.91	3.69	1.12	99.00	0.00	99.00	0.00
Ab-Tran	1.50	0.87	99.00	0.00	99.00	0.00	99.00	0.00

Table C-2: Retrofitted MSC Steel Component Fragility Curves.

As-built								
	Slight		**Moderate**		**Extensive**		**Complete**	
Component	med_{comp}	β_{comp}	med_{comp}	β_{comp}	med_{comp}	β_{comp}	med_{comp}	β_{comp}
Column	0.37	0.62	0.49	0.59	0.66	0.64	0.84	0.64
Fxd-Long	0.83	0.65	1.78	0.65	2.75	0.70	99.00	0.00
Fxd-Tran	0.52	0.69	1.01	0.69	1.48	0.72	3.46	0.77
Exp-Long	0.23	0.65	0.45	0.63	0.55	0.64	0.68	0.67
Exp-Tran	0.26	0.53	0.48	0.53	0.68	0.57	1.51	0.61
Ab-Pass	0.95	0.82	1.73	0.82	99.00	0.00	99.00	0.00
Ab-Act	99.00	0.00	99.00	0.00	99.00	0.00	99.00	0.00
Ab-Tran	0.89	0.98	99.00	0.00	99.00	0.00	99.00	0.00
Steel Jacket								
	Slight		**Moderate**		**Extensive**		**Complete**	
Component	med_{comp}	β_{comp}	med_{comp}	β_{comp}	med_{comp}	β_{comp}	med_{comp}	β_{comp}
Column	1.34	0.59	1.96	0.56	2.47	0.61	2.70	0.61
Fxd-Long	0.74	0.61	1.52	0.61	2.30	0.66	99.00	0.00
Fxd-Tran	0.51	0.69	0.98	0.69	1.43	0.73	3.30	0.77
Exp-Long	0.23	0.65	0.46	0.62	0.56	0.64	0.69	0.67
Exp-Tran	0.27	0.53	0.51	0.53	0.74	0.58	1.69	0.62
Ab-Pass	1.06	0.88	1.97	0.88	99.00	0.00	99.00	0.00
Ab-Act	99.00	0.00	99.00	0.00	99.00	0.00	99.00	0.00
Ab-Tran	0.80	0.93	3.46	1.12	99.00	0.00	99.00	0.00
Elastomeric Isolation Bearing								
	Slight		**Moderate**		**Extensive**		**Complete**	
Component	med_{comp}	β_{comp}	med_{comp}	β_{comp}	med_{comp}	β_{comp}	med_{comp}	β_{comp}
Column	0.60	0.67	0.86	0.64	1.24	0.69	1.65	0.70
EB-Long	0.35	0.80	0.50	0.77	0.64	0.79	1.05	0.83
EB-Tran	99.00	0.00	99.00	0.00	99.00	0.00	99.00	0.00
Ab-Pass	0.75	0.75	1.34	0.75	3.02	0.72	3.02	0.72
Ab-Act	99.00	0.00	99.00	0.00	99.00	0.00	99.00	0.00
Ab-Tran	0.35	0.79	0.80	0.87	1.24	0.85	99.00	0.00
Restrainer Cables								
	Slight		**Moderate**		**Extensive**		**Complete**	
Component	med_{comp}	β_{comp}	med_{comp}	β_{comp}	med_{comp}	β_{comp}	med_{comp}	β_{comp}
Column	0.41	0.66	0.56	0.63	0.77	0.67	0.98	0.68
Fxd-Long	1.29	0.68	3.09	0.68	99.00	0.00	99.00	0.00
Fxd-Tran	0.53	0.68	1.04	0.68	1.53	0.71	3.61	0.76
Exp-Long	0.26	0.66	0.55	0.64	0.67	0.65	0.85	0.69
Exp-Tran	0.26	0.52	0.48	0.52	0.69	0.56	1.53	0.61
Ab-Pass	1.51	0.92	3.03	0.92	99.00	0.00	99.00	0.00
Ab-Act	0.40	0.81	0.84	0.86	1.24	0.85	99.00	0.00
Ab-Tran	0.84	0.97	3.85	1.16	99.00	0.00	99.00	0.00

Seat Extenders								
	Slight		Moderate		Extensive		Complete	
Component	med_{comp}	β_{comp}	med_{comp}	β_{comp}	med_{comp}	β_{comp}	med_{comp}	β_{comp}
Column	0.37	0.62	0.49	0.59	0.66	0.64	0.84	0.64
Fxd-Long	0.83	0.65	1.78	0.65	2.75	0.70	99.00	0.00
Fxd-Tran	0.52	0.69	1.01	0.69	1.48	0.72	3.46	0.77
Exp-Long	0.23	0.65	0.45	0.63	0.55	0.64	1.02	0.67
Exp-Tran	0.26	0.53	0.48	0.53	0.68	0.57	1.51	0.61
Ab-Pass	0.95	0.82	1.73	0.82	4.01	0.80	99.00	0.00
Ab-Act	99.00	0.00	99.00	0.00	99.00	0.00	99.00	0.00
Ab-Tran	0.89	0.98	4.23	1.18	99.00	0.00	99.00	0.00

Shear Keys								
	Slight		Moderate		Extensive		Complete	
Component	med_{comp}	β_{comp}	med_{comp}	β_{comp}	med_{comp}	β_{comp}	med_{comp}	β_{comp}
Column	0.43	0.65	0.59	0.62	0.82	0.67	1.06	0.67
Fxd-Long	0.87	0.63	1.85	0.63	2.86	0.68	99.00	0.00
Fxd-Tran	0.79	0.68	1.78	0.68	2.85	0.73	99.00	0.00
Exp-Long	0.23	0.66	0.47	0.63	0.57	0.65	0.71	0.68
Exp-Tran	0.34	0.45	0.76	0.45	1.21	0.52	3.43	0.60
Ab-Pass	1.02	0.83	1.89	0.83	4.48	0.81	99.00	0.00
Ab-Act	99.00	0.00	99.00	0.00	99.00	0.00	99.00	0.00
Ab-Tran	0.64	0.86	2.42	1.02	4.84	0.98	99.00	0.00

Restrainer Cables and Shear Keys								
	Slight		Moderate		Extensive		Complete	
Component	med_{comp}	β_{comp}	med_{comp}	β_{comp}	med_{comp}	β_{comp}	med_{comp}	β_{comp}
Column	0.43	0.66	0.58	0.63	0.81	0.67	1.04	0.68
Fxd-Long	1.36	0.68	3.30	0.68	99.00	0.00	99.00	0.00
Fxd-Tran	0.71	0.65	1.55	0.65	2.44	0.71	99.00	0.00
Exp-Long	0.26	0.66	0.55	0.63	0.67	0.65	0.85	0.68
Exp-Tran	0.34	0.45	0.77	0.45	1.23	0.53	3.51	0.61
Ab-Pass	1.38	0.89	2.72	0.89	99.00	0.00	99.00	0.00
Ab-Act	0.40	0.80	0.83	0.86	1.22	0.84	99.00	0.00
Ab-Tran	0.59	0.85	2.12	1.00	99.00	0.00	99.00	0.00

Seat Extenders and Shear Keys								
	Slight		Moderate		Extensive		Complete	
Component	med_{comp}	β_{comp}	med_{comp}	β_{comp}	med_{comp}	β_{comp}	med_{comp}	β_{comp}
Column	0.43	0.65	0.59	0.62	0.82	0.67	1.06	0.67
Fxd-Long	0.87	0.63	1.85	0.63	2.86	0.68	99.00	0.00
Fxd-Tran	0.79	0.68	1.78	0.68	2.85	0.73	99.00	0.00
Exp-Long	0.23	0.66	0.47	0.63	0.57	0.65	1.07	0.68
Exp-Tran	0.34	0.45	0.76	0.45	1.21	0.52	3.43	0.60
Ab-Pass	1.02	0.83	1.89	0.83	99.00	0.00	99.00	0.00
Ab-Act	99.00	0.00	99.00	0.00	99.00	0.00	99.00	0.00
Ab-Tran	0.64	0.86	2.42	1.02	99.00	0.00	99.00	0.00

Table C-3: Retrofitted MSSS Concrete Component Fragility Curves.

As-built								
	Slight		**Moderate**		**Extensive**		**Complete**	
Component	med_{comp}	β_{comp}	med_{comp}	β_{comp}	med_{comp}	β_{comp}	med_{comp}	β_{comp}
Column	0.61	0.68	0.93	0.63	1.43	0.71	2.00	0.71
Fxd-Long	0.51	0.77	1.54	0.74	1.93	0.76	2.54	0.80
Fxd-Tran	1.60	1.45	99.00	0.00	99.00	0.00	99.00	0.00
Exp-Long	0.33	0.79	1.27	0.75	1.67	0.78	2.32	0.83
Exp-Tran	1.36	1.42	99.00	0.00	99.00	0.00	99.00	0.00
Ab-Pass	3.14	0.73	99.00	0.00	99.00	0.00	99.00	0.00
Ab-Act	0.49	1.07	2.32	1.26	99.00	0.00	99.00	0.00
Ab-Tran	0.78	0.82	2.88	0.99	99.00	0.00	99.00	0.00
Steel Jacket								
	Slight		**Moderate**		**Extensive**		**Complete**	
Component	med_{comp}	β_{comp}	med_{comp}	β_{comp}	med_{comp}	β_{comp}	med_{comp}	β_{comp}
Column	3.74	0.70	99.00	0.00	99.00	0.00	99.00	0.00
Fxd-Long	0.55	0.79	1.74	0.75	2.22	0.78	2.95	0.82
Fxd-Tran	2.47	1.64	99.00	0.00	99.00	0.00	99.00	0.00
Exp-Long	0.35	0.80	1.36	0.76	1.81	0.79	2.53	0.84
Exp-Tran	2.61	1.64	99.00	0.00	99.00	0.00	99.00	0.00
Ab-Pass	3.02	0.73	99.00	0.00	99.00	0.00	99.00	0.00
Ab-Act	0.47	1.03	2.09	1.20	99.00	0.00	99.00	0.00
Ab-Tran	0.88	0.89	3.43	1.06	99.00	0.00	99.00	0.00
Elastomeric Isolation Bearing								
	Slight		**Moderate**		**Extensive**		**Complete**	
Component	med_{comp}	β_{comp}	med_{comp}	β_{comp}	med_{comp}	β_{comp}	med_{comp}	β_{comp}
Column	0.60	0.63	0.88	0.58	1.32	0.65	1.81	0.66
EB-Long	0.86	0.90	1.36	0.85	1.87	0.88	3.52	0.94
EB-Tran	99.00	0.00	99.00	0.00	99.00	0.00	99.00	0.00
Ab-Pass	0.79	0.67	1.41	0.67	3.21	0.65	3.21	0.65
Ab-Act	99.00	0.00	99.00	0.00	99.00	0.00	99.00	0.00
Ab-Tran	0.43	0.84	1.26	0.95	2.20	0.92	99.00	0.00
Restrainer Cables								
	Slight		**Moderate**		**Extensive**		**Complete**	
Component	med_{comp}	β_{comp}	med_{comp}	β_{comp}	med_{comp}	β_{comp}	med_{comp}	β_{comp}
Column	0.67	0.70	1.03	0.65	1.61	0.74	2.29	0.74
Fxd-Long	0.51	0.77	1.54	0.74	1.95	0.77	2.56	0.80
Fxd-Tran	1.92	1.63	99.00	0.00	99.00	0.00	99.00	0.00
Exp-Long	0.37	0.87	1.65	0.82	2.25	0.86	3.23	0.92
Exp-Tran	1.64	1.51	99.00	0.00	99.00	0.00	99.00	0.00
Ab-Pass	3.40	0.79	99.00	0.00	99.00	0.00	99.00	0.00
Ab-Act	0.45	0.97	2.10	1.17	99.00	0.00	99.00	0.00
Ab-Tran	0.98	0.91	99.00	0.00	99.00	0.00	99.00	0.00

Seat Extenders								
	Slight		Moderate		Extensive		Complete	
Component	med_{comp}	β_{comp}	med_{comp}	β_{comp}	med_{comp}	β_{comp}	med_{comp}	β_{comp}
Column	0.65	0.66	0.97	0.61	1.50	0.69	2.09	0.70
Fxd-Long	0.51	0.77	1.54	0.74	1.93	0.76	99.00	0.00
Fxd-Tran	1.60	1.45	99.00	0.00	99.00	0.00	99.00	0.00
Exp-Long	0.33	0.79	1.27	0.75	1.67	0.78	99.00	0.00
Exp-Tran	1.36	1.42	99.00	0.00	99.00	0.00	99.00	0.00
Ab-Pass	3.14	0.73	99.00	0.00	99.00	0.00	99.00	0.00
Ab-Act	0.49	1.07	2.32	1.26	99.00	0.00	99.00	0.00
Ab-Tran	0.78	0.82	2.88	0.99	99.00	0.00	99.00	0.00

Shear Keys								
	Slight		Moderate		Extensive		Complete	
Component	med_{comp}	β_{comp}	med_{comp}	β_{comp}	med_{comp}	β_{comp}	med_{comp}	β_{comp}
Column	0.57	0.68	0.84	0.63	1.28	0.70	1.77	0.71
Fxd-Long	0.46	0.76	1.31	0.73	1.63	0.75	2.12	0.79
Fxd-Tran	99.00	0.00	99.00	0.00	99.00	0.00	99.00	0.00
Exp-Long	0.31	0.75	1.07	0.71	1.39	0.74	1.89	0.79
Exp-Tran	99.00	0.00	99.00	0.00	99.00	0.00	99.00	0.00
Ab-Pass	2.43	0.71	99.00	0.00	99.00	0.00	99.00	0.00
Ab-Act	0.65	1.12	99.00	0.00	99.00	0.00	99.00	0.00
Ab-Tran	0.85	0.84	3.28	1.02	99.00	0.00	99.00	0.00

Restrainer Cables and Shear Keys								
	Slight		Moderate		Extensive		Complete	
Component	med_{comp}	β_{comp}	med_{comp}	β_{comp}	med_{comp}	β_{comp}	med_{comp}	β_{comp}
Column	0.63	0.70	0.95	0.65	1.46	0.73	2.04	0.74
Fxd-Long	0.51	0.78	1.56	0.75	1.97	0.77	2.59	0.81
Fxd-Tran	99.00	0.00	99.00	0.00	99.00	0.00	99.00	0.00
Exp-Long	0.36	0.82	1.44	0.77	1.93	0.80	2.73	0.86
Exp-Tran	99.00	0.00	99.00	0.00	99.00	0.00	99.00	0.00
Ab-Pass	2.72	0.76	99.00	0.00	99.00	0.00	99.00	0.00
Ab-Act	0.42	0.90	1.78	1.08	3.78	1.03	99.00	0.00
Ab-Tran	0.87	0.86	3.39	1.04	99.00	0.00	99.00	0.00

Seat Extenders and Shear Keys								
	Slight		Moderate		Extensive		Complete	
Component	med_{comp}	β_{comp}	med_{comp}	β_{comp}	med_{comp}	β_{comp}	med_{comp}	β_{comp}
Column	0.62	0.68	0.93	0.64	1.42	0.71	1.97	0.72
Fxd-Long	0.46	0.76	1.31	0.73	1.63	0.75	3.44	0.79
Fxd-Tran	99.00	0.00	99.00	0.00	99.00	0.00	99.00	0.00
Exp-Long	0.31	0.75	1.07	0.71	1.39	0.74	3.38	0.79
Exp-Tran	99.00	0.00	99.00	0.00	99.00	0.00	99.00	0.00
Ab-Pass	2.43	0.71	99.00	0.00	99.00	0.00	99.00	0.00
Ab-Act	0.65	1.12	99.00	0.00	99.00	0.00	99.00	0.00
Ab-Tran	0.85	0.84	3.28	1.02	99.00	0.00	99.00	0.00

Table C-4: Retrofitted MSC Concrete Component Fragility Curves.

As-built								
	Slight		**Moderate**		**Extensive**		**Complete**	
Component	med_{comp}	β_{comp}	med_{comp}	β_{comp}	med_{comp}	β_{comp}	med_{comp}	β_{comp}
Column	0.59	0.69	0.87	0.65	1.33	0.72	1.84	0.73
Fxd-Long	0.34	0.78	1.08	0.75	1.38	0.77	1.84	0.81
Fxd-Tran	2.04	1.46	99.00	0.00	99.00	0.00	99.00	0.00
Exp-Long	0.33	0.86	1.32	0.82	1.76	0.85	2.48	0.90
Exp-Tran	2.39	1.51	99.00	0.00	99.00	0.00	99.00	0.00
Ab-Pass	2.03	0.94	99.00	0.00	99.00	0.00	99.00	0.00
Ab-Act	0.49	1.88	99.00	0.00	99.00	0.00	99.00	0.00
Ab-Tran	0.51	1.03	2.17	1.20	99.00	0.00	99.00	0.00
Steel Jacket								
	Slight		**Moderate**		**Extensive**		**Complete**	
Component	med_{comp}	β_{comp}	med_{comp}	β_{comp}	med_{comp}	β_{comp}	med_{comp}	β_{comp}
Column	2.89	0.67	99.00	0.00	99.00	0.00	99.00	0.00
Fxd-Long	0.34	0.76	1.06	0.73	1.35	0.75	1.79	0.79
Fxd-Tran	2.24	1.50	99.00	0.00	99.00	0.00	99.00	0.00
Exp-Long	0.33	0.84	1.28	0.80	1.69	0.83	2.36	0.88
Exp-Tran	2.55	1.53	99.00	0.00	99.00	0.00	99.00	0.00
Ab-Pass	1.80	0.88	99.00	0.00	99.00	0.00	99.00	0.00
Ab-Act	0.49	1.83	99.00	0.00	99.00	0.00	99.00	0.00
Ab-Tran	0.51	1.02	2.18	1.19	99.00	0.00	99.00	0.00
Elastomeric Isolation Bearing								
	Slight		**Moderate**		**Extensive**		**Complete**	
Component	med_{comp}	β_{comp}	med_{comp}	β_{comp}	med_{comp}	β_{comp}	med_{comp}	β_{comp}
Column	0.65	0.68	0.96	0.63	1.46	0.71	2.01	0.71
EB-Long	1.11	1.09	1.94	1.03	2.88	1.07	99.00	0.00
EB-Tran	99.00	0.00	99.00	0.00	99.00	0.00	99.00	0.00
Ab-Pass	1.06	0.76	1.25	0.76	1.41	0.76	1.77	0.77
Ab-Act	99.00	0.00	99.00	0.00	99.00	0.00	99.00	0.00
Ab-Tran	0.66	0.64	1.65	0.64	99.00	0.00	99.00	0.00
Restrainer Cables								
	Slight		**Moderate**		**Extensive**		**Complete**	
Component	med_{comp}	β_{comp}	med_{comp}	β_{comp}	med_{comp}	β_{comp}	med_{comp}	β_{comp}
Column	0.59	0.68	0.87	0.63	1.33	0.71	1.83	0.71
Fxd-Long	0.35	0.75	1.13	0.71	1.44	0.74	1.92	0.78
Fxd-Tran	2.71	1.56	99.00	0.00	99.00	0.00	99.00	0.00
Exp-Long	0.37	0.87	1.62	0.82	2.20	0.85	3.16	0.91
Exp-Tran	3.22	1.63	99.00	0.00	99.00	0.00	99.00	0.00
Ab-Pass	2.27	0.91	99.00	0.00	99.00	0.00	99.00	0.00
Ab-Act	0.31	1.25	1.80	1.46	99.00	0.00	99.00	0.00
Ab-Tran	0.51	1.01	2.17	1.18	99.00	0.00	99.00	0.00

Seat Extenders								
	Slight		Moderate		Extensive		Complete	
Component	med_{comp}	β_{comp}	med_{comp}	β_{comp}	med_{comp}	β_{comp}	med_{comp}	β_{comp}
Column	0.59	0.69	0.87	0.65	1.33	0.72	1.84	0.73
Fxd-Long	0.34	0.78	1.08	0.75	1.38	0.77	3.15	0.81
Fxd-Tran	2.04	1.46	99.00	0.00	99.00	0.00	99.00	0.00
Exp-Long	0.33	0.86	1.32	0.82	1.76	0.85	99.00	0.00
Exp-Tran	2.39	1.51	99.00	0.00	99.00	0.00	99.00	0.00
Ab-Pass	2.03	0.94	99.00	0.00	99.00	0.00	99.00	0.00
Ab-Act	0.49	1.88	99.00	0.00	99.00	0.00	99.00	0.00
Ab-Tran	0.51	1.03	2.17	1.20	99.00	0.00	99.00	0.00
Shear Keys								
	Slight		Moderate		Extensive		Complete	
Component	med_{comp}	β_{comp}	med_{comp}	β_{comp}	med_{comp}	β_{comp}	med_{comp}	β_{comp}
Column	0.63	0.71	0.95	0.66	1.46	0.74	2.04	0.74
Fxd-Long	0.33	0.77	1.05	0.74	1.33	0.76	1.77	0.80
Fxd-Tran	3.32	1.47	99.00	0.00	99.00	0.00	99.00	0.00
Exp-Long	0.33	0.85	1.27	0.81	1.68	0.84	2.35	0.89
Exp-Tran	99.00	0.00	99.00	0.00	99.00	0.00	99.00	0.00
Ab-Pass	1.73	0.86	99.00	0.00	99.00	0.00	99.00	0.00
Ab-Act	0.49	1.88	99.00	0.00	99.00	0.00	99.00	0.00
Ab-Tran	0.40	0.86	1.39	1.01	2.68	0.97	99.00	0.00
Restrainer Cables and Shear Keys								
	Slight		Moderate		Extensive		Complete	
Component	med_{comp}	β_{comp}	med_{comp}	β_{comp}	med_{comp}	β_{comp}	med_{comp}	β_{comp}
Column	0.65	0.69	0.98	0.65	1.52	0.72	2.13	0.73
Fxd-Long	0.35	0.75	1.13	0.71	1.44	0.74	1.91	0.78
Fxd-Tran	5.56	1.67	99.00	0.00	99.00	0.00	99.00	0.00
Exp-Long	0.37	0.87	1.61	0.82	2.18	0.85	3.13	0.91
Exp-Tran	99.00	0.00	99.00	0.00	99.00	0.00	99.00	0.00
Ab-Pass	2.11	0.88	99.00	0.00	99.00	0.00	99.00	0.00
Ab-Act	0.30	1.24	1.72	1.44	99.00	0.00	99.00	0.00
Ab-Tran	0.40	0.84	1.39	1.00	2.68	0.95	99.00	0.00
Seat Extenders and Shear Keys								
	Slight		Moderate		Extensive		Complete	
Component	med_{comp}	β_{comp}	med_{comp}	β_{comp}	med_{comp}	β_{comp}	med_{comp}	β_{comp}
Column	0.63	0.71	0.95	0.66	1.46	0.74	2.04	0.74
Fxd-Long	0.33	0.77	1.05	0.74	1.33	0.76	3.01	0.80
Fxd-Tran	3.32	1.47	99.00	0.00	99.00	0.00	99.00	0.00
Exp-Long	0.33	0.85	1.27	0.81	1.68	0.84	99.00	0.00
Exp-Tran	99.00	0.00	99.00	0.00	99.00	0.00	99.00	0.00
Ab-Pass	1.73	0.86	99.00	0.00	99.00	0.00	99.00	0.00
Ab-Act	0.49	1.88	99.00	0.00	99.00	0.00	99.00	0.00
Ab-Tran	0.40	0.86	1.39	1.01	2.68	0.97	99.00	0.00

APPENDIX D

PERCENT DIFFERENT IN MEDIAN VALUES FOR RETROFIT SELECTION

Chapter 8 presented a simplified approach for comparing retrofits based on the percent difference in the median values of the system fragility relative to the as-built bridge. The percent change is listed in Table D-1 - Table D-4 for the four typical classes of bridges evaluated as a part of this work.

Table D-1: Percent Difference in Fragility Medians for Retrofitted MSSS Steel Relative to As-Built Bridge.

	% Difference in med_{sys} from As-Built			
Retrofit Measure	**Slight**	**Moderate**	**Extensive**	**Complete**
Steel Jackets	+6%	+6%	+7%	+13%
Elastomeric Isolation Bearings	**+57%**	**+32%**	**+37%**	**+39%**
Restrainer Cables	+3%	+3%	+4%	+11%
Seat Extenders	0%	0%	0%	+26%
Shear Keys	-1%	-2%	-2%	-3%
Restrainer Cables and Shear Keys	+2%	+2%	+4%	+9%
Seat Extenders and Shear Keys	-1%	-2%	-1%	+23%

Table D-2: Percent Difference in Fragility Medians for Retrofitted MSC Steel Relative to As-Built Bridge.

	% Difference in med_{sys} from As-Built			
Retrofit Measure	**Slight**	**Moderate**	**Extensive**	**Complete**
Steel Jackets	+4%	+14%	+14%	+18%
Elastomeric Isolation Bearings	**+37%**	**+21%**	**+27%**	**+61%**
Restrainer Cables	+3%	+5%	+11%	+17%
Seat Extenders	-1%	+1%	0%	+21%
Shear Keys	+8%	+14%	+13%	+9%
Restrainer Cables and Shear Keys	+9%	+17%	+21%	+21%
Seat Extenders and Shear Keys	+9%	+15%	+15%	+41%

Table D-3: Percent Difference in Fragility Medians for Retrofitted MSSS Concrete Relative to As-Built Bridge.

	% Difference in med_{sys} from As-Built			
Retrofit Measure	**Slight**	**Moderate**	**Extensive**	**Complete**
Steel Jackets	+5%	**+30%**	**+33%**	**+41%**
Elastomeric Isolation Bearings	**+62%**	+1%	+5%	+17%
Restrainer Cables	+1%	+7%	+10%	+13%
Seat Extenders	-1%	+3%	+2%	+32%
Shear Keys	+4%	-3%	-8%	-13%
Restrainer Cables and Shear Keys	+6%	+3%	+6%	+7%
Seat Extenders and Shear Keys	+4%	+1%	-5%	+22%

Table D-4: Percent Difference in Fragility Medians for Retrofitted MSC Concrete Relative to As-Built Bridge.

	% Difference in med_{sys} from As-Built			
Retrofit Measure	**Slight**	**Moderate**	**Extensive**	**Complete**
Steel Ja Steel Jackets	+3%	+16%	+17%	+20%
Elastomeric Isolation Bearings	**+194%**	**+31%**	**+21%**	+17%
Restrainer Cables	+4%	-4%	+1%	+5%
Seat Extenders	+1%	0%	0%	+31%
Shear Keys	+1%	-2%	-1%	+1%
Restrainer Cables and Shear Keys	+4%	-4%	+4%	+12%
Seat Extenders and Shear Keys	+1%	-3%	-1%	**+37%**

References

AASHTO (1999). *Guide Specifications for Seismic Isolation Design*. American Association of State Highway Transportation Officials, Washington, D.C.

Abrams, D. (2003). "6th Year MAE Center Annual Report." *Report no.*, University of Illinois.

Anderson, R. E. and Gruendler, J. J. (1995). "Illinois department of transportation seismic bridge condition survey." *Proceedings of the 13th Structures Congress. Part 2 (of 2), Apr 3-5 1995*, Vol. 2 of *Structures Congress - Proceedings*, Boston, MA, USA. ASCE, New York, NY, USA, 1169–1181.

ATC (1985). "Earthquake Damage Evaluation Data for California." *Report No. ATC-13*, Applied Technology Council.

ATC (1991). "Seismic Vulnerability and Impact of Disruption of Lifelines in the Conterminous United States." *Report No. ATC-25*, Applied Technology Council.

Baker, J. and Cornell, A. C. (2006). "Which Spectral Acceleration Are You Using?." *Earthquake Spectra*, 22(2).

Basoz, N., Kiremidjian, A., King, S. A., and Law, K. H. (1999). "Statistical Analysis of Bridge Damage Data from the 1994 Northridge, CA, Earthquake." *Earthquake Spectra*, 15(1).

Basoz, N. and Kiremidjian, A. S. (1999). "Development of empirical fragility curves for bridges." *Technical Council on Lifeline Earthquake Engineering Monograph Proceedings of the 1999 5th U.S. Conference on Lifeline Earthquake Engineering: Optimazing Post-Earthquake Lifeline System Reliability, Aug 12-Aug 14 1999*, (16), 693–702.

Basoz, N. and Mander, J. (1999). "Enhancement of the Highway Transportation Module in HAZUS." *Report No. National Institute of Building Sciences*.

Boore, D. M. (1983). "Stochastic Simulation of High-Frequency Ground Motions Based on Seismological Models of the Radiated Spectra." *Bulletin of the Seismological Society of America*, 73(6), 1865–1894.

Bostrom, A., Turaga, R. M. R., and Ponomariov, B. (2006). "Earthquake Mitigation Decisions and Consequences." *Earthquake Spectra*, 22(2), 313–327.

Bruneau, M. (1998). "Performance of steel bridges during the 1995 Hyogoken-Nanbu (Kobe, Japan) earthquake - a North American perspective." *Engineering Structures*, 20(12), 1063.

Caltrans (1990). *Caltrans Structures Seismic Design References*. California Department of Transportation, Sacramento, CA, first edition.

Caltrans (1997). *Seismic Design References*. State of California Department of Transportation Division of Structures.

Caltrans (1999). *Caltrans Seismic Design Criteria*. California Department of Transportation, Sacramento, CA, first edition.

Caltrans (2003). "Seismic Retrofit Program.

Caner, A., Dogan, E., and Zia, P. (2002). "Seismic performance of multisimple-span bridges retrofitted with link slabs." *Journal of Bridge Engineering*, 7(2), 85–93.

Chai, Y. H., Priestley, M. N., and Seible, F. (1991). "Seismic Retrofit of Circular Bridge Columns for Enhanced Flexural Performance." *ACI Structural Journal (American Concrete Institute)*, 88(5), 572–584.

Chang, S. E. and Shinozuka, M. (1996). "Life-cycle cost analysis with natural hazard risk." *Journal of Infrastructure Systems*, 2(3), 118.

Chang, S. E., Shinozuka, M., and Moore, James E., I. (2000). "Probabilistic earthquake scenarios: Extending risk analysis methodologies to spatially distributed systems." *Earthquake Spectra*, 16(3), 557.

Choi, E. (2002). "Seismic Analysis and Retrofit of Mid-America Bridges." *Report no.*, Georgia Institute of Technology.

Choi, E., DesRoches, R., and Nielson, B. (2004). "Seismic Fragility of Typical Bridges in Moderate Seismic Zones." *Engineering Structures*, 26(2), 187–199.

Cimellaro, G. P. and Domaneschi, M. (2006). "Reliability of a Cable Stayed Bridge." *8th U.S. National Conference on Earthquake Engineering*, San Francisco, California.

Collaboration, A. . N. S. B. (2005). "G 9.1-2004 Steel Bridge Bearing Design and Detailing Guidelines." *Report No. AASHTO: SBB-1*.

Cooper, J., Friedland, I. M., Buckle, I. G., Nimis, R. B., and Bobb, N. M. (1994). "The Northridge: Progress Made, Lessons Learned in Seismic Design of Bridges." *Public Roads*, 58(1).

Cornell, A. C., Jalayer, F., and Hamburger, R. O. (2002). "Probabilistic Basis for 2000 SAC Federal Emergency Management Agency Steel Moment Frame Guidelines." *Journal of Structural Engineering*, 128(4), 526–532.

CUSEC (2000). "Earthquake Vulnerability of Transportation Systems in the Central United States." *Report no.*, Central U. S. Earthquake Consortium and U. S. Department of Transportation.

DesRoches, R., Choi, E., Leon, R. T., and Pfeifer, T. (2004). "Seismic Response of Multiple Span Steel Bridges in Central and Southeastern United States. I: As Built." *Journal of Bridge Engineering*, 9(5).

DesRoches, R., Leon, R. T., Choi, E., and Pfeifer, T. (2000). "Seismic Retrofit of Bridges in Mid-America." *16th US-Japan Bridge Engineering Workshop*, Reno, Nevada.

DesRoches, R., Pfeifer, T., Leon, R. T., and Lam, T. (2003). "Full-Scale Tests of Seismic Cable Restrainer Retrofits for Simply Supported Bridges." *Journal of Bridge Engineering*, 8(4), 191–198.

Dicleli, M. and Mansour, M. (2003). "Seismic retrofitting of highway bridges in Illinois using friction pendulum seismic isolation bearings and modeling procedures." *Engineering Structures*, 25(9), 1139–1156.

Dillman, D. A., Tortora, R. D., and Bowker, D. (1998). "Principles for Constructing Web Surveys." *Report no.*

Drosos, V. A. (2003). "Synthesis of Earthquake Groundmotions for the New Madrid Seismic Zone," Master's, Georgia Institute of Technology.

Dutta, A. and Mander, J. B. (1998). "Seismic Fragility Analysis of Highway Bridges." *Center-to-Center Project Workshop on Earthquake Engineering Frontiers in Transportation Systems*, H. Kameda and I. M. Friedland, eds., Tokyo, Japan. International Center for Disaster-Mitigation Engineering (INCEDE).

Ellingwood, B. R. and Wen, Y. K. (2005). "Risk-benefit-based design decisions for low-probability/high consequence earthquake events in Mid-America." *Progress in Structural Engineering and Materials*, 7(2), 56–70.

Elnashai, A., Borzi, B., and Vlachos, S. (2004). "Deformation-based Vulnerability Functions for RC Bridges." *Structural Engineering and Mechanics*, 17(2), 215–244.

FEMA (1997). "NEHRP Recommended Provisions for Seismic Regulations for New Buildings and Other Structures, Part 1: Provisions." *Report No. FEMA 302*, Federal Emergency Management Agency.

FEMA (2005). "HAZUS-MH.

Fenves, G. L., Huang, W.-H., Whittaker, A. S., Clark, P. W., and Mahin, S. A. (1998). "Modeling and Characterization of Seismic Isolation Bearings." *?*

FHWA (1995). *Seismic Retrofitting Manual for Highway Bridges*, Vol. FHWA-RD-94-052. Office of Engineering and Highway Operations R and D, McLean, 16 edition.

FHWA (2006). "Seismic Retrofitting Manual for Highway Structures: Part 1 - Bridges." *Report No. FHWA-RD (MCEER-06-xxxx)*, Federal Highway Administration.

Frankel, A. and Leyendecker, E. (2001). "Seismic Hazard Curves and Uniform Hazard Response Spectra for the United States." *Report No. 01-436 CDROM*, U.S. Geological Survey.

Frankel, A., Mueller, C., Barnhard, T., Perkins, D., Leyendecker, E., Dickman, N., Hanson, S., and Hopper, M. (1996). "National Seismic-Hazard Maps: Documentation." *Report No. OFR-96-532*, U.S. Geological Survey.

Galambos, T. V. and Ravindra, M. K. (1978). "Properties of Steel for Use in LRFD." *Journal of Structural Division*, 104(9), 1459–1468.

Ghobarah, A. and Ali, H. M. (1988). "Seismic Performance of Highway Bridges." *Engineering Structures*, 10(3), 157–166.

Gupta, S. and Hartnagel, B. A. (2003). "Seismic Design and Retrofit of Bridges on Missouri's Earthquake Priority Routes." *19th US - Japan Bridge Engineering Workshop*, Tsukuba, Japan.

Hess, P., Bruchman, D., Assakkaf, I., and Ayyub, M. (2002). "Uncertainties in Material Strength, Geometric, and Load Variables." *Naval Engineerings Journal*, 114(2), 167–180.

Hines, W., Montgomery, D., Goldsman, D., and Borror, C. (2003). *Probability and Statistics in Engineering*. John Wiley & Sons, Inc., New York.

Hipley, P. (1997). "Bridge Retrofit Construction Techniques." *Second National Seismic Conference on Bridges and Highways*, Sacramento, CA.

HITEC (1998). "Summary of Evaluation Findings for the Testing of Seismic Isolation and Energy Dissipating Devices." *Report No. CERF REPORT: HITEC 98-06*, Highweay Innovative Technology Evaluation Center.

Housner, G. W. and Thiel, Charles C., J. (1995). "The Continuing Challenge: Report on the Performance of State Bridges in the Northridge Earthquake." *Earthquake Spectra*, 11(4), 607–636.

Hwang, H. and Huo, J. R. (1994). "Generation of Hazard-Consistent Ground Motion." *Soil Dynamics and Earthquake Engineering*, 13(6), 377–386.

Hwang, H. and Huo, J. R. (1998). "Probabilistic Seismic Damage Assessment of Highway Bridges." *6th US National Conference on Earthquake Engineering*, Seattle, WA. EERI.

Hwang, H. and Jaw, J. W. (1990). "Probabilistic Damage Analysis of Structures." *Journal of Structural Engineering*, 116(7), 1992–2007.

Hwang, H., Jernigan, J. B., Billings, S., and Werner, S. D. (2000). "Expert Opinion Survey on Bridge Repair Strategy and Traffic Impact." *Post Earthquake Highway Response and Recovery Seminar*, St. Louis, MO. CERI.

Hwang, H., Jernigan, J. B., and Lin, Y.-W. (2000). "Evaluation of Seismic Damage to Memphis Bridges and Highway Systems." *Journal of Bridge Engineering*, 5(4), 322–330.

Hwang, H., Liu, J. B., and Chiu, Y.-H. (2000). "Seismic Fragility Analysis of Highway Bridges." *Report No. MAEC RR-4*, Center for Earthquake Research Informaion.

Hwang, J. S., Wu, J. D., Wu, T.-C., and Yang, G. (2002). "A Mathematical Hysteretic Model for Elastomeric Isolation Bearings." *Earthquake Engineering and Structural Dynamics*, 31(4), 771–789.

INDOT (2000). "Handbook for the Post-Earthquake Safety Evaluation of Bridges and Roads." *Report no.*, Indiana Department of Transportation.

Jangid, R. S. (2004). "Seismic Response of Isolated Bridges." *Journal of Bridge Engineering*, 9(2), 156–166.

Jernigan, J. B. and Hwang, H. (2002). "Development of Bridge Fragility Curves." *7th US National Conference on Earthquake Engineering*, Boston, Mass. EERI.

Karim, K. R. and Yamazaki, F. (2001). "Effect of earthquake ground motions on fragility curves of highway bridge piers based on numerical simulation." *Earthquake Engineering and Structural Dynamics*, 30(12), 1839.

Karim, K. R. and Yamazaki, F. (2003). "A simplified method of constructing fragility curves for highway bridges." *Earthquake Engineering and Structural Dynamics*, 32(10), 1603–1626.

Keady, K. I., Alameddine, F., and Sardo, T. E. (2000). "Seismic Retrofit Technology." *Bridge Engineering Handbook*, W.-F. Chen and L. Duan, eds., CRC Press.

Kelly, J. M. (1997). *Earthquake-Resistant Design with Rubber*. Springer, London, second edition.

Kelly, J. M. (1998). "The Analysis and Design of Elastomeric Bearings for Application in Bridges." *US-Italy Workshop on Seismic Protective Systems for Bridges*, I. M. Friedland and M. C. Constantinou, eds., Vol. MCEER-98-0015, NY, NY, USA. MCEER, 73–88.

Kelly, J. M. and Quiroz, E. (1992). "Mechanical Characteristics Neoprene Isolations Bearings." *Report No. UBC/EERC-92/11*, University of California at Berkeley.

Khan, R. A., Datta, T. K., and Ahmad, S. (2005). "A simplified fragility analysis of fan type cable stayed bridges." *Earthquake Engineering and Engineering Vibration*, 4(1), 83.

Kim, S.-H. and Shinozuka, M. (2003). "Fragility Curves for Concrete Bridges Retrofitted by Column Jacketing and Restrainers." *Proceedings of the Sixth U.S. Conference and Workshop on Lifeline Earthquake Engineering, Aug 10-13 2003*, Technical Council on Lifeline Earthquake Engineering Monograph, Long Beach, CA, United States. American Society of Civil Engineers, 906–915.

Kim, S.-H. and Shinozuka, M. (2004). "Development of fragility curves of bridges retrofitted by column jacketing." *Probabilistic Engineering Mechanics*, 19(1), 105–112.

Kiremidjian, A. S., Fan, Y., Hortacsu, A., Burnell, K., and LeGrue, J. (2002). "Earthquake Risk Assessment for Transportation Systems: Analysis of Pre-Retrofitted System." *7th National Conference on Earthquake Engineering*, Boston. EERI, III–2109–2116.

Koh, C. G. and Kelly, J. M. (1989). "Viscoelastic Stability Model for Elastomeric Isolation Bearings." *Journal of Structural Engineering*, 115(2), 285–302.

Liao, W.-I., Loh, C.-H., and Lee, B.-H. (2004). "Comparison of dynamic response of isolated and non-isolated continuous girder bridges subjected to near-fault ground motions." *Engineering Structures*, 26(14), 2173–2183.

Mackie, K. (2004). "Fragility Based Seismic Decision Making for Highway Overpass Bridges," PhD thesis, University of California, Berkeley.

Mackie, K. and Stojadinovic, B. (2001). "Probabilistic Seismic Demand Model for California Bridges." *Journal of Bridge Engineering*, 6(6), 468–480.

Mackie, K. and Stojadinovic, B. (2003). "Seismic Demands for Performance-Based Design of Bridges." *Report No. PEER 312*.

Mackie, K. and Stojadinovic, B. (2005). "Comparison of Incremental Dynamic, Cload, and Stripe Method for Computing Probabilistic Seismic Demand Models." *2005 Structures Congress*, New York, NY. American Society of Civil Engineers.

Mackie, K. R. and Stojadinovic, B. (2006). "Post-earthquake functionality of highway overpass bridges." *Earthquake Engineering and Structural Dynamics*, 35(1), 77.

Maleki, S. (2004). "Effect of side retainers on seismic response of bridges with elastomeric bearings." *Journal of Bridge Engineering*, 9(1), 95–100.

Mander, J. B. (1999). "Fragility Curve Development for Assessing the Seismic Vulnerability of Highway Bridges." *Report No. 99-SP01*, MCEER.

Mander, J. B. and Basoz, N. (1999). "Seismic Fragility Curve Theory for Highway Bridges." *5th US Conference on Lifeline Earthquake Engineering*, Seattle, WA, USA. ASCE.

Mander, J. B., Kim, D. K., Chen, S. S., and Premus, G. J. (1996). "Response of Steel Bridge Bearings to the Reversed Cyclic Loading." *Report No. NCEER 96-0014*, NCEER.

Maroney, B., Kutter, B., Romstad, K., Chai, Y. H., and Vanderbilt, E. (1994). "Interpretation of Large Scale Bridge Abutment Test Results." *Proceedings of 3rd Annual Seismic Research Workshop*, Sacramento, CA. Caltrans.

Maroney, B., Romstad, K., and Kutter, B. (1993). "Experimental Testing of Laterally Loaded Large Scale Bridge Abutments." *Structural Engineering in Natural Hazards Mitigation*, Irvine, CA. ASCE.

Martin, G. R. and Yan, L. (1995). "Modeling Passive Earth Pressure for Bridge Abutments." *Earthquake-Induced Movements and Seismic Remediation of Existing Foundations and Abutments, ASCE 1995 Annual National Convention*, Vol. Geotechnical Special Publication 55, San Diego, CA. ASCE.

McKenna, F. and Fenves, G. L. (2001). "OpenSees Command Language Manual.

Melchers (1999). *Structural Reliability Analysis and Prediction*. John Wiley and Sons, Chichester, second ed. edition.

Mellon, D. E. and Post, T. J. (1999). "Caltrans Bridge Research and Applications of New Technologies." *Unknown Journal*.

MODOT (2004). "Post Earthquake Bridge Inspection Training." *Report no.*, Missouri Department of Transportation.

Moehle, J., Fenves, G. L., Mayes, R., Priestley, N., Seible, F., Uang, C.-M., Werner, S., and Aschheim, M. (1995). "Highway Bridges and Traffic Management." *Earthquake Spectra*, 11(S2), 287–372.

Mori, A., Moss, P. J., Carr, A. J., and Cooke, N. (1997). "Behaviour of Laminated Elastomeric Bearings." *Structural Engineering and Mechanics*, 5(4), 451–469.

Mori, A., Moss, P. J., Cooke, N., and Carr, A. J. (1999). "Behavior of bearings used for seismic isolation under shear and axial load." *Earthquake Spectra*, 15(2), 199–224.

Muthukumar, S. (2003). "A Contact Element Approach with Hysteresis Damping for the Analysis and Design of Pounding in Bridges," PhD thesis, Georgia Institute of Technology.

Nielson, B. (2005a). "Analytical Fragility Curves for Highway Bridges in Moderate Seismic Zones," PhD thesis, Georgia Institute of Technology.

Nielson, B. (2005b). "Personal Communication: Analytical Fragility Curves for Highway Bridges in Moderate Seismic Zones.

Nielson, B. and DesRoches, R. (2007a). "Probabilistic Seismic Analysis of Highway Bridges Using a Component Level Approach." *Earthquake Engineering and Structural Dynamics*, In Press.

Nielson, B. and DesRoches, R. (2007b). "Seismic Fragility Curves for Typical Highway Bridge Classes in the Central and Southeastern United States." *Earthquake Spectra*, In Press.

Nielson, B. G. and DesRoches, R. (2006). "Influence of modeling assumptions on the seismic response of multi-span simply supported steel girder bridges in moderate seismic zones." *Engineering Structures*, 28(8), 1083–1092.

Nuti, C. and Vanzi, I. (2003). "To retrofit or not to retrofit?." *Engineering Structures*, 25(6), 701–711.

Priestley, M. J. N., Seible, F., and Calvi, G. M. (1996). *Seismic Design and Retrofit of Bridges*. John Wiley and Sons, New York.

Priestley, M. J. N., Seible, F., Xiao, Y., and Verma, R. (1994a). "Steel Jacket Retrofitting of Reinforced Concrete Bridge Columns for Enhanced Shear Strength-Part 1: Theoretical Considerations and Test Design." *ACI Structural Journal*, 91(4), 394–405.

Priestley, M. J. N., Seible, F., Xiao, Y., and Verma, R. (1994b). "Steel Jacket Retrofitting of Reinforced Concrete Bridge Columns for Enhanced Shear Strength-Part 2: Test Results and Comparison with Theory." *ACI Structural Journal*, 91(5), 537–551.

Ranf, R. T., Eberhard, M. O., and Berry, M. P. (2001). "Damage to Bridges during the 2001 Nisqually Earthquake." *Report No. PEER 2001/15*, Pacific Earthquake Engineering Research Center.

Rix, G. J. and Fernandez, J. A. (2004). "Earthquake Ground Motion Simulation.

Saadeghvaziri, M. and Rashidi, S. (1998). "Effect of Steel Bearings on Seismic Response of Bridges in Eastern United States." *6th US National Conference on Earthquake Engineering*, Seattle, WA. EERI.

Saiidi, M., Maragakis, E. A., and Feng, S. (1996). "Parameters in Bridge Restrainer Design for Seismic Retrofit." *Journal of Structural Engineering*, 122(1), 61–68.

Saiidi, M., Randall, M., Maragakis, E. A., and Isakovic, T. (2001). "Seismic Restrainer Design Methods for Simply Supported Bridges." *Journal of Bridge Engineering*, 6(5), pp. 307–315.

SAS (2004). "JMP: Statistical Discovery Software" Cary, NC.

Seible, F. and Priestley, M. J. N. (1999). "Lessons Learned from Bridge Performance During Northridge Earthquake." *Seismic Response of Concrete Bridges*, F. Seible and M. J. N. Priestley, eds., ACI, Farmington Hills, Michigan, 29–55.

Selna, L. G., Malvar, L. J., and Zelinski, R. (1989). "Bridge Retrofit Testing: Hinge Cable Restrainers." *Journal of Structural Engineering*, 115(4), 920–934.

Shinozuka, M., Feng, M. Q., Dong, X., Uzawa, T., and Ueda, T. (2000). "Damage Assessment of a Highway Network Under Scenario Earthquakes for Emergency Response Decision Support." *Proceedings of SPIE - The International Society for Optical Engineering*, Vol. 3988, Newport Beach, CA, USA. Society of Photo-Optical Instrumentation Engineers, p264–275.

Shinozuka, M., Feng, M. Q., Kim, H., Uzawa, T., and Ueda, T. (2003). "Statistical Analysis of Fragility Curves." *Report No. MCEER-03-0002*, MCEER.

Shinozuka, M., Feng, M. Q., Lee, J., and Naganuma, T. (2000). "Statistical analysis of fragility curves." *Journal of Engineering Mechanics*, 126(12), 1224.

Shinozuka, M., Feng, Maria, Q., Kim, H.-K., and Kim, S.-H. (2000). "Nonlinear Static Procedure for Fragility Curve Development." *Journal of Engineering Mechanics*, 126(12), 1287–1296.

Shinozuka, M., Kim, S.-H., and Zhou, Y. (2004). "Effect of Retrofit, Skew and Number of Spans on Bridge Fragility." *Second PRC-US Workshop on Seismic Analysis and Design of Special Bridges*, G. C. Lee and L.-C. Fan, eds., Vol. MCEER-04-006, Buffalo, NY. MCEER, 61–73.

Skinner, R. I., Robinson, W. H., and McVerry, G. H. (1993). *An Introduction to Seismic Isolation*. John Wiley and Sons, Chichester.

Smyth, A. W., Altay, G., Deodatis, G., Erdik, M., Franco, G., Gulkan, P., Kunreuther, H., Lus, H., Mete, E., Seeber, N., and Yuzugullu, O. (2004). "Probabilistic Benefit-Cost Analysis for Earthquake Damage Mitigation: Evaluating Measures for Apartment Houses in Turkey." *Earthquake Spectra*, 20(1), 171.

Smyth, J. D., Dillman, D. A., Christian, L. M., and Stern, M. J. (2004). "How Visual Grouping Influences Answers on Internet Surveys." *Report no.*, Washington State University Social and Economic Sciences Research Center.

Stanton, J. F. (1997). "The 1997 AASHTO Seismic Isolation Guide Specifications.

Stanton, J. F. and Roeder, C. W. (1992). "Elastomeric Bearings: An Overview." *Concrete International: Design and Construction*, 14(1), 41–46.

Tekie, P. B. and Ellingwood, B. R. (2003). "Seismic fragility assessment of concrete gravity dams." *Earthquake Engineering and Structural Dynamics*, 32(14), 2221–2240.

Thiel, Charles C., J. and Hagen, S. H. (1998). "Economic analysis of earthquake retrofit options: An application to welded steel moment frames." *Structural Design of Tall Buildings*, 7(1), 1.

Wen, Y. K., Ellingwood, B. R., Veneziano, D., and Bracci, J. (2003). "Uncertainty Modeling in Earthquake Engineering." *Report No. MAE Center Projet FD-2 Report*, Mid-America Earthquake Center.

Wen, Y. K. and Wu, C. L. (2001). "Uniform Hazard Ground Motions for Mid-America Cities." *Earthquake Spectra*, 17(2), 359–384.

Wendichansky, D. A., Chen, S. S., and Mander, J. B. (1995). "In-Situ Performance of Rubber Bearing Retrofits." *National Seismic Conference on Bridges and Highways*, Progress in Research and Practice, San Diego, CA.

Werner, S. D. and Taylor, C. E. (2002). "Component Vulnerability Modeling Issues for Analysis of Seismic Risks to Transportation Lifeline Systems." *Acceptable Risk Processes – Lifelines and Natural Hazards*, Council on Disaster Reduction and Technical Council for Lifeline Earthquake Engineering.

Werner, S. D., Taylor, C. E., and Moore, J. E. (1997). "Loss Estimation Due to Seismic Risks to Highway Systems." *Earthquake Spectra*, 13(4), 585–604.

Werner, S. D., Taylor, C. E., Moore, J. E., Walton, J. S., and Cho, S. (2000). "A Risk-Based Methodology for Assessing Seismic Performance of Highway Systems." *Report No. MCEER-00-0014*, MCEER.

Wu, C.-F. J. and Hamada, M. (2000). *Experiments: Planning, Analyisis, and Parameter Design Optimization*. John Wiley & Sons, Inc., New York.

Yamazaki, F., Hamada, T., Motoyama, H., and Yamauchi, H. (1999). "Earthquake Damage Assessment of Expressway Bridges in Japan." *Technical Council on Lifeline Earthquake Engineering Monograph*, (16), p 361–370.

Yan, G., Zhao, G., and Zhong, T. (2004). "Aseismic Performance of Base-Isolated Bridges using Lead-Rubber Bearings." *Second PRC-US Workshop on Seismic Analysis and Design of Special Bridges*, G. C. Lee and L.-C. Fan, eds., Vol. MCEER-04-006, Buffalo, NY. MCEER, 283–297.

Yashinsky, M. (2006). "Personal Communication Regarding State of Retrofit Practice.

Zahrai, S. M. and Bruneau, M. (1999). "Ductile End-Diaphragms for Seismic Retrofit of Slab-on-Girder Steel Bridges." *Journal of Structural Engineering*, 125(1), 71.

Zhang, Y., Cofer, W. F., and McLean, D. I. (1999). "Analytical Evaluation of Retrofit Strategies for Multicolumn Bridges." *Journal of Bridge Engineering*, 4(2), 143–150.

Zhou, Y., Murachi, Y., Kim, S.-H., and Shinozuka, M. (2004). "Seismic Risk Assesment of Retrofitted Transportation Systems." *13th World Conference on Earthquake Engineering*, Vancouver, B.C., Canada.

VITA

Jamie Ellen Padgett was born on December 5, 1980 in Melbourne, Florida. Upon graduating High School, she entered the University of Florida in Gainesville, FL. She obtained her Bachelor's of Science in Civil Engineering with a minor in Business Administration and Sales Engineering from UF in 2003. Jamie continued to graduate school at the Georgia Institute of Technology pursuing a Master's and Doctoral Degree in Civil Engineering with a minor in Probability and Statistics.